


2013

# Development and application of a rapid sampling technique for identification and quantification of compounds in high temperature process gas streams produced from biomass gasification and pyrolysis

Patrick John Woolcock  
*Iowa State University*

Follow this and additional works at: <http://lib.dr.iastate.edu/etd>

 Part of the [Analytical Chemistry Commons](#), [Chemical Engineering Commons](#), and the [Mechanical Engineering Commons](#)

---

## Recommended Citation

Woolcock, Patrick John, "Development and application of a rapid sampling technique for identification and quantification of compounds in high temperature process gas streams produced from biomass gasification and pyrolysis" (2013). *Graduate Theses and Dissertations*. 13241.

<http://lib.dr.iastate.edu/etd/13241>

This Dissertation is brought to you for free and open access by the Graduate College at Iowa State University Digital Repository. It has been accepted for inclusion in Graduate Theses and Dissertations by an authorized administrator of Iowa State University Digital Repository. For more information, please contact [digirep@iastate.edu](mailto:digirep@iastate.edu).

**Development and application of a rapid sampling technique for identification and  
quantification of compounds in high temperature process gas streams produced from  
biomass gasification and pyrolysis**

by

**Patrick J. Woolcock**

A dissertation submitted to the graduate faculty  
in partial fulfillment of the requirements for the degree of

DOCTOR OF PHILOSOPHY

Co-majors: Agricultural & Biosystems Engineering; Biorenewable Resources & Technology

Program of Study Committee:  
Robert C. Brown, Co-major Professor  
Jacek Koziel, Co-major Professor  
Steven Hoff  
Derrick Rollins  
Young-Jin Lee

Iowa State University

Ames, Iowa

2013

Copyright © Patrick J. Woolcock, 2013. All rights reserved.

*Dedication:*

The following were essential ingredients for this recipe ...

1. The Head Honcho above, who blesses me with each day
2. Family, without which I ultimately would not have had this opportunity
3. Friends, both in grad school and a mere phone call away, without which opportunities like these remain empty
4. Colleagues (Karl and CSET) and Professors, who have instructed me and learned along with me
5. Inspiration and dedication, thank you Morgan
6. And knowing when to claim dgaff, thank you Josh

**Table of Contents**

List of Figures .....	vi
List of Tables .....	x
Abstract .....	xii
Chapter 1: Introduction .....	1
Big Picture Motivation .....	1
Syngas & Tar Analytical Techniques.....	3
Project Objectives .....	10
Dissertation Outline.....	11
Chapter 2. Literature Review: Understanding Syngas and Cleanup .....	12
Introduction .....	13
Description of Contaminants.....	15
Hot Gas Cleanup (HGC) .....	25
Cold Gas Cleanup (CGC).....	69
Warm Gas Cleanup (WGC) .....	85
Conclusion.....	92
Acknowledgments .....	93

Chapter 3. Proof of concept work for developing a novel analytical method for hot gas stream analysis based on TWA-SPME.....	94
Introduction .....	95
Experimental Section .....	101
Results & discussion .....	106
Conclusion.....	119
Chapter 4. Pilot scale validation of the novel TWA-SPME based analytical method for measurement of analytes in hot process gas.....	121
Abstract .....	121
Introduction .....	122
Experimental Section .....	127
Results & Discussion .....	131
Conclusions .....	144
Author Information .....	145
Acknowledgements .....	145
Chapter 5. Challenges and potential solutions to analyzing alternative thermochemical process gas streams .....	146
Chapter 6. Conclusions.....	155
Appendix .....	159
GC-FID calibration issues using TWA-SPME .....	159

Supplementary material for proof-of-concept work.....	167
Supplementary Work for TWA-SPME Pilot-Scale Validation Manuscript .....	179
Gas cleaning system design: optimizing oil scrubbing for tar removal .....	190
References .....	201

## LIST OF FIGURES

<b>Figure 1:</b> Syngas conversion technologies as adapted from Spath and Dayton [45].....	14
<b>Figure 2:</b> Tar evolution as suggested by Elliott [65] .....	19
<b>Figure 3:</b> Hydrogen sulfide removal processes (adapted from Lovell) [72].....	22
<b>Figure 4:</b> Cyclone [52].....	28
<b>Figure 5:</b> Filtration mechanisms for removal of particulate matter: (a) diffusion, (b) inertial impaction, (c) direct interception, (d) gravitational settling. (Adapted from [58]).....	29
<b>Figure 6:</b> Candle filter element (Adapted from [58]) .....	31
<b>Figure 7:</b> Cross-flow filter (Adapted from [58]).....	32
<b>Figure 8:</b> Operation of moving bed filter[108] .....	35
<b>Figure 9:</b> A tube-type ESP concept for high temperatures and pressures (adapted from [58]).....	39
<b>Figure 10:</b> Plate type turbulent flow precipitator TFP [125] .....	43
<b>Figure 11:</b> Wet dynamic scrubber [198] .....	71
<b>Figure 12:</b> Simplified OLGA process diagram [34, 35] .....	87
<b>Figure 1:</b> Simulated TWA SPME sampling system for hot process gas. ....	105
<b>Figure 2:</b> Benzene adsorbed on the CAR/PDMS fiber at atmospheric pressure for 10 min sampling times at 115 °C, $\delta = 5$ mm.....	107
<b>Figure 3:</b> TWA SPME extraction at 115 °C ( $\delta = 3.3$ mm) of $0.39 \text{ g cm}^{-3}$ (160 ppm <sub>w</sub> ) benzene in N <sub>2</sub> (standard errors all below 4 ng).....	108

<b>Figure 4:</b> Amount of benzene (ng) collected (minus a baseline) at 115 °C as a function of t (s) and $\delta$ (mm) for the treatment combinations (t = 5, 10, and 15 min; $\delta$ = 3.3, 5, and 10 mm; $C_g = 0.39 \text{ g m}^{-3}$ (160 ppm <sub>w</sub> )).	111
<b>Figure 5:</b> Experimental (apparent) diffusivity ( $D_g$ ) as a function of $\delta$ for different t. All tests performed at normal conditions of 115 °C, $0.39 \text{ g m}^{-3}$ (160 ppm <sub>w</sub> ), 1 atm, and 5.7 SLPM N <sub>2</sub> flow rate.	112
<b>Figure 6:</b> TWA-SPME analysis of syngas generated from biomass gasification and passed through a tar condensation vessel. Conditions of sample taken directly from process piping: CAR/PDMS fiber, 3.3 mm retraction depth, 10 min exposure, ~150 °C syngas temperature.	116
<b>Figure 1:</b> Schematic of the conventional tar sampling and collection system (all process piping and sampling lines are heat traced to reduce probability of tar condensation).	129
<b>Figure 2:</b> Schematic of the gasifier and gas cleaning system (gas samples taken immediately prior to and downstream of the tar/char scrubber	130
<b>Figure 1:</b> Pyrolysis Free-Fall Reactor	147
<b>Figure 2:</b> TWA-SPME chromatograms of port 14 of the free fall reactor (top) and port 18 (bottom) taken with CAR/PDMS	148
<b>Figure 3:</b> Schematic for the internally-cooled SPME device.	149
<b>Figure 4:</b> The original (top) and new (bottom) internally-cooled SPME devices	151
<b>Figure 5:</b> Chromatograms taken in the free-fall reactor with cellulose, showing the main peak of levoglucosan that was targeted for the extraction conditions.	153



<b>Figure 1:</b> $D_g$ values calculated with the calibration curve developed from the initial autosampler values for the BTSIN Mixture.....	165
<b>Figure 2:</b> $D_g$ values calculated with the calibration curve developed from the autosampler values for the BTSIN Mixture adjusted for the extra 20 % injection volume (0.2 uL extra). .....	165
<b>Figure S-1:</b> Analyses of the syngas tar scrubbing oil taken at 100 °C, 1 minute exposure time, and mass spectroscopy for analyte identification.....	174
<b>Figure S-2:</b> SPME device with fiber exposed from the needle housing (top) and fiber retracted (bottom).....	175
<b>Figure S-3:</b> SPME temperature probe developed to measure temperature profile along depth of retraction .....	175
<b>Figure S-4:</b> Heated sampling apparatus for TWA passive sampling at 115°C.....	176
<b>Figure S-5:</b> Sampling rates of benzene at different $t$ . All tests performed at normal conditions of 115 °C, 0.39 g m <sup>-3</sup> (160 ppm <sub>w</sub> ), 1 atm, and 5.7 SLPM N <sub>2</sub> flow rate. ..	177
<b>Figure S-6:</b> 3-D plot of experimental $D_g$ values at 115 °C versus time and inverse depth according to Equation 3. ....	178
<b>Figure S-7:</b> 3-D plot of experimental $D_g$ values at 25 °C versus time and inverse depth according to Equation 3. ....	178
<b>Figure S-1:</b> SPME device with fiber exposed from the needle housing (top) and fiber retracted (bottom).....	179
<b>Figure S-2:</b> Mass of the target analytes adsorbed on SPME fiber vs. changes in sampling time and SPME fiber retraction depth.....	180
<b>Figure S-3:</b> Benzene response to changes in time and depth. ....	181

<b>Figure S-4:</b> Toluene response to changes in time and depth..	182
<b>Figure S-5:</b> Benzene $n(t)$ residual by predicted plot. Note the over estimation at the extreme ends of the model calibration.	182
<b>Figure S-6:</b> Impingers from comparison run 3.	185
<b>Figure S-7:</b> Impinger 4 (first impinger downstream of pressure cooker) analyzed for tar compounds.	186
<b>Figure S-8:</b> TWA-PSME sample taken from the slipstream during the sample of Figure S-7 above.	187
<b>Figure S-9:</b> TWA-SPME analysis of post-pressure cooker tar at 170° C for high temperature identification of tar compounds.	188
<b>Figure 1:</b> Pilot-scale 20 kg/h fluidized bed gasifier and gas cleaning PDU	191
<b>Figure 2:</b> Oil scrubber for tar removal in the PDU	192
<b>Figure 3:</b> Oil scrubber column original design	193
<b>Figure 4:</b> Oil scrubber decanter design	194
<b>Figure 5:</b> Oil scrubber column new design	195
<b>Figure 6:</b> Oil scrubber system P&ID	196
<b>Figure 7:</b> Oil scrubber column schematic and sectors for tar removal	199
<b>Figure 8:</b> Oil scrubber column top view	200

## LIST OF TABLES

<b>Table 1:</b> Common feedstock impurity levels [48-51] .....	16
<b>Table 2:</b> Typical syngas applications and associated cleaning requirements .....	17
<b>Table 3:</b> Basic approximations for tar compound classification [15, 33] .....	21
<b>Table 4:</b> Summary of hot gas particulate cleanup technology (adapted from Seville) [58].....	26
<b>Table 5:</b> Examples of sulfur sorbents and theoretical capacities [75].....	58
<b>Table 1:</b> The means of nine depth and time combinations statistically compared to the average of the WL, FSG, and Huang theoretical equations (at $\alpha = 0.05$ unless otherwise stated) .....	115
<b>Table 2:</b> TWA-SPME analysis of syngas generated from biomass gasification and calculated tar concentration.. .....	118
<b>Table 1:</b> Gasification trials using switchgrass. Equivalence ratio indicates the amount (kg) of O <sub>2</sub> used compared to the amount (kg) actually required for complete stoichiometric combustion of the feedstock.. .....	134
<b>Table 2:</b> $D_g$ values derived experimentally from lab scale testing and adjustments made for PDU experiments at sampling locations A and B. ....	137
<b>Table 3:</b> Quantified analytes compared between TWA-SPME and conventional impingers (L.D. represents values below limit of detection for method) .....	138
<b>Table 4:</b> Total light tar estimations from conventional solvent impinger measurements and TWA-SPME analysis. ....	142
<b>Table S-1:</b> Statistical analysis of variance (ANOVA) testing the effects of $t$ and $\delta$ treatments.....	173

<b>Table S-2:</b> Statistical analysis of covariance (ANCOVA). Testing the effects of time assuming depth as a covariate (i.e. confounding variable) .....	173
<b>Table S-1:</b> ANOVA, model parameters, and LOF results for Benzene.....	183
<b>Table S-2:</b> ANOVA, model parameters, and LOF results for Toluene .....	184
<b>Table S-3:</b> TWA-SPME analysis of post-pressure cooker tar at 170 °C for high temperature identification of tar compounds. ....	189
<b>Table 1:</b> Key calculations for oil scrubber column .....	198

## Abstract

A commercially applicable measurement technique for measuring volatile organic compounds (VOCs) in hot process gas streams was developed. The method was validated by quantifying the amount “tar” in a syngas stream generated from a pilot-scale gasification reactor and gas cleaning process development unit (PDU) and comparing the value to that of conventional measurements. Conventional approaches to measuring VOCs suffer from extensive amounts of equipment and require substantial preparation time in the lab before data are recovered. This makes them impractical for use in rapid process monitoring and drastically inhibits attempts to optimize new tar removal techniques for syngas. The novel method is capable of sampling directly from process piping and provides results within the time-resolution of the analytical equipment (typically 1-2 h for mass spectrometry or flame ionization detection).

The method is based on time-weighted average solid-phase microextraction (TWA-SPME) theory. Testing the theory on a lab scale system for the analytes of interest (benzene, toluene, styrene, indene, and naphthalene) yielded important limitations to the technique using high temperature (>115 °C) process environments. The TWA-SPME method was applied on the pilot-scale (20 kg/h of switchgrass feed) PDU within appropriate sample extraction conditions dictated by the lab-scale testing. The method returned results within 10% of the conventional impinger approach for most analytes, and within 20% for all analytes downstream of the gas cleaning unit. When coupled with a new rapid measurement technique for heavy tar using a pressure cooker, the new method is capable of providing the concentration of tar for any syngas stream in an hour or less compared to the conventional method that requires several days for wet-chemical analysis. Additional applications of the technique are currently underway including the measurement of key light VOCs generated in a free-fall pyrolysis reactor in an attempt to gain

valuable process kinetics data. An extension of this research is based on the development of a method for measurement of VOCs at much higher temperatures (exceeding 300 °C) using an internally-cooled SPME fiber.

## CHAPTER 1: INTRODUCTION

### Big Picture Motivation

The world consumed over 87 million barrels a day of oil in 2011, and will continue to increase consumption with the rapid rise in demand of developing countries to over 100 million barrels a day in 2035 [1]. Along with other fossil fuels and net carbon emitting sources of energy, energy-related carbon dioxide (CO<sub>2</sub>) emissions are slated to increase from 31.2 Gt in 2010 to 37 Gt in 2035 without substantial investment in carbon capture and storage.[2] The resulting 3.6 °C rise in average global temperature has obvious catastrophic impacts on climate and sea levels, evidence of which has been prominent even in mainstream media and literature. Other less obvious impacts include the mass destruction and possible extinction of numerous species, as well as ocean acidification and eventual human suffering due to famine.

All of these issues have led to a surging interest in renewable and clean sources of energy for today's world. Global subsidies for renewable energy grew by 24% to over \$88 billion from 2010 to 2011.[1] Continued development of renewable sources of energy, cleaner fossil fuels, and improved efficiencies are expected in the coming decades given the tremendous financial incentives to avoiding any preventable environmental damages.[1] A substantial amount of the new investment in renewable carbon is also geared toward very water efficient feedstock such as perennial grasses (i.e. switchgrass) and waste streams (agricultural and municipal), given the significant water use of both fossil fuel and current first generation renewables.

Deployment of these alternative carbon feedstocks on a grand scale requires a means converting them into higher valued products such as transport fuels and chemicals.

Thermochemical conversion (TC) technologies such as gasification and pyrolysis are a rapidly

growing and commercially viable means of making these carbon sources compatible with current infrastructure.

TC uses heat and catalysts to convert carbon polymers into fuels, chemicals or electric power. Pyrolysis work is largely focused on fast pyrolysis, which is the rapid thermal depolymerization and subsequent rapid cooling of the organic vapors to yield a primarily bio-oil product with non-condensable gas (NCG) and a solid char byproduct. Pyrolysis oil is typically high in water content with low pH, making it necessary to upgrade the oil prior to use in many applications or long term storage. Much of the current work is focused on upgrading the oil after pyrolysis, or creating an alternative reactor to create a superior crude bio-oil product via in-situ deoxygenation or hydrogenation [3, 4].

Alternatively, gasification yields a primarily NCG product stream of which carbon monoxide (CO) and hydrogen (H<sub>2</sub>) are typically the desired gas species. The raw producer gas must be cleaned of contaminants and impurities before combustion for heat and power applications or catalytically converted to fuels (see Chapter 1).

Overall, both technologies are promising routes to replacing traditional fossil carbon in our current infrastructure with renewable or cleaner carbon. Widespread deployment depends on developing the processes to be economically competitive with fossil-derived products. Equally as important as process development is the development of sampling and analysis techniques for the products, without which no measure of improvement or optimization can be effectively attained. Efforts to characterize both bio-oil and syngas have been made, but significant impediments still exist.



## Syngas & Tar Analytical Techniques

One of the most important analytical challenges still without a feasible solution is a means of monitoring the volatile organic compounds in gasification and pyrolysis process gas streams in real time. Measurement of the volatile organics in both pyrolysis and gasification are commonly approached in two ways: condensable medium and heavy organic molecules are quenched and collected for later analysis, and non-condensable gases are measured in the gas phase using a number of well-known detection methods.

Non-condensable gases have received considerable attention in the past given their prominence in combustion gas streams.  $\text{CO}_2$ ,  $\text{CO}$ ,  $\text{N}_2$ ,  $\text{H}_2$ , and even light hydrocarbons like acetylene and propane are easily measured using micro gas chromatographs (microGCs), thermal conductivity detectors, and other dedicated gas analyzers [5]. Compounds with inorganic atoms such as ammonia ( $\text{NH}_3$ ) and hydrogen sulfide ( $\text{H}_2\text{S}$ ) can also now be measured online using a number of conductivity or chemiluminescence detection devices [5, 6]. The expense of some equipment to monitor more hard to determine species such as carbon disulfide or hydrogen cyanide can be substantial, but the technology and commercial equipment is available to perform the necessary process gas measurements.

Larger condensable volatile compounds are a more challenging issue. In nearly all cases the compounds are condensed and collected either with aid of a solvent or simple heat transfer, and are separated and analyzed with conventional wet chemistry methods [7-9]. Measurement in the gas phase for bio-oil is not currently performed. The instability and high reactivity of the pyrolysis products also suggests that differences in compounds and concentrations will exist between gas and liquid phases. Analyzing pyrolysis vapors prior to condensation is typically only possible with micro-pyrolyzers connected to a gas chromatograph and mass spectrometer

(GC-MS) [10, 11]. This does not however reflect the kind of processing environment expected at larger scale commercial facilities, and is not a feasible means of gaining valuable process data for optimization at larger scales. Devising a method for in-situ measurement of the pyrolysis vapors is of great importance for the future of commercial scale pyrolysis, and is also important for understanding the chemistry of pyrolysis vapors in larger than micro sized reactions.

Analyzing syngas from gasification processes has also received considerable attention in recent years given the mature and commercial nature of gasification technology.[12] However, the larger condensable volatile compounds found in syngas continue to be a difficult collection of compounds for sampling and analysis. Commonly known as tars, these aromatic, polyaromatic, or heteroaromatic hydrocarbons are a detrimental byproduct of the gasification process rather than the primary desired product as in fast pyrolysis [13]. Conventional approaches to the syngas tar analysis often resulted in varied definitions between researchers, which made it difficult to compare technologies and process improvements as well as ensure accurate sampling was being performed by independent groups [14]. Over a decade, an international effort was made to develop, test, and validate a protocol for standardizing tar collection and analysis, which is summarized by the fairly recent international tar protocol [15-17]. This method utilizes an extensive array of equipment including an isokinetic probe and thimble filter for particulate collection, a series of glass impingers for collection of condensable analytes, and extensive sampling line heat tracing to avoid premature condensation of desired analytes.[18] It also discusses the analytical equipment and procedures necessary for sample preparation and analysis (such as evaporation of solvent and separation of non-GC detectable compounds). Although this method successfully standardized a feasible approach to tar analysis, it often suffers from poor repeatability (high variability) during analysis, is incredibly complex,

and is performed completely offline over a period of several hours if not days, which makes it useless for rapid process monitoring and optimization.

Some recent efforts have been made to improve on the speed, reliability, and/or simplicity of the tar protocol. Solid-phase adsorption/extraction (SPA/SPE) methods were developed to simplify tar collection by eliminating the need for extensive glassware and solvents in the processing environment [7, 19-21]. In lieu of the solvent train, tars collect on an intermediate solid phase which is thermally desorbed or washed later in the laboratory to separate the collected analytes for further sample preparation and analysis. The technique drastically reduces preparation time and time for collecting a sample. However, tar analysis still requires substantial time in the laboratory performing solvent extractions and sample preparation for analysis.

Among the more common methods for analysis are those used in conventional tar quantification, such as gas chromatography coupled with flame ionization or mass spectrometry (GC-FID, GC-MS) or high performance liquid chromatography (HPLC) [22, 23].

Online analytical techniques have also been attempted in order to gain real-time syngas tar data. Heated sampling lines transport syngas from the sampling point to the analytical device. Pressure reduction, gas dilution, or some other means to reduce the dew point of tar compounds is generally required to avoid analyte condensation prior to reaching the analytical device [22, 24, 25]. One recently developed technique immediately quenches the heated slipstream with an alcohol to form a biphasic mixture of analytes: a non-condensable gas stream free of particulates and heavy tars that can be analyzed by micro-GC, and a liquid phase that can be analyzed using on-line density measurements for water concentration and UV-vis spectroscopy to provide real time tar concentration [22, 25]. Apparent shortcomings of this recently developed technique

remain the complexity of the analysis and the extravagant analytical equipment and wet chemistry still required for full understanding of tar quantification.

Another approach has been developed at Iowa State University to simplify the IEA tar protocol by eliminating the solvent evaporation step. The solvent-free tar measurement technique flows syngas through a polymer tube (Santoprene®) submerged within a water-filled pressure cooker set at 105 °C [26]. Tars with a dew point higher than ~105 °C condense and deposit in the pressure cooker tubing. The tubing is weighed before and after a test to gravimetrically determine the heavy tar fraction. The water dew point depends on syngas composition and pressure of the gasifier, but is generally several degrees below 100 °C and is not a confounding factor in the gravimetric tar analysis. This approach showed less than 5% deviation between measurements and came within 10% of the IEA tar protocol for the heavy tars. A comparison for lighter tar compounds was not performed, and syngas water concentration measurements were substantially different from the IEA tar protocol. The data also reflected very poor precision for both methods in the quantification of syngas water vapor.

Measurement of heavy tars with the pressure cooker method has several benefits. The simple gravimetric response without any required preparation provides immediate feedback on the process. The simplicity of the technique overall also enables a rapid turnaround between tests, as only the tubing inside the pressure cooker needs changed and the system can be ready for sampling again. The equipment is also very robust with no sensitive analytical equipment to guard against. However, the light tar in syngas that is missed by this method can be a significant portion of the total tar compounds. Aigner et al. reported aromatics as 15-30% of the total tar compounds from fluidized bed gasification of wood chips [27]. Single ring aromatics were also consistently 40-50% by weight of the total tar collected in a series of 6 tests conducted on a

fluidized bed gasifier operating feeding willow trees in Europe [14]. Many other researchers using a variety of feedstock and gasifier types have shown benzene and light aromatics to be anywhere from 20-65% of the total tar compounds [7, 17, 28-31].

Reliably measuring the gravimetric tars is important for ensuring piping and equipment remains free of heavy tar deposits. Light tars that are not quantified reliably with the conventional method can however be very detrimental for downstream processes requiring high purity syngas. It also becomes harder to quantify these tars reliably after cleaning processes have removed a majority of the tar compounds. For instance, an oil-based gas washing technique, OLGA, was developed in the Netherlands for removing tars from syngas [32-35]. This and other techniques are discussed in greater detail in Chapter 1. Similar to older methods based on water as the washing fluid, it works on the principal of cooling and absorbing tars with the liquid solvent. Both techniques are very efficient at removing tars below a given threshold for downstream processes. However, the process parameters can be varied to increase the intensity of the cleaning and remove a higher percentage of unwanted compounds depending on the requirements of downstream applications. This generally requires higher flow rates and more washing fluid, which in turn increases operational costs. Depending on the end-use application, the light tars may serve as additional feedstock (combustion processes) or they may cause substantial process disruptions (catalysis or fuel cells). Differences may exist within applications as well, such as new catalysts that are more tolerant to contaminants than others. Knowing the concentration of light tars can be advantageous economically: measuring the tar content and reducing the tar concentration to levels required by the downstream application may create substantial economic benefits by balancing cleaning expense with maintenance expense.

Conventional methods for measuring tar using slipstream collection and solvent washing are poorly suited for such precise measurements. Gravimetric measurements may take hours to collect enough sample mass downstream of a cleaning process to provide clear and accurate measurements. Similarly, time for washing sorbents with solvents and preparing samples for analysis can also be substantial. Both methods also suffer from large solvent peaks that confound data during analysis in analytical devices.

Solid-phase micro extraction (SPME) combines sample extraction and preparation into a single step, which mitigates the extensive laboratory work required in conventional wet chemical methods to provide much more rapid results. As discussed in chapter 2, SPME is essentially a micro-sized version of an SPE device. A thin coating is placed on a small wire inside of a syringe and acts as an adsorption or absorption phase to collect and preconcentrate analytes for analysis. The small size also enables direct injection of the phase into the injection port of conventional analytical devices (GC-FID, GC-MS, HPLC, etc.). The method effectively reduces the time resolution for sampling to that of the analytical device.

SPME is a relatively new technique developed in Canada by Pawliszyn [36]. Used widely for agricultural and environmental research, the device can be used in two primary configurations. The first and most commonly used method is based on the partitioning (i.e. distribution constants) of analytes between the extraction phase (fiber's coating) and the sample environment (surrounding environment). This method basically revolves around the estimations of distribution constants based on a variety of conditions including pressure, temperature, pH, salt, analyte concentrations and other sample matrix characteristics. Multiple methods of calibration are possible for this technique which can be performed with several common extraction phases depending on the nature of the analytes (polar, non-polar, aromatic, etc.)

A second method used more recently is the time-weighted average (TWA) approach. SPME-TWA operates on the principle of diffusion. Each analyte of interest will diffuse through a stagnant boundary layer at a given rate based on environmental conditions. The amount collected after a set time of exposure to the sample environment then corresponds to a concentration in the environment. This is discussed in greater detail in chapter 2.

A limited number of researchers have begun to approach SPME as potentially valuable in thermochemical research operations. Micro-scale pyrolysis operations have received the most attention, followed by combustion or residue analysis [37-40]. To date, the only syngas tar measurement attempt was performed with equilibrium-based SPME, and showed poor performance compared to SPA/SPE [41]. Based on the type of extraction phases and method of calibration utilized at the time, this result is not extraordinary. Larger compounds have a tendency to displace smaller compounds given enough time, and the different extraction phases will preferentially extract certain classes of molecules leaving an incomplete picture. Diffusion based sampling with the TWA-SPME approach may potentially reduce these effects given the small amount of analyte collected on the fiber coating during experimentation. Several other advantages to TWA-SPME compared to previous attempts and conventional measurements are thoroughly discussed in chapters 2 and 3.

The importance of gasification and pyrolysis in producing a clean and sustainable future is evident. With the growth of both technologies, a substantial gap has grown in the ability to rapidly analyze the process environments and provide real-time optimization for commercial operations. Developing a new analytical technique to address these issues is vital to continued research and development of these thermochemical technologies.

## **Project Objectives**

Objective 1: To design, construct, and operate a syngas cleaning system of the appropriate size for a steam/oxygen fluidized bed gasifier operating at 20 kg/h of biomass feed, and successfully generate a syngas stream with trace concentrations of tar that represents feed streams typical to commercial syngas applications.

Objective 2: To develop a rapid tar measurement technique capable of supplementing and/or fully replacing the available techniques for identification and quantification of syngas tar compounds measured at elevated temperatures.

Objective 3: Test the novel concept for analyzing syngas tar using a lab-scale controlled environment, followed by validation by comparison to a conventional tar measurement technique using syngas generated by the fluidized bed gasifier, with the intention to apply the technique to other thermochemical process environments such as pyrolysis or combustion vapors.



## **Dissertation Outline**

Development of a new technique for high-temperature analysis of process gas based on TWA-SPME has highlighted the substantial weakness in the current state of technology with regard to syngas tar analysis. It has also led to a more detailed understanding of high-temperature behavior for the TWA-SPME technique. The following chapter aims to provide background information on the challenging process environment of gasification, as well as the cleaning techniques that are likely to be used upstream of the TWA-SPME technique. Chapter 3 discusses the development process for the novel application and potentially limiting factors found in the gasification environment. The final paper discusses an overall comparison between a conventional impinger based approach to that of the TWA-SPME approach, as well as future potential of the technique.

## CHAPTER 2. LITERATURE REVIEW: UNDERSTANDING SYNGAS AND CLEANUP

The following article was published in the Journal of Biomass and Bioenergy to serve as a single resource for all current understanding of contaminant generation and contaminant removal in syngas [42]. Extensive literature review was performed to develop a working knowledge of producer gas and syngas streams, as well as identify the technological gaps hindering widespread commercial application of thermochemical processing technologies.

Syngas from gasification of carbonaceous feedstocks is used for power production and synthesis of fuels and commodity chemicals. Impurities in gasification feedstocks, especially sulfur, nitrogen, chlorine, and ash, often find their way into syngas and can interfere with downstream applications. Incomplete gasification can also produce undesirable products in the raw syngas in the form of tar and particulate char. This paper reviews the origins and chemistry of the major contaminants in raw syngas, as well as the technologies for gas cleanup. These technologies are classified according to the gas temperature exiting the cleanup device: hot ( $T > 300^{\circ}\text{C}$ ), cold ( $T < \sim 100^{\circ}\text{C}$ ), and warm gas cleaning regimes. Cold gas cleanup uses relatively mature techniques that are highly effective although they often generate waste water streams and may suffer from energy inefficiencies. The majority of these techniques are based on using wet scrubbers. Hot gas cleaning technologies are attractive because they avoid cooling and reheating the gas stream. Many of these are still under development given the technical difficulties caused by extreme environments. Warm gas cleaning technologies include traditional particulate removal devices along with new approaches for removing tar and chlorine.

## Introduction

Syngas is a mixture of hydrogen ( $H_2$ ) and carbon monoxide (CO) produced from the gasification of carbonaceous feedstocks. Since its first commercial use by the London Gas, Light, and Coke Company in 1812, syngas and its coal based antecedents (town gas, producer gas, coal gas) have been influential in the development of human society [43]. They have illuminated cities, provided heat and power, and fueled vehicles through both direct use and conversion to liquid fuels. As global energy demand rises by nearly 44 % from 2006 to a projected 715 EJ in 2030, syngas will become increasingly important for process heat, electric power generation, and liquid fuels [2]. There is renewed emphasis on coal gasification for enhancing national security, while mounting environmental sustainability issues have increased interest in biomass gasification. Raw product gas generated from gasification contains contaminants that must be mitigated to meet process requirements and pollution control regulations. This paper provides a comprehensive overview of the technologies used to remove these contaminants.

The term ‘syngas’ is widely used as industry shorthand to refer to the product gas from all types of gasification processes. However, syngas is technically a vapor stream composed of only  $H_2$  and CO derived from a steam and oxygen gasification process. While not entirely accurate, this industry shorthand will be used in this paper with appropriate adjectives to maintain clarity and simplicity of discussion with regard to the industry and published literature [44].

Syngas has many uses which range from heat or power applications such as IGCC to a variety of synthetic fuels as shown below. With such applications, each contaminant creates specific downstream hazards. These include minor process inefficiencies such as corrosion and

pipe blockages as well as catastrophic failures such as rapid and permanent deactivation of catalysts.

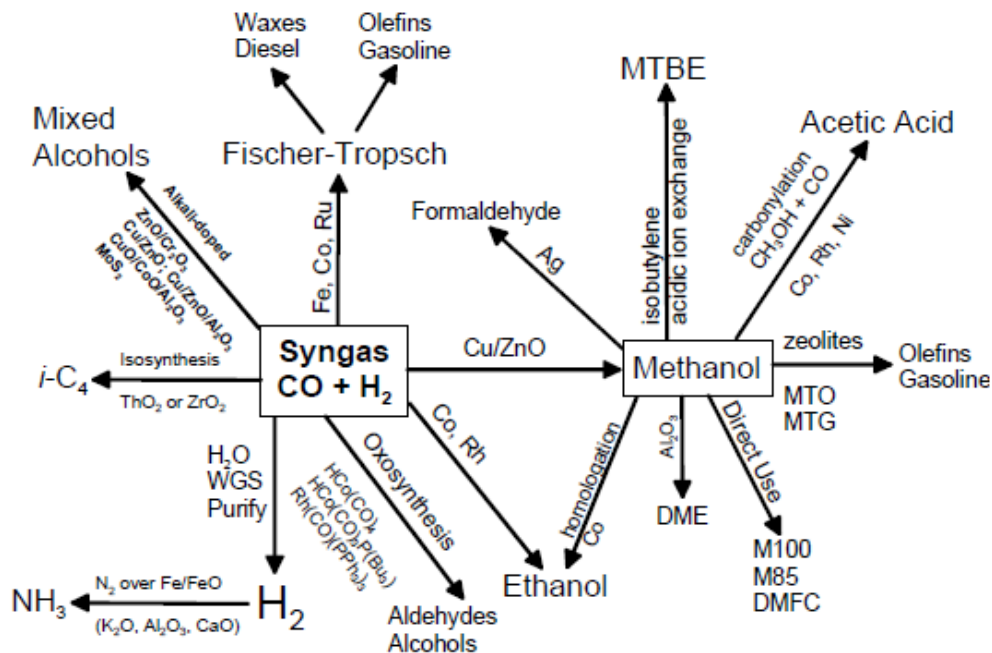


**Figure 1:** Syngas conversion technologies as adapted from Spath and Dayton [45]

A multitude of technologies exist to purify the raw synthesis gas stream that is produced by gasification. Some methods are capable of removing several contaminants in a single process, such as wet scrubbing, while others focus on the removal of only one contaminant. Techniques are available that minimize the syngas contamination by reducing the contaminants emitted from within the gasifier; an approach typically termed ‘primary’ or ‘in-situ’ cleanup. Also available are a variety of secondary techniques that clean the syngas downstream of the reaction vessel in order to meet the stringent requirements of today’s applications.

Gas clean-up technologies are conveniently classified according to the process temperature range: hot gas cleanup (HGC), cold gas cleanup (CGC), or warm gas cleanup (WGC). There is considerable ambiguity in these definitions with no accepted guidelines to distinguish among

them. Cold gas cleanup generally describes processes that occur near ambient conditions, while hot gas cleanup has been used to describe applications at a broad range of conditions from as low as 400 °C to higher than 1300 °C.

A more rigorous definition of these classifications might be constructed based on condensation temperatures of various compounds. Cold gas cleanup technologies, which often employ water sprays, result in exit temperatures that allow water to condense. Contaminants will either absorb into the water droplets or serve as nucleation sites for water condensation. Warm gas cleanup is often assumed to occur at temperatures higher than the boiling point of water but still allow for ammonium chloride condensation. This typically implies an upper limit of temperatures around 300 °C. Hot gas cleanup occurs at higher temperatures, but still often results in condensation of several alkali compounds [46]. Few hot gas cleanup operations will extend beyond 600 °C in order to avoid expensive piping materials, but exceptions to this generalization operate at temperatures as high as 1000 °C [47]. Before reviewing these different kinds of gas cleaning, the nature of the contaminants to be removed from the gas stream is described.

### **Description of Contaminants**

Contaminants removed from syngas generally include particulate matter, condensable hydrocarbons (i.e. tars), sulfur compounds, nitrogen compounds, alkali metals (primarily potassium and sodium), and hydrogen chloride (HCl). Carbon dioxide (CO<sub>2</sub>) is also removed in various industrial applications concerned with acid gases or carbon sequestration, but it is not considered in this review.

Contaminant levels vary greatly and are heavily influenced by the feedstock impurities and the syngas generation methods (see **Table 1**). The level of cleaning that is required may also vary substantially depending on the end-use technology and/or emission standards (see Figure 2).

**Table 1:** Common feedstock impurity levels [48-51]

Note: Results may vary depending on database selection.

The above is intended only as average comparisons. Ex:

Several types of wood may be considered for slow-growth biomass, such as oak, poplar, and other hardwoods.

	Wood	Wheat Straw	Coal
<b>Impurity</b>	(moisture-free; percent by mass)		
<b>Sulfur</b>	0.01	0.2	0.1 - 5
<b>Nitrogen</b>	0.25	0.7	1.5
<b>Chlorine</b>	0.03	0.5	0.12
<b>Ash</b>	1.33	7.8	9.5
(Major Components)			
K <sub>2</sub> O	0.04	2.2	1.5
SiO <sub>2</sub>	0.08	3.4	2.3
Cl	0.001	0.5	0.1
P <sub>2</sub> O <sub>5</sub>	0.02	0.2	0.1

**Table 2:** Typical syngas applications and associated cleaning requirements

Contaminant	Application			
	IC Engine	Gas Turbine	Methanol Synthesis	FT Synthesis
<b>Particulate</b> (soot, dust, char, ash)	<50 mg m <sup>-3</sup> (PM10)	<30 mg m <sup>-3</sup> (PM5)	<0.02 mg m <sup>-3</sup>	n.d. <sup>a</sup>
<b>Tars (condensable)</b> Inhibitory Compounds (class 2-heter atoms, BTX)	<100 mg m <sup>-3</sup>		<0.1 mg m <sup>-3</sup>	<0.01 µL L <sup>-1</sup> <1 µL L <sup>-1</sup>
<b>Sulfur</b> (H <sub>2</sub> S, COS)		<20 µL L <sup>-1</sup>	<1 mg m <sup>-3</sup>	<0.01 µL L <sup>-1</sup>
<b>Nitrogen</b> (NH <sub>3</sub> , HCN)		<50 µL L <sup>-1</sup>	<0.1 mg m <sup>-3</sup>	<0.02 µL L <sup>-1</sup>
<b>Alkali</b>		<0.024 µL L <sup>-1</sup>		<0.01 µL L <sup>-1</sup>
<b>Halides (primarily HCl)</b>		1 µL L <sup>-1</sup>	<0.1 mg m <sup>-3</sup>	<0.01 µL L <sup>-1</sup>

<sup>a</sup>n.d. = not detectable; tars described in further detail in section 2.2

Note: All values are at STP unless explicitly stated otherwise.

### **Particulate matter**

Particle matter elutriated from a gasifier range in size from less than one micrometer to over 100 µm, and can vary widely in composition depending on the feedstock and process [52]. Inorganic compounds and residual solid carbon from the gasification of biomass constitutes the bulk of the particulate matter, although bed material or catalysts can also be elutriated. The inorganic content includes alkali metals (potassium and sodium); alkaline earth metals (mostly calcium); silica (SiO<sub>2</sub>); and other metals such as iron and magnesium [53, 54]. Minor constituents present in trace amounts are primarily derived from solid fossil carbon feedstocks and include arsenic, selenium, antimony, zinc, and lead [55].

Many syngas applications require greater than 99 % particulate removal (all particulate matter discussions are provided on a mass basis unless stated otherwise). Even direct combustion processes, which are relatively tolerant of particulate matter, usually demand particulate reduction to concentrations below 50 mg m<sup>-3</sup>. Common issues with particulate matter

are fouling, corrosion and erosion, which cause efficiency and safety concerns if they are not addressed. These have been studied extensively, with a heavy focus on the erosion on turbine blades, in both pressurized fluidized bed combustors (PFBC) and integrated gasification combined cycle (IGCC) power facilities [56-58].

Particulate matter is classified according to aerodynamic diameter. For instance, PM<sub>10</sub> are particles smaller than 10  $\mu\text{m}$ , and PM<sub>2.5</sub> are particles smaller than 2.5  $\mu\text{m}$  [59]. Common practice is to remove particulate of a certain size below a given level, such as removing PM<sub>5</sub> below 30  $\text{mg m}^{-3}$  for gas turbine applications as described in Table 2.

### **Tars**

Tars are composed of condensable organic compounds. They vary from primary oxygenated products to heavier deoxygenated hydrocarbons and polycyclic aromatic hydrocarbons (PAHs) [60]. Thermochemical conversion processes create hundreds or even thousands of different tar species in response to the operating parameters. Particularly important are feedstock composition and processing conditions, especially temperature, pressure, type and amount of oxidant, and feedstock residence time [61, 62]. For instance, gasification of wood shows higher tar concentrations with greater amounts of stable aromatics in comparison to coal or peat [63]. An updraft gasifier operates very differently from a downdraft gasifier and may yield 10 % to 20 % tar composition, while the latter may yield less than 1 % tar (unless otherwise stated these discussions are also provided on a mass basis) [64]. Regardless of the amount or type, tar is a universal challenge of gasification because of its potential to foul filters, lines, and engines, as well as deactivate catalysts in cleanup systems or downstream processes [61].

The complex chemical nature of tar creates difficulties in collecting, analyzing, and even defining what constitutes tar [15]. A recent intergovernmental effort has produced an explicit



definition of “tar” as “all hydrocarbons with molecular weights greater than that of benzene” [16]. In addition to this definition, a widely recognized “tar standard” was created which now provides technical specifications for sampling and analysis of tars [18, 49]. This guideline was designed to provide a consistent basis of tar measurement among researchers. Essential to measuring and controlling this contaminant is a fundamental understanding of the nature and formation of tar compounds.

The formation of tar is commonly understood to be a progression from highly oxygenated compounds of moderate molecular weight to heavy, highly reduced compounds. Longer reaction times and higher temperatures (referred to as increased reaction severity) reduce tar yields but result in more heavy hydrocarbons, which are very refractory to further reaction. These compounds are conveniently grouped into primary, secondary, and tertiary tars (see Figure 2). Primary tars are organic compounds, such as levoglucosan and furfurals, which are released from devolatilizing feedstock (i.e. coal or biomass pyrolysis) [60]. Higher temperatures and longer residence times result in secondary tars, including phenolics and olefins. These compounds are more present during fast pyrolysis reactions and are a large portion of bio-oil. Further increases in temperature and reaction time encourage the formation of tertiary tars, such as polyaromatic hydrocarbons (PAHs) [61].

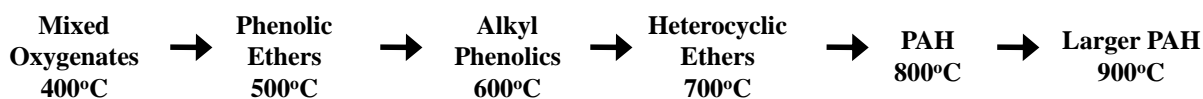


**Figure 2:** Tar evolution as suggested by Elliott [65]

Overall, the severe conditions of thermochemical processes produce an array of tarry compounds with diverse properties that can be differentiated by structure as shown in **Table 3**. Tars in classes 1, 4 and 5 can readily condense even at high temperature, making them

responsible for severe fouling and clogging in gasification-based fuel and power systems [65]. Class 2 and 3 tars, including heterocyclic aromatics and benzene/toluene/xylene (BTX) compounds, are problematic in catalytic upgrading because they compete for active sites on the catalysts. These tars are also water soluble and create issues with waste water remediation in water based cleanup processes. In general, removal or decomposition of all organic compounds is encouraged as they represent impurities in the synthesized product [66].

Although eliminating all tar is desirable, a more practical strategy is to simply remove sufficient tar for its dew point to be less than the minimum temperature experienced by the gas stream. The Energy Research Center of the Netherlands (ECN) has developed an extensive database with information on more than 50 common tar compounds, as well as calculation procedures for estimating the tar dew point [67]. An analyzer has also been developed that is capable of online tar dew point measurements, which are critical to preventing tar problems in biomass gasification systems [32, 68].

**Table 3:** Basic approximations for tar compound classification [15, 33]

Class	Description	Properties	Representative Compounds
1	GC-undetectable	Very heavy tars; cannot be detected by GC	Determined by subtracting the GC-detectable tars from the total gravimetric tar
2	Heterocyclic aromatics	Tars containing hetero atoms; highly water soluble	Pyridine, phenol, quinoline, isoquinoline, dibenzophenol cresols
3	Light aromatic (1 ring)	Usually single ring light hydrocarbons; do not pose a problem regarding condensation or solubility	Toluene, ethylbenzene, xylenes, styrene
4	Light PAH compounds (2-3 rings)	2 and 3 ring compounds; condense at low temperatures even with low concentrations	Indene, naphthalene, methylnaphthalene, biphenyl, acenaphthalene, fluorene, phenanthrene, anthracene
5	Heavy PAH compounds (4-7 rings)	Larger than 3 ring; condensation occurs at high temperatures even with low concentrations	Fluoranthene, pyrene, chrysene, perylene, coronene

### Sulfur

Sulfur contaminants occur mostly as hydrogen sulfide ( $\text{H}_2\text{S}$ ) with lesser amounts of carbonyl sulfide ( $\text{COS}$ ). Sulfur contaminants like  $\text{H}_2\text{S}$  may range in concentration from  $0.1 \text{ mL L}^{-1}$  to more than  $30 \text{ mL L}^{-1}$  depending on the feedstock [69]. Biomass has significantly less sulfur than coal. It usually contains only  $0.1 \text{ g kg}^{-1}$  to  $0.5 \text{ g kg}^{-1}$  sulfur compared to as much as  $50 \text{ g kg}^{-1}$  sulfur compounds for some coal-derived syngas [60]. Some forms of biomass, including a few grasses and black liquor (a byproduct of the pulp and paper industry), can still have sulfur contents exceeding  $1 \text{ g kg}^{-1}$  [61, 70, 71].

Sulfur compounds corrode metal surfaces [72]. If syngas is burned, sulfur contaminants are oxidized to sulfur dioxide ( $\text{SO}_2$ ), a regulated pollutant. Even small amounts of sulfur can eventually poison catalysts used to clean or upgrade syngas [73]. Sulfur removal to parts per

billion levels is often required in order to avoid these kinds of detrimental effects (as noted in Table 2).

More than 30 gas cleanup technologies have been developed for removing sulfur compounds and other so-called acid gases (including CO<sub>2</sub>) [72]. These include both dry and liquid-based processes that cover a temperature range from sub-zero to several hundred degrees Celsius. Physical and chemical removal processes exist, many of which can yield elemental sulfur or sulfuric acid as a useful byproduct. Recent hot gas removal research focuses on the use of dry sorbents. These various approaches are summarized in Figure 3 [47, 72, 74, 75]. Further details are found in the sections on hot gas and cold gas cleaning.

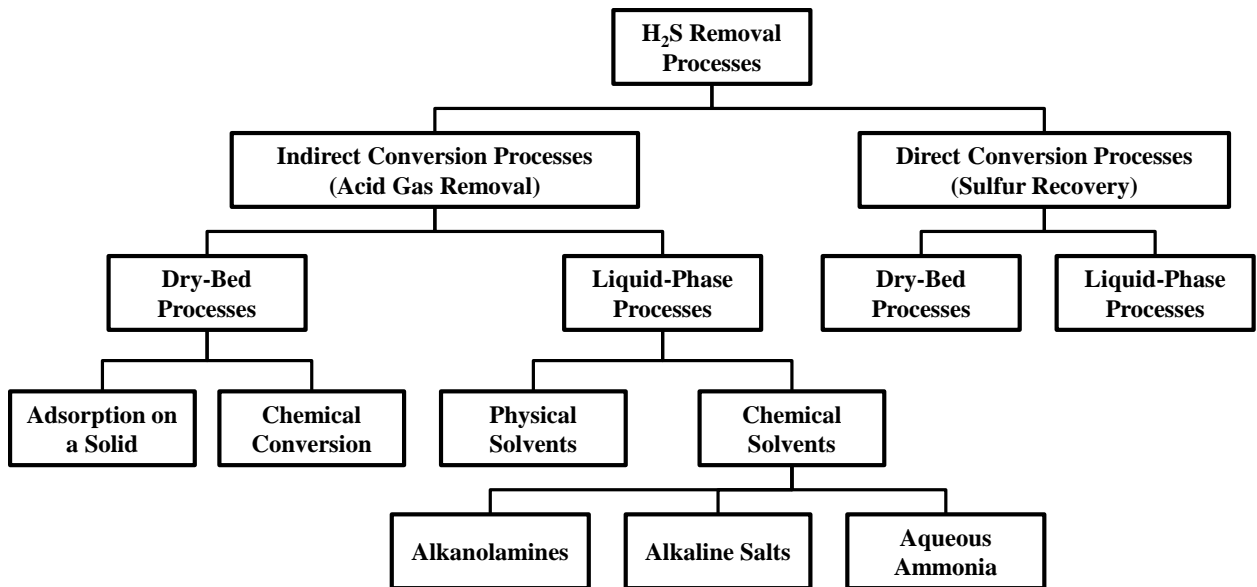


**Figure 3:** Hydrogen sulfide removal processes (adapted from Lovell) [72]

### **Nitrogen Compounds (NH<sub>3</sub>, HCN)**

Most nitrogen (N) contaminants in syngas occur as ammonia (NH<sub>3</sub>) with smaller amounts of hydrogen cyanide (HCN). The pyrolysis stage of gasification and combustion releases nitrogen from protein structures or heterocyclic aromatic compounds in the feedstock [76]. The amount of NH<sub>3</sub> and HCN released is heavily dependent on intrinsic properties (N content, functionalities) and physical properties (particle size) as well as process conditions. Ammonia is typically the dominant form of nitrogen contaminants by at least an order of magnitude. It can be formed directly from biomass in primary reactions or from HCN in secondary gas phase reactions [77-79]. As the temperature increases from feedstock conversion, secondary reactions increase HCN concentration as well as NH<sub>3</sub>. However increased availability of H<sub>2</sub> and residence time will convert the HCN to NH<sub>3</sub>. Given sufficient temperature and time, N<sub>2</sub> is the predominant equilibrium product, but this is rarely attained in practice [78, 79].

The nitrogen content of many biomass feedstocks can produce ammonia concentrations of several weight percent. However, up to two-thirds of this ammonia decomposes to molecular nitrogen (N<sub>2</sub>) at typical gasification temperatures. Thus, the concentration of ammonia in syngas is usually no more than several hundred to a few thousand parts per million. Even these low levels can be detrimental in some applications. Gas turbines usually demand ammonia concentrations less than 0.05 mL L<sup>-1</sup> to control nitrogen oxide emissions, while less than 0.05 μL L<sup>-1</sup> may still poison some catalysts used to upgrade syngas [77]. Acid gas removal units used for sulfur recovery can also experience problems unless nitrogen is substantially reduced [72].

### **Alkali Compounds**

Many gasification feedstocks naturally contain alkali and alkaline earth metals. Concentrations of alkali in biomass can vary substantially but are typically much greater than in coal.[80] Woody biomass tends to contain more alkaline earth metals, while herbaceous biomass

contains higher levels of alkali metals [81]. The alkali metals are primarily potassium and to a lesser extent sodium, and are more problematic in syngas applications than alkaline earth metals due to their higher reactivity.

Alkali in feedstock is both reactive and volatile. Some reactions of alkali with other ash components of biomass yield non-volatile compounds that remain as bottom ash in the gasifier. However, some alkali compounds melt or even vaporize above 600° C and can leave the reactor as aerosols and vapors, respectively [82, 83]. Alkali compounds transported out of the reactor, usually in the form of chlorides, hydroxides, and sulfates, can cause substantial fouling and corrosion in downstream processes [83, 84].

Biomass is not the only source of alkali metal contaminants in gasification-based systems. Some catalysts used to remove syngas contaminants or alter the syngas composition incorporate alkali-based catalysts and transition metal promoters, such as cobalt, molybdenum, rubidium, cesium, and lithium. Along with potassium and sodium from the biomass, these metals vaporize in high temperature sections of the system and condense in cooler sections where they can cause corrosion or ash fouling [85-87].

Removing alkali metal contaminants is important to avoid sintering and slagging of ash in boilers and hot corrosion in gasification power systems [84]. Catalysts are also extremely sensitive to alkali contents and can be easily poisoned by the alkali levels found in biomass. Alkali must sometimes be reduced from as high as a few grams per kilogram to as little as a few micrograms per kilogram [88].

### **Chlorine**

Chlorides are the predominant halide in syngas, usually in the form of hydrochloric acid

(HCl). Chlorine in biomass occurs as alkali metal salts, which readily vaporize in the high temperature environment of combustors, pyrolyzers, or gasifiers and react with water vapor to form HCl [58, 89-91]. Raw syngas may contain up to several milliliters of chloride for every liter of syngas. Despite its relatively low concentration compared to other contaminants, it can create serious materials problems. Chlorine levels as low as  $20 \mu\text{L L}^{-1}$  will cause performance loss in nickel anodes of molten carbonate and solid oxide fuel cells [92]. Substantial hot corrosion of gas turbine blades can occur with concentrations of chlorine and alkali as low as  $0.024 \mu\text{L L}^{-1}$  [89, 90]. Reactions can also occur between HCl and other contaminant species in the gas phase, which creates more compounds such as ammonium chloride ( $\text{NH}_4\text{Cl}$ ) and sodium chloride ( $\text{NaCl}$ ). These compounds can cause fouling and create deposits when they condense in cooler downstream piping and equipment. Chlorides have also caused poisoning of catalysts used for ammonia, methanol and other chemical syntheses.

### **Hot Gas Cleanup (HGC)**

Hot gas cleanup has historically focused on removal of particulate matter and tar, with the goal of minimizing maintenance of syngas combustion equipment. Beginning with the 1970 Clean Air Act, more stringent environmental standards have increased the need to remove contaminants that would otherwise be emitted to the environment as pollutants.[93] Increasing interest in synfuels production also provides impetus to improve the quality of the syngas stream. With temperatures above  $200^\circ\text{C}$ , many syngas applications benefit thermodynamically by cleaning the gas at elevated temperatures. In general, benefits of hot gas cleanup may include reduced waste streams, increased efficiencies or improved syngas conversions with fewer byproducts.

### Particulate Matter

High temperature particulate cleanup is one of the most important improvements to commercial syngas applications in the past 30 years [91]. Many techniques have been applied to hot gas particulate cleanup, most of which are based upon one or more of the following physical principles: inertial separation, barrier filtration, and electrostatic interaction.

**Table 4:** Summary of hot gas particulate cleanup technology (adapted from Seville) [58]

Device	Collection Efficiency (%)	Pressure Drop (kPa)	Flow Capacity ( $\text{m}^3 \text{s}^{-1} \text{m}^{-2}$ )	Energy Required
<b>Cyclones:</b>				
Conventional	Low (>90)	Moderate to High (7.5-27.5)	Very High	Low
Enhanced	(>90-95)	Moderate to High	Very High	Moderate to High
<b>Granular Filters:</b>				
Fixed		Moderate (6-10)	High (0.15-0.2)	High
Moving <sup>a</sup>		Moderate	High	Moderate to High
Electrostatic Precipitators	Good (>99)	Very Low (0.3-0.6)	Low to Moderate (0.01-0.03)	Moderate to High
Thermal Plasma <sup>a</sup>		Low	Low to Moderate	High
Turbulent Flow Precipitator		Low	High	Low to Moderate
Ceramic Bags		Low (1-3.5)	Low to Moderate (0.01-0.03)	Low
<b>Rigid Barrier Filters:</b>				
Ceramic Candle		Moderate to High (5-25)	Moderate to High (0.03-0.07)	Moderate
Cross Flow	Excellent (>99.5)	Low to Moderate (2.5-7.5)	Moderate to High (0.03-0.07)	Low to Moderate
Ceramic Tube		Moderate (8-12.5)	Moderate to High (0.03-0.05)	Moderate
Metallic		Moderate to High	Moderate to High	Moderate

<sup>a</sup>Some variations of these technologies exist that are capable of excellent removal rates.



### **Inertial Separation**

Inertial separation devices operate using mass and acceleration principles for separation of heavier solids from lighter gases. The most significant device in this category is the cyclone, but alternative options do exist such as impact separators and dust agglomerators [55, 94]. Operating sometimes in excess of 1000 °C, cyclones are one of the oldest and most commonly employed devices for solids separation. They utilize centripetal acceleration to reduce the long times otherwise required for small particles to settle by gravity. As shown in Figure 4, the gas stream enters a ‘double vortex’ that first forces particulate outward and downward in an outer vortex. This outer swirling motion separates particulate matter from the vapors by inertial forces. The gas stream is then redirected into an inner and upward moving vortex before exiting the device through a ‘vortex finder’.

Several approaches to cyclone design exist, which are based on the characteristics of the particle and the gas stream [52, 95-97]. Typically, a ‘cut point’ is established where a certain size particle obtains a balance between centrifugal and drag forces. The particle size at this point is the ‘cut size’ (typically denominated as  $x_{50}$  or  $d_{50}$ ) and has a 50 % removal efficiency [52]. For instance, a cyclone designed with an  $x_{50}$  of 10  $\mu\text{m}$  indicates that a 10  $\mu\text{m}$  particle has a 50% chance of being removed. Larger particles are removed more efficiently given the greater centrifugal force compared to the drag force, and vice-versa for smaller particles.

Although cyclones are a mature technology, process advancements are still occurring. One new design operates as a reverse flow gas cyclone using partial recirculation. It has shown separation efficiency that is superior to the classical Stairmand high efficiency (HE) designs [95]. Particulate removal efficiency in pilot and industrial scales has consistently surpassed 99.6 %, which is comparable to more demanding lower temperature devices such as venturi devices and

pulse jet bag filters [98].

The simple design and lack of moving parts in cyclones enable high temperature operation that is typically limited only by mechanical strength of the construction materials. They are often operated hot to prevent condensation of water, tar, and other contaminants that might otherwise foul or corrode the cyclone. With their robust nature and efficient removal of particulate matter larger than  $5\ \mu\text{m}$ , cyclones are typically the first cleanup device applied to a gas stream. Many processes require more stringent particulate matter removal down to sizes below  $1\ \mu\text{m}$ . While up to 90 % of particulate matter as small as  $0.5\ \mu\text{m}$  may also be removed with cyclones, this can require multiple stages which is not typically economical for large volume gas streams [52].

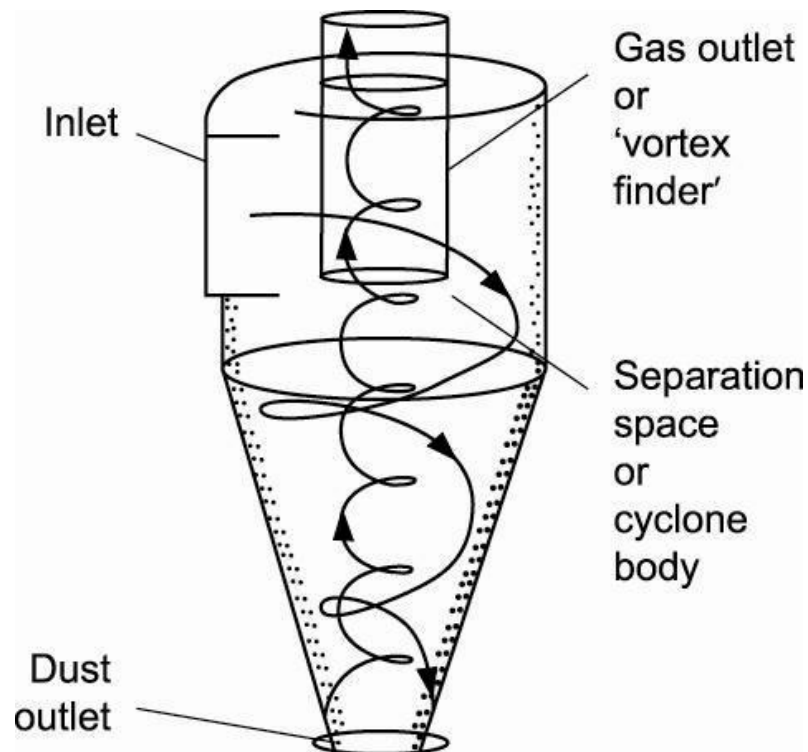


**Figure 4:** Cyclone [52]

### **Barrier Filtration**

Filters are one of the most common methods for removing particulate matter. Barrier filtration occurs when a gas stream passes around fibers or granules or through a porous monolithic solid. Particulate matter is removed during filtration by a combination of four different mechanisms as shown in Figure 5. Diffusion, inertial impaction, and gravitational settling will collect particles due to random collisions with the filter media as they deviate from the gas streamlines [58]. Particles that follow the gas streamline may also be removed by direct interception if the streamline passes close enough to the filter media (i.e. within a particle's radius). Porous media also removes particulate matter by restricting particles larger than a specified pore size. As particulate matter builds up on a surface, the efficiency is increased by the formation of a filter cake, which hinders successively smaller particles from passing through. Once a maximum desired pressure drop is attained, the filter cake is removed and the process repeated. A more detailed description of particulate collection is available in the literature [58, 99].

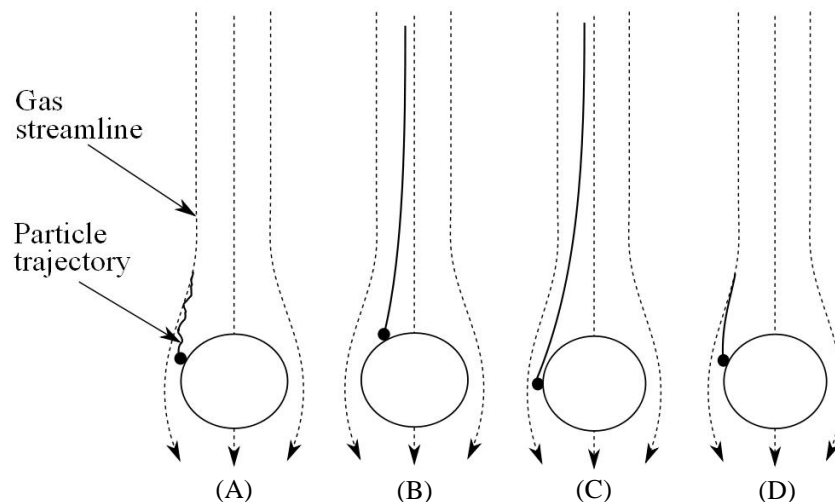


**Figure 5:** Filtration mechanisms for removal of particulate matter: (a) diffusion, (b) inertial impaction, (c) direct interception, (d) gravitational settling. (Adapted from [58])

Several types of filtration devices exist, including: fabric filters, rigid filters, and both fixed and moving bed granular filters. Filtration has also been combined with other cleanup processes, such as incorporating tar reduction catalysts into filter elements. Fabric filters have been employed since the early 1960's for gas cleanup and can effectively remove particulate matter larger than  $1\ \mu\text{m}$  to concentrations less than  $1\ \mu\text{g m}^{-3}$  [58]. However, the typical construction materials for these types of filters limit their operation temperature to  $250^\circ\text{C}$ , which classifies them as warm gas cleanup [58, 100].

Rigid filters are usually constructed of either ceramic or metallic materials. They have advanced in recent years to the extent that they can remove 99.99 % of particulate matter smaller than  $100\ \mu\text{m}$  while operating at temperatures exceeding  $400^\circ\text{C}$  [101]. Candle filters are a common example of a barrier filter for high temperature gas cleaning. These are hollow tubes primarily composed of porous ceramic, as illustrated in Figure 6. Dirty gas passes through the outside of a long, closed-end tube (or cone), depositing the particles on the surface before exiting through the top of the tube. The resulting accumulation of particulate matter, known as filter cake, is periodically removed with a reversed pulse of gas, typically nitrogen. Several candle elements are placed in parallel to form an array so that several filters are always operating while others are being cleaned.

Candle filter are commonly constructed of clay-bonded silicon carbide (SiC) as well as more exotic materials such as monolithic and composite ceramics [94, 102]. The material's porosity is influenced by using either granules or fibers of alumina and aluminosilicates during construction [58]. Metals may also be incorporated into the ceramics to reduce damage in hostile environments and provide catalytic activity [103]. Layered constructions also exist that use a

base structure of coarse (usually 100  $\mu\text{m}$  to 125  $\mu\text{m}$ ) granular media, such as SiC, accompanied by a thin sprayed or painted layer of fine media (usually 8  $\mu\text{m}$  to 10  $\mu\text{m}$ ) [58]. The fine layer inhibits excessive and sometimes irreversible dust penetration into the candle element.

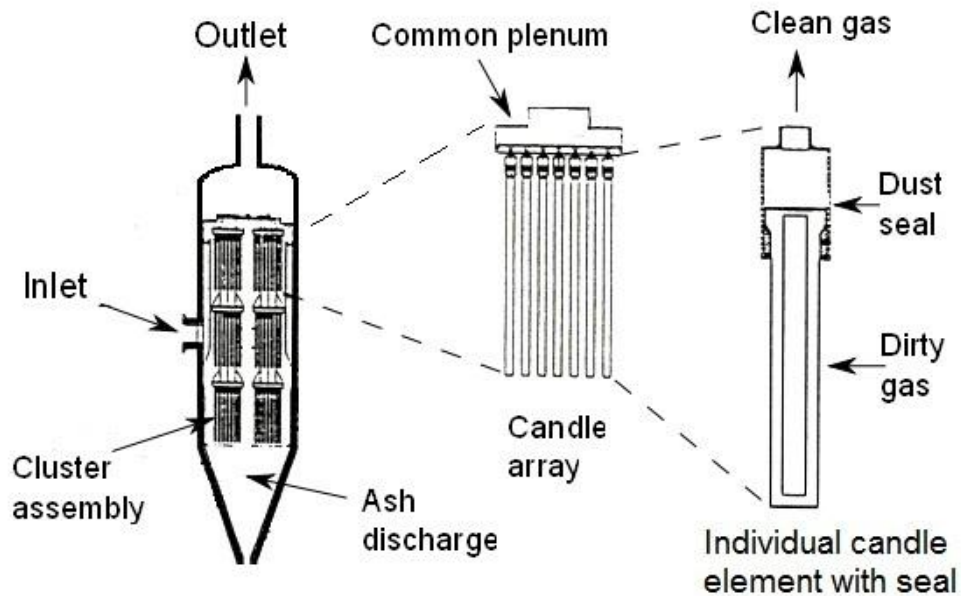


**Figure 6:** Candle filter element (Adapted from [58])

Variations of the candle filter are the cross-flow and tube filters produced by manufacturers such as Westinghouse and Asahi Glass Company (AGC). A cross-flow filter is constructed as a monolithic block with channels created by layered filter material (see Figure 7). This design allows greater filter area in a specified volume. Unlike more conventional designs, the reverse pulse used to dislodge the filter cake must also move the cake to an outlet, which may increase operational complexity or stress on the filter element.

The AGC tube filter can reduce this filter stress by altering the orientation of the filter cake. The filter is constructed with both ends of the 'candle' open, thus forming a tube rather than a candle. The dirty gas flow enters the interior of the candle where it forms the filter cake, instead

of forming it on the exterior surface as in the conventional candle filter. The reverse pulse used to dislodge the cake will then place the candle in compression (rather than tension) by pulsing the surrounding chamber [58].

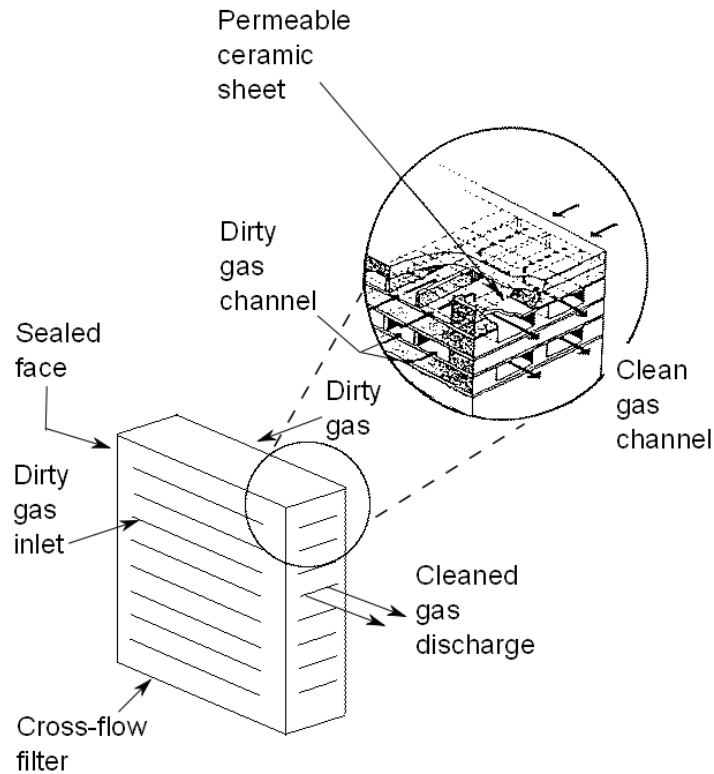


**Figure 7:** Cross-flow filter (Adapted from [58])

Stress is only one of several factors affecting filter life and overall down-time, which are critical issues for commercial deployment. Reactions with gas phase alkali can also reduce filter life by attacking aluminosilicate binders and non-oxide based ceramics [58]. The fundamental relationship between porosity, mechanical strength, and thermal conductivity naturally decreases the lifetime of the porous material as temperatures are increased: smaller pores require smaller fibers that are not as durable [101]. Finally, the reverse pressure pulses most often used to remove the filter cake have a high pressure drop and are usually done with gas that is substantially cooler than the dirty process gas. This can induce significant thermal stress and

shock.

Stress and shock are the primary contributors to high down times associated with commercial hot gas cleanup devices for particulate matter. While some commercial technologies have achieved 99 % particulate matter removal at temperatures above 400 °C, continuous operation before failure rarely exceeds 2700 h [101]. This is less than desired for commercial deployment. Online times approaching 8000 h at temperatures between 650 °C and 850 °C are possible with the Asahi Glass Ceramic Tube Filter (CTF), although insufficient information is available to fully assess the performance of this filter [101].

Increases in filter lifetime without sacrificing efficiency are possible with the pulse-less candle system developed by the Centre for Low Emission Technologies (cLET) in Australia [102]. This system maintains a filter cake of constant thickness on the filter element by flowing a jet of gas perpendicular to the filter element surface. Sustaining the filter cake rather than periodically removing it enhances efficiency and reduces corrosion/erosion on the surface of the filter. This design also simultaneously reduces pressure drops and the possible temperature shocks associated with conventional pulsed cleaning. This design uses air or exhaust for the gas jet since it was developed for cleaning flue gases from coal combustion. An oxygen-free gas would be mandated for use in a syngas environment, which may add complexity and cost to the system for compressing recycle syngas or using inert gases such as nitrogen [102].

The fragile nature of ceramic at higher temperatures led to the development of sintered metal barrier filters, which have material strengths well suited to higher temperatures. Operational temperatures can approach 1000 °C depending on the alloys used and the pore sizes that are created during the sintering process. Particulate matter concentrations are usually reduced below

10 mg m<sup>-3</sup> with filtration efficiencies closely approaching 100 % [94, 104]. Metallic filters are also relatively simple to construct. Metallic powders, often iron aluminide, are heated within a mold to a temperature where the material begins to fuse together [105]. The resulting structure is resistant to thermal shock that often occurs during cleaning, and is less susceptible to corrosive syngas components, such as alkali, that can degrade other cleaning elements [58, 94].

Commonly employed powder construction techniques result in filters with fairly substantial pressure drops. One approach to overcoming this problem may be to construct the filter with metal fibers. Fibers are inherently more robust than powders, and can provide similar strength with less flow resistance [105]. To test this theory, the Power Systems Development Facility (PSDF) created a fiber-based metal sintered filter for comparison with a standard Pall Fuse filter constructed from powders. The Pall filter showed 34 % higher flow resistance compared with the PSDF filter. The PSDF filter was however much less reliable and plugged multiple times, whereas the conventional powdered filter reduced particulate below 0.1 mg kg<sup>-1</sup> throughout a 5000 h period.

Several fundamental limitations of the metallic and ceramic filter elements can be avoided with fixed or moving granular bed filters. Granular material is placed in a vessel through which particulate-laden gas is passed. Materials can be as unusual as low-silica lapilli (volcanic rock) or as common as limestone or sand. A spherical form of sintered bauxite (alumina-oxide) with particle diameters typically on the order of several hundred micrometers is a common example [94, 106, 107]. During fixed-bed operation, pores in the granular material become filled when particulate matter contacts and adheres to the surfaces. Dust can also agglomerate at the entrance to the filter and form a filter cake similar to those created on candle filters. This further increases filtration efficiency, but adds pressure drop. Panel bed filters are a common example of this



approach. Filtration efficiencies of this filter are similar to baghouse (fabric) filters, but with much higher operating temperatures ( $550^{\circ}\text{C}$  to  $600^{\circ}\text{C}$ ) and superficial velocities [106]. Once a critical pressure drop is reached, the filter beds are cleaned, usually by reverse pulses, or are replaced. The more robust nature of the granules and filter construction enable the filters to withstand higher temperatures and stresses with less down-time than conventional candle filters.

The moving bed filter attempts to eliminate the periodic operation of fixed bed filters. Slowly moving granular material flows through the filter at a rate that still allows for high efficiency filtration. This configuration balances the continuous buildup of particulate matter in the bed with a continual replacement of clean bed media (see Figure 8). The result is a constant and acceptable pressure drop.

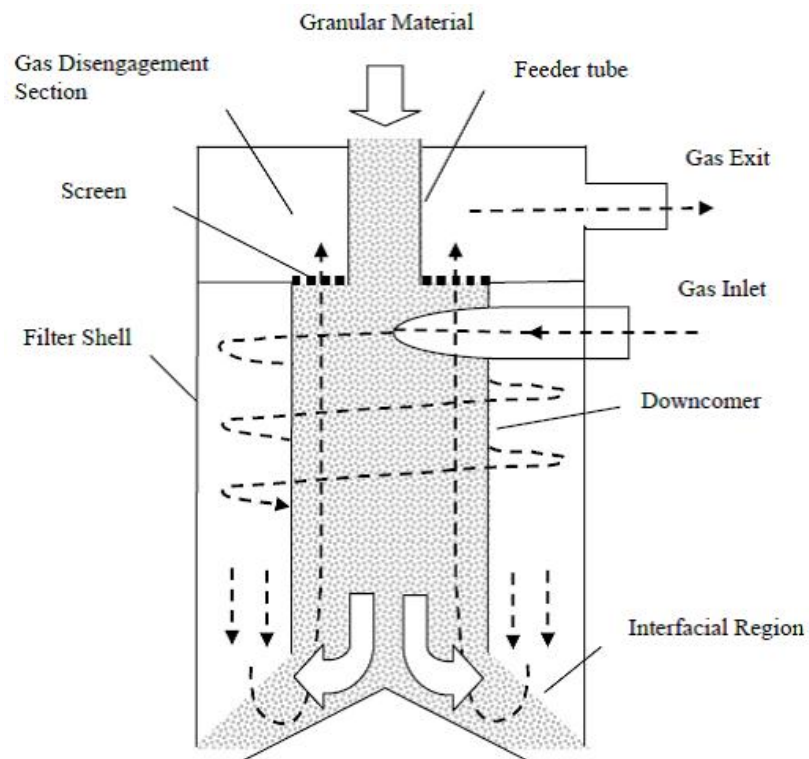


**Figure 8:** Operation of moving bed filter[108]

Several factors affect the efficiency of a moving bed filter. The flow rate of the granular

media and the size of the granules will affect the pore sizes and surface area available for particle impaction. They also affect the pressure drop by altering the thickness of the dust cake that forms at the interfacial region, where a majority of the cleaning occurs [108, 109]. Other factors affecting the efficiency are the particulate shapes and loadings in the gas, as well as maintaining the filter's gas velocity below the minimum fluidization velocity of the granules [110].

Multiple variations of the moving bed granular filter have been developed. Various granular media have been employed, including alumina and mullite, and different design modifications have been used, such as enhancing removal with electrostatic forces [111]. At temperatures up to 840 °C, removal efficiencies have been attained that exceed 99 % for 4 µm particles and 93 % for 0.3 µm particles [111]. Tests using a stand-leg moving granular-bed filter system (SMGBF) at up to 870 °C have shown efficiency increases above 99.9 % (see references for details) [112]. Moving granular-bed filters show promise for high temperature and robust operation with minimal maintenance. Completely continuous operation has been shown feasible on a MBGF at Iowa State under the condition that a certain granular residence time is not exceeded [113]. Removal of gaseous contaminants may also be possible if adsorbents or catalysts are incorporated into the granular material.

Catalytic materials can also be incorporated into other filter constructions to enable simultaneous removal of particulate matter and tars. For example, a catalytic filter was created by adding active nickel (Ni) and magnesium oxide (MgO) components to the pores of a common  $\alpha$ -alumina ( $\text{Al}_2\text{O}_3$ ) candle filter material [114]. In order to include the Ni/MgO catalyst, additional layers of  $\text{ZrO}_2$ ,  $\text{Al}_2\text{O}_3$ , or a  $\text{ZrO}_2$ - $\text{Al}_2\text{O}_3$  mixture were first added to the base  $\text{Al}_2\text{O}_3$  filter material to increase the available surface area. Activity for tar reduction and stabilization

of the materials was enhanced, resulting in a potentially superior Ni-based catalytic filter. At the testing conditions of 850 °C, little or no loss in activity was observed over an extended period of 170 h. Over 99 % removal of benzene and naphthalene was achieved even with sulfur concentrations of 100 mg kg<sup>-1</sup>. This was attributed to the MgO component, which has previously been shown to increase the sulfur tolerance of nickel catalysts. Increasing the surface area may provide a simple and effective improvement to this catalytic filter, which could be possible by using a better layering approach than the urea method that was used in this study.

In a similar application, a silicon carbide candle filter was impregnated with an MgO-Al<sub>2</sub>O<sub>3</sub> supported Ni catalyst and placed in the freeboard of a biomass gasifier for in-situ reduction of tar [115]. Compared against a non-catalytic filter, a 58 % conversion of tar and a 28 % conversion of methane yielded improved hydrogen content and a 15 % increase in overall gas yield.

Incorporating these catalytic filters may simplify the production of clean syngas for many applications, as well as provide substantial cost savings by eliminating some secondary cleanup elements. However, these hot gas filtration combinations only show ‘proof of concept’. Major remaining challenges include: the catalytic filter optimization, removing solids from the filter material at high temperatures in a syngas environment, and integrating the filters into commercial gasification designs (i.e. primary and/or secondary applications).

### **Electrostatic Separations**

Electrical properties can also be exploited to remove particles from gas flows. Essentially, particles become charged by a strong electric field and are removed due to their difference in dielectric properties compared with the gas molecules (discussed in detail below) [116].

Electrostatic forces acting on fine particulate matter (less than 30 μm) can be more than 100 times stronger than the force of gravity, making electrostatic precipitators (ESPs) very effective

in removing particulate matter from gas streams [116].

ESPs are widely used for removing fly ash in coal-fired power plants at temperatures up to 200 °C, and have also been applied on occasion at temperatures above 400 °C [58, 117].

Synthetic fuel plants may also apply higher temperature ESPs between 300 °C and 450 °C for oil vapor separation [118]. At higher temperatures, ESPs become less effective although some research projects have been conducted at temperatures as high as 1000 °C [58].

Two configurations are commonly employed in the design of ESPs: a tube-type precipitator and a parallel-plate precipitator. Although simple in concept, performance depends on several factors including geometry of the device, applied voltage, electrical resistivity of gas and particles, and size and shape of particles. A tube-type ESP, illustrated in Figure 9, utilizes electrified wires placed within an insulated vessel through which hot gas passes. Most commonly, a negative direct current is passed through a centrally located discharge electrode, which is surrounded by the grounded collection electrode(s). Gas molecules passing close to the discharge electrode will lose electrons and become ionized, resulting in an electrical corona discharge [119]. Electrons in close proximity to the discharge electrode, where the electric field intensity is highest, will ionize additional molecules in the gas stream in the presence of the strong electric field. Electrons and negative ions migrating from the discharge electrode to the collection electrode collide with particles suspended in the gas stream, thereby charging the particles. Charge builds on particles until they become saturated, which is primarily determined by particle diameter, applied electric field, ion density, exposure time, ion mobility, and relative (static) permittivity of the particles [117]. The charged particles experience a force due to the electrical field that accelerates them to a velocity in the direction of the collection electrode,

known as the drift velocity. This velocity may be many times that of the velocity due to the drag force on a particle. The result is rapid particle movement toward the collection electrode relative to the bulk flow velocity of the gas [117]. Upon migrating to the oppositely charged electrode, the accumulating particles collecting on the electrode are periodically removed by mechanical rapping. Alternative ESP configurations and specific ESP design based on current-densities and other operating principles are discussed in greater detail in several publications [58, 116, 117].

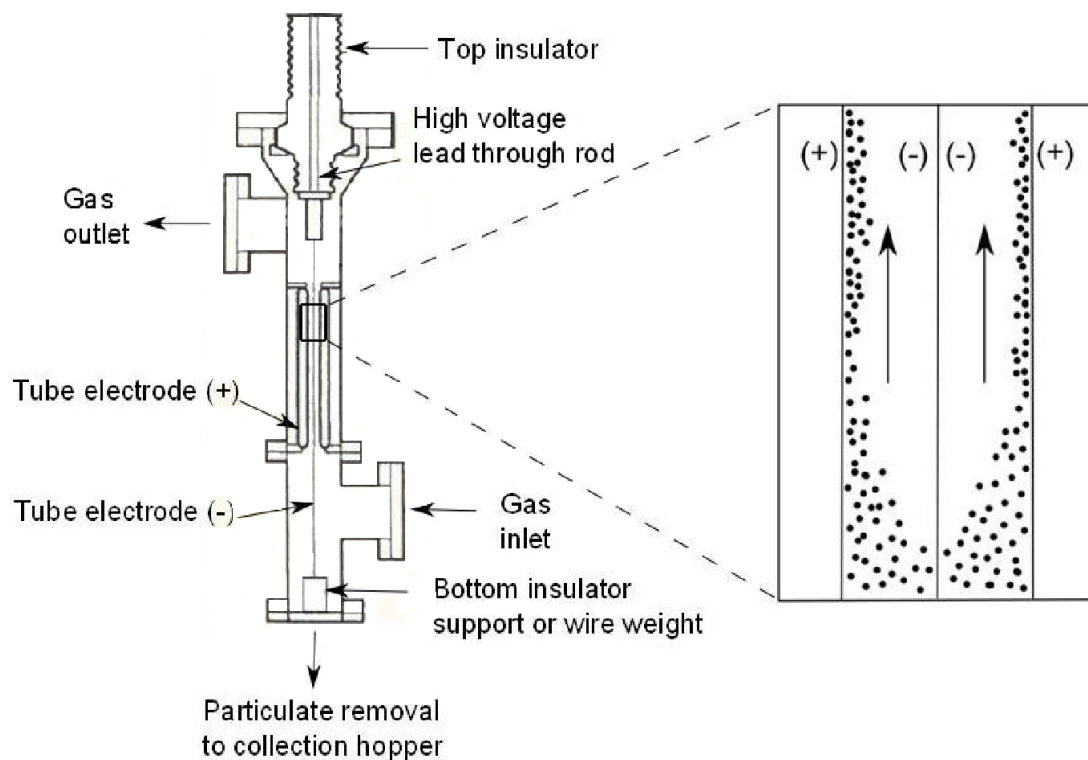


**Figure 9:** A tube-type ESP concept for high temperatures and pressures (adapted from [58])

The operating voltage range of ESPs extends from the onset of gas molecule ionization (i.e. corona onset voltage) to the point where electrical breakdown (sparkover) occurs in the gas [58]. Sparkover occurs as either a spark or back-corona [119]. Imperfections in the metal surfaces can concentrate the electric field strength, which may create a spark. Alternatively, a layer of high resistivity particulate matter may cause positive ions to emanate toward the negative discharge electrode and cause a back-corona. In either case, particle charging ceases and so does

collection; hence the need to maintain the voltage within the operating range [120].

The limited use of ESPs at very high temperatures is largely due to the temperature effects on basic properties affecting ESP operation, such as density, viscosity, and resistivity. Increased temperature lowers the gas density, decreasing the concentration of gas molecules within the ESP. The increased spacing between gas molecules in a lower density gas stream reduces the frequency of impacts responsible for slowing molecules in higher density gas streams. Thus, the mean free path of the gas molecules is longer and the mobility of the gas ions increases [58]. These changes permit more time for accelerating gas molecules to ionization velocity, which lowers the required strength of the electrical field. In other words, a lower voltage is required at increased temperatures for initiating a corona and starting particle collection. Although this is beneficial, the amount of voltage that can be applied before electrical breakdown occurs is also reduced as gas density decreases. This reduction in critical voltage unfortunately occurs at a faster rate than the reduction in initiation voltage. The end result is a reduced range of voltages at which the ESP can operate. A smaller operational region with reduced current density increases the frequency of sparking or back-coronas, and reduces efficiency [58, 117].

Gas viscosity also increases with temperature, according to the square root of the temperature ratio  $(T+\Delta T)/T$  [58]. Increasing viscosity increases the drag force on the particle, while the electrostatic force remains unaffected. This results in a lower drift velocity for the particle relative to the increased drag velocity. Thus, increasing gas temperatures reduce collection efficiency because gas flow carries particles out of the ESP before they can drift to the collection electrode.

ESP operation is also heavily affected by the particle resistivity. Particles with excessively

high or low resistivity are not readily removed due to charge dissipation effects upon contact with the collector element. Low resistivity particles ( $<100 \Omega \text{ m}$ , such as carbon black) dissipate charge too quickly upon reaching the collection electrode, which causes them to acquire the same charge as that electrode and become repelled back into the gas stream [58]. High resistivity particles ( $> 10 \text{ G}\Omega \text{ m}$ , such as elemental sulfur) dissipate charge too slowly and can result in excessive charge buildup that has been implicated in inefficient and dangerous ‘back-corona’ phenomenon [116, 117]. Particles with very high resistivity (greater than  $100 \text{ G}\Omega \text{ m}$ ) may also have an effective migration velocity less than  $2 \text{ cm s}^{-1}$ , which may be too slow to be captured by the collection electrode [116]. Increasing temperature first increases resistivity due to moisture evaporating from the surface of the particle and reducing its surface conductivity. Additional increases in temperature beyond about  $150^\circ \text{ C}$  reduces resistivity by increasing the conductivity through the particle’s core [116, 117]. Reducing resistivity can provide substantial efficiency improvements. For instance, industrial precipitator efficiency can increase from 81 % to 98 % with a decrease in dust resistivity from  $5 \text{ G}\Omega \text{ m}$  to  $0.1 \text{ G}\Omega \text{ m}$  [117]. However, excessive reductions in particle resistivity will increase the charge dissipation rate and can lead to particle re-entrainment [58].

Higher pressures are one method for counteracting temperature-induced complications. Higher pressures increase the gas density and allow higher voltages to be applied before electrical breakdown occurs [58]. While increases in pressure also increase the density and raise the onset voltage, the higher temperatures minimize this effect. The result is a wider range of voltages at which the ESP can operate. This combination of high temperatures and pressures makes ESP operation potentially more efficient than at ambient conditions, as has been empirically proven [58]. However, there will also be an additional cost of compression in

atmospheric or low pressure gasification processes.

Despite the potential benefits, the combination of high temperature and high pressures introduces additional challenges. The mechanical strength of materials decreases with temperature while the stress on these materials increases with pressure. The resistivity of insulating materials used in the charged atmosphere is also reduced as temperatures increase. The need to empty pressurized hoppers of collected particulate matter also leads to system complexity.

Closely related to ESP operation are several non-thermal plasma techniques developed for gas cleaning applications including pulsed-corona, dielectric barrier discharges, DC corona discharges, RF plasma, and microwave plasma [121]. These systems develop high energy pulses in the gas stream that release high-energy electrons, which then generate other electrons and ions similar to ESP operation [122, 123]. However, these more powerful devices can break apart larger molecules as well as collect particles, which is useful in eliminating tar compounds, as discussed in section 0.

#### **Additional particulate removal technologies**

Another particle collection device, the turbulent flow precipitator (TFP), operates by separating the gas stream into two sections: an unobstructed turbulent flow area adjacent to an essentially stagnant flow area. The turbulent flow area directs gas flow through the device while the adjacent section induces settling. A system of parallel plates, honeycomb structures, or similar structures is used in the settling section to halt axial flow. Turbulent eddies penetrate this area perpendicular to flow and subsequently dissipate, thus depositing their entrained particles (see Figure 10) [124].



TFPs achieve separation comparable to other techniques and have some important advantages. They operate at high temperatures and with no moving parts like cyclones, but they operate over wider particle and velocity ranges with high separation efficiency for particles as small as  $0.5\ \mu\text{m}$ . They also have very small pressure drops and are less likely to plug than other filter types of similar efficiencies. They also typically do not present the operational complications, power constraints, and overall expense of electrostatic devices. TFP designs have achieved removal efficiencies as high as 99.8 % for particles between  $2\ \mu\text{m}$  and  $3\ \mu\text{m}$ , and 78.5 % for particles as small as  $0.43\ \mu\text{m}$  [125].

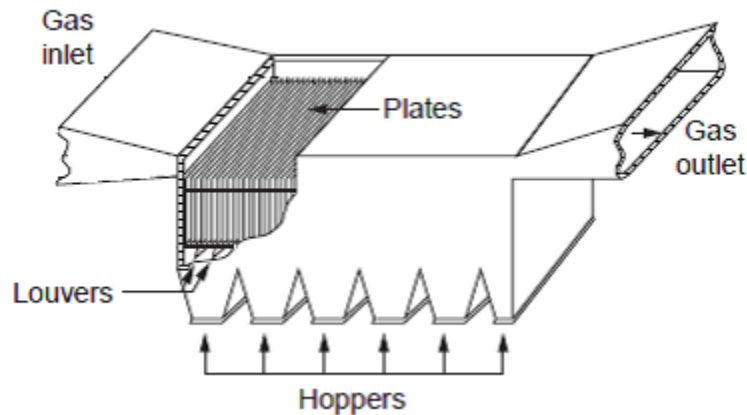


**Figure 10:** Plate type turbulent flow precipitator TFP [125]

### Tars

There are four basic approaches to removing tar from producer gas: thermal cracking, catalytic cracking, non-thermal plasmas and physical separation. Chemical equilibrium predicts the absence of tarry compounds under conditions of gasification. In practice however, there is always some tar (condensable organic compounds) in the product gas, which decreases as gasification temperature increases [91]. However, even at relatively modest gasification temperatures, tar is not expected if chemical equilibrium was attained. Thermal cracking, catalytic cracking, and non-thermal plasmas attempt to more closely approach chemical

equilibrium by increasing reaction rates of tar decomposition. Physical separation of tars, on the other hand, cools the product gas to condense vapors as liquids, which are then removed by purely physical means.

These methods are applied in both primary (in-situ) and secondary (post-gasifier) environments for tar removal, depending on the type of gasifier and the intended application of the product gas. Primary cleanup measures are limited to thermal and catalytic cracking, and use approaches such as high temperatures, oxygen feed in lieu of air, or different bed materials. Gasifiers using these methods may achieve tar concentrations as low as  $50 \text{ mg m}^{-3}$ , which is sufficient for robust applications like direct combustion [126, 127]. Secondary cleanup downstream of the gasifier employ one of four basic methods. These methods are capable of removing tar to undetectable levels, which is necessary for more stringent application such as fuel cells or catalytic conversion processes.

The end-use of the gas stream is also an important consideration when deciding which cleanup method to utilize. Applications such as combustion may benefit from methods that convert tar to other compounds rather than remove them from the gas stream. Converting tars may only provide moderate tar reduction, but it maintains the heating value of the gas stream by retaining the carbon and hydrogen compounds. Applications such as synthetic fuel production may require more stringent removal than may be feasible with conversion. Conversion methods may also alter the gas composition (such as increased carbon dioxide), which can also negatively affect fuel synthesis applications [61, 128-130]. These applications may therefore favor physical removal methods that sacrifice tars in favor of gas stream purity.

### **Thermal Cracking**

Thermal cracking uses high temperatures to decompose large organic compounds into

smaller non-condensable gases. Temperatures between 1100 °C to 1300 °C are typically employed, with lower temperatures requiring longer residence times for effective cracking [122, 131]. Naphthalene for instance can be reduced by more than 80 % in about one second at 1150 °C, but it can take more than five seconds to achieve similar reductions at 1075 °C [132, 133]. Brandt and Henriksen have shown that at temperatures of 1250 °C only 0.5s is required for effective tar reduction [134].

High temperatures for thermal cracking may be generated in a variety of ways. High temperature gasifiers are intended to operate at conditions that promote tar decomposition. Low temperature gasifiers are known to produce excessive tar emissions, which can be reduced by raising the temperature of the product gas stream through admission of a small amount of air or pure oxygen downstream of the gasifier [135]. Tar reduction in low temperature gasifiers can also be accomplished using heat exchangers that indirectly heat the gas stream using hot surfaces. Heat exchangers have the disadvantages of higher energy input and good gas mixing [63].

Thermal cracking can reduce tar levels by more than a factor of 80 depending on initial tar concentrations [127]. Tar concentrations have even been achieved down to 15 mg m<sup>-3</sup> at 1290 °C, which is tolerated by many combustion engines [127, 134].

Despite the conceptual simplicity of thermal cracking of tar, it has proved difficult and expensive to implement downstream of the gasifier. For example, Dutta compared synthetic alcohol production using high temperature gasification with previous studies using low temperature gasification. High temperature gasification largely eliminated downstream tar cleanup, but it still proved more expensive than the low temperature gasification scenarios. This

was attributed to significant cost increases for the more sophisticated gasification equipment, which was more expensive than employing a tar reformer downstream of a less expensive low temperature gasifier [136-138].

Thermal cracking approaches downstream of a gasifier may also increase soot production, which increases the particulate load on cleanup or processing equipment [133, 139, 140]. Indirectly heating syngas downstream of a fluidized bed gasifier showed the polymerization of tar compounds into large PAHs and soot [140]. A similar tendency was shown with the partial oxidation of naphthalene using increasing amounts of air [133]. Sufficient hydrogen:methane syngas ratio favors cracking in lieu of soot production, but this limits the application to low methane, high hydrogen gas streams. Removing tars as soot is also an option, but will reduce the energy content of the syngas. Furthermore, the cleanup achieved may not be suitable for many stringent applications such as fuel cells.

### **Catalytic Cracking**

Catalytic cracking occurs at lower temperatures than thermal cracking by reducing the activation energy for decomposing tar compounds. It has the potential to reduce the thermal penalties and costs associated with higher temperature operation. On the other hand, catalysts present operational challenges due to reductions in catalyst activity, which typically involves poisoning, fragmentation, or carbon deposition [141].

Catalyst poisoning occurs when contaminant molecules in the gas stream adsorb irreversibly onto active sites of the catalyst. Sulfur is a common poison for cracking catalysts, especially metal catalysts [63].

Fragmentation can be a result of physical or chemical forces. The extreme temperatures,

pressures, and abrasive environments often encountered by in-situ catalysts can break them into smaller pieces that are easier to elutriate from the reactor. Gas streams can also chemically strip away part of a catalyst (similar to a reverse poisoning reaction), such as sulfided metal catalysts becoming reduced in gas streams with a low  $\text{H}_2\text{S}:\text{H}_2\text{O}$  ratio [142].

Carbon deposition (coking) is the phenomena of organic compounds absorbed on active sites being dehydrated or decarboxylated to fine solid carbon, which accumulates and fouls the catalyst [135]. Several methods are available to reduce the impact of coking. Altering the geometries of the active sites can limit coking by modifying the adsorption/desorption characteristics of the catalyst surface. Optimizing the operating conditions, such as temperatures, pressures, or feed compositions, may promote desired products to form rather than coke. Modifying catalyst compositions can also be effective by altering reaction rates or by increasing the attrition resistance (i.e. durability) of the catalyst. Increasing catalyst durability improves tolerance for extreme conditions that are often encountered during regeneration, when the coke is periodically burned from the catalyst. This high temperature process leads to catalyst sintering, but increased durability enables the catalyst to withstand more of these cycles and increases catalyst lifetime [143].

Catalysts for tar cracking can be classified in several different ways. Torres [61] classifies tar cracking catalysts according to chemical mechanism, which includes acidic, basic, iron-based, and nickel-based catalysts. Dou [144] focuses on temperature conditions and coking response and classifies only the nickel-based catalysts and less expensive mineral catalysts such as calcined dolomite or limestone catalysts. Sutton [145] concentrates on dolomites, alkali-based, and Ni-based catalyst compositions, which are the more common materials. Dayton [135] classifies only the reforming catalysts used downstream of the gasifier, including both non-

metallic oxides and supported metallic oxides. Yung [146] expands upon Dayton's classification of catalysts. He includes essential design parameters such as surface area, the chemical element upon which the catalyst is based, the inclusion of promoters to increase catalytic activity or stability, and the presence of compounds that deactivate catalyst. Xu [147] provides a discussion broken down by the most recent advances in catalysts based on dolomite, iron, nickel (and other metals as supports), and carbon as a support. Abu El-Rub [148] classifies catalysts by their origin: mineral or synthetic. This approach has been adopted below as it is both simple and comprehensive.

Mineral-based or synthetic-based catalysts differ according to the presence or absence of treatments. Mineral-based catalysts are homogeneous solids as opposed to layered materials, and have variable but distinct compositions [148]. These catalysts can be physically but not chemically altered. They are generally less expensive than synthetic catalysts and include materials such as calcined rocks, olivine, clay minerals, and ferrous metal oxides. Synthetic catalysts are more expensive due to required chemical treatments. These catalysts include transition metal-based catalysts (nickel or iron usually), alkali metal carbonates, activated alumina, FCC catalysts used in traditional refining (typically zeolite based), and char.

Minerals are abundant and low cost. Calcined rocks are frequently explored as tar cracking catalysts, of which dolomites are a common example. Calcined dolomites are created by heating dolomite to release bound  $\text{CO}_2$ , and have shown up to 95 % tar conversion [148]. Although it is easily deactivated, dolomite is often used in guard beds as a low cost alternative to more expensive materials, such as activated carbon and  $\text{ZnO/CuO}$ . Minerals such as limestone ( $\text{CaCO}_3$ ) and magnesium carbonate ( $\text{MgCO}_3$ ) are comparable to dolomite when they are calcined to form calcite and magnesite. One issue with calcined catalysts is their need for high  $\text{CO}_2$

partial pressures to maintain their active calcined form [149].

The iron and magnesium content of the silicate mineral known as olivine ((Mg,Fe)SiO<sub>4</sub>) enhances its catalytic properties. The activity of olivine is slightly lower than dolomite when applied directly to the gasification environment, but it has greater attrition resistance. Used as bed material in fluidized bed gasifiers, olivine serves as an in-situ catalyst. For example, olivine has been observed to increase carbon conversion during the gasification of recycled polyethylene pellets [143].

The catalytic activity of clay minerals is primarily due to their silica (SiO<sub>2</sub>) and alumina (Al<sub>2</sub>O<sub>3</sub>) content [148]. Unfortunately their porous structure tends to degrade at the temperatures common in gasification (850 °C). Clay minerals also promote coking, which reduces catalytic activity. The catalytic activity of clays is typically less than that of dolomite [150].

Many iron-rich minerals display significant catalytic activity. The iron often exists as oxides, representing between 35 % and 70 % of the mineral composition. They are commonly found in a reduced metallic form when prepared as catalysts, as opposed to their oxide, carbonate, silicate, or sulfide form [148, 151]. Additional discussions on iron catalyst activities and attrition rates, as well as comparisons of iron catalysts are available in the literature [135, 143, 151, 152].

Although synthetic catalysts are produced from many kinds of materials, nickel has proved particularly effective in decomposing tar [135]. Nickel catalysts are often used in steam reforming to enhance gas yields [94]. Their activities are 8-10 times higher than that of dolomite, which improves H<sub>2</sub> levels in some instances by 0.06 L L<sup>-1</sup> to 0.11 L L<sup>-1</sup> (on a dry syngas basis) [122, 148]. Nickel-based catalysts are also used for industrial naphtha and methane reforming or biomass syngas production. In these applications, nickel increases CO levels and

decreases methane and tar levels, especially above 740 °C. They have also shown water-gas shift capability, and possible reduction of ammonia via catalytic decomposition [135, 153]. Nickel catalysts are readily poisoned by hydrogen sulfide (H<sub>2</sub>S) and fouled by coking, both of which can be reduced by operating at temperatures exceeding 900 °C.

Transition metal-based catalysts have been prepared from platinum (Pt), zirconium (Zr), rhodium (Rh), rutherfordium (Ru), and iron (Fe). These show increased activity toward tar conversion in the following order: Rh > Pd > Pt > Ni = Ru.[122] A Rh/CeO<sub>2</sub>/SiO<sub>2</sub> catalyst, for example, showed significantly higher tar conversion and activity compared to typical steam reforming Ni-based catalysts [61, 154]. This was attributed to superior coking resistance and H<sub>2</sub>S tolerance of up to 180 μL L<sup>-1</sup>.

Tungsten (W) is another promising transition metal for creating catalysts, such as calcined tungsten/zirconia or tungsten carbide [155]. These catalysts show tar conversion similar to a stable zeolite in experiments with toluene as a tar proxy compound. In addition, tungsten catalysts showed significant ammonia decomposition. While these transition metals are superior cracking catalysts, they are expensive and have not demonstrated long term stability, activity, or mechanical strength. These problems can be mitigated by combining a transition metal with supporting and promoting materials.

Activated alumina is commonly employed in catalyst formulations due to its high mechanical and thermal stability, as well as a relatively high activity that is similar to dolomite [114, 148]. Alumina can be activated by heating, which removes hydroxyl groups found in many minerals such as bauxite and aluminum oxide. The resulting compounds can only be approximated as Al<sub>2</sub>O<sub>3</sub> because they typically do not reach equilibrium and still contain partially hydroxylated



components [148]. Alumina is often combined with other materials to overcome the rapid deactivation from coking that occurs on pure alumina catalysts. For instance, reduced coking and H<sub>2</sub>S poisoning can be achieved by adding an MgO promoter and Ni active sites [114]. Tar is effectively reduced to 2 g m<sup>-3</sup> with this catalyst at temperatures above 830 °C. Other alumina based metal oxides include V<sub>2</sub>O<sub>5</sub>, Cr<sub>2</sub>O<sub>3</sub>, Mn<sub>2</sub>O<sub>3</sub>, Fe<sub>2</sub>O<sub>3</sub>, CoO, NiO, CuO, and MoO<sub>3</sub> [62]. The most favored of these is NiO/Al<sub>2</sub>O<sub>3</sub>, since it produced an H<sub>2</sub>:CO ratio of nearly 2:1, an ideal composition for many synthesis reactions [62].

Another common group of aluminum-based catalysts are aluminosilicate zeolites (SiO<sub>4</sub><sup>4-</sup> and AlO<sub>4</sub><sup>5-</sup>). Known as fluid catalytic cracking (FCC) catalysts in the petroleum industry, these acidic catalysts are widely used for converting heavy fuel oil components to lighter middle distillate products. Partial sulfur tolerance, low price, and greater stability compared with regular alumina-based catalysts also make zeolites promising tar removal catalysts [148, 156].

However, zeolites have limitations as tar cracking catalysts. In a gasification environment, the zeolites are also active to the water-gas shift reaction, producing a competition for active sites and reducing tar conversion. Nitrogen and alkali compounds found in biomass can poison active sites, and coking occurs prominently in the presence of zeolites.

These problems can be mitigated by combining other active elements with the zeolite. Zeolites combined with Ni, for example, showed significantly improved tar conversion and longer lifetime compared with pure zeolites, which tended to coke [157]. There was also a positive correlation between increasing acidity of the zeolite and increasing tar conversion. Zeolite-supported Ni catalysts have increased specific surface area, which improves coking resistance compared to the conventional Ni-reforming catalysts [156].

Char is a synthetic, non-metallic catalyst. Because it is a coproduct of thermochemical processing of carbon-rich feedstocks, it is relatively inexpensive compared to other kinds of synthetic catalysts. Because biomass varies greatly in structure and mineral content and processing conditions can vary widely, the resulting chars can display significant variations in physical and chemical properties [158].

Multiple forms of char have been used for catalysts including semicoke, charcoal, activated carbon, char-dolomite mixtures, and char from poplar wood [127, 159-161]. In a comparison of several inexpensive catalysts, pinewood-derived char and commercial biomass char showed greater catalytic activity than biomass ash, calcined dolomite, olivine, used FCC catalyst, and silica sand [152]. Commercial Ni catalysts were the only catalysts evaluated that outperformed char. However, Ni catalysts lack the stability of char afforded by continual replenishment from the thermochemical process. New char is continually generated within the process and is then activated by the steam and CO<sub>2</sub> present in the environment [152, 162, 163]. While carbon deposition in the micropores (i.e. coking) can reduce its activity, subsequent gasification of the coke/char mixture regenerates the catalyst [164].

Char has been combined with thermal destruction techniques to enhance the catalytic conversion of tar [127]. This approach reduced tar by factors of 75-500, yielding consistently less than 15 mg m<sup>-3</sup> of tar contaminants with no heavy tar (i.e. non-GC/MS detectable tar). The sorption of alkali, sulfur contaminants, and fine particulate matter has also been attempted. When impregnated with iron it has also shown significant water-gas shift activity at temperatures as low as 300 °C [165]. One roadblock still remaining is to determine the best approach for utilizing in-situ generated char.

Char may potentially be utilized by establishing a filter cake. Retaining the tar vapors at high temperature by creating a filter cake increases the vapor residence time and enables the highly reactive compounds to undergo secondary reactions. These reactions occurring above 400 °C have been shown to create or add to coke and char deposits at the expense of tar [60]. The final gas stream then has a lower concentration of tar due to its breakdown or its addition to solid carbon compounds.

Both natural and synthetic alkali compounds have been investigated as gasification catalysts. A majority of alkali catalysts are applied directly to the gasification process, but tar reduction downstream of the reactor has also been attempted with alkali [83, 84, 135, 166, 167]. Alkali metals catalyze the decomposition of pyrolysis products like levoglucosan to smaller molecules like hydroxacetaldehyde [168]. Although naturally occurring alkali in biomass enhances tar decomposition, further improvement can be gained by adding alkali minerals to the reactor.

Multiple forms of mineral alkali have been investigated, of which potassium carbonate is most promising. Potassium carbonate ( $K_2CO_3$ ) is a prominent constituent of fast-growing biomass, present in species such as switchgrass on the order of half a percent. Brown et al. added switchgrass with 0.38 % potassium in the form of ash (at 5.9 % potassium) to an Illinois No.6 coal char and increased the rate of gasification by nearly 8-fold [169]. Hauserman also added biomass ash to a gasifier and increased the reactivity of bituminous coal by 9 fold and by 32 fold for wood [145, 166].

Potassium carbonate and other forms of alkali are added to the reactor primarily by mixing alkali into the dry biomass or by wet impregnation of the biomass with alkali carbonates [145]. Compared to the mixing approach, impregnation methods tend to decrease agglomeration, which

reduces the deactivation attributed to coking [145]. Sodium carbonate ( $\text{Na}_2\text{CO}_3$ ) and potassium carbonate ( $\text{K}_2\text{CO}_3$ ) are common alkali catalysts added by these impregnation methods. These are applied both individually and in combination with other common materials such as supported alumina. When individually impregnated into biomass, they showed higher activity than trona ( $\text{Na}_3\text{H}(\text{CO}_3)_2 \cdot 2\text{H}_2\text{O}$ ) and borax ( $\text{Na}_2\text{B}_4\text{O}_7 \cdot 10\text{H}_2\text{O}$ ) with no carbon deposition [139]. A slight decrease in gas yield during gasification was observed with these particular catalysts when supported alumina was included.  $\text{CsCO}_3$  has also been used and has shown even higher activity than  $\text{K}_2\text{CO}_3$  and  $\text{Na}_2\text{CO}_3$ . Many other alkali combinations have had similar results to these catalysts, including materials such as Li, Ba, Fe, and Ni [148]. An unfortunate side effect of adding alkali to any process is the subsequent increase in ash byproduct.

#### **Non-thermal Plasma**

Plasmas are reactive atmospheres of free radicals, ions, and other excited molecules. These reactive species are able to initiate decomposition of tar molecules [170]. Plasmas can be generated by operation at temperatures far exceeding what is possible in gasification (thermal plasmas) or from high energy electron-molecule collisions (non-thermal plasmas) [170].

Several types of non-thermal plasmas are available, including pulsed corona, dielectric barrier discharges, DC corona discharges, RF plasma, and microwave plasma. While these technologies have been effective, the cost, energy demand, device lifetime and operational complexities have limited their application [61]. Pulsed corona plasma is the most promising of these techniques, and reduces tar at optimal temperatures of about  $400^\circ\text{C}$  [123, 171].

Commercial scale development may be possible with a new DC/AC power source, but the operational energy use at about 20 % of the output energy continues to inhibit large scale feasibility [58, 123, 171]. More detailed descriptions of plasma processes are available in the

literature [122, 170].

### **Physical Separation**

Many physical removal methods such as scrubbing and electrostatic precipitation require lower temperatures in order to operate effectively. However, tar reduction by physical devices may still occur at higher temperatures by exploiting their partial condensation.

When temperatures fall below  $\sim 450^{\circ}\text{C}$ , tars begin to condense and form aerosols within the gas stream. These aerosols have a sufficiently larger mass than the vapors and more closely resemble the particulate matter that can be removed by physical forces with techniques such as ESP and inertial separation devices. The rotating particle separator (RPS) used for particulate was recently applied to tar removal for this purpose, but was reported to have limited success [122]. Mechanical separation of tar aerosol droplets still requires partial cooling of the gas stream, which limits high temperature potential and efficiency of these devices [60, 172].

### **Sulfur**

Sulfur removal at high temperatures focuses on one of two compounds: sulfur dioxide ( $\text{SO}_2$ ) or hydrogen sulfide ( $\text{H}_2\text{S}$ ). Historically, sulfur removal at high temperatures has been performed by ‘scrubbing’ the  $\text{SO}_2$  products emitted from a combustion process. However, there are several strong motivators for focusing on  $\text{H}_2\text{S}$  removal rather than  $\text{SO}_2$ .

The growth of syngas applications in recent years has made removing  $\text{H}_2\text{S}$  a primary focus for hot sulfur removal. Many stringent applications require low sulfur levels down to levels as low as picoliters per liter of syngas to avoid equipment failures. Some combustion applications that do not require these low levels may still require sulfur removal in order to satisfy increasingly stringent environmental standards for emissions. These applications benefit economically when sulfur is removed from the syngas fuel ( $\text{H}_2\text{S}$ ) rather than as a combustion

byproduct ( $\text{SO}_2$ ), since the addition of oxygenate during combustion increases the mass flow and therefore the size and power required in subsequent cleaning equipment [55].

Many cleanup processes also recover the removed sulfur, especially those associated with coal, petroleum, and natural gas. Sulfur recovery from these processes accounts for a majority of the elemental sulfur and sulfuric acid currently required in the United States [173]. Recovering sulfur is therefore an important consideration for new removal technologies.

Most hot gas cleanup technologies utilize adsorption, in which gaseous species combine physically or chemically to solid materials. Physical adsorption involves weak van der Waal's intermolecular dipole interactions formed from polarizations within molecules. Chemical adsorption (i.e. chemisorption) involves covalent bonding of adsorbate molecules onto the surface of adsorbents. The forces involved in physical adsorption can allow several layers of adsorption to take place on the sorbent material and are weak enough to allow relatively easy desorption. Alternatively, chemisorption may be too strong for easy desorption of contaminants and occurs only where the sorbent surface is available for reaction.

Adsorption occurs either reversibly or irreversibly. Reversible processes allow for regeneration of the sorbents and is favored for more expensive synthetic materials. Irreversible reactions require cheaper once-through materials but ensure that adsorbed contaminants are permanently removed from the gas stream.

A sulfur adsorption process usually follows three stages: reduction, sulfidation, and regeneration. The solid sorbent is first reduced as a preparation step for chemical adsorption with the sulfur species. The sulfidation reaction typically combines a metal oxide with sulfur, creating a metal sulfur compound such as  $\text{ZnS}$  or  $\text{FeS}$ . A reversible process then follows this

step with regeneration to form the original oxide sorbent and an enriched sulfur dioxide gas stream. Larger commercial installations concerned with byproduct sulfur recovery then direct the sulfur rich gas to a sulfur recovery unit, which primarily yields sulfuric acid or elemental sulfur.

Metal oxides exhibit the best chemical properties for high temperature sulfur adsorption. An extensive list of potential metals was screened by Westmoreland and Harrison according to high temperature desulfurization capability and free energy minimization [174]. Subsequent research has narrowed their list of potential desulfurization metals to the most promising seven single oxides based on Zn, Fe, Cu, Mn, Mo, Co, and V [75].

Mixed metal oxides are common and widely applied adsorption materials (see **Table 5** below). Combinations of metals can be designed to enhance specific characteristics, such as sulfur capacity, regeneration effectiveness, thermal tolerances, or removal of additional contaminants. Some exotic oxides, such as Mn mixed with V and Cu, have shown high sulfur removal at temperatures above 600 °C [61]. Copper and zinc oxides (CuO and ZnO) are more abundant and have removal efficiencies that still exceed 99 %. ZnO in particular may be the most common component of the increasingly popular renewable sorbents, despite its original development for one-time use [175].

**Table 5:** Examples of sulfur sorbents and theoretical capacities [75]

Sorbent	Chemical formula	Capacity % <sup>a</sup>	Equil. H <sub>2</sub> S <sup>b</sup> $\mu\text{L L}^{-1}$	Temperature range °C
Zinc copper ferrite	0.86ZnO·0.14CuO·Fe <sub>2</sub> O <sub>3</sub>	39.83	<1 <sup>c</sup>	540-680
Copper manganese oxide	CuMn <sub>2</sub> O <sub>4</sub>	53.78	<1 <sup>d</sup>	510-650
Zinc oxide	ZnO	39.51	7 <sup>d</sup>	450-650
Iron oxide	Fe <sub>3</sub> O <sub>4</sub>	41.38	560 <sup>d</sup>	450-700
Copper oxide	Cu <sub>2</sub> O	22.38	<1 <sup>c</sup>	540-700
Lime	CaO	57.14	150 <sup>e</sup>	815-980

<sup>a</sup>Theoretical loading of sulfur as kg kg<sup>-1</sup> of fresh sorbent; <sup>b</sup>Notestein states this environment contains a molar ratio of H<sub>2</sub>O to H<sub>2</sub> of 25 % to 20 %; <sup>c</sup>at 590 °C; <sup>d</sup>at 650 °C; <sup>e</sup>at 980 °C; all temperatures are approximate as converted from °F; original data cited from the Update on DOE hot gas cleanup programs from Notestein, 1989.

Many zinc-based sorbents contain multiple components, primarily iron oxides, nickel oxides, copper oxides, and zinc titanates. Combinations with iron oxides are typically called zinc ferrites, and have better capacity and regeneration properties than pure zinc oxides [175]. Both zinc and iron have an affinity for sulfur which gives zinc ferrites a high sulfur loading capacity of more than 300 g kg<sup>-1</sup> of fresh catalyst [61]. Iron-based materials, however, tend to suffer from carbon deposition, which worsens with increased H<sub>2</sub>O content during sulfidation reactions [128]. Techniques such as oxidation are available to remove deposited carbon (i.e. coke), but this leads to sorbent sintering and attrition. Thus, minimizing coking can increase sorbent lifetimes.

Coking on zinc sorbents has been heavily researched. High temperatures are typically used to avoid coking. However, zinc is easier to vaporize than other metals and is easily removed from a



catalyst at elevated temperatures [176]. An optimal temperature range that increases zinc stability and performance was determined using zinc ferrite ( $\text{ZnFe}_2\text{O}_4$ ) [177]. Zinc vaporization was avoided at temperatures below  $600^\circ\text{C}$ , but excessive temperature reductions led to increased carbon deposition and sorbent deactivation. When supported by  $\text{TiO}_2$ , the sorbent successfully reduced  $\text{H}_2\text{S}$  from  $1\text{ mL L}^{-1}$  to less than  $1\text{ }\mu\text{L L}^{-1}$  at temperatures as low as  $450^\circ\text{C}$ .

Coking has also been attributed to high CO concentrations, as indicated by the same  $\text{TiO}_2$ -supported  $\text{ZnFe}_2\text{O}_4$  catalyst. Increasing the syngas CO concentration from 25 % to 55 % resulted in carbon deposition that largely diminished the desulfurization ability. A slight improvement in CO tolerance was shown by impregnating brown coal to create carbon-supported  $\text{ZnFe}_2\text{O}_4$  and  $\text{CaFe}_2\text{O}_4$ . These sorbents showed up to 120 %, or roughly double, the desulfurization capacity of unsupported ferrites using a 33 % CO syngas at temperatures  $\geq 400^\circ\text{C}$ . Of these two carbon-supported catalysts, the Zn compound was more suitable as a sorbent since it experienced insignificant activity loss over 40 regeneration cycles. These zinc ferrites indicate the need for improved tolerance to coking in high CO content syngas [177].

Another common technique is “doping” ZnO and other sorbents with CuO. ZnO/CuO sorbents have been used extensively in guard beds to ensure low sulfur concentrations, and are becoming more prominent in regeneration processes for first stage sulfur removal. Other combinations with CuO include  $\text{Fe}_2\text{O}_3$ , and  $\text{Al}_2\text{O}_3$  [75]. Adding CuO increases sulfur capacity and regeneration ability. The better thermodynamic equilibrium between CuO and  $\text{H}_2\text{S}$  enhances sulfur adsorption and provides more stable performance [175]. A ZnO sorbent can consistently remove  $\text{H}_2\text{S}$  to nearly  $10\text{ }\mu\text{L L}^{-1}$ , but begins to volatilize as average operational temperatures reach  $600^\circ\text{C}$  to  $650^\circ\text{C}$ . Alternatively, CuO shows minimal vaporization losses and may remove  $\text{H}_2\text{S}$

to concentrations of  $1\text{-}5\ \mu\text{L L}^{-1}$  [75]. Combining CuO with ZnO also minimizes sorbent surface area loss, leading to a longer lifetime in regeneration applications [175].

Improvements in ZnO/CuO sorbents have led to their commercial development by Sud-Chemie and other companies. Although specifics are proprietary, they produce several sorbents for sulfur removal at commercial scale. Sorbent compositions range from pure ZnO to mixtures of ZnO/CuO/Al<sub>2</sub>O<sub>3</sub>. Sorbent geometry is also important for addressing different mass transfer and flow issues, and includes a variety of sizes and forms such as granules, tablets, or extrusions [178].

ConocoPhillips has also developed commercial sorbent combinations with ZnO [179]. Their proprietary ZsorbIII zinc oxide sorbent is composed of less than  $100\ \text{g kg}^{-1}$  Ni-oxide and less than  $500\ \text{g kg}^{-1}$  zinc oxide. This sorbent achieved greater than 99 % H<sub>2</sub>S removal by reducing  $10\ \text{mL L}^{-1}$  H<sub>2</sub>S to near zero concentration. Repeated regenerations resulted in no loss in performance or structure. During testing with simulated syngas at high temperature and pressure, optimal performance was achieved at temperatures between  $400\ ^\circ\text{C}$  to  $600\ ^\circ\text{C}$  and higher pressures ( $2026.5\ \text{kPa}$  compared to  $202.65\ \text{kPa}$ ). These regeneration experiments indicated no loss of activity, which implies potential for long lifetimes. Consistently 90 % of sulfur loading capacity was attainable even after 40 runs. A regeneration gas of  $20\ \text{mL L}^{-1}$  oxygen with a balance of nitrogen eliminated the sintering and active site migration caused by highly exothermic regeneration reactions [75]. The periodic temperature spikes that occur during regeneration were held below  $770\ ^\circ\text{C}$ , which minimized zinc vaporization. One additional benefit for the zinc-nickel sorbent is an indication of COS reduction. This is attributed to either direct COS adsorption, or nearly complete elimination of H<sub>2</sub>S from which COS is assumed to

form [180]. These high removal efficiencies and potential for increased lifetimes of zinc oxides are driving factors for continued Zn sorbent research.

The potential for regenerating metal sorbents is very important, since regeneration can drastically reduce material inputs and waste streams. Regeneration is limited by several phenomena, and substantial effort has been placed on this regeneration step in order to extend sorbent lifetimes. Agglomeration of active sites after successive regenerations will reduce the surface area and ultimately decrease sorption capability. Other design factors affecting sorbent regeneration are poisoning (irreversibly adsorbing other chemicals), coking, and possible loss of the metals at high temperatures due to vaporization.

Another important consideration is the effect of other gas phase components on the adsorption process and catalyst/sorbent lifetime. Biomass-derived syngas can have widely varying amounts of nitrogen, alkali, and chloride contaminants compared with coal-derived syngas. Since many techniques are adapted from previous commercial applications for cleaning coal-derived syngas, they must be modified to account for these different contaminant levels.

HCl can be particularly detrimental, but zinc-titanate sorbents such as  $\text{ZnTiO}_3$ ,  $\text{Zn}_2\text{TiO}_4$ , and  $\text{Zn}_2\text{Ti}_3\text{O}_8$  have been used to reduce its effect. The Research Triangle Institute has developed proprietary, attrition-resistant zinc titanate-based sorbent that minimizes the activity loss experienced by previous zinc titanates [61, 181]. With this sorbent, desulfurization capacity was actually enhanced by HCl in the syngas, as long as temperatures remained below  $550^\circ\text{C}$ . One disadvantage of this zinc titanate is its dependence on water. The lack of steam (less than  $\sim 60\text{ mL L}^{-1}$ ) in syngas increases the reduction capacity of gas streams caused by acidic compounds such as HCl. This leads to instability of zinc compounds, which become easily volatilized.

Fortunately, many syngas streams contain adequate H<sub>2</sub>O to avoid this volatilizing situation.

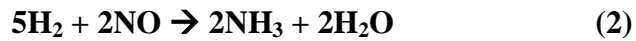
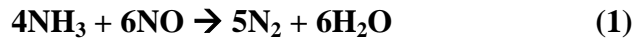
Ideally, a single sorbent or catalyst will eliminate multiple gas stream contaminants. For example, Ni and Co promoters added to Zn-Ti sorbents have enabled simultaneous removal of NH<sub>3</sub> and H<sub>2</sub>S [182]. Mixed oxides have shown promising results for simultaneous removal of tars along with the nitrogen and sulfur compounds [61]. Simultaneous adsorption of HCl and H<sub>2</sub>S at the gasifier outlet has been done with a natural trona material (Na<sub>2</sub>CO<sub>3</sub>, NaHCO<sub>3</sub>·2H<sub>2</sub>O) combined with Zn/Ti material [71]. Many other simultaneous removal examples exist, some of which are more thoroughly discussed in the following hot gas cleanup sections for nitrogen and alkali.

### **Nitrogen**

Hot gas cleanup of nitrogen compounds focuses on decomposing ammonia rather than removing it from gas streams. Very little ammonia should exist in syngas at elevated temperatures if chemical equilibrium is attained. However, ammonia released during gasification of biomass does not decompose rapidly enough to achieve the low part per million concentrations required for many syngas applications. Thus, selective catalytic oxidation or thermal catalytic decomposition may potentially be employed for hot gas cleaning.

Normal oxidation of gas streams containing ammonia leads to thermal destruction of NH<sub>3</sub> into N<sub>2</sub>, H<sub>2</sub>, and NO<sub>x</sub>. Minimizing the production of NO and N<sub>2</sub>O is possible, but they are inevitably formed despite the greater stability of CO<sub>2</sub> and N<sub>2</sub> [183]. Simply oxidizing syngas also has obvious undesired effects on methane, CO and H<sub>2</sub> compositions. Using catalysts has been proposed in a 'selective oxidation approach' to minimize these effects and decrease the severity of conditions required for NH<sub>3</sub> decomposition [61].

Catalysts must be chosen that selectively oxidize the nitrogen compounds with oxygen molecules (equation 1), thereby avoiding undesired reactions with other gas species (equation 2). Carefully adding an oxidizer such as NO is one promising oxidation agent, and several catalysts including those common in the thermal catalytic decomposition approach (continued below) such as nickel and zeolites.



Thermal catalytic decomposition of  $\text{NH}_3$  essentially occurs via the opposite mechanism of  $\text{NH}_3$  formation [61].  $\text{NH}_x$  molecules are consecutively dehydrogenated, and the  $\text{N}^*$  and  $\text{H}^*$  radicals are recombined to form  $\text{N}_2$  and  $\text{H}_2$ . High  $\text{NH}_3$  conversions typically occur above  $500^\circ\text{C}$ , but higher temperatures between  $700^\circ\text{C}$  to  $800^\circ\text{C}$  are currently required to avoid catalyst deactivation from CO-induced coking. Reducing these temperatures closer to  $500^\circ\text{C}$  is still within the ideal temperature range for many syngas applications.

Typical tar cracking or hydrocarbon reforming catalysts such as dolomites and nickel or iron-based catalysts have shown promising  $\text{NH}_3$  reductions and are inexpensive alternatives to materials such as Ru, W, and alloys thereof, as well as nitrides, oxynitrides, and carbides [61] [60].

Common industrial Ni-based reforming catalysts have shown up to 75 % reduction of  $\text{NH}_3$  when using actual coal-derived syngas. Sulfur deactivation is a frequent problem with these catalysts, and can occur after only 60 h of operation. Increases in pressure will exacerbate the

sulfur poisoning [184].

Many of these catalysts are already applied for other commercial processes, but require testing and refinement for their ammonia reduction capability. Commercial tungsten based catalysts, specifically tungsten carbide (WC) and tungstated zirconia (WZ), are partially resistant to sulfur and possess good activity, physical hardness, and multiple types of available active sites [155]. During  $\text{NH}_3$  reduction in a simulated hot syngas, both catalysts performed similarly to commercially ultrastable Y zeolite (USY) for the reduction of toluene [155]. Near total conversion of  $4 \text{ mL L}^{-1} \text{ NH}_3$  was possible at  $700^\circ \text{C}$  with only  $\text{H}_2$  and He as a carrier gas mixture. Benefits with this catalyst were mechanical strength and thermal stability, as well as abilities to simultaneously reduce tar and resist sulfur poisoning. These catalysts may also be easily improved by an increase in surface area.

An inherent disadvantage of the above catalysts, as with other acid catalysts, is a reduction in the  $\text{NH}_3$  conversion in the presence of water. The slight reduction in  $\text{NH}_3$  decomposition seen with the WC and WZ catalysts may have been due to competitive reactions between CO and  $\text{H}_2\text{O}$  on the active sites. The decrease in  $\text{NH}_3$  conversion to 80 % was still comparable to other catalysts used for ammonia conversion.

Deactivation from sulfur is a primary focus of nickel catalyst research. A commercial Ni-based catalyst combined with  $\text{MnO}_3$  and  $\text{Al}_2\text{O}_3$  overcomes some sulfur effects to remove tars and ammonia simultaneously [73, 185]. In several tests, this combination outperformed 15 other nickel, iron, Zn-Ti, and Cu-Mn based catalysts. A 92 % removal efficiency was attained and more than 80 % conversion was maintained during high  $\text{H}_2\text{S}$  ( $6 \text{ mL L}^{-1}$ ) concentrations. Longer term tests are needed to prove sustained sulfur resistance and decomposition capability of this

sorbent.

Ferrous dolomite and sintered and palletized iron ores are less expensive approaches to  $\text{NH}_3$  catalytic decomposition. Although still inferior to the Ni-based commercial catalysts, they have achieved nearly 85 % conversion of  $\text{NH}_3$  in syngas at  $900^\circ\text{C}$  for concentrations of  $2.2 \text{ mL L}^{-1}$  to  $2.4 \text{ mL L}^{-1}$  [177]. Iron rich coals containing between  $2 \text{ g kg}^{-1}$  to  $20 \text{ g kg}^{-1}$  of iron can form char that is applicable for use as a catalyst. Higher iron content samples can yield 70 % to 80 %  $\text{NH}_3$  reduction to  $\text{N}_2$ .  $\text{FeOOH}$  precipitated on an Australian brown coal is an alternative approach. The heated Fe nanoparticles on this catalyst almost completely decomposed  $2 \text{ mL L}^{-1}$  of  $\text{NH}_3$  in inert gas at  $750^\circ\text{C}$ . High activities are a result of the fine metallic Fe particles present in the catalyst. This realization led to the pursuit of limonite, a goethite ( $\alpha\text{-FeOOH}$ ) rich mineral, as another possibly inexpensive catalyst. It showed the best results of all the iron rich or impregnated specimens including ferrous dolomite, sintered iron ore,  $\text{Fe}_2\text{O}_3$  with  $\text{TiO}_2$  or  $\text{MnO}_2/\text{TiO}_2$ , and coal char. 90 %  $\text{NH}_3$  reduction was achieved at  $750^\circ\text{C}$  in simulated syngas with low CO content ( $200 \text{ mL L}^{-1}$ ), and even 70 %  $\text{NH}_3$  reduction was possible at high CO content ( $500 \text{ mL L}^{-1}$ ).

High CO contents in lower temperature gas streams still pose a problem with coking, even with these inexpensive catalysts. Also of concern are the remaining nitrogen compounds, primarily HCN, which is typically around a tenth of the  $\text{NH}_3$  quantity [177].

### **Alkali**

Two processes are commonly employed to reduce alkali concentrations in syngas at elevated temperatures: removal with other contaminants via condensation, and hot adsorption onto solid sorbents. As gas stream temperatures fall below alkali condensation points, alkali vapors will nucleate and agglomerate to form or add to particulate matter in the gas stream. In order to be

effective, temperatures lower than 600 °C are necessary to minimize the alkali vapors that bypass particulate removal equipment [86, 91]. Solid sorbents however may be applied at various temperatures for alkali in any form, which allows even higher temperatures for applications such as combustion or fuel cells.

A sorbent in alkali removal is generally termed a ‘getter’, and is selected using several criteria. It must tolerate high temperatures, possess a high adsorption rate and loading capacity, and preferably form irreversible adsorptions (i.e. have the ability to retain alkali despite fluctuations in process conditions) [186]. However, selecting the best ‘getter’ from this constantly growing list of possibilities is dependent on the specific process. Important factors determining sorbent lifetime include the presence of other contaminants, application temperature, and the ability to regenerate the sorbent.

Sorbents include a variety of natural minerals such as diatomaceous earth (silicas), clays, or kaolinite. Sorbent can also be synthesized such as activated alumina from bauxite minerals [58, 89, 187]. Minerals such as kaolinite and bauxite are capable of high temperature (1000 °C) removal applications both inside and downstream of the gasifier. Other minerals, like emathlite, can only be used at lower temperatures because they form low melting point eutectics with the alkali [188]. Kaolinite irreversibly chemisorbs alkali, which helps explain its very high adsorption capacity [186]. Bauxite removes alkali by rapid physical adsorption. It can achieve removal efficiencies as high as 99 % in as little as 0.2 seconds. Bauxite is readily regenerated by boiling water, allowing it to be reused [94]. Activated  $\text{Al}_2\text{O}_3$  also uses physisorption and has both a high capture capacity and adsorption efficiency. At 840°C, activated  $\text{Al}_2\text{O}_3$  out performed bauxite, second grade alumina, kaolinite and acidic white clay with 98.2 % removal efficiency



and an alkali loading (sodium in this case) of  $6.2 \text{ mg g}^{-1}$  [189].

Some sorbents, such as alumina ( $\text{Al}_2\text{O}_3$ ) and silica ( $\text{SiO}_2$ )-based materials are able to remove both alkali and chlorine from gas streams at temperatures approaching  $800^\circ\text{C}$ . One study utilized a solid sorbent comprised of  $\text{Mg}(\text{OH})_2$  and montmorillonite (alumina/silica mineral) placed in tandem with other known alkali sorbents such as activated alumina, bauxite, kaolinite, and clay [89]. Excess chlorine vapors are released by chemical adsorption of the alkali component (Na in this instance), and are subsequently adsorbed by the  $\text{Mg}(\text{OH})_2$  and montmorillonite. Simultaneous removal of alkali and chlorine has been demonstrated at temperatures up to  $550^\circ\text{C}$  for HCl and  $840^\circ\text{C}$  for alkali.

Another study suggested the removal of alkali and halides as particulate matter by injecting aluminosilicates and sodium carbonate into the gas stream [102]. The injected compounds created alkali carbonates in the gas stream, which then transformed to oxides and combined with halides to form particulate. Any alkali vapors could then be removed as a solid alkali silicate once captured by the silica or alumina. Interactions with multiple other compounds present in syngas might substantially affect these sorption processes, which would be evident in actual gasification trials.

### **Chlorine**

Chlorine is commonly found in biomass, and while chloride salts can form under certain conditions, a substantial portion evolves as hydrogen chloride (HCl). Cold gas cleaning typically removes HCl along with alkali, tars and particulate matter. Hot gas cleaning more typically employs a sorbent that only removes the HCl and sometimes the alkali [190].

Adsorption removes gaseous HCl to a solid surface at elevated temperatures. This often

generates a salt product through chemisorptions. High temperature removal of HCl is most effective between 500 °C and 550 °C due to chemical equilibrium between the gases and solids involved [191]. Calcium-based sorbents begin to decompose as temperatures exceed 500 °C, thereby decreasing their binding capacity and releasing adsorbed HCl [192].

Commercial operations most commonly employ cold-gas cleaning to remove HCl. For hot gas cleaning, activated carbon, alumina and common alkali oxides in fixed beds are most commonly employed. Alternatives such as alkali-based multioxides can provide efficiency improvements or environmental benefits, but these are higher in cost than traditional sorbents [89, 193].

Several less expensive materials have been suggested as alternatives for removing HCl at elevated temperatures. A variety of sodium-rich minerals have been evaluated including nahcolite, trona, and their derivatives sodium bicarbonate ( $\text{NaHCO}_3$ ) and sodium carbonate ( $\text{Na}_2\text{CO}_3$ ). Other naturally occurring alternatives are  $\text{Ca}(\text{OH})_2$  and  $\text{Mg}(\text{OH})_2$ , as well as their calcined forms ( $\text{CaO}$  and  $\text{MgO}$ ) [58, 190]. Additions of limestone in the past for sustained, high temperature gasification have also motivated research for using limestone and solid-slaked lime as inexpensive HCl sorbents [58, 190, 194].

Factors to consider in HCl adsorption include tolerance to the presence of other contaminants, effects of sorbent material combinations, and methods of application. For instance, a commercial HCl-sorbent,  $\text{NaCO}_3$ , was enhanced to minimize sulfur effects by adding  $\text{Al}_2\text{O}_3$  to form  $\text{NaAlO}_2$ . The combined material tolerated  $0.2 \text{ mL L}^{-1}$  sulfur while reducing  $0.2 \text{ mL L}^{-1}$  HCl to less than  $1 \mu\text{L L}^{-1}$  at 400 °C [177]. The addition of calcium and magnesium oxides to sodium carbonate, reduced HCl concentrations from  $1000 \text{ mg m}^{-3}$  to less than  $1 \text{ mg m}^{-3}$ .

This strategy is not always effective as illustrated by attempts to enhance  $\text{NaCO}_3$  sorption by the addition of  $\gamma\text{-Al}_2\text{O}_3$ , possibly due to an inadequate ratio of reactive component and structure [195].

As an alternative to fixed bed sorption filters, direct injection of sorbent into hot gas streams ( $600^\circ\text{C}$  to  $1000^\circ\text{C}$ ) has been attempted. Tests with calcium-based powders showed up to 80 % HCl removal [196].

### **Cold Gas Cleanup (CGC)**

While HGC processes are ‘dry’ due to the high temperatures, cold gas cleanup (CGC) is characteristically a ‘wet’ process. Liquid adsorbents are typical in CGC processes, and their upper temperature is usually the limit of the CGC process. This may be as high as the condensation point of the water used for tar and particulate scrubbing, or as low as  $-62^\circ\text{C}$  for chilled methanol used in removing acid gases [47]. A general shortcoming of these first generation cleaning technologies is that the cooler temperatures of CGC also induce thermal penalties on the overall plant efficiency. Treating the scrubbing medium in these ‘wet’ technologies also incurs added expense in order to meet increasing environmental standards. Despite these downfalls, however, CGC techniques will continue to be important gas treatment technologies in the future due to their high efficiency and proven reliability.

### **Particulate Matter**

Particulate matter is typically removed at ambient temperatures using water as a “wet scrubbing” agent. Wet scrubbing is widely deployed in industry, given its relative simplicity and effectiveness. The reader is directed toward the literature for more detailed information than provided in this review [59, 197].

Cold gas scrubbing has been characterized according to operating principles: spray scrubbers, wet dynamic scrubbers, cyclonic spray scrubbers, impactor scrubbers, venturi scrubbers, and electrostatic scrubbers [197]. These techniques are ranked according to increasing removal efficiency for submicron particulate matter. The most basic methods use primarily inertial forces to separate particles, which becomes more effective as particles increase beyond 3  $\mu\text{m}$  in size. With smaller particles, however, electrostatic forces, temperature gradients, higher liquid vapor pressures and smaller liquid droplet sizes become increasingly important for adequate removal. Atomizers and other nozzle variations, velocity and pressure changes, and induced electric charges are common methods of attaining optimal performance. However, increasing the particulate removal efficiency of these techniques typically involves higher energy consumption.

The most basic design is the spray scrubber. Spray nozzles or atomizers inside a chamber disperse liquid into either a concurrently or counter-currently flowing gas stream. This design assures a large surface area for impaction and interception of particulate by the water. These systems have efficiencies ranging from 90 % for particulate larger than 5  $\mu\text{m}$  (>PM<sub>5</sub>) down to around 40 % for submicron particles [197]. Wet scrubbers are also effective in absorbing water soluble gaseous contaminants. Unfortunately, using water as an efficient removal media requires costly waste water treatment facilities.

Wet dynamic scrubbers and cyclonic scrubbers have slightly higher removal efficiencies than the spray scrubbers, up to 95 % for PM<sub>5</sub> and 60 % to 75 % for submicron particles. Integrating these systems into a single device has also been done as shown in Figure 11.

Dynamic scrubbers use the mechanical motion of fan blades to turbulently mix the water droplets with the gas stream, increasing the chances of inertial impaction of particles with water

droplets. Comparable removal efficiencies are attained with cyclonic scrubbers, which are based on principles similar to that of gas cyclones, previously described. In wet scrubber applications, cyclonic scrubbers introduce an additional water spray at the inlet area. Increasing velocity at this location and closer proximity of droplets increases the probability that water captures the particulate. The dynamic scrubber in Figure 11 essentially repeats a series of separation and wetting stages in order to capture progressively smaller sized particles. The tangential inlet removes larger particles by inertial separation followed by a wetted vane to capture smaller particulate. Following the dynamic section of the system, any remaining particles are removed by the final cyclonic motion.

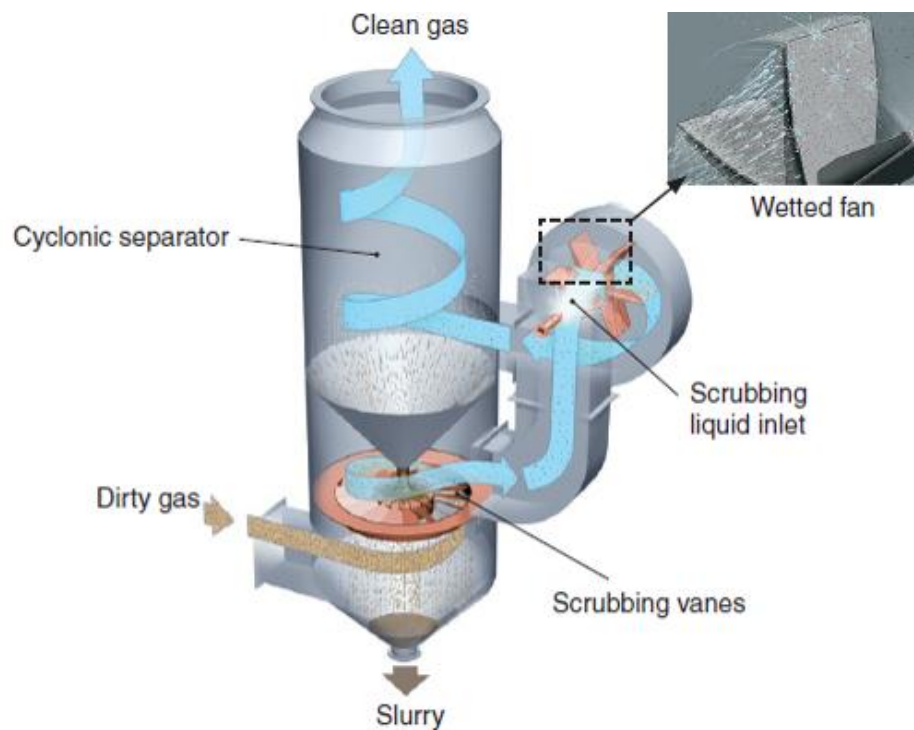


**Figure 11:** Wet dynamic scrubber [198]

Impinger or impactor wet scrubbers closely resemble the trayed columns widely employed in cold gas absorption processes. Dirty gas passes through perforated plates or trays for impaction on a smaller plate which is continually cleansed with water. These scrubbers can remove larger

particles with greater than 98 % efficiency. Multiple trays in series within the column are required to remove submicron size particles, but even this technique has little to no effect on particles smaller than 0.6  $\mu\text{m}$  [197]. This scrubbing method uses essentially static water flow compared with the atomizing spray, although some water circulation is required in order to maintain a low solids loading in the cleaning water and limit clogging.

Venturi devices, or gas-atomizing scrubbers, operate on the principle of increasing gas velocity by reducing the flow area, thus shearing water sprays into very fine droplets. The high density of very fine droplets absorbs submicron particulate matter at efficiencies greater than 50 % [197]. Maximum efficiencies are achieved through optimal sizing of the throat area and the contacting volume. Devices with adjustable throat sections have improved the original fixed square or round designs, and enable a variety of pressure drops and collection characteristics with a single venturi. The scrubbing liquid can also be applied either before or after the velocity transition area, typically termed the 'wet' or 'dry' approach. At the transition from dry to wet, a 'liquid line' is present and a slight buildup of particulate will occur. Both wet and dry venturis must maintain this liquid line either before or after the constricting throat section in order to operate efficiently. Venturis may incorporate different kinds of geometries, nozzle designs, and even multi-venturi zone configurations. In the latter case, rows of rods are utilized to provide the increased velocity area for a more equally distributed result. In most configurations the resulting mass of particulate and liquid drops are removed by cyclonic or demisting separation.

Submicron particles, with their smaller mass, respond less to inertial forces and require additional techniques to achieve removal efficiencies greater than seen in venturis. One preferred technology is the wet electrostatic scrubber, which can be applied in venturi applications or in systems similar to the hot ESP. Unlike the hot ESP, water is sprayed into the

stream before or after applying an electrical charge [197, 199]. Electronegative water molecules can attract positively charged particles prior to the wetting stage, and the combined material can then be separated downstream. Alternatively, the water/particulate mixture can be charged together and separated downstream with oppositely charged plates. Traditional separation methods of cyclonic or packed tower design are also employed.

Wet ESPs are gaining popularity due to reduced power consumption, operation at reduced velocities and lower pressure drops, and increased removal efficiencies compared to traditional venturis [118]. In a recent investigation of a two-field electrostatic precipitator, submicron aerosols of  $(\text{NH}_4)_2\text{SO}_4$ , HCl, and  $\text{NH}_4\text{Cl}$  were successfully removed in both laboratory and pilot scale facilities at efficiencies approaching 99 %. Power consumed when removing  $\text{H}_2\text{SO}_4$  particulate matter was reduced in industrial scale tests to 0.2 kWh for every 1000 m<sup>3</sup> of syngas. Removal efficiency at this scale was also greater than 95 % [199]. Wet ESPs however still suffer from increased complexity, a residual waste stream, and other CGC disadvantages.

### **Tars**

Wet scrubbers can remove tar as well as particulate matter in the same process. Although many tar compounds are non-soluble in water, wet scrubbing drops gas temperature sufficiently for many tarry vapors to condense as fine aerosols that are readily absorbed into water droplets. Lighter class two and three tars, such as phenol, remain as vapors but they are sufficiently water soluble to be readily absorbed by water droplets.

Water leaving the wet scrubber, heavily contaminated with tar compounds, enters a settling tank where water-insoluble tar compounds are separated from the water, allowing the water to be recirculated to the scrubber. Eventually, the water-soluble tars accumulate and reduce the effectiveness of the wet scrubber. This waste water cannot be discharged to the environment

without chemical and/or biological waste water treatments.

Biological gas treatments have been developed for certain kinds of environmental remediation at ambient conditions, which eliminates waste water streams. A biofilm absorbs organic compounds from the gas stream and metabolizes them to CO<sub>2</sub> and water [200].

Although biological processes may appear to be too slow to match the high production rates of syngas, in fact, a whole field called syngas fermentation is emerging around the concept [201].

### **Sulfur**

There are many approaches to low temperature sulfur removal. Chemical, physical or mixed chemical/physical solvent processes are most often employed. Chemical redox processes as well as biological processes are also heavily utilized, especially in systems concerned with sulfur recovery.

Chemical solvent methods use a liquid solvent to create a weak chemical bond between an amine component and an acid gas, most commonly H<sub>2</sub>S and CO<sub>2</sub>. Amines are classified by the number of hydrogen atoms on the nitrogen molecule that are displaced by another atom or group. In these applications, an amine or hindered amine first extracts acidic gases in an absorber unit. A stripper unit then regenerates the sorbent for recycling to the absorber and yields a concentrated acid gas stream. Many commercial fuel facilities use primary, secondary, or tertiary amines in these absorption processes.

The oldest methods of commercial sulfur removal were developed using alkanolamines by R.R. Bottoms in 1930 for the absorption of acidic gases [202]. The first commercially available triethanolamines (TEA) were later replaced by other alkanolamines such as the more widely utilized monoethanolamine (MEA), diethanolamine (DEA), and the recently favored



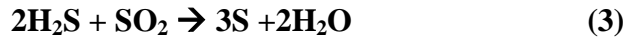
methyldiethanolamine (MDEA, a tertiary amine) [47]. More stringent regulations have required development of new processes, such as a glycol-amine process used to simultaneously dehydrate and purify natural gas for pipelines [202]. Regardless of the particular solvent, utilizing these liquid sorbents with regeneration enables continuous online sorbent use and the ability to generate elemental sulfur via Claus processes or chelating agents, subsequently discussed.

Organic forms of sulfur such as COS are not efficiently removed in these processes, and can degrade several solvents (MEA being more significantly affected than DEA). Therefore, COS hydrogenation to H<sub>2</sub>S is necessary before using these solvents in most synthesis gas streams. This adds additional complexity to the process. Another disadvantage is continuous solvent replacement due to loss of the amine known to occur during operation.

Physical absorption processes are also available. These utilize solvents such as methanol and dimethyl ether. While these processes are not favored in the petrochemical industry due to their tendency to also absorb hydrocarbons, this does not represent a shortcoming in syngas cleaning. These methods are also advantageous for Claus and other sulfur recovery processes as they remove COS and H<sub>2</sub>S without extracting large amounts of other acid gases such as CO<sub>2</sub>. Minimal solvent loss, high loadings and minimal heating requirements are additional benefits compared with the chemical removal processes. Substantial energy and infrastructure investment is sometimes required for pressurization and refrigeration. The *Rectisol* process, for instance, is commonly employed in ammonia, hydrogen, and other fuel synthesis operations for deep sulfur removal (<0.1 μL L<sup>-1</sup> H<sub>2</sub>S and COS) and uses chilled methanol at -62 °C [47]. Overall, acid-gas scrubbing units used for sulfur or carbon dioxide removal can be highly efficient and selective, but have a high capital and operating cost due to multiple columns and absorbents. On occasion, this cost may contribute well over 10 % of total plant costs [203].

Given the large variety of processes available, including several mixed chemical/physical processes, the reader is encouraged to visit the literature for further information [47].

The sulfur-rich, so called sour gas emitted from regeneration units of these processes are typically fed to sulfur recovery units (SRU). Many operations use the classic Claus process, governed by the following reaction:

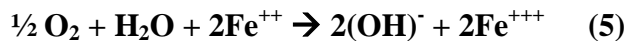
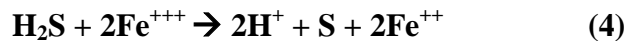


The Claus process is only utilized with separated and concentrated sour gas streams rather than raw syngas because partial combustion of the gas is required to generate one part  $\text{SO}_2$  and two parts  $\text{H}_2\text{S}$ . The elemental sulfur formed during the combustion stage is condensed and recovered, after which the gas stream is passed to a catalytic reactor. Catalysts typically employed are aluminum oxide materials such as natural bauxite or alumina. This adds cost and complexity to a process that only recovers 85 % to 95 % of total sulfur, yielding  $\text{SO}_2$  emissions often approaching 10 % of the inlet sulfur mass [47, 74]. Other equipment (combustors, heat recovery equipment, boilers, condensers, etc.) and the multiple stages that are often required will also impact the profitability of recovering sulfur with this process.

Newer techniques have improved Claus method efficiencies, primarily the SuperClaus 99 and 99.5 processes. These applications employ catalysts that selectively oxidize the low concentration  $\text{H}_2\text{S}$  stream remaining after the primary Claus reactions, and increase  $\text{H}_2\text{S}$  removal above 99 % [202]. Additional sulfur removal attained by the SuperClaus 99.5 approach is obtained with a hydrogenation stage that converts  $\text{COS}$ ,  $\text{CS}_2$  and other sulfur compounds to  $\text{H}_2\text{S}$  [74, 91]. These processes attain similar removal efficiencies as those of newer redox and biological approaches, but with added thermal penalties and generally more complex construction. Depending on the gas characteristics and the feasibility of utilizing newer

techniques, the Claus processes are rapidly becoming uneconomical.

Liquid redox is a rapidly expanding approach for direct H<sub>2</sub>S removal as well as sulfur recovery from sour gas streams exiting scrubbers. Several liquid redox systems exist, ranging from a classic vanadium-catalyst approach to newer iron based processes. Vanadium-based catalytic approaches began with the Stretford process in 1959, and now include the Unisulf and Sulfolin processes as well [74]. These techniques apply a dissolved vanadium catalyst to the gas stream via wet scrubbing techniques. Following removal of the vanadium-sulfur compound, anthraquinone disulfonic acid (ADA) is applied for vanadium regeneration. Alternative iron-based approaches such as the popular LOCAT process utilize slurries of chelated iron and a biocide according to Equations 4 and 5 for sulfur removal and regeneration:



Venturis or similar devices are often used to apply the chelate, or the gas stream can be bubbled into auto-circulating tanks of chelate solution [204, 205].

Commercial liquid redox processes have achieved sulfur concentrations lower than 0.5 μL L<sup>-1</sup> in applications such as acetic acid production and Fischer-Tropsch fuels synthesis. Sulfur removal from 100 kg d<sup>-1</sup> to 36 t d<sup>-1</sup> has been conducted in a wide range of environments. High pressures and feedstocks varying from coal to municipal waste have been used [205]. Properly operated, these liquid redox approaches show nearly 100 % removal efficiency with increased catalyst activity, non-toxic reactions, and process flexibility compared to other gas-phase redox approaches (i.e. Claus). Additional advantages are the lack of tail-gas and the production of elemental sulfur via sulfate rather than more harmful SO<sub>2</sub>. The sulfur attained from these

processes is also hydrophilic in nature and has fast soil adsorption rates, making it an ideal agricultural additive for adjusting soil pH. Lower equipment, operation, and maintenance costs are several economic benefits compared with the similarly efficient Superclaus redox method. Liquid redox approaches can suffer from plugging problems created as a result of poor process management; a situation that can lead to microbial growth and environmentally dangerous sulfur salt formations. When operated correctly however, liquid redox achieves superior sulfur removal and recovery compared to the traditional gas-phase redox or solvent absorption methods [74, 205].

A third type of liquid redox reaction is the low-severity process [206].  $\text{H}_2\text{S}$  is absorbed into a polar solvent (*n*-methyl-2 pyrrolidone) where it reacts with *t*-butyl anthraquinone to form hydroquinone and elemental sulfur. The elemental sulfur precipitates out of solution and the hydroquinone is dehydrogenated to regenerate the *t*-butyl anthraquinone, thereby producing solid sulfur and gaseous hydrogen as the primary products. The formation of hydrogen and sulfur rather than sulfur dioxide or water is a major benefit of this liquid redox technique compared with other sulfur recovery processes. Other benefits include atmospheric pressure operation and low energy input. However, *t*-butyl anthraquinone can be lost during the dehydrogenation process by selectivity to anthrone instead of anthraquinone, which would create a waste stream and require constant makeup of anthraquinone. This undesired reaction is reduced by using catalysts that are sufficiently basic. Operating within the ideal temperature range during regeneration also minimizes this occurrence. Separating and oxidizing anthrone in order to recover the anthraquinone is also possible, but this increases cost. Improving the catalysts and optimizing operational conditions are essential to proving large scale feasibility and developing commercial applications that are economical.

In addition to the chemical and physical approaches to sulfur removal, biological and chemobiological processes can be employed [207]. Many kinds of micro-organisms have been studied ranging from photosynthetic autotrophs, such as members of the genus *Chlorobiaciae*, to chemolithotrophs and autotrophs, such as *Thiobacillus denitrificans* [207]. Among potential benefits of a biological approach are generally less extreme reaction conditions and simultaneous removal of H<sub>2</sub>S and other contaminants. For instance, the van Niel reaction common in these processes can remove other acid gases like CO<sub>2</sub>, in addition to target contaminants such as dimethylsulfide (DMS), methyl mercaptan, and other sulfur species (CS<sub>2</sub>, etc.) However, one shortcoming that must be overcome is the extreme susceptibility to process fluctuations. Processes based on living organisms are naturally slower to respond than chemical processes in which a reaction environment can be modified essentially at will. Living creatures also tend to have smaller feasible zones of operating conditions than chemical reactions.

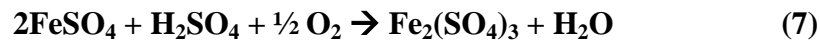
There are several intriguing concepts to overcome the inherent disadvantages of processes based on living organisms. The Thiopaq® and Biopuric® processes, both available on a commercial level, utilize conventional chemical or physical techniques to remove H<sub>2</sub>S from a gas stream prior to a second stage biological process [208]. Recent laboratory attempts with lithoautotrophic organisms, such as common sulfur oxidizers of the genus *Thiobacillus*, have increased potential application to vapor streams with H<sub>2</sub>S concentrations as high as 12 mL L<sup>-1</sup>. Long-term efficiencies greater than 90 % were achieved, with sulfur reduction to concentrations less than 0.5 mL L<sup>-1</sup>. Compared to some other biological processes, the bioreactors tested were able to adjust relatively well to fluctuations in temperatures and concentrations. Unfortunately, 0.5 mL L<sup>-1</sup> is insufficient in many advanced syngas applications. Some recovery rates were also as long as 48 h following some severe process agitations, which is also insufficient for reliable

commercial syngas applications [208]. These processes are also still dependent on the costly conventional chemical and physical techniques to remove sulfur, and only eliminate them from the sulfur recovery process.

A combined chemobiological approach could eliminate some of these cost and performance issues. The two stage BIO-SR process chemically reacts ferric sulfate with hydrogen sulfide and then regenerates the ferric sulfate by biological oxidation using *Thiobacillus ferrooxidans*:



(sulfur precipitates out of solution)



(biological oxidation for regeneration)

The chemical step is carried out by bubbling a sour-gas stream through a liquid solution containing the ferric sulfate. Tested on an industrial scale, it rapidly removes 99.99 % of H<sub>2</sub>S from former Claus feed gas streams, making it potentially attractive for the high volumetric flow rates of syngas [74, 207, 209]. The chemical reaction in the first stage is also better suited to withstand more drastic fluctuations in the syngas streams. Repositioning the biological process to the second step allows for better control of the environment for living organisms and enables complete regeneration of ferric sulfate. Provisions for waste treatment can also be eliminated, as no harmful products or potential byproducts are generated (such as the salts of improperly operated liquid redox processes). These factors reduce energy use and operational costs by <sup>2</sup>/<sub>3</sub> compared to conventional approaches. Although capital costs are comparable, this may lead to savings of nearly 50 % compared to conventional approaches. Large scale process demonstrations and techno-economic analyses are also important for future widespread

acceptance in syngas treatment.

### **Nitrogen Compounds (NH<sub>3</sub>, HCN)**

Cold gas cleaning of nitrogen contaminants, which are primarily NH<sub>3</sub> and HCN, is primarily accomplished with absorption in water. Ammonia is highly soluble in water, which makes it a common absorption liquid for ammonia removal. Even the condensation of water vapor contained in syngas is capable of substantially removing nitrogen compounds when it condenses. For instance, partial condensation of a gas stream with 400 mL L<sup>-1</sup> of water vapor occurred during tar scrubbing at 50 °C with rape oil methyl ester (RME) organic solvent [210]. The condensate removed ammonia at 30 % efficiency with initial concentrations of 2 mL L<sup>-1</sup> ammonia. Efficiency increased to 50 % with lower initial ammonia concentrations. Similarly, the condensate created while using a chilled condenser to remove the water in a syngas stream derived from sewage sludge resulted in more than 90 % reduction in NH<sub>3</sub> [211]. Additional water introduced by conventional wet scrubbers (as previously discussed) will improve these removal efficiencies. Ammonia can be removed down to the picoliter per liter levels depending on the upstream processing and feedstock, which is suitable even for low tolerance applications [212].

Other gas species such as CO<sub>2</sub> and SO<sub>2</sub> can impact the absorption of ammonia into the aqueous scrubbing medium. Substantial amounts of CO<sub>2</sub> in syngas for instance will encourage both the acid gases and the ammonia to move to the aqueous phase, thereby enhancing syngas purification. (The complex reactions responsible for this phenomena are discussed in detail by Bai and Yeh [213].) This phenomenon is actually exploited in several applications, such as acid gas removal with aqueous ammonia as the scrubbing agent. Aqueous ammonia can actually outperform conventional amine-based processes such as MEA (see section 4.3), with acid gas

removal capacities approaching  $\text{CO}_2$  900  $\text{g kg}^{-1}$  of  $\text{NH}_3$ . In syngas streams with high ammonia concentrations, this process chemistry can be an important contributor in determining the final composition of the gas stream.

Multiple other techniques including adsorption and biological processing are widely used for cleaning air, but many have disadvantages when applied to synthesis gas streams. For instance, activated carbons and zeolites have been widely applied for air purification [214]. However, the high levels of gaseous species in syngas that could be adsorbed make throw-away (single use) sorbent applications uneconomical. Selectivity of the sorbents for compounds such as COS and  $\text{H}_2\text{S}$  also makes it difficult to safely and economically regenerate the sorbent. Biological processes such as trickling filters offer similar performance as seen with sulfur removal (section 4.3). Nitrogen is effectively removed with zero hazardous waste generation, but large sizes are required for the relatively slow removal rate and  $\text{CO}_2$  is produced as a byproduct. Difference between air and syngas compositions may also inhibit biological activity. These issues with adsorption and biological treatments, coupled with the efficiency and ease of water scrubbing makes absorption with water the most logical approach for CGC of nitrogen in the near future.

### **Alkali Compounds**

Temperature reduction allows alkali vapors to condense and agglomerate into small particles or combine with tars [46]. Most alkali compounds condense out of the gas stream by  $300^\circ\text{C}$ , and are thus removed simultaneously with particulate and tar in wet scrubbers. The cleaning techniques for removing tar and particulate at low temperatures are also therefore adequate for alkali removal.

However, an additional technique that is available to reduce the alkali content of syngas that is not feasible for tars and particulate is removing the alkali from gasification feedstock. There is



widespread interest in this approach, known as pretreatment, but it is not extensively discussed here because it is not a direct gas cleanup technique. The reader is encouraged to visit the literature below for further details.

Biomass pretreatment is a preventative measure that takes place at low temperatures with one of two approaches. Low alkali content biomass can simply be selected as the feedstock, possibly by using the alkali index (low alkali content to heating value ratio). Biomass can also be leached of the primarily water soluble alkali content via washing and mechanical dewatering [94].

A majority of alkali in biomass is water soluble, and up to 95 % of some feedstock is in either water soluble or ion exchangeable forms [215]. Water washing or leaching is therefore a common approach for removing many alkali compounds. An additional possibility is to mechanically dewater the washed biomass with processes similar to those commercially used for sugar extraction from sugarcane. A study in which banagrass was mechanically dewatered, rinsed, and dewatered again removed a majority of the alkali as well as other compounds, resulting in an overall ash reduction of 45 % [216]. 90 % of potassium was removed along with 68 % of magnesium and sodium, 72 % of phosphorous, 98 % of chlorine, and even 55 % of sulfur. Washing with acid can also be used instead of water. Pyrolysis of wood waste and wheat straw showed that an acid pretreatment could reduce alkali emissions by 70 %, compared to only 30% reduction with a water wash [217].

The feasibility of using a particular alkali pretreatment depends on the feedstock and overall cost analysis for the end-use application. Additional costs incurred for the washing, drying, waste treatment, and any mechanical processes involved may be uneconomical in certain circumstances. For instance, alkali is easily removed from herbaceous biomass with water or

acid leaching, but woody biomass contains more organically bound alkali which is not as easily removed [217].

### Chlorine

Chlorine compounds exist in syngas as either gaseous HCl or solid particles of ammonium chloride (NH<sub>4</sub>Cl). Wet scrubbing is commonly employed, which also is effective in removing particulate matter, tar, and alkali. Chloride removal takes place via two primary mechanisms: deposition of ammonium chloride salts and absorption of HCl vapor.

Gasification generates HCl and NH<sub>3</sub>, which exist as gases until the syngas is cooled to about 300 °C. At this point the HCl reacts with ammonia in the gas stream to form ammonium chloride:



Although this salt is entrained in the gas flow, the fine particles can agglomerate to form larger particles and accumulate on surfaces, leading to fouling of process equipment. A well designed gasifier system will maintain syngas above 300 °C until gas cleaning can be accomplished.

In a wet scrubber, cooling occurs very quickly, potentially limiting the amount of NH<sub>4</sub>Cl formed. Regardless, the wet scrubber is effective in absorbing both forms of chlorine from the gas stream. Although HCl is highly soluble in water, its removal can still be enhanced by addition of sodium carbonate to the water [202].

These very efficient techniques also create highly acidic compounds and filter cake, which can reduce process efficiency and damage equipment. Depending on the inlet gas temperatures, choosing proper non-reactive materials, such as tantalum, specific alloys, glassware, ceramic,

etc. can mitigate corrosion concerns [202]. Alternative methods have recently been developed to minimize these corrosion concerns and are subsequently described in the following WGC section.

### **Warm Gas Cleanup (WGC)**

Several cleanup processes operate at temperatures higher than ambient conditions, but lower than the hot cleanup applications. Although some may be capable of operating at hot cleanup conditions, they are widely employed at more moderate temperatures due to several process advantages. In general, the risks associated with extreme operating conditions as well as higher costs of materials are avoided. These processes all avoid water condensation, but allow some tars, alkalis and chlorides to be condensed and removed. Maintaining temperatures above the point of water condensation also eliminates water treatment often required in CGC.

#### **Particulate Matter**

Three particulate removal technologies are suitable for WGC. Two of these, gas cyclones and electrostatic precipitators have been previously discussed. The third is fabric filters, which utilize fabrics woven from temperature-resistant fibers. These fabric filters operate on the same principle as barrier filters, which capture particulate matter by inertial impaction, interception, and diffusion into the filter media. They also consider several similar factors in their construction, such as the maximum allowable pressure drop before the filter cake is removed and the type of cleaning technique utilized. In fabric filters, filter cleaning can be accomplished by methods of varying severity, including mechanical shaking, reverse flow, rapping, or compressed gas pulses. Methods using reverse flows must use a gas that is acceptable for a syngas environment, which make them slightly more complicated than typical air-cleaned particulate applications.

Another important consideration when designing the fabric filter is establishing an acceptable filtration velocity, usually stated as the flowrate per area of fabric (i.e.  $\text{m}^3 \text{s}^{-1} \text{m}^{-2}$ ). This is used to determine the total effective fabric area of the filter, which is then used to size the filter equipment.

Cleaning media are a final factor crucial in the design of fabric filters. Materials can be various sizes with very different characteristics depending on their composition. For instance, synthetic polymers with very little crystallinity such as polyvinylchloride tend to melt before reaching their combustion temperature and are limited to lower temperatures [58]. The fabrics utilized are typically restricted to between  $90^\circ\text{C}$  and  $250^\circ\text{C}$  in order to limit exposure to liquids and remain under the temperature tolerance of the materials [58]. Higher temperatures are possible, but demand costly metallic composites. For instance, Nextel's 3M material can withstand temperatures greater than  $700^\circ\text{C}$ , but is an expensive aluminum, boron and silica oxide composite [100]. In lieu of these exotic materials, lower temperature construction fabrics include common materials such as polyester, polypropylene, and polypeptide (wool). Some materials such as co-polyamide, silicate glass, or polytetrafluorethylene (PTFE) can tolerate slightly higher temperatures approaching  $260^\circ\text{C}$ .

### **Tars**

WGC technologies are now being developed for tar removal. These techniques attempt to combine the environmental and economic benefits of HGC and CGC removal techniques, without succumbing to their disadvantages.

The OLGA technique (a Dutch acronym for oil-based gas washer) removes and reuses valuable tar components without costly waste remediation [218]. Operating between  $60^\circ\text{C}$  and

450 °C, the process shown in Figure 12 uses oil rather than water to scrub tars from the gas stream. Similar to water scrubbing, condensable tars (classes 1, 4, and 5) are recovered by condensation as temperature is reduced below the tar dew point. Lighter tar compounds such as phenols and 1 or 2 ring aromatics (classes 2 and 3) are subsequently removed via absorption into a second liquid scrubbing medium. When applied downstream of an air blown biomass gasifier producing 500 kW of thermal energy, this process completely removed heavy tars and over 99 % of phenol and light heterocyclic tars. This correlates to a tar dew point reduction below 10 °C from an original gas stream containing tar concentrations of 10 g m<sup>-3</sup> to 20 g m<sup>-3</sup>. The cleaned gas stream was used in an IC engine and had effects that were similar to that of operation on natural gas, indicating overall success of the cleanup process.

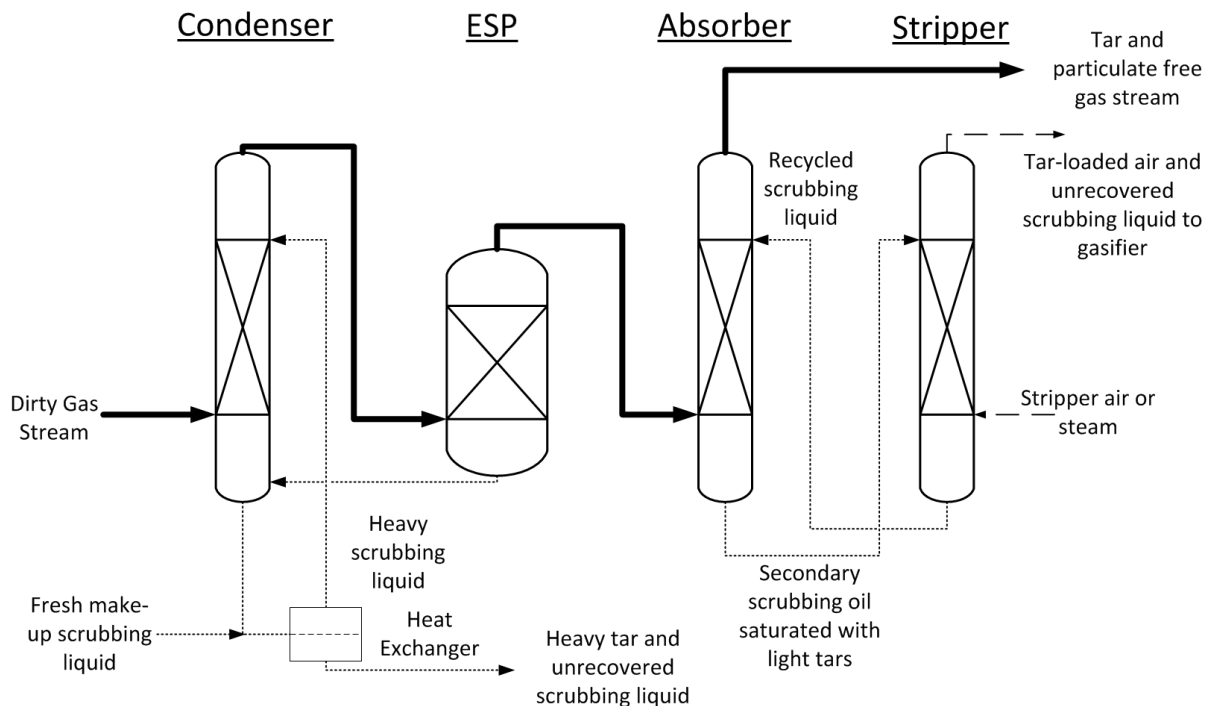


**Figure 12:** Simplified OLGA process diagram [34, 35]

The OLGA process offers several advantages compared to conventional CGC and HGC techniques. This approach eliminates the operational and economic challenges of catalytic and

high temperature tar removal. Eliminating waste water remediation is another prominent example. Highly toxic PAH compounds are always a concern, but these tars are generally easier to remove from water given their volatility and low water solubility [33]. The greater issue is highly soluble tar, particularly phenol. These smaller polar compounds dissolve easily in water and are more difficult to remove. Costly waste water treatment is avoided by removing these tars with oil. The oil can then be easily regenerated or used as feedstock.

The valued products of gasification also remain unaffected by OLGA. Primary light components, such as  $C_2H_4$ ,  $CH_4$ ,  $CO$ , and  $H_2$ , remain relatively unchanged when compared to the use of thermal and catalytic tar reduction methods. Valuable tar compounds that are extracted with the oils can also be utilized rather than discarded as they are during water scrubbing. The primary condensed tars can serve as additional feedstock in many carbon-conversion processes, such as those in petroleum refineries. Even the acceptably small losses of scrubbing liquid and the remaining tar that escapes during regeneration could be recycled to the gasifier [218].

The patent holders, the Energy Research Center of the Netherlands (ECN), have successfully demonstrated OLGA at several facilities [32, 122, 218]. Applications now include syngas cleanup from gasifiers producing as much as 800 kW of thermal energy, and have reduced tar dew points to below  $0^\circ C$ . The unit operations involved in OLGA are commercially mature, and enable these larger facilities to capture benefits associated with economies of scale. The low tar dew points have now also made expansion to more demanding applications possible, such as catalysis for synthetic natural gas (SNG) [32].

### **Chlorine (HCl)**

The semi-wet removal process for removing HCl occurs at temperatures just above the condensation point of water. Originally developed to treat flue gas from waste incineration, this

process uses a lime-slurry injected with a state-of-the-art atomization disk. The atomizer uses a rotational disk rather than variation in flow rate to atomize the spray. Improved dispersion and absorption characteristics of the spray enhance overall efficiency with minimal slurry addition. Upon contacting the gas stream,  $\text{Ca}(\text{OH})_2$  rapidly reacts with HCl to ultimately form  $\text{CaCl}_2$  and  $\text{H}_2\text{O}$ . A majority of the particles are then carried along in the gas stream where they are removed with a bag filter at around  $130^\circ\text{C}$  to  $140^\circ\text{C}$ . This avoids the previous complications of caked particulate deposits and corrosive liquids. Results indicated that greater than 99.5 % HCl was removed with an additional 94 % removal of  $\text{SO}_2$  [219].

Formation of  $\text{CaCl}_2$  and  $\text{H}_2\text{O}$  facilitates easier waste handling and cleanup. However, leachate produced from the landfill disposal of  $\text{CaCl}_2$  can cause environmental damage if left untreated. One alternative may be a semi-wet scrubbing process involving an Mg-Al oxide. Adding Mg-Al oxide at  $130^\circ\text{C}$  has removed up to 97 % of HCl. The resulting Cl-Mg-Al LDH (layered double hydroxide) compound can then be calcinated. This regenerates the Mg-Al oxide sorbent for reapplication, and results in a concentrated HCl stream. This process eliminates the unwanted  $\text{CaCl}_2$  and produces HCl as a byproduct with little additional treatment and no waste. Optimal efficiency for scalable designs is contingent upon further experimentation and a better understanding of other chemical reactions complicating the process [220].

### **Additional Contaminants**

Trace contaminants are mineral and metallic elements present in all carbonaceous feedstock, usually in quantities less than 0.1 % [221]. Hg, As, Se, Cd and Zn have received the most attention due to public health concerns and government legislations. Mercury has been the most emphasized contaminant because of numerous equipment failures associated with mercury amalgam formations, especially in natural gas applications [47]. This past focus on mercury is

now supplemented with current techniques that remove most other trace contaminants as well.

Initially, the Low Temperature Separation (LTS) process was used in 1972 to remove mercury by condensation. It used glycol and a system of heat exchange and expansion to condense mercury from the gas stream, but removal to levels of  $1 \mu\text{g m}^{-3}$ – $15 \mu\text{g m}^{-3}$  are orders of magnitude higher than the required purity for current applications [47]. Thus, trace contaminant removal is currently done with either regenerable or non-regenerable adsorption onto a solid sorbent.

IGCC and other combustion applications use solid sorbents such as silica, bauxite, kaolinite, zeolite, lime, activated carbon, and other combinations of active elements and supports. Limestone, fly ash, alumina, and metal oxide mixtures have also been tested in conditions similar to gasification environments. Fly ash, limestone, and metal oxides show the highest As and Se removal, while fly ash is also effective in removing Cd and Zn. These promising materials are an important focus as they are currently relevant in gasification, especially limestone, mixed metal oxides, and fly ash [221].

Industrial natural gas applications have long utilized adsorption onto activated carbon for mercury removal. When it is impregnated with  $100 \text{ g kg}^{-1}$  to  $150 \text{ g kg}^{-1}$  sulfur, mercury in the gas stream reacts with the sorbent to form very stable HgS. The sorbent and HgS mixture is then disposed of, or it is incinerated for condensation and recovery of the Hg. In the past, activated carbons have typically provided 90-95 % removal efficiency of Hg. A new activated carbon from Calgon Carbon Corporation improved this removal in commercial applications to 99.99 %, even for levels up to  $\sim 50 \mu\text{g m}^{-3}$  (indicative of bituminous coal-derived syngas). Mercury carrying capacity of activated carbon beds are often affected by other trace contaminants, such as



nickel and iron carbonyls ( $\text{Ni}(\text{CO})_4$  and  $\text{Fe}(\text{CO})_5$ ). The adsorption of these contaminants is usually an acceptable compromise in applications such as IGCC or Claus Sulfur Recovery Units, since those compounds also form deposits on catalysts or turbines [47].

Zeolites are another common adsorbent, also developed by the natural gas industry. Zeolites with a small outside coating of silver such as HgSIV were created principally for drying of natural gas, but have a secondary purpose of removing mercury. These sorbents generally have a low removal capacity, which limits their use as a throw away sorbent. However they still warrant attention in commercial gasification trials since they can be regenerated and have a high mercury removal efficiency to less than  $0.01 \mu\text{g m}^{-3}$  [47].

Operating at higher temperatures and pressures offers efficiency improvements for many syngas applications, such as IGCC or catalytic synthesis. A new regenerable sorbent developed by TDA Research Inc. can be applied at high temperature and pressure. Greater than 95 % mercury removal was demonstrated with syngas derived from various lignite and bituminous coals, as well as the additional removal of trace metals Cd, As, and Se. Waste is also minimized by using regeneration. Mercury desorption during regular operation is also reduced due to substantially different conditions required for regeneration. The sorbent also functioned well as a guard bed for removing residual sulfur by three or more orders of magnitude from as much as  $10 \mu\text{L L}^{-1}$  to picoliter levels, although exposure to higher levels would cause more rapid sorbent deactivation. Primary benefits for this adsorbent are industrial-scale production capability and the high contaminant removal at warm temperatures and pressures up to 1825 kPa [222].

Silver-loaded adsorption beds are another category of promising adsorbents for trace contaminants. Past research has concluded that silver on activated carbon achieved high removal

efficiency and high capacity, but was however non-regenerable. In order to commercially use expensive silver adsorption, a regenerable sorbent must be developed [47].

## Conclusion

Syngas has many applications, ranging process heat and power to chemical and fuels synthesis. Gasifying contaminated feedstock to syngas offers an opportunity to transform otherwise polluting combustion fuels or idle waste into relatively useful materials. Gasified biomass is a versatile supplement to a primarily fossil-based energy infrastructure, and provides an alternative renewable source of chemicals and fuels for a growing populace. Raw syngas unfortunately contains contaminants derived from the thermochemical process or impurities in the feedstock that cause problems during use. Syngas must therefore be relatively purified of the contaminants, specifically particulate matter, tar,  $\text{H}_2\text{S}$ ,  $\text{NH}_3$ , alkali formations, halides and trace contaminants.

There are numerous processes available to provide a relatively clean  $\text{H}_2$  and CO syngas stream. These technologies can be roughly classified into three regimes according to their operational temperature: hot gas cleanup (HGC), cold gas cleanup (CGC), and warm gas cleanup (WGC).

HGC has received the greatest attention in the recent past, especially in the removal of tars, particulate matter, and sulfur. Several mature technologies have existed for decades to remove particulate matter, including cyclones, electrostatic precipitators, and barrier filtration. The complex tars that are created in gasification reactions are typically reduced to lighter compounds by thermal and catalytic methods. Thermal techniques experience some losses and inefficiencies when raising the temperature by partially combusting the syngas stream. Most research has

therefore focused on overcoming the coking, deactivation and economic challenges associated with catalytic methods for use at slightly lower temperatures. Removing sulfur at high temperatures is primarily done with adsorption onto a variety of solid sorbents. These methods may provide gains in thermal efficiency, process simplicity and the potential for cost reduction using regenerable sorbents, but overcoming activity losses and increasing sorbent lifetime remains challenging.

CGC is a mature area of gas cleanup and typically uses water or liquid absorption to remove contaminants. Wet scrubbers are perhaps the most common, and are effective for removal of nearly all contaminants. Sulfur has also been a prime focus of CGC, and mature technologies have been employed globally that also recover sulfur as a byproduct. Disadvantages of conventional CGC sulfur scrubbing have led to attempts in combining rapid and robust chemical approaches with the cost effectiveness of biological applications.

WGC is becoming increasingly important with respect to tar and chlorine removal. A new oil based washing technique is particularly promising for tar and residual particulate removal. This approach may eliminate the problematic waste water treatment required with current scrubbing techniques, while simultaneously capturing the valuable tar components for further use.

### **Acknowledgments**

The authors gratefully acknowledge financial support from the ConocoPhillips and the US Department of Energy during the preparation of this review article. We also appreciate the assistance of the numerous individuals who made the information above available for writing this review.

### **CHAPTER 3. PROOF OF CONCEPT WORK FOR DEVELOPING A NOVEL ANALYTICAL METHOD FOR HOT GAS STREAM ANALYSIS BASED ON TWA-SPME**

The following article was published in the Journal of Chromatography A to highlight the novel analytical technique developed for syngas tar measurement based on solid-phase microextraction [223]. Time-weighted average (TWA) passive sampling using solid-phase microextraction (SPME) and gas chromatography was investigated as a new method of collecting, identifying and quantifying contaminants in process gas streams. Unlike previous TWA-SPME techniques using the retracted fiber configuration (fiber within needle) to monitor ambient conditions or relatively stagnant gases, this method was developed for fast-moving process gas streams at temperatures approaching 300 °C. The goal was to develop a consistent and reliable method of analyzing low concentrations of contaminants in hot gas streams without performing time-consuming exhaustive extraction with a slipstream. This work in particular aims to quantify trace tar compounds found in a syngas stream generated from biomass gasification. This paper evaluates the concept of retracted SPME at high temperatures by testing the three essential requirements for TWA passive sampling: (1) *zero-sink assumption*, (2) *consistent and reliable response by the sampling device to changing concentrations*, and (3) *equal concentrations in the bulk gas stream relative to the face of the fiber syringe opening*. Results indicated the method can accurately predict gas stream concentrations at elevated temperatures. Evidence was also discovered to validate the existence of a second boundary layer within the fiber during the adsorption/absorption process. This limits the technique to operating within reasonable mass loadings and loading rates, established by appropriate sampling depths

and times for concentrations of interest. A limit of quantification for the benzene model tar system was estimated at  $0.02 \text{ g m}^{-3}$  (8 ppm) with a limit of detection of  $0.5 \text{ mg m}^{-3}$  (200 ppb). Using the appropriate conditions, the technique was applied to a pilot-scale fluidized-bed gasifier to verify its feasibility. Results from this test were in good agreement with literature and prior pilot plant operation, indicating the new method can measure low concentrations of tar in gasification streams.

## Introduction

*Sampling and Analysis in Thermochemical Processing.* Thermochemical processing of carbonaceous materials, such as biomass or municipal solid waste, is a potential pathway for producing renewable fuels and chemicals. Gasification in particular is a robust technology that is capable of converting contaminated feedstock into a useable product, in this case, a hot (800 to 1200 °C) synthetic gas stream composed primarily of carbon monoxide (CO) and hydrogen (H<sub>2</sub>). This ‘syngas’ is valuable for many commercial applications, from fuel and chemical synthesis to raw heat and power operations.

Raw syngas produced by gasification contains numerous contaminants either derived from impurities in the feedstock or created as a byproduct of the process. These contaminants include particulate matter, ammonia (NH<sub>3</sub>), hydrogen chloride (HCl), hydrogen sulfide (H<sub>2</sub>S), and heavier oxygenated compounds known as “tars.” Tars are a particularly serious issue as they tend to condense from the vapor-phase as the temperatures fall below 400 °C, which leads to deposits that clog pipes and equipment. Cleaning methods often leave residual contamination that can still be problematic in several highly sensitive technologies, such as catalysis [224].

Numerous analytical techniques are available for quantifying these contaminants, but they are largely based on preparation steps that use wet chemical methods [225]. These methods are performed offline, which is a significant disadvantage to monitoring and quickly controlling a process in real-time to maintain optimum efficiency. Some devices may monitor specific contaminants online during the process, including GC-TCD (thermal conductivity detector), NCD (nitrogen chemiluminescence detector), and SCD (sulfur chemiluminescence detector) among others. However these devices are typically expensive and limited to detecting single types of contaminants (i.e.  $\text{NH}_3$  or  $\text{H}_2\text{S}$ ).

Heavy molecular weight, slightly oxygenated compounds known as tars are a particularly difficult contaminant to quantify [224]. Due to their varied composition (usually hundreds of different compounds), they are typically collected by exhaustive extraction and gravimetrically measured. A slipstream (i.e. a small sample stream diverted from the main process stream) of the syngas is passed through a series of condensers or impingers, sometimes with isopropanol as a solvent. Differences in mass are calculated for the equipment before and after the tars are collected. Clear guidelines for this conventional tar measurement and a closely related solvent-free technique have been documented in the literature [16, 26].

The method of exhaustive extraction is difficult to apply at low concentrations due to low mass accumulation. For example, removing tar by 99% from a typical fluidized bed gasifier would still yield  $\sim 100 \text{ mg m}^{-3}$  of tar ( $\sim 30 \text{ ppm}_w$  at standard conditions) [226]. Only  $\sim 0.5 \text{ g}$  of sample would be collected after nearly 17 h of sampling at a higher than typical flow rate of 5 SLPM. In addition to this inefficient data gathering technique, maintaining steady-state process conditions and the sampling equipment for that extended timeframe is often difficult. The

conventional tar measurement techniques are therefore impractical for monitoring low concentrations, which can still cause damage to catalysts and reduce process efficiency.

Sampling and sample preparation are notorious for taking the most time during an analytical process, typically accounting for over 80% of analysis time [36]. In the case of trace tar analysis, this could be even greater due to the long sample times required for collecting significant gravimetric tar data. More likely is the inability of maintaining steady state conditions long enough to collect meaningful samples. In the event that a statistically meaningful amount of tar can be collected, the light tars condensed in the impinger train are likely to be highly diluted with water that has condensed from the many hours of sampling. This makes it increasingly difficult to obtain accurate and precise data on the quantity of light tar that has also condensed. Any ability to obtain information on process kinetics also becomes extremely complicated if not impossible with such a slow and time-consuming technique. The result in many cases is that potentially useful data is discarded as unquantifiable. Developing an alternative analytical technique based on representative sampling to quantify trace tars will eliminate these issues of tar quantification. This in turn will improve the performance of gas cleaning equipment and downstream applications.

*Time-weighted average (TWA) sampling with SPME.* Solid-phase microextraction (SPME) is a sample collection and preparation method that does not require long sample times to obtain a representative sample using exhaustive extraction. It is a relatively new approach that has been extensively applied to environmental, agricultural, and pharmaceutical applications [227-229]. It operates by collecting volatile analytes on a small fiber that is coated with an extraction phase,

which is then directly injected into a gas chromatograph (GC) or liquid chromatograph (LC) coupled to a detector, such as flame ionization (FID) or mass spectrometry (MS) [228, 230, 231].

SPME can detect pico-grams or less of some compounds, equating to part per trillion (ppt) levels or lower [36, 232]. Tar concentrations can be several hundred parts per million (ppm), and can easily saturate a fiber's extraction phase when exposed to the gas stream. This leads to samples that may not be representative of the average concentration in the gas stream. Retracted time-weighted average (TWA) SPME sampling addresses this issue by keeping the extraction phase retracted within the protective needle housing. Diffusion of the analytes from the environment to the extraction phase occurs through the stagnant boundary layer between the tip of the fiber and the tip of the needle housing. Under conditions where diffusion can be approximated as a constant value, the rate of sample collection can be controlled by the depth of fiber retraction. Retracting the fiber farther within the needle housing can facilitate sampling at higher concentrations, or the sampling time can be extended to several minutes or hours to establish a more representative average analyte concentration.

Other advantages of SPME-TWA using a retracted fiber include (a) reducing analysis time from several hours per sample to several minutes (b) simplified quantification because a retracted fiber is independent of gas stream velocity [233-235], (c) small particles in the gas stream are not a concern since the fiber is protected by the outer needle housing, (d) the SPME sampler is sealed at the top to eliminate the possibility of gas flowing through the fiber syringe, which could alter results or damage the fiber. Unlike the equilibrium SPME techniques, applying the TWA-SPME method avoids the need for extra sampling equipment (heated chambers, sampling lines, and vacuum pumps) since it is used directly on process piping, and



may potentially eliminate the need to calibrate the fiber for compounds of interest [236]. Finally, SPME sampling experience continues to grow, offering information on many different organic and inorganic compounds at a wide range of molecular weights and sampling environments, which aids in more rapid development for future applications [227, 237-240].

The principle of the TWA sampling technique follows Fick's first law of diffusion: the amount collected on the fiber is proportional to the molecular diffusion rate ( $D_g$ ) of the analytes in the vapor and the area ( $A$ ) of the needle housing opening, and is inversely proportional to the diffusion path length ( $\delta$ ), which is the boundary layer of stagnant gas inside the needle housing between the tip of the needle and the tip of the coated fiber. As long as the concentration at the tip of the coated fiber is small compared to the free-stream value, the amount extracted is proportional to the integral of the concentration over a sampling time ( $t$ ):

Equation 1: 
$$n = D_g \frac{A}{\delta} \int C_g(t) dt$$

where:

$A =$  open area of needle housing [ $L^2$ ]

$t =$  sampling time [ $t$ ]

$D_g =$  molecular diffusion coefficient for the sample in the gas stream [ $L^2 t^{-1}$ ]

$C_g =$  instantaneous concentration in the gas stream [ $M L^{-3}$ ]

$n =$  mass extracted (determined by analytical equipment) [ $M$ ]

$\delta =$  boundary layer (or length of diffusion path inside the needle) [ $L$ ]

The overall objective of this work is to develop a TWA-SPME technique to improve the speed and accuracy of analyzing process gas streams for difficult-to-measure species. Unlike previous TWA applications, this research involves rapidly moving gas streams at elevated temperatures (~115 °C), with application to a complicated gas matrix in actual process environments. This paper in particular examines the TWA-SPME passive sampling concept for application to trace tar measurements in syngas process streams. As the authors are unaware of any application of SPME directly to gasification streams, this work also forms a basis for future analysis of syngas. Specifically, the three necessary requirements for TWA passive sampling were addressed: (1) *zero-sink assumption*, (2) *consistent and reliable response by the sampling device to changing concentrations*, and (3) *equal concentrations in the bulk gas stream relative to the face of the fiber syringe opening*. Benzene in nitrogen was used as a model compound in this proof-of-concept evaluation. Multiple concentrations, sampling times, and boundary layer lengths (i.e. depths of SPME fiber retraction) were tested to determine the limits of method application.

The experimental program included both bench-top experiments and pilot plant trials in a biomass gasifier. The bench-top experiments were conducted to develop the TWA-SPME method, while the pilot plant trials provided an opportunity to test the technique in a realistic gas matrix.

## Experimental Section

**Chemicals.** Benzene (Sigma-Aldrich CHROMASOLV®Plus, for HPLC  $\geq 99.9\%$ ) was used as a model tar compound within an ultra-high-purity nitrogen gas stream (99.995%) to prove the concept of predicting tar concentrations in syngas using SPME. All work with chemicals was performed following lab safety protocols, using vented fume hoods and approved personal protection gear.

**Materials.** A manual SPME device was equipped with a Carboxen/polydimethylsilosane (85  $\mu\text{m}$  CAR/PDMS - Supelco) fiber. This fiber was recommended by the Supelco fiber selection guide for gases and low molecular weight compounds, which are the prominent compounds in the sample matrix. An additional benefit for TWA passive sampling is the high capacity of Carboxen, which facilitates sampling at higher concentrations or longer periods of time [241].

This fiber was also chosen in large part based on its performance during preliminary tests on the process development unit (PDU) in which final method testing will be performed. (An overview of this gasification and cleanup system is available in Woolcock et al [6].) The gasifier in this pilot scale PDU produces a syngas that is passed through an oil scrubbing unit for tar removal. Tests were performed downstream of the oil scrubbing unit using several different fibers, of which CAR/PDMS showed the best results (Figure S1). (See supplementary material.)

**SPME-TWA Procedure.** The SPME concept uses the TWA passive sampling method with a retracted fiber to provide quantitative information on compound concentrations. Equation 1 can be simplified to determine TWA gas stream concentration (assuming a steady average concentration is used during the time interval) according to the following relationship:

Equation 2: 
$$C_g(t) = \frac{n(t)\delta}{D_g At}$$

where:

$A$  = SPME needle opening (based on inside diameter)[ $\text{cm}^2$ ]

$t$  = sampling time [s]

$D_g$  = gas-phase molecular diffusion coefficient [ $\text{cm}^2 \text{s}^{-1}$ ]

$n(t)$  = mass extracted in a given amount of time [g]

$\delta$  = boundary layer (or length of diffusion path) during extraction [cm]

$A$ ,  $t$ , and  $n(t)$  are known values or can be determined using common analytical equipment, such as mass spectrometry (MS) or flame ionization detection (FID) [242].  $\delta$  represents the diffusion path length, and depends on the position of the fiber retracted within the needle (see Figure S-1). Similar to the work by Koziel et al. (1999, 2001), a special SPME housing was modified to enable retraction depths of 5 mm, 10 mm, 15 mm, and 20 mm in addition to the 3.3 mm depth possible with the original device [243, 244].

The final unknown parameter in Equation 2 is  $D_g$ . Diffusivity is a function of pressure, temperature, and gas stream composition (i.e. the molecular sizes of compounds) [245]. Several theoretical models are available to estimate  $D_g$ , such as the Wilke-Lee (WL), Fuller-Schettler-Giddings (FSG) and Huang *et al* [245-247]. At the temperatures of interest for measuring trace tars in syngas (100 to 125 °C), these models estimate  $D_g$  for benzene as 0.130 to 0.164  $\text{cm}^2 \text{s}^{-1}$ . Assumptions necessary in these models also cause variability, e.g., at  $T = 115$  °C (the temperature ultimately used in lab-scale experiments here) the models suggest a theoretical  $D_g$  value of 0.138 to 0.156  $\text{cm}^2 \text{s}^{-1}$ .

Although it is possible to model molecular diffusion coefficients in a mixture, the complexity of the calculations and accuracy of the results are diminished as more components are added to the mixture [248]. Syngas is composed of multiple gases and real tar consists of hundreds of compounds. While several compounds will likely be present at higher concentrations than the majority of other compounds, the system is far from the simple binary systems used by many models. The use of SPME for quantitative analysis of tar requires an experimental method that can establish a collective (apparent)  $D_g$  value for several of the important compounds while in the presence of other compounds. Benzene in  $N_2$  is used as a proof-of-concept approach that can be compared to theoretical models because it is a bimolecular system. Once the experimental system is proven to produce results similar to theory (i.e. an experimental  $D_g$  value similar to the theoretical  $D_g$  value), the number of quantifiable compounds in the system can be expanded to include other major tar compounds.

Three prerequisites must be satisfied when experimentally determining  $D_g$  using retracted SPME:

(1) The rate of mass loading must not change due to the collection of analytes onto the fiber. This is known as satisfying the ‘zero-sink’ assumption [249]. It only occurs during early stages of extraction when the amount of analyte extracted on the fiber is significantly less than when at equilibrium with the sample matrix or at fiber coating saturation [36]. As more analytes are collected onto the fiber, the rate of mass collection is reduced as a consequence of the decreasing concentration gradient, resulting in a deviation from the zero-sink behavior.

(2) The concentration of the sampled species in the bulk gas of the experimental system ( $C_{\text{bulk}}$ ) and at the face of the SPME needle opening ( $C_{\text{face}}$ ) must be equal. This assures that a

secondary diffusion boundary layer does not exist outside the tip of the needle (i.e. the diffusion path length ends at the syringe opening). Previous work with BTEX gas standard [233] has shown that a minimum gas flow velocity of  $\sim 10$  to  $25 \text{ cm s}^{-1}$  will make any potential resistance from a secondary diffusion layer negligible. In fact, maintaining a gas flow higher than  $0.6 \text{ cm s}^{-1}$  has shown no significant differences between the face and bulk concentrations for multiple compounds of similar nature to syngas proxy-tars [241].

(3) The sampling system must respond to changing concentrations in a consistent or predictable fashion. A design of experiments is necessary to satisfy this requirement. Specifically,  $n(t)$  must change proportionally to  $t$ ,  $n(t)$  must be inversely proportional to  $\delta$ , and no significant differences should exist between the  $D_g$  values calculated at each of the experimental conditions; the experimental  $D_g$  value must also be reasonably similar to theoretical estimations at the experimental temperature and pressure.

The constant  $D_g$  assumption was tested by maintaining a steady concentration and systematically varying  $t$  and  $\delta$ . Changing  $t$  and  $\delta$  should effectively alter the  $n(t)$  so that no statically significant differences in the experimental  $D_g$  can be detected:

Equation 3: 
$$D_g = \frac{n(t)\delta}{C_g(t)At}$$

Precise concentrations of benzene in  $\text{N}_2$  ( $C_g$ ) for use in Equation 3 were generated via the experimental system shown in Figure 1 (adapted from [250]) An Alicat flow controller provided precise flow of  $\text{N}_2$  gas into the system. A <sup>kd</sup>Scientific Model 200 series syringe injector was used to inject benzene with a Hamilton 1 mL gastight syringe. An online mass spectrometer (Pfeiffer

ThermoStar/GSD 301 T3) verified consistent benzene concentrations throughout experiments. Near atmospheric conditions were maintained, and individual heat tracing zones sustained proper temperatures so that conditions for constant diffusivity (according to pressure, temperature and molecular composition in equation 3) could be sustained.

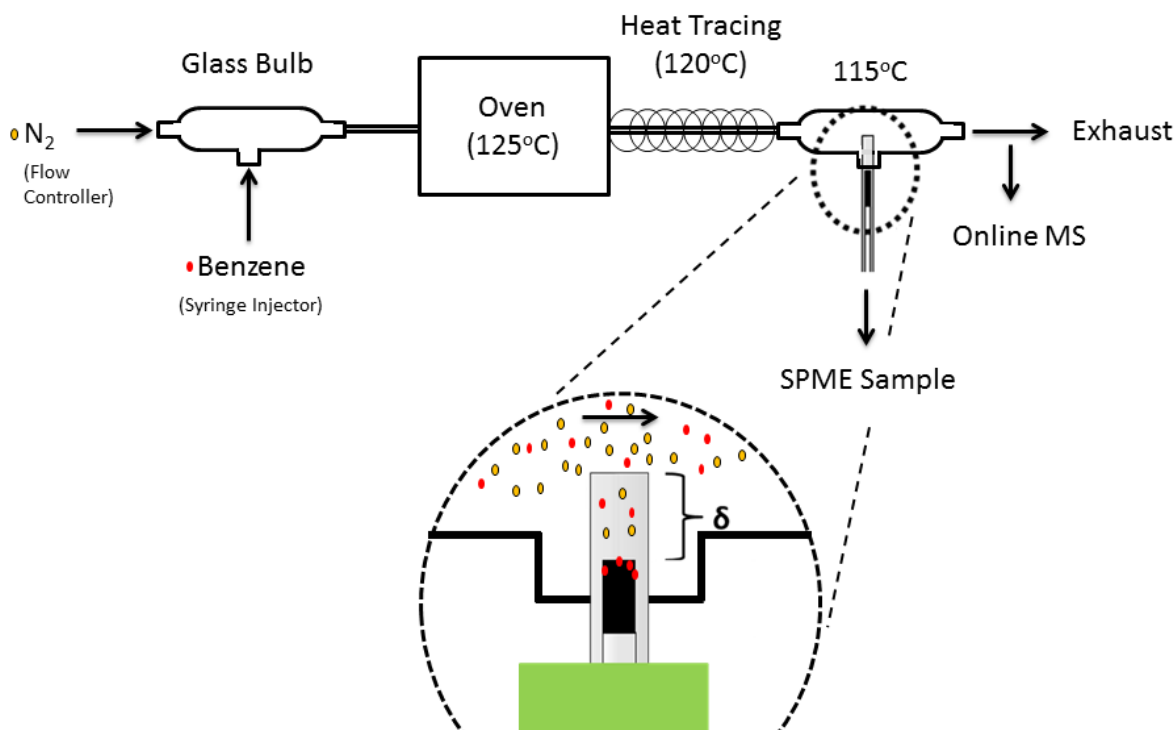


**Figure 1**

**Figure 1:** Simulated TWA SPME sampling system for hot process gas.

Gas samples were analyzed using a GC-FID (Varian GC-430), supplied with UHP hydrogen (30 mL min<sup>-1</sup>), air (300 mL min<sup>-1</sup>), and helium (25 mL min<sup>-1</sup>). The GC injection port was held 250 °C and fitted with a 0.75 mm SPME injection sleeve (Supelco 2-6375,05); no split was utilized. A Phenomenex Zebron ZB-5ms column (60 m × 0.25 mm × 0.25 μm) was held at a constant flow of 1.2 mL/min and used a temperature program of 50 °C for 1 min followed by

heating at  $10\text{ }^{\circ}\text{C min}^{-1}$  to  $150\text{ }^{\circ}\text{C}$ . The FID was operated at  $280\text{ }^{\circ}\text{C}$  and the acquisition frequency was set at 20 Hz.

## Results & discussion

The reliability of the sample system and its practical limitations were determined to establish acceptable conditions for a statistical design of experiments (DOE).

*Testing zero sink assumption.* Accurate and consistent responses were acquired at several  $C_g$  values. Three repetitions of  $C_g$  ranging from  $0.05\text{-}0.4\text{ g m}^{-3}$  (16 to 160 ppm<sub>w</sub>) benzene in N<sub>2</sub> resulted in a very high correlation as displayed in Figure 2. (This correlates to 20 to 200 times reduction in tar concentration in a real syngas.) The relative standard deviations (RSD, or standard deviation divided by the average) were between <1 to 4%, which indicates a high degree of precision. In fact, limits in spectroscopy are generally considered 10% RSD for quantification and 33% RSD for detection, both of which are much larger than the 1 to 5% RSD values determined here [251]. If a simple approach is taken to linearly extrapolate based on these data using the 10% and 33% rules, an estimated limit of quantification (LOQ) for the benzene model tar could be calculated on the order of  $0.02\text{ g m}^{-3}$  (8 ppm) with a limit of detection (LOD) of  $0.5\text{ mg m}^{-3}$  (200 ppb). Sampling times longer than 10 min would theoretically enable LOD and LOQ at much lower concentrations, limited only by the homogeneity and stability of the process stream.



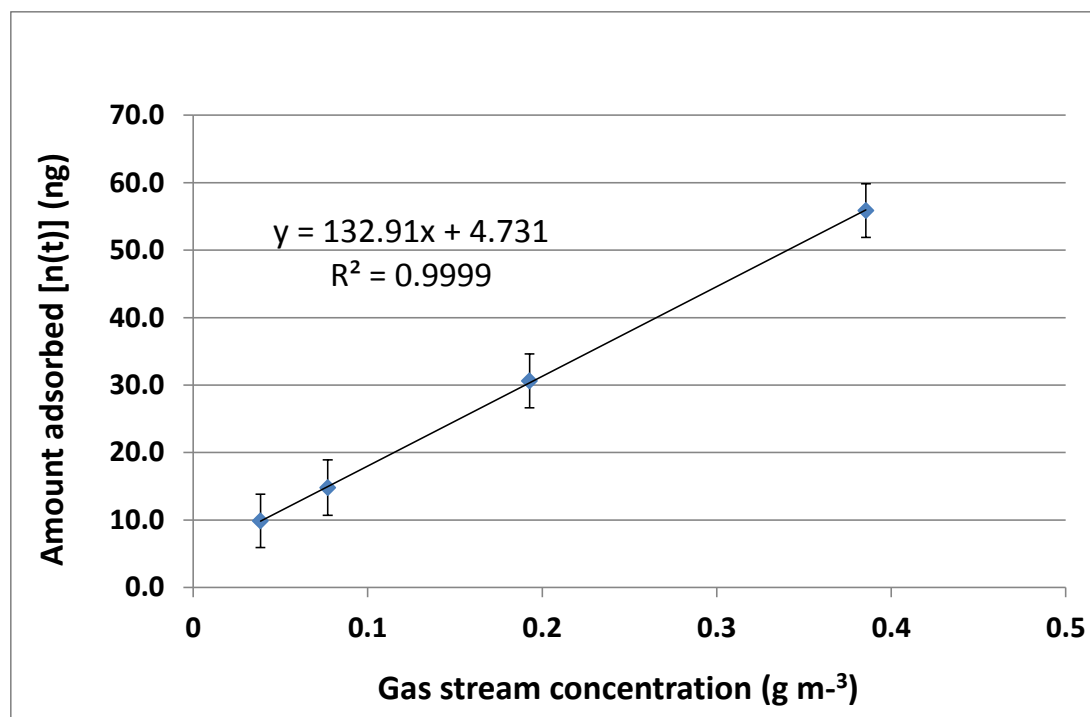


**Figure 2:** Benzene adsorbed on the CAR/PDMS fiber at atmospheric pressure for 10 min sampling times at 115 °C,  $\delta = 5$  mm. Concentration calculated as 0.5 g m<sup>-3</sup> at room temperature (23 °C) as a function of the gas flow meter and syringe pump settings, and subsequently adjusted for temperature [249]. (Standard errors for amount adsorbed were nearly identical and ranged from 3.9 to 4.1 ng.)

The zero-sink limit was determined next by sampling the highest  $C_g$  of interest at the smallest  $\delta$  for gradually longer  $t$ . These conditions result in ‘worst-case’ scenario for meeting the zero-sink conditions for benzene adsorbed on the fiber. The zero-sink specification is met as long as adsorption is occurring linearly with  $t$  [231]. Once the adsorption begins to slow with time in the kinetic regime, the mass adsorption rate becomes a dynamic variable and Fick’s Law is no longer easily applied.

Figure 3 indicates that adsorbed mass below approximately 110 ng remains within this linear adsorption regime for  $0.39 \text{ g m}^{-3}$  (160  $\text{ppm}_w$ ). This equates to  $t = 15 \text{ min}$ , with approximately 10% deviation from the theoretical maximum  $n(t)$ . According to Equation 2, this theoretically indicates ability to measure  $C_g$  with an upper bound of  $1.2 \text{ g m}^{-3}$  (480  $\text{ppm}_w$ ) for 5 min intervals at  $\delta = 3.3 \text{ mm}$ . At longer  $\delta$ , the theoretical maximum  $C_g$  will increase proportionally with  $\delta$  (e.g.,  $12 \text{ g m}^{-3}$  (0.5% $_w$ ) could be measured at  $\delta = 33 \text{ mm}$  and  $t = 5 \text{ min}$ ).

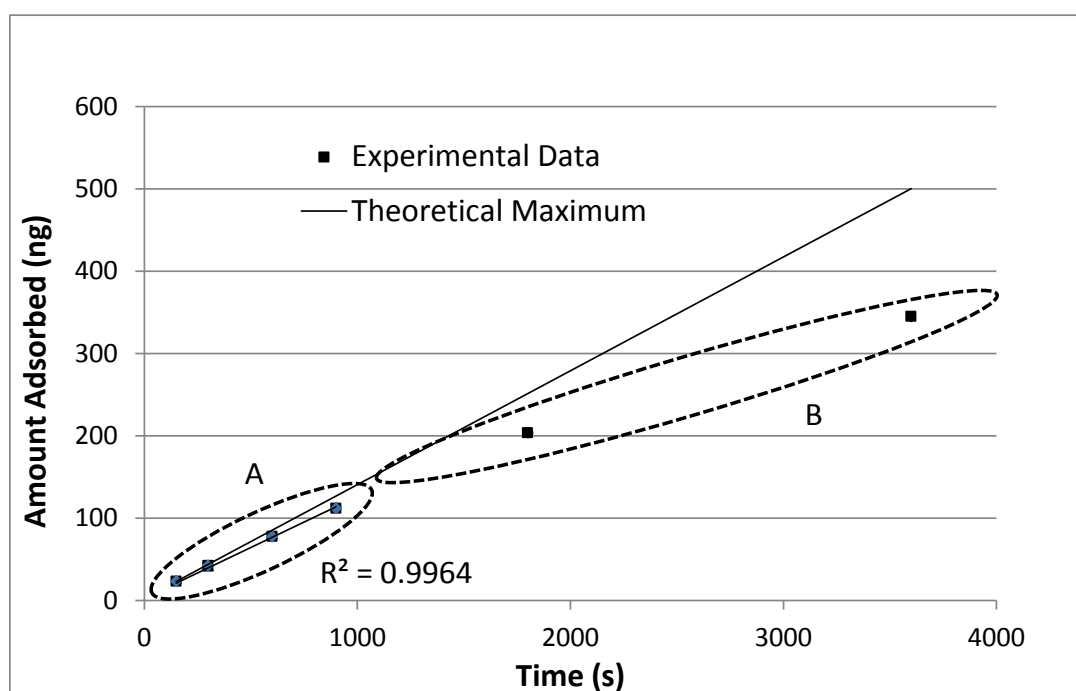


**Figure 3:** TWA SPME extraction at  $115 \text{ }^\circ\text{C}$  ( $\delta = 3.3 \text{ mm}$ ) of  $0.39 \text{ g cm}^{-3}$  (160  $\text{ppm}_w$ )

benzene in  $\text{N}_2$  (standard errors all below 4 ng). “A” represents zero-sink behavior. “B” represents clear loss of zero-sink behavior.

*Verifying  $C_{face}$  is equal to  $C_{bulk}$ .* A constant  $\text{N}_2$  flow rate of 5.7 SLPM resulted in a mean gas velocity in the sampling bulb of  $0.75 \text{ cm s}^{-1}$ , which guaranteed this second requirement of TWA passive sampling. The faster velocity also more accurately represents gas velocities in process piping. This larger flow rate was also necessary to avoid severe temperature fluctuations in the

sampling zone of the glass bulb (Supelco #28526-u), due to its initial lack of heat tracing. A steady 115 °C was achieved in the center of the glass bulb with this flow rate.

*Testing consistent and predictable response to changing  $C_g$ .* Despite the highly linear response at different concentrations (Figure 2), testing still showed severe fluctuations in  $n(t)$  at different depths. This was possibly due to changes in the actual diffusion rate of compounds occurring as a result of temperature differences at different depths in the sampling zone. (Maintaining constant temperature is essential to collecting accurate data, since  $D_g$  is a function of temperature and thermophoresis can also alter the mass adsorption rate.) Temperatures at different depths within the SPME syringe housing were measured using a SPME temperature probe that was created by removing the stainless steel inner rod and fiber coating from a broken fiber and replacing it with a thermocouple (Figure S-3). A temperature of 115 °C at the fiber tip resulted in a temperature of 75 °C at  $\delta = 10$  mm. Tracing was placed on the entire sampling zone, including a sampling well for the fiber so that the entire depth of the extracted fiber was heated appropriately (Figure S-4). The adjustments resulted in a temperature variation of less than 1 °C from the fiber tip to a depth of 10 mm.

Initial testing also identified replacement of syringes in the syringe injector as a potential nuisance variable. This variation was dealt with by using a block design for the DOE: a single syringe was used to perform one repetition of all treatment conditions, and a fresh syringe was used for each repetition of the treatments. The quantity of treatment conditions was therefore constrained to fit within the time provided by one syringe.

Another potential source of error involved retraction depth, since variation in depths by more than 0.1 mm from the assumed depth may cause substantial changes in the amount adsorbed.

This variability was addressed using a single SPME fiber during each repetition, and having the SPME fiber holder professionally machined at each of the required depths [244]. This resulted in variation of less than 0.1 mm retraction depth and high precision as indicated in the results (See Figure 3 and caption for an example of high precision).

The high degree of linearity in Figure 2 suggested that  $C_g$  could also be removed as a variable from the DOE as long as similar conditions were utilized. A  $C_g$  of  $0.5 \text{ g m}^{-3}$  (160 ppm<sub>w</sub>) at room temperature was chosen given the promising initial results and the understanding that longer  $\delta$  significantly diminishes  $n(t)$ . In this manner, the linear portion of the adsorption curve shown in Figure 3 is preserved for the data and the amount adsorbed is within the quantification limits.

Two potential variables remained that could cause variation in the experimentally determined  $D_g$  values, as described in Equation 3:  $\delta$ , and  $t$ .

A maximum sampling time of 4.5 h was possible when testing a tar concentration in the sampling zone of  $0.39 \text{ g m}^{-3}$  (160 ppm<sub>w</sub>, or  $0.5 \text{ g m}^{-3}$  at room temperature) at a  $\text{N}_2$  flow rate of 5.7 SLPM. In addition to  $t$ , the fiber was submitted to 5 min of desorption and 5 min of cooling time following extraction and desorption. A full factorial design using 10 min as the average  $t$  enabled 9 treatment combinations within the time frame of a single syringe. A full factorial design was applied for three different  $\delta$  (3.3, 5, and 10 mm) and three  $t$  (5, 10, and 15 min).

Results from this DOE are illustrated in Figure 4. The linear correlation suggests that passive TWA sampling using SPME is applicable for detection of contaminants in elevated temperature (>100 °C) process gas streams. According to Equation 3, the amount collected on the fiber

should be inversely proportional to  $\delta$  and directly proportional to  $t$ . The  $R^2$  value of 0.979 suggests that this relationship holds true.

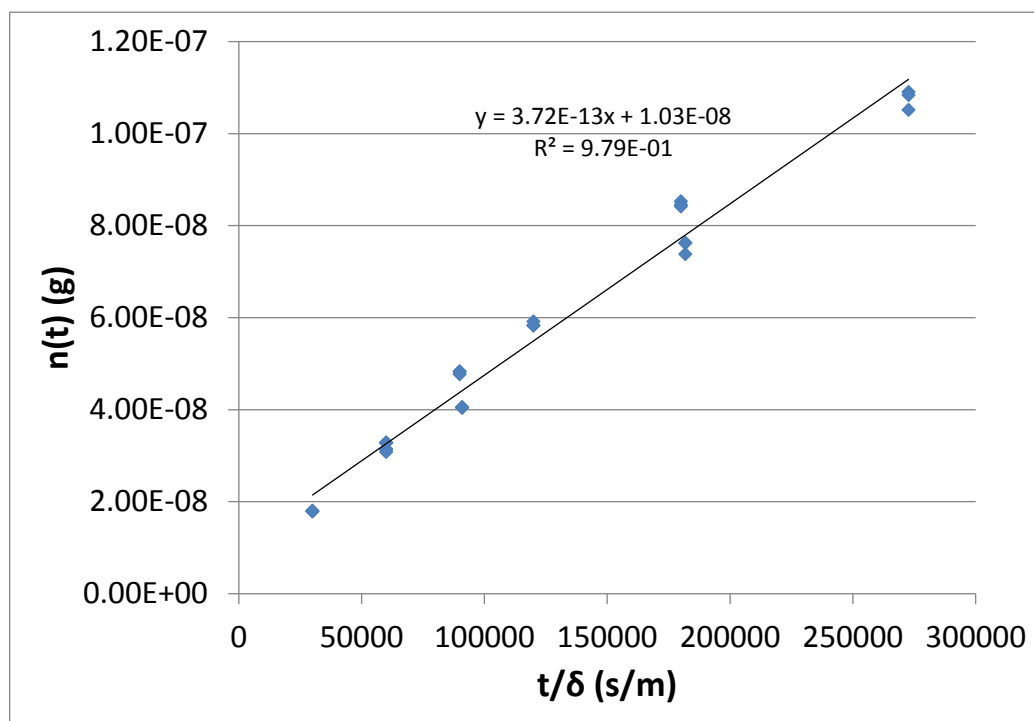


**Figure 4:** Amount of benzene (ng) collected (minus a baseline) at 115 °C as a function of  $t$  (s) and  $\delta$  (mm) for the treatment combinations ( $t = 5, 10,$  and  $15$  min;  $\delta = 3.3, 5,$  and  $10$  mm;  $C_g = 0.39 \text{ g m}^{-3}$  (160 ppm<sub>w</sub>)).

Prior to calculating the experimental  $D_g$  with Equation 3,  $n(t)$  must be adjusted to account for the amount adsorbed on the stainless steel syringe barrel that houses the fiber. For this purpose, a decommissioned SPME fiber that had its 1 cm coating completely removed was subjected to the same testing conditions as the CAR/PDMS fiber. The quantities of benzene adsorbed onto the bare steel at these conditions were 5.3, 5.8, and 6.1 ng for the 5, 10, and 15 min time intervals, respectively (changes in the amount adsorbed with depth were not significant at any

level). The final apparent  $D_g$  values for all 27 tests were 0.101 to 0.157  $\text{cm}^2 \text{s}^{-1}$  with an average of 0.129  $\text{cm}^2 \text{s}^{-1}$ . RSDs were all 1% or less for  $\delta = 5$  and 10 mm, and less than 2% for  $\delta = 3.3$  mm. These data compare well to WL, FSG, and Huang theoretical predictions (0.138 to 0.156  $\text{cm}^2 \text{s}^{-1}$ ), but do show a slightly larger range of  $D_g$  values. Plotting the larger range of experimental  $D_g$  values versus inverse depth (as Equation 3 suggests) shows a strong correlation in lieu of random scatter for each time interval (Figure 5). The experimentally determined  $D_g$  increases with increasing  $\delta$  and decreasing sampling time.

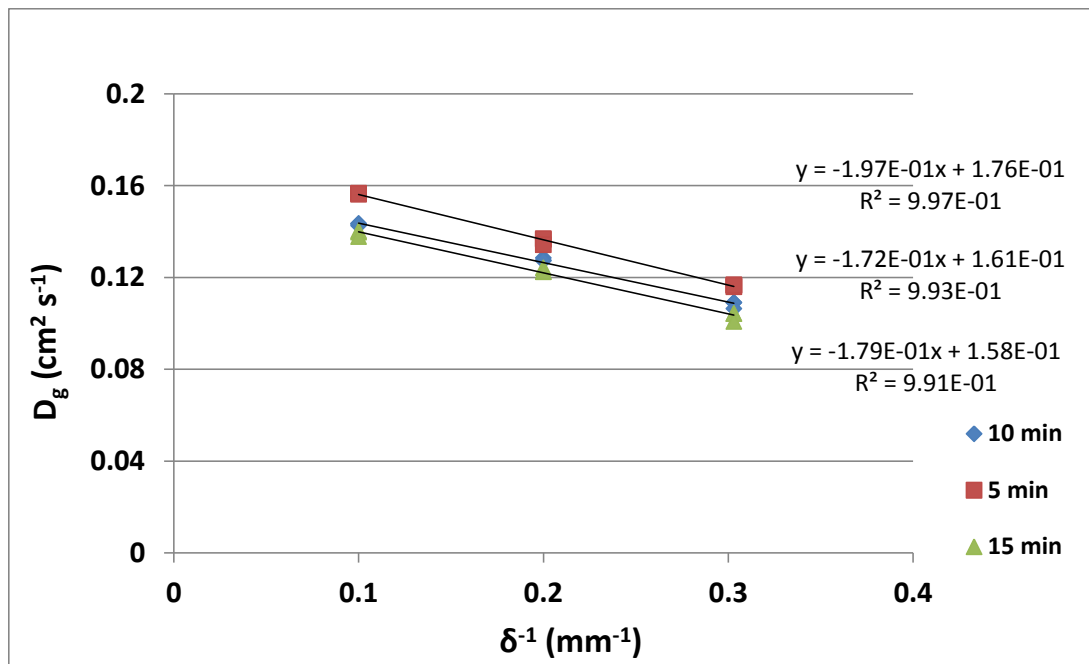


**Figure 5:** Experimental (apparent) diffusivity ( $D_g$ ) as a function of  $\delta$  for different  $t$ . All tests performed at normal conditions of 115 °C, 0.39  $\text{g m}^{-3}$  (160 ppm<sub>w</sub>), 1 atm, and 5.7 SLPM  $\text{N}_2$  flow rate.

Statistical analysis (using JMP software) showed that the value measured for diffusivity was dependent upon the time interval and diffusion length employed in the measurement at a 95% confidence level (See Tables S-1 and S-2). The analysis of variance (ANOVA) for the

experiment estimated p-values of less than 0.0001 for both  $t$  and  $\delta$ . Even after addressing all major factors potentially impacting  $n(t)$  (including: temperature, experimental system flow rates, sinks and leaks for the analyte),  $\delta$  and  $t$  had a significant effect on  $D_g$  as determined by Equation 3.

Several possibilities were tested to explain why the experimental value of  $D_g$  depended upon the time of collection and the diffusion length. Any potential eddy effects from the high gas velocity were discounted by testing a velocity of  $0.03 \text{ m s}^{-1}$  in the heat-traced sampling zone, which produced no change in the resulting pattern (see Figures S-6 and S-7). Intermittent exposure to benzene could have been caused by a syringe injector malfunction or a variation in the delay between sample extraction and analysis for different samples. Such effects should have been avoided by the use of randomized test order. In the event that randomization did not fully address potential effects of intermittent exposure, an experiment was performed similar to Martos et al. in which the samples were immediately subjected to a helium-only environment for varied lengths of time before analysis [249]. As was expected with the high affinity for the analytes by the CAR/PDMS fiber, the amount of sample lost from the fiber was not detectable. This verified the study by Martos et al. and eliminated intermittent exposure to the sample environment as a possible explanation for the significant pattern in the data. Exposure to elevated temperatures may also expand the fiber/syringe tip over time – i.e.  $A$  and  $\delta$  are no longer constant and expand. This was tested by performing an experiment at room temperature, with no change in the resulting pattern.

One remaining explanation is the apparent deviation from linear analyte adsorption, as indicated in Figure 3. There is a slight reduction of approximately 10% from the theoretical

maximum adsorption at 15 min. Less deviation than 10% may be necessary to apply Equation 2. Chen et al. (2003) chose conditions in which the fiber performance remained within 5% of theoretical [241]. This implies that the limit of application for TWA passive sampling is a point at which  $n(t)$  lies between 5% and 10% of the theoretical SPME mass adsorption capacity.

Despite the significant variation in experimentally derived  $D_g$  values, several were very similar to values predicted by the three theoretical equations. Determining which particular values were not statistically different from theory can establish a maximum  $n(t)$  at which this method can make valuable use of theoretical  $D_g$  calculations. Establishing the conditions of this TWA-SPME method in a practical application under which a simple theoretical calculation of  $D_g$  for analytes of interest could be used in place of these types of experiments would save substantial amounts of time during analysis. The user could simply identify what compounds are of interest, calculate the  $D_g$  at sampling process gas conditions, select a depth and time at which the mass adsorbed is within this theoretical limit, and calculate analyte concentration. Experimentally determining diffusivity for all compounds would become unnecessary for estimating their concentration.

Certain combinations of conditions will collect lower amounts of benzene than others, and identifying which conditions specifically differ from theory can determine if a practical maximum  $n(t)$  value was surpassed. If the conditions that differ from theory all collected higher amounts of benzene, this will support the notion that a practical maximum  $n(t)$  value was exceeded. The averages of each combination of conditions (nine averages of 3 repetitions) are shown in Table 1 tested against the average of the three theoretical equations (see Equation S-2).



**Table 1:** The means of nine depth and time combinations statistically compared to the average of the WL, FSG, and Huang theoretical equations (at  $\alpha = 0.05$  unless otherwise stated)

Condition	Depth	Sampling Time	Empirical $D_g$ average (n = 3)	$n(t)$	$D_g$ different from theory (n = 3)
	(mm)	(s)	$cm^2 s^{-1}$	$(g) \times 10^{-9}$	
1	3.3	5	0.124	43.1	Yes
2	3.3	10	0.108	75.4	Yes
3	3.3	15	0.103	107.5	Yes
4	5	5	0.136	31.2	No
5	5	10	0.128	58.6	No*
6	5	15	0.123	84.7	Yes
7	10	5	0.156	17.9	No
8	10	10	0.143	32.8	No
9	10	15	0.139	48.0	No
(Theoretical)			(0.146)		

\*when taken at @  $\alpha = 0.01$  instead of 0.05

Analyzing all nine combinations of retraction depths and sampling times indicated that a critical  $n(t)$  value was reached. Each mean value that was significantly different from theory had collected more benzene than those that were not significantly different, except for one. The first condition of 3.3 mm and 5 min collected less benzene than both condition 9 and 5 (10 mm and 15 min; 5 mm and 10 min), yet still showed a molecular diffusion coefficient that was significantly different from the average of the theoretical equations. This suggests that the rate of analyte collection on the surface of the fiber tip can create a localized area of high concentration, which can negate the zero-sink assumption if the system becomes limited by mass transfer deeper into the fiber coating. This second boundary layer of pre-concentrated analyte located at the surface of the fiber tip is similar to a phenomenon suggested by Semenov (2000), in which a certain degree of oversaturation on the fiber surface was essentially responsible for moving the analyte deeper into the sorbent layer and achieving equilibrium [252].

*Pilot-scale gasification trial.* Given the close proximity of the theoretical values to many of the experimental values, a preliminary test was performed on the pilot scale gasifier to test the overall feasibility of the concept in a real-world situation. The CAR/PDMS fiber was subjected to the process gas stream existing downstream of a tar condensation vessel using a retracted TWA sampling configuration. The chromatogram in Figure 6 illustrates the impurities found in the syngas stream, primarily benzene, toluene, styrene, indene, and naphthalene. These 5 compounds represent the major components existing in the vapor phase after the syngas cools down to the 100 to 150 °C temperature of the condensation vessel. The remaining compounds in the chromatogram were shown in a baseline sample taken of the vessel prior to use, and were subtracted from the syngas tar chromatogram to ensure only the additional mass of syngas tar compounds were used in concentration calculations.

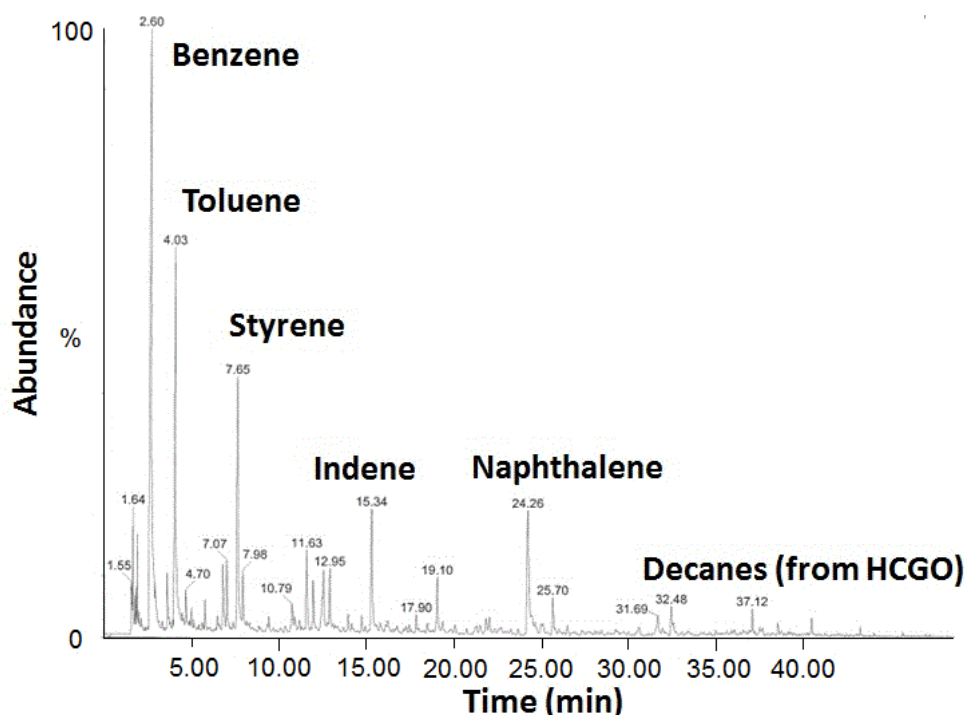


**Figure 6:** TWA-SPME analysis of syngas generated from biomass gasification and passed through a tar condensation vessel. Conditions of sample taken directly from process

pipng: CAR/PDMS fiber, 3.3 mm retraction depth, 10 min exposure, ~150 °C syngas temperature.

A CAR/PDMS fiber was inserted directly into the gas stream via a compression fitting attached to the 1.5" process piping and outfitted with a GC septa (11 mm). Results shown in the chromatogram of the process gas are feasible (Figure 6), given the simple condensation process used to remove tar directly upstream of the sampling area. Exit temperatures in the piping from the condensation vessel were higher than desired (i.e., ~150 to 175 °C as opposed to desired 95 °C), thereby condensing only the heavier tars and allowing most of the lighter tars to remain in the vapor phase.

The TWA-SPME measurement resulted in a total tar concentration of approximately 3 g m<sup>-3</sup> (Table 1). This is the same order of magnitude of tar concentration indicated by the conventional tar measurement methods performed further upstream (~7 g m<sup>-3</sup>). The discrepancy may reflect the lower overall quantity of tar where TWA-SPME sampling was performed, due to upstream condensation of the heavier tar molecules (see lower response of heavier molecular weight compounds in Figure 6).

**Table 2:** TWA-SPME analysis of syngas generated from biomass gasification and calculated tar concentration. Empirical calculation at 150 °C was adjusted by the same ratio as theory, since it is outside the experimental conditions of 115 °C, and is provided only for comparison. Theoretical diffusivity was calculated using the average of the WL, FSG, and Huang correlations at the temperature stated in the table. Literature values were provided by Karaiskakis [246]. Benzene concentrations were calculated for theoretical and literature comparisons by reorganizing Eq. (3) to obtain  $n(t)$  with the  $D_g$  provided.

	Empirical		Theoretical		Literature	
	<i>(D<sub>g</sub> estimated from controlled TWA-SPME experiments)</i>		<i>(D<sub>g</sub> estimated using WL, FSG, and Huang models)</i>		<i>(D<sub>g</sub> from Karaiskakis 2004)</i>	
Molecular diffusivity, $D_g$ (cm <sup>2</sup> s <sup>-1</sup> )	0.143	0.163	0.146	0.167	0.140	0.165
<i>At Temperature (°C)</i>	<i>115</i>	<i>150</i>	<i>115</i>	<i>150</i>	<i>105</i>	<i>150</i>
Benzene conc. (g m <sup>-3</sup> )	2.28	2.00	2.23	1.95	2.32	1.97
<u>Tar % by Benzene*</u>	<u>71.1</u>	<u>71.1</u>	<u>71.1</u>	<u>71.1</u>	<u>71.1</u>	<u>71.1</u>
Total tar concentration $C_g$ (g m <sup>-3</sup> )	3.21	2.81	3.13	2.74	3.26	2.77

\*‘Tar % by Benzene’ indicates the fraction of all tar peaks in the chromatogram accounted for by the benzene peak.

## Conclusion

Proof-of-concept was established for passive TWA sampling of contaminants found in process streams at high temperatures ( $> 100\text{ }^{\circ}\text{C}$ ) using a retracted SPME fiber. Concentration of a model tar compound (benzene) was tested in a model syngas stream ( $\text{N}_2$ ) at multiple retraction depths ( $\delta$ ) and sampling times ( $t$ ). Empirical diffusion coefficients ( $D_g$ ) calculated from known concentrations ( $C_g$ ) of the model tar compound were in good agreement with theoretical estimates at  $115\text{ }^{\circ}\text{C}$  and 1 atm pressure. However, empirically determined  $D_g$  values appeared to depend on the diffusion path length and sampling time employed in its measurement. Despite this limitation of the method under some of the tested conditions, the TWA model can nevertheless be applied to quantification of trace contaminants in process gas streams at elevated temperature, provided that the amount collected ( $n(t)$ ) at the exposure time and depth of retraction deviates by 5% or less from the theoretical SPME fiber adsorptive capacity (i.e. the zero-sink assumption is not violated). If several depths fall within the limits of  $n(t)$  that satisfy the zero-sink assumption, the preferred configuration uses the greatest depth and longest time of extraction. These experiments provide strong evidence supporting Semenov's hypothesis that a secondary boundary layer initially develops at the front edge of the SPME fiber.

The TWA-SPME technique was also tested on a pilot-scale gasification process, yielding tar concentrations that are reasonable considering the relatively cooler gas temperature where the SPME sampling was performed compared to the conventional tar measurement. Future tests will attempt comprehensive evaluations of the TWA-SPME method in the pilot-scale gasifier for the five major compounds identified in the current study, including comparing the method to currently accepted conventional tar measurements.

**Supporting Information.** Includes: more detailed description of TWA sampling techniques, custom devices for high temperature TWA testing, and full statistical analysis results.

**Acknowledgements.** The authors of this work appreciate the financial contributions of Phillips66 to fund this work. Appreciation to Dr. Derrick Rollins is also expressed for his assistance with statistical analysis.

## **CHAPTER 4. PILOT SCALE VALIDATION OF THE NOVEL TWA- SPME BASED ANALYTICAL METHOD FOR MEASUREMENT OF ANALYTES IN HOT PROCESS GAS**

The following article is currently being reviewed by co-authors for submission to *Analytical Chemistry* (secondary, *Journal of Chromatography A*). The title of the manuscript is, “Analysis of trace contaminants in hot gas streams using time-weighted average solid-phase microextraction: pilot-scale validation.”

### **Abstract**

A new method was developed for collecting, identifying and quantifying contaminants in hot process gas streams using time-weighted average (TWA) passive sampling with solid-phase microextraction (SPME). Specifically, the original lab scale proof-of-concept with benzene was expanded to include the remaining major tar compounds of interest in syngas: toluene, styrene, indene, and naphthalene. It was then tested on high temperature ( $\geq 100^\circ\text{C}$ ) process gas from a pilot-scale fluidized bed gasifier feeding switchgrass at 20 kg/h. The TWA-SPME technique was compared side-by-side with a conventional tar measurement technique involving isokinetic sampling and chilled solvent impinger trains. The TWA-SPME technique performed consistently well in two different sampling locations and was able to identify and quantify 40 to 60% more compounds than the conventional approach. Differences between the two measurement methods in the gas cleaning section were 1 to 20%, and differences were as much as 40 to 100% in the raw gas stream with SPME-based measurements always yielding lower concentrations than the conventional approach. Compared to the difficult and inconsistent conventional tar measurement

techniques, the SPME-TWA approach offers a solvent-free, simplified approach (passive sampling) capable of drastically reducing sample time and improving analytical reliability. Additionally, SPME presents an opportunity to identify and quantify VOCs beyond the capability of the conventional approaches, reaching concentrations in the ppb range (low  $\text{mg}/\text{m}^3$ ). Despite the variability in gasifier process conditions, relative standard deviations (RSDs) during SPME testing were lower than 10%, with most lab-based trials yielding less than 2% RSDs. Lab scale calibrations were performed down to the lowest expected values of tar concentrations in ppb ranges (low  $\text{mg}/\text{Nm}^3$ , where N indicates STP), with successful measurement of gasification tar concentrations at times exceeding 4000 ppm (up to  $10 \text{ g}/\text{Nm}^3$ ). Overall results indicate the TWA-SPME technique can be a valid alternative to the standard impinger-based method for light tar quantification under certain conditions. The opportunity also exists to exploit this technique for analysis of other process gas streams such as pyrolysis vapors and combustion exhaust.

## **Introduction**

Thermochemical processing is the application of heat and catalysts to break apart solid carbonaceous materials to produce heat, power, fuels, and chemicals [201]. Many thermochemical processes create a vapor stream as either a direct or intermittent product. These vapor phases must be analyzed to determine product purity and process efficiency. However, many conventional methods of analysis require substantial time and material investment. Developing an alternative means of analysis using fewer steps and less material (i.e. solvents), while maintaining or improving levels of detection and quantification are highly desirable.

Solid-phase microextraction (SPME) is a relatively recent analytical technique that has been developed to address these issues by combining sampling and sample preparation into a single



step [36]. Volatile analytes are collected on a thin extraction phase that is located at the tip of a fused-silica or metal alloy fiber, which can be retracted into a syringe-like housing. The SPME-based samples can then be introduced into a gas chromatograph (GC) or liquid chromatograph (LC) coupled with a detector such as a flame ionization detector (FID) or mass spectrometer (MS) [228, 230, 231].

Unlike conventional SPME in which the fiber is exposed to the sampling environment, time-weighted average sampling keeps the fiber coating retracted a known distance within the syringe opening [249]. TWA-SPME applies Fick's first law of diffusion to the SPME apparatus to determine the time-weighted average concentration of analytes using their molecular diffusion coefficient and the retraction depth of the fiber. This protects the fiber coating while enabling sampling in a variety of conditions by simply varying the fiber retraction depth and the sampling time.

Similar to the work by Koziel et al. (1999, 2001), a special SPME housing was modified to enable retraction depths of 5 mm, 10 mm, 15 mm, and 20 mm (Figure S-1) [243, 244].

The objective of this work is to further test the proof-of-concept work performed in a previous article [223]. Specifically, this paper expands the quantification of a single analyte (benzene) in a high-temperature (115 °C) gas stream (nitrogen) to include a matrix of benzene, toluene, styrene, indene, and naphthalene (BTSIN). These analytes represent the primary components of syngas tar existing downstream of a syngas cleaning device [223]. The lab testing was then demonstrated on a pilot-scale gasification and syngas cleaning unit feeding 20 kg/h of switchgrass to compare the technique with conventionally approved quantification methods for syngas tar [16].

*Syngas tar analysis*

Syngas exiting a gasification process is contaminated by feedstock impurities as well as an array of larger molecular weight aromatic hydrocarbons developed from the process known as ‘tar’ compounds. These tars are typically found in concentrations ranging from 10-100 g/m<sup>3</sup> (3-30 ppm<sub>w</sub> at standard conditions) or higher depending on the method of gasification [253]. They are a particularly menacing problem given their tendency to start condensing as temperatures fall below ~400 °C, potentially clogging pipes and fouling downstream equipment. Tar reduction also usually becomes more intense and expensive as the removal efficiency is increased, making it beneficial to only reduce tar to levels necessary for downstream applications [253, 254].

Conventional analysis of syngas tar is performed offline using wet chemical methods to analyze tars [5, 17, 225]. They typically involve passage of a slipstream (i.e. a small sample stream diverted isokinetically from the main process stream) into a series of impingers containing solid or liquid-phase sorbents, where the condensable components in the syngas are collected and the non-condensable gases (NCGs) are passed to a gas measurement device such as a micro-gas chromatograph (microGC). The gas stream is ultimately passed through a flow meter to determine the volume of gas analyzed (See Figure 1). The final stage is a multi-step sample preparation process to analyze the collected components via gas chromatography and mass spectroscopy (GC-MS) or flame ionization detection (GC-FID) for the volatile analytes, and gravimetric analysis for the non-GC detectable components. The concentration is then derived by the overall mass of analytes collected divided by the standardized volume of gas analyzed. These methods suffer from long and complicated solvent extraction steps, often requiring days for analysis and suffering from a plethora of potential errors, such as inherently difficult isokinetic sampling trains (see description in Materials section), glassware

contamination, insufficient measurement accuracy and precision, and complicated sample matrices and solvent separations. In addition, experimental errors typically result in relative standard deviations ranging from 20 to 50% for concentration measurements, but can extend beyond 100% for many kinds of analytes [16, 17].

Previous attempts to mitigate the challenges presented in the conventional tar measurement technique have included adoption of a pressure cooker (PC) vessel for collection of non-GC detectable components [26]. This dry-condenser process was compared to the conventional analysis and showed accuracy within 10% of the heavy tar fraction from the conventional approach. However, the light tar fraction, i.e. compounds with vaporization temperatures near or below the 105 °C set point of the PC (such as benzene and toluene), could make up a substantial fraction of the syngas tar. Benzene, toluene, and other light tars may typically represent 10 to 30%, and as much as 50% or more of the overall tar fraction [5, 28, 30, 254-256]. These compounds are still a significant threat to end-use applications that require high purity syngas, like catalysis for synthetic fuels [42]. Due to their low condensation temperatures, their presence also creates significant challenges for cleaning processes that prefer little-to-no water condensation such as oil washing of the syngas [33, 218]. Determining the concentration of light tar fractions in the syngas is therefore of great importance to identify the optimal operating conditions for a gasification-based synthetic fuels facility.

There is an obvious need for an accurate, rapid, and dependable light tar quantification method. The syngas temperatures found downstream of cleaning equipment and the dry condenser typically fall between 100 to 150 °C and provide an ideal side-by-side testing environment for the TWA-SPME method. The TWA-SPME-based method has been tested previously in the lab to determine if the benefits of the technique found in its typical ambient

environmental applications would still apply to contaminant measurement in hot process gas streams [223]. The results indicated potential for the method to effectively determine contaminant concentrations at elevated temperatures in a variety of concentrations. The benefits might potentially include lower detection limits than conventional methods, shorter sample preparation and analysis time, and more accurate measurements. The TWA-SPME approach also avoids potential challenges associated with conventional equilibrium SPME, such as controlling sample extraction conditions and minimizing the fouling and mechanical stress on the exposed fiber [236]. This work aims to test the TWA-SPME-based method in a pilot-scale gasifier for quantification of BTSI and to compare results with the impinger based dry-condenser gas sampling technique. The TWA-SPME approach can close the gap on analytical methods capable of avoiding problematic condenser trains and providing rapid process response. Numerous additional analytically challenging process gas environments can benefit from successful application of this technique, such as combustion exhaust and pyrolysis vapor streams, and may also enable monitoring of reaction kinetics.

*Theory of TWA-SPME sampling*

TWA-SPME operates on the premise that the amount extracted is proportional to the integral of the concentration over a sampling time ( $t$ ):

Equation 1: 
$$n = D_g \frac{A}{\delta} \int C_g(t) dx$$

where:

$A = \text{open area of needle housing } [L^2, \text{ cm}^2]$

$t = \text{sampling time } [t, \text{ s}]$

$D_g = \text{molecular diffusion coefficient for the sample in the gas stream } [L^2/t, \text{ cm}^2/\text{s}]$

$C_g$  = instantaneous concentration in the gas stream [ $M/L^3$ ,  $g/cm^3 \rightarrow g/m^3$ ]

$n$  = mass extracted (determined by analytical equipment) [ $M$ , g]

$\delta$  = boundary layer (or length of diffusion path = retraction of SPME fiber inside the needle)[ $L$ , cm]

In practice, this can be reduced to the following relationship as long as a few essential sampling requirements are met, which are detailed thoroughly in [36, 223].

Equation 2: 
$$C_g(t) = \frac{n(t)\delta}{D_g A t}$$

The work aims to tailor and expand the original lab scale proof of concept to the environment expected in the syngas process streams located downstream of the dry-condenser and the start of the gas cleaning system (see Figure 1) [223]. The TWA-SPME method is ultimately compared against the conventional tar analysis technique for validation on the pilot scale gasification and gas cleaning unit.

## Experimental Section

**Chemicals.** Benzene, toluene (Sigma-Aldrich CHROMASOLV®Plus, for HPLC  $\geq 99.9\%$ ), styrene (Sigma-Aldrich ReagentPlus®  $\geq 99\%$ ), indene and naphthalene (Sigma-Aldrich  $\geq 99\%$ ) were used to generate a model tar stream within an ultra-high-purity  $N_2$  gas stream (99.995%). Impingers in the sampling train were filled with either DI water (18.2  $M\Omega$ -cm) or 2-Propanol (Sigma-Aldrich CHROMASOLV®Plus, for HPLC  $\geq 99.9\%$ ) depending on the testing. 2-Propanol and dry ice were used in the impinger ice bath during later experiments to ensure analyte capture by reducing impinger temperature. Permanent gases calibrated and analyzed in the Agilent micro-gas chromatograph (microGC) included  $CO_2$  (6 - 45%), carbon monoxide (1 –

45%), H<sub>2</sub> (2 – 22.5%), CH<sub>4</sub> (2 – 6%), N<sub>2</sub> (0 – 66.5%), ethane (0.25 – 1%), ethylene (0.75 – 5%), acetylene (0.15 – 1%), and O<sub>2</sub> (0.2 – 1%). All work with chemicals was performed following lab safety protocols, using vented fume hoods and approved personal protection gear.

**Materials.** A manual SPME device was equipped with a Carboxen/Polydimethylsilosane (85 µm Carb/PDMS - Supelco) fiber. This fiber was chosen based on performance criteria for testing syngas streams (see [223]). The high sorptive capacity of Carboxen was an additional benefit for TWA sampling of the high analyte concentration potentially found in process gas [241].

This work was performed in two phases requiring different experimental setups. Figure 1 in [223] shows the laboratory setup used for experimental validation of  $D_g$  values. This original setup was modified with extensive heat tracing upstream of the oven to preheat the gas flowing through the glass bulb to 80 °C. Initial testing showed this was necessary to maintain a homogenous concentration of the synthetic tar mixture (benzene, toluene, styrene, and indene) in the gas stream. SPME samples were analyzed both from the lab-scale testing and the pilot plant testing using an identical GC-FID setup as described previously in [223]. The conventional tar sampling system was significantly more complex. Glassware used on the pilot-scale testing included two sets of impinger trains (seven impingers total) for sampling multiple locations in the syngas process lines simultaneously. Other gas sampling equipment included an isokinetic probe, thimble filter system, pressure cooker (PC), rotameter, vacuum pump, wet type gas flow meter, and microGC for permanent gas analysis (see Figure 1).

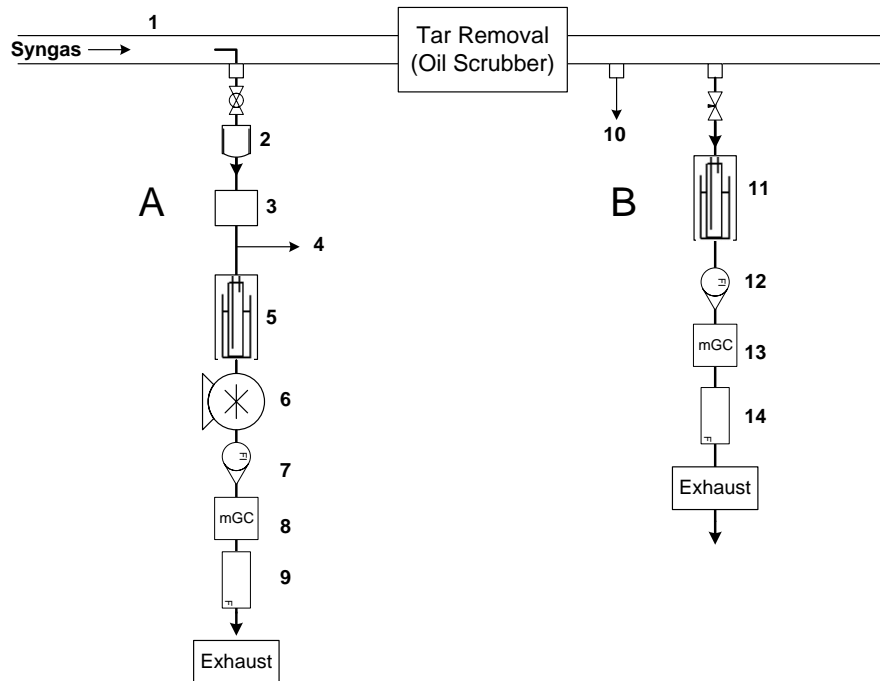


**Figure 1:** Schematic of the conventional tar sampling and collection system (all process piping and sampling lines are heat traced to reduce probability of tar condensation): (1) syngas process piping; (2) isokinetic sampling probe and particulate thimble filter; (3) pressure cooker (PC) heavy tar sampling system (refer to [26]); (4) SPME sampling port; (5) 4 impingers each with 200 mL 2-propanol immersed in a dry ice 2-propanol bath; (6) vacuum pump; (7) rotameter; (8) micro gas-chromatograph (mGC); (9) wet-test meter calibrated for lab environment; (10) SPME sampling port sample; (11) 3 impingers each with 200 mL 2-propanol immersed in a dry ice 2-propanol bath; (12) rotameter; (13) mGC; (14) wet-test meter calibrated for lab environment.

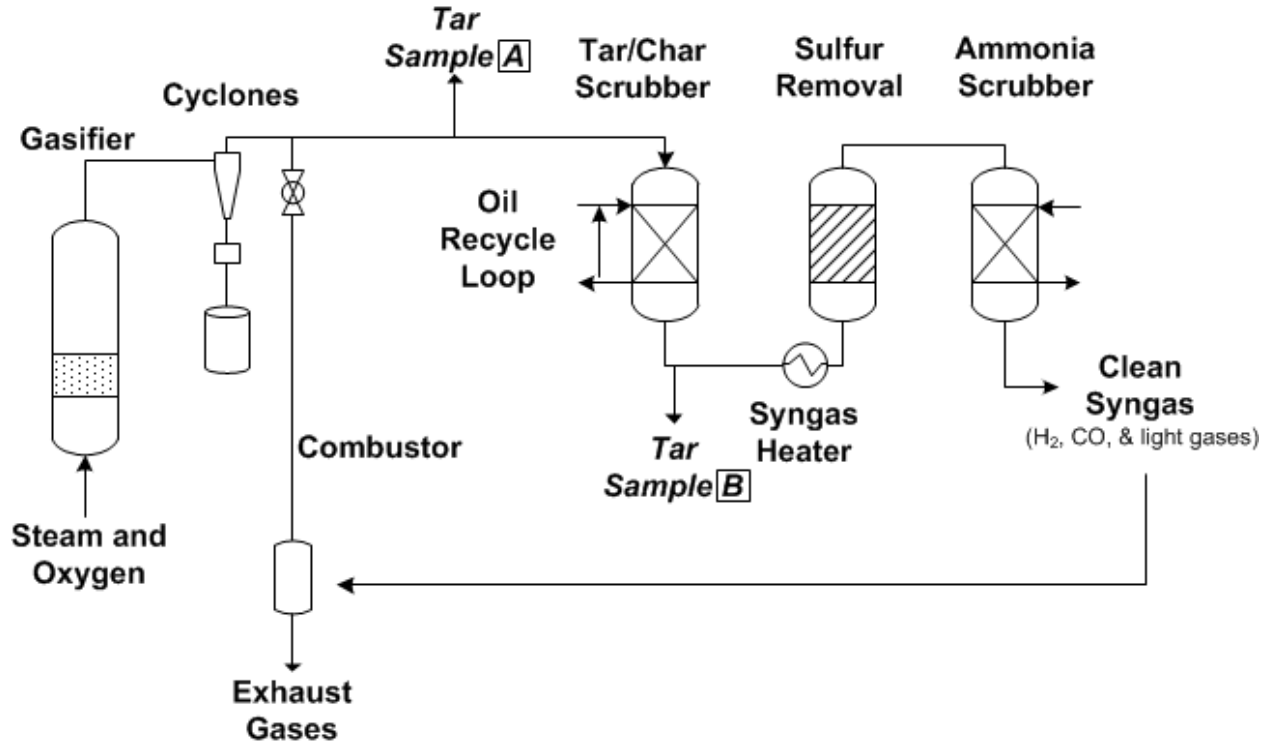


**Figure 2:** Schematic of the gasifier and gas cleaning system (gas samples taken immediately prior to and downstream of the tar/char scrubber, with A taken at  $\sim 135^{\circ}\text{C}$  and B at  $\sim 110^{\circ}\text{C}$ )

Syngas exits the gasifier and enters the cleaning system as described in [6] and shown in Figure 2. The hot syngas is maintained at  $400^{\circ}\text{C}$  or higher using high performance cable heaters (Tempco©) on the process piping. Cyclones remove a bulk of the particulate matter, and the remaining char is quantified using the thimble filter located in the isokinetic sampling line (A). This heat traced sampling line enters a pressure cooker downstream of the thimble filter, where syngas passes through a three meter polymer tube (Santoprene or Trelleborg) submerged in water heated to  $105^{\circ}\text{C}$ . This environment rapidly transfers heat from the syngas to condense the heavier molecular weight tars from the vapor stream. Syngas exiting the PC enters another heat traced  $\sim 9.5\text{ mm}$  ( $3/8''$ ) sampling line equipped with a stainless steel tee, which serves as an



SPME sampling port by placing an 11 mm septum into the top nozzle of the tee. Four impingers filled 1/3 full with 200 mL of 2-propanol follow this ~ 0.5 m sampling line.

## Results & Discussion

Validating the TWA-SPME concept for analysis of syngas tar at elevated temperatures required two separate experimental segments: (1) verifying the molecular diffusion coefficients ( $D_g$ ) for the primary analytes of interest in a laboratory scale testing system, and (2) comparing the technique to conventional tar measurement techniques on a pilot-scale gasification and gas cleaning system.

*Phase I:* Laboratory-scale experiments to estimate  $D_g$  for target analytes at elevated T.

$D_g$  is the only parameter on the right side of Equation 2 that is not provided by analytical equipment or known a priori. Proof-of-concept work performed in [223] on a benzene/N<sub>2</sub> gas stream indicated the possibility of a secondary boundary layer existing at the face of the SPME fiber's CAR/PDMS extraction phase [243, 249]. This boundary layer has the potential to significantly affect  $D_g$  under certain conditions. In order to determine this phenomenon's impact on a sample matrix that includes additional analytes, an identical series of tests was performed as described in [223] using a mixture of compounds that reflect the main tars remaining in cleaned syngas: benzene, toluene, styrene, indene, and naphthalene (BTSIN). An equal weight mixture of these five compounds was created and used in the injection syringe of the sampling system depicted in Figure 1 of [223]. Despite several attempts to address repeated sampling difficulties with naphthalene (described in supplementary information), this equal weight mixture was reduced to BTSI.

The design of experiments (DOE) for this work included testing the effects of SPME fiber retraction in the needle (5, 10, and 15 mm diffusion path lengths), and testing the effects of

sampling time (5, 10, 15, and 20 min), resulting in 12 different treatment conditions. Results from the previous work [223] indicated that the 3.3 mm depth was the worst performing depth setting (i.e., deviating from the behavior described by Eq. 1 and 2), and was therefore discarded from this DOE. The potentially higher tar concentrations expected in the gas stream also suggested that 5, 10, and 15 mm depths would be more suitable for the actual gasification environment. The overall number of treatment conditions possible was also still constrained by the laboratory sampling system, as depicted thoroughly in [223]. The DOE was slightly improved to enable the additional sampling time of 20 min. The 33% increase in treatment conditions allows a better interpretation of the data than was possible previously with only 9 treatment conditions in the proof of concept work. Gas stream concentrations were held constant at  $0.4 \text{ g/m}^3$  for the total sum of all analytes (roughly 42, 37, 32, and 29 ppm<sub>v</sub> for B, T, S, I).

According to theory, the change in response ( $n(t)$ ) should be directly proportional to time of sampling and inversely proportional to changes in depth (See Equation 2). In the previous work using benzene, the data suggested a secondary boundary layer was present at the surface of the fiber tip, which was created by the preconcentration effect of the CAR/PDMS coating [223, 249]. This effect was not substantial enough to reduce the coefficient of determination ( $R^2$ ) value to below 0.979 between  $t/\delta$  and  $n(t)$  with benzene alone. However, if the effect were to be more severe in a matrix of compounds, the constant  $D_g$  assumption may be affected to the point at which the method becomes unusable in practice.

A Lack of Fit (LOF) test was performed as a formal test on the data collected in order check the response of  $n(t)$  to changes in  $t/\delta$ . A model was developed from the data (displayed in Figures S-1 and S-2) and the test was performed on the response  $n(t)$  to the changes in time/depth  $t/\delta$ .

$$H_0: \mu_i = \beta_0 + \beta_1 x + \epsilon_{ij} \text{ (where } i = 1, 2, \dots, 12; j = 1, 2, 3)$$

$$H_A: \mu_i = \beta_0 + \beta_1 x + \epsilon_{ij} \text{ is not the model}$$

The null hypothesis shows the linear equation that was determined by the estimates for the intercept and t/d (see Table S-1 and S-2). The alternative hypothesis states that there was sufficient evidence to prove the linear model is not the model.

The lack of fit tests showed that benzene followed the same trend in the mixture of compounds as it did in the previous work as a single analyte. The terms in the linear model are significant and a high degree of linearity is also promising. However there is a significant lack of fit to a linear relationship (p value less than .0001). While sufficient evidence was available to suggest a lack of fit for Toluene as well, it was less significant than that of benzene. This implies benzene (the smallest analyte and also fastest moving analyte to the fiber surface based on diffusion theory) may be the worst case scenario for effects from the preconcentration phenomenon on the fiber tip. In addition, a plot of the residuals for benzene (Figure S-4) clearly illustrates the tendency of the model to over predict the conditions at the extreme ends of the testing, and under predict the conditions in the middle. This result verifies the lack of fit analysis, and substantiates the results from the original proof-of-concept paper that a secondary boundary layer may affect the stability of the  $D_g$  term.

Despite the secondary boundary layer effect, a highly linear nature of the response was noted in addition to small sample deviations. RSDs for benzene were all less than 5% with an average of 3.0%, and remaining RSD averages were 2%, 3.5%, and 5% for T, S, and I respectively). These data highly encouraged continuing trials of the TWA-SPME method in pilot-scale testing to compare the ability of measuring tar concentration to that of a conventional tar analysis technique.

*Phase II: Method comparison between TWA-SPME and conventional impingers*

Field testing of the TWA-SPME analytical method was performed on a fluidized bed gasification and gas cleaning pilot-plant located at Iowa State University's BioCentury Research Farm (BCRF) [257]. Due to the scale of the system and the expense of operation, the comparison between the conventional analytical approach and the TWA-SPME approach was performed jointly with other research. (*Broer, 2013 – in preparation*) A battery of tests using switchgrass as feedstock was performed on the reactor system over a period of 6 months. The joint research that was performed on the gasifier required a very steady state condition in the reactor, which was difficult to maintain for more than 1-2 h. In the few cases that a steady state was retained for longer periods of time, only the three samples shown in Table 1 were taken without complications in the conventional tar measurement equipment. A series of maintenance operations followed this battery of tests and required several months of downtime for the reactor, which limited the comparison data available to only the three tests listed below in Table 1.

**Table 1:** Gasification trials using switchgrass. Equivalence ratio indicates the amount (kg) of O<sub>2</sub> used compared to the amount (kg) actually required for complete stoichiometric combustion of the feedstock. Heavy tar is described as tar that condenses and is collected in the PC at a temperature of 105 °C.

Run	Feedrate	Equivalence Ratio	Reactor Temperature	Reactor Pressure		Heavy Tar	Char
	kg/h		C	kPa	PSIG	g/m <sup>3</sup>	g/m <sup>3</sup>
1	10.8	0.26	900	129	4	26.4	89
2	12.5	0.17	700	129	4	40.7	149
3	11.4	0.23	850	129	4	34.5	

Syngas samples were taken at two different locations during each test. Sampling location A was located approximately 3 m upstream of the tar scrubber where the syngas temperature remained around 425 °C. The slipstream was heated to 450 °C prior to entering the PC, where gas temperature dropped to ~105 °C for collection of heavy tar. Syngas exiting the PC entered the impinger train via a short sampling line that was heat traced to 130 °C to avoid continued tar condensation. This line included a thermocouple port and a TWA-SPME sampling port (Figure 1). The impinger train was cooled with a dry ice and 2-propanol bath, as simple water chilling did not completely remove all analytes of interest. A vacuum pump was used to draw the syngas through the particulate thimble filter and sampling train, and a rotameter was used to adjust flow rates for isokinetic sampling depending on gasification conditions.

The TWA-SPME sampling location for B was located immediately downstream of the tar scrubber and ~1.5 m upstream from the impinger sampling point at a process temperature of between 110-125 °C depending on the test. A compression fitting equipped with a septum was attached directly to the 1.5" stainless steel syngas piping for TWA-SPME sampling directly from the process stream. A 2 m heat traced slipstream passed syngas to the second set of impingers, which were also cooled with a dry ice/2-propanol bath. The tar scrubber removed remaining particulate matter prior to sampling at this location, which eliminated the need for a particulate filter and enabled successful sampling using only pressure from the system rather than a vacuum pump.

Raw results from the TWA-SPME analysis required multiple adjustments to account for temperature, pressure, and sampling variables. Initial  $D_g$  values were based on lab experiments (discussed in *Phase I* results) conducted at 115 °C and atmospheric pressure using a gas stream composed only of N<sub>2</sub> and the analytes of interest. However, the samples taken from the PDU

were at different conditions which varied slightly with each testing environment. Accounting for these conditions was done using a combination of approaches. The temperature and pressure were easily accounted for by utilizing the three theoretical equations used previously (Wilke-Lee, FSG, and Huang et. al) [223, 246, 247, 258]. The baseline analyte adsorption was also accounted for as in previous work by alternating samples in the PDU with SPME fibers that were missing a CAR/PDMS coating. The corresponding quantity of analytes that adsorbed onto the stainless steel outer syringe was then subtracted from the amount collected on the CAR/PDMS coated fibers.

The gas composition required a more thorough investigation. Most molecular diffusion coefficients are calculated only in a bimolecular mixture, and very few theoretical equations are available to adjust for multiple gas phase species [259]. Adjustments were made using the technique described in [259], in which the FSG equation is calculated for each bimolecular species and adjusted for the total depending on concentration of each major species. The microGC used at the end of the impinger trains during all PDU research was used to calculate the average gas composition during each test. This composition was normalized to the five major gas species ( $N_2$ ,  $CO_2$ ,  $CO$ ,  $H_2$ ,  $CH_4$ , and  $H_2O$ ) which accounted for 95% or more of the gas phase. Unfortunately  $H_2O$  has at times been shown to affect the CAR/PDMS adsorption process as well, by taking up active sites in the Carboxen [233, 260, 261]. However its effect is varied and may sometimes be insignificant due to molecular analyte size and hydrophobicity [262, 263]. Due to this uncertainty, mathematical adjustments were not made for the effect of  $H_2O$  on the SPME adsorption process, and this is cited as a potential source of error to be considered for further analysis in future experiments.

**Table 2:**  $D_g$  values derived experimentally from lab scale testing and adjustments made for PDU experiments at sampling locations A and B. Note:  $D_g$  was only significant to 2 digits and adjustments for  $H_2O$  were only for molecular diffusion effects and not the effect of humidity on the CAR/PDMS adsorption process.

	<u>Original</u>		<u>Revised</u>
		A	B
Benzene	0.133	0.164	0.120
Toluene	0.109	0.134	0.097
Styrene	0.101	0.124	0.090
Indene	0.083	0.103	0.075
<i>Conditions</i>			
Temperature (°C)	115	131	115
Pressure (kPa)	101	101	129
Gas Composition	$N_2$	$(N_2, CO_2, CO, H_2, CH_4, H_2O^*)$	

\*Note:  $D_g$  only significant to 2 digits

$H_2O$  was accounted for via Molecular weight only, not any effect due to CAR/PDMS coating interference

Initial results from the Impinger analysis also required substantial revision. The 2-propanol impingers were chilled to ~200K, which caused significant amounts of non-condensable gas (NCG) to dissolve and collect into the impingers. This dissolved gas was subsequently not counted for in the wet-test meter results. Immediately after sampling, the impinger samples were allowed to sit at room temperature after initial weights were taken and the dissolved gases were allowed to vent. This was done to prevent violent release of the samples once bottled and readied for transport. Once the dissolved NCGs were released, the samples were weighed again and the difference was accounted for in the wet-test meter as  $CO_2$ . The complicated matrix of 2-

Propanol, water from the steam/O<sub>2</sub> gasification process, and similarly low boiling point analytes of interest also created significant problems in GC-FID analysis. A separate analysis was performed by an independent lab (Minnesota Valley Testing Laboratory – MVTL) and showed potential matrix effects were possible with the varied concentration of water in the impinger samples. All subsequent tests were also sent to MVTL for verification of analyte concentrations prior to final comparison of the conventional and TWA-SPME analytical methods.

**Table 3:** Quantified analytes compared between TWA-SPME and conventional impingers (L.D. represents values below limit of detection for method)

Location	A		B	
	TWA-SPME	Impinger	TWA-SPME	Impinger
			<u>Run 1</u>	
	g/m <sup>3</sup>	g/m <sup>3</sup>	g/m <sup>3</sup>	g/m <sup>3</sup>
Benzene	9.0	16.2	6.4	7.7
Toluene	0.25	0.33	0.41	0.26
Styrene	0.26	0.45	0.07	L.D.
			<u>Run 2</u>	
Benzene	4.9	13.6	6.9	7.2
Toluene	2.2	5.1	0.69	0.29
Styrene	1.0	2.0	0.14	L.D.
			<u>Run 3</u>	
Benzene	7.4	17.8	10.3	10.5
Toluene	1.1	2.2	0.83	0.54
Styrene	0.59	0.96	0.13	L.D.



Final results from the three successful comparison trials (stated in Table 3) indicate a general level of success in terms of a comparable quantity of light syngas tars identified by both the TWA-SPME method and the conventional impinger approach. Differences between runs are expected given the different operating conditions. The heavy tar values in Table 1 correspond as expected with the equivalence ratios: lower equivalence ratio yields more heavy tar [23, 254]. The overall trend in light tar is difficult to discern from the two different methods of measurement, but may indicate according to data from location A (prior to the cleanup stage in the tar scrubber) a tendency of heavy tar to crack at higher temperatures and yield larger quantities of lighter tars (Runs 1 and 3 compared to 2). This phenomenon directly corresponds to conventional knowledge of tar formation and methods of destruction, at which multi-ring tars may crack above 850 °C and single ring tars remain intact until temperatures exceed 1000 °C [14, 42]. More fundamental kinetic studies in the laboratory may further confirm this phenomenon.

The tar samples taken with the TWA-SPME method at sampling point A were always less than that of the impinger approach, but more closely align with literature values. Typical literature values for benzene for instance may range from a few g/m<sup>3</sup> to up to 45% by weight of the total tar volume quantified [5, 28, 30, 254, 256].

The conventional and TWA-SPME analyses were substantially more similar at sampling location B, with relative differences typically less than 10%. This is beneficial when considering deployment in commercial gasification systems since trace tars are of greatest concern downstream of the cleaning processes. The inability of the impingers to detect the styrene present in the TWA-SPME analysis also shows the significance of the new method's ability to quantify otherwise undetected compounds.

A variety of potential issues could be responsible for differences occurring between samples taken at different locations. The different methods of removal for heavy tar may play a primary role. The pressure cooker method utilizes indirect contact heat exchange limited by convection to reduce the syngas temperature. Tar is collected via condensation and deposition on the surface of the tubing and small canister of glass wool inside the PC. The tar scrubber utilizes a much more efficient direct-contact heat exchange process with cooler oil. In addition to rapid condensation, it also applies a counter-flowing oil spray to achieve a very efficient removal of aerosol vapors. Compounds such as naphthalene should condense in the pressure cooker and be included in the heavy tar fraction of Table 1 as its dew point is higher than the 105 °C set point. However, as seen by the coloration in Figure S-6 and noted in Table S-3, compounds such as naphthalene are less efficiently removed with the PC and may also deposit in the impinger train, yielding much higher tar values when compared against the post cleanup location. Lower tar concentrations at location B compared to location A may also be due to the much lower temperatures attained at times in the syngas cleaning unit. Due to the short sampling times allowed by the gasifier, there was insufficient time to reach a steady operating state in the oil scrubber. Typical operating conditions were ~115 °C, but periods of operation occurred below 80 °C. This results in greater condensation of tar and potentially absorption into liquid water that is condensed from the high concentration of steam in the syngas.

Some discrepancy between the two sampling methods at location A could also be explained by the inconsistent vacuum pump and thimble filter pressure disturbances located on the sampling line. These devices made it difficult to accurately predict the pressure at the SPME sampling point for proper adjustment of the  $D_g$  values during analysis.

The high variability in the conventional method may also be a source of discrepancy between the two techniques. According to [12 and 14], the overall variability in the conventional approach is typically 20-40% for many analytes. In addition, the high quantity of water vapor in the syngas from the steam/O<sub>2</sub> gasification process may cause analytes to preferentially separate in the impinger containers and vials while awaiting analysis. GC-FID trials were conducted to test this theory using a calibration standard of the analytes of interest that was spiked with 20% water. Results reflected the hydrophobicity of the analytes with a minimal but noteworthy 2%, 5%, 10%, 14% and 17% increase in response for B, T, S, I, and N respectively. The sampling at location A also requires isokinetic sampling to maintain proper collection of heavy tars. Data analysis later indicated that isokinetic rates were missed by as much as 30% on occasion during the 6 months of trials, with no discernible pattern to the wet-test and rotameter discrepancies. This would also affect the collection of heavy tars giving a false indication of the light/heavy tar ratio.

TWA-SPME sampling configurations during gasification were also altered from the lab-scale analysis due to higher than expected tar concentrations. Despite the higher concentrations, the adjustments in sampling depth and time of extraction were able to keep analyte quantity on the fiber for all tests within an order of magnitude of the calibrations performed in the lab [223]. This should be noted however as a potential source of error, resulting in a possible underestimate of tar via the TWA-SPME technique at location A. However, because there was zero carry over in the fiber after analysis and the samples stayed below the 5-10% saturation levels required by the zero-sink hypothesis (the high capacity of Carboxen is orders of magnitude higher yet), it is unlikely that the under-estimate was off by more than a few percent [264].

Evidence for this is seen by the linear response in the higher concentration lab experiments of previous work.

**Table 4:** Total light tar estimations from conventional solvent impinger measurements and TWA-SPME analysis. All totals calculated using BTSI calibrated compounds and adjusting for the percentage of the total tar compounds present in the chromatogram. BTSI in all cases was 50% to 90% of the total peak area.

Location	A		B	
	TWA-SPME	Impinger	TWA-SPME	Impinger
	<u>Run 1</u>			
Total Tars (g/m <sup>3</sup> )	15.4	25.4	10.4	9.6
W/out Light Ends	12.4	24.2	7.7	7.7
STDEV T (g/m <sup>3</sup> )	4.0		4.4	
STDEV WoLE	3.4		3.0	
RSD TT (%)	26%		42%	
RSD WoLE	27%		39%	
	<u>Run 2</u>			
Total Tars (g/m <sup>3</sup> )	16.0	43.8	18.1	13.4
W/out Light Ends	12.0	38.0	8.3	7.2
STDEV T (g/m <sup>3</sup> )	3.1		3.4	
STDEV WoLE	1.4		3.0	
RSD TT (%)	19%		19%	
RSD WoLE	12%		36%	
	<u>Run 3</u>			
Total Tars (g/m <sup>3</sup> )	9.3	28.6	17.6	14.0
W/out Light Ends	8.2	26.7	11.2	10.5
STDEV T (g/m <sup>3</sup> )	1.7		2.0	
STDEV WoLE	2.2		1.4	
RSD TT (%)	18%		11%	
RSD WoLE	27%		12%	

Total light tar calculations were estimated in Table 4 from the relative abundance of quantified compounds in the chromatograms. The light tars were calculated as BTSI and then a correction was applied to account for the missing mass percentage in the chromatograms that was not due to

those 4 calibrated compounds. A second calculation was performed by discounting all compounds smaller than benzene (termed: without light ends, or WoLE). This adjustment was made to reflect the inability to read some analytes in the impingers due to the co-elution in the GC-FID with the 2-propanol solvent. It also more accurately reflects the true definition of ‘tar’, which is typically considered as benzene compounds and larger [253].

The discrepancies between samples become exacerbated when comparing total tars using only 4 calibrated analytes, but the table is useful for comparing typical light tar values to those reported in literature. A majority of the compounds displayed in the chart are single ring aromatics, as shown in Table S-3. For each test three extractions and three baselines were taken successively for TWA-SPME in the PDU trials, which allowed for a standard deviation and RSD calculation. Unfortunately the impinger analysis was not amenable to taking several different impinger samples from each location. RSD information for the impingers is limited to the 2% or less RSD values attained during direct injection of liquid samples into the GC-FID for analysis.

Large RSD values for the SPME samples in the pilot scale trials may reflect the drastic changes that occur in the pilot scale sampling train. Samples for the conventional method were collected over a 50 min period on average, whereas TWA-SPME samples were collected over several different 5 min sampling periods. Inconsistent pump performance, changes in sampling line pressure drop, or changes in gas composition are captured by the TWA-SPME method but are averaged out in the conventional analysis. Unlike commercial-scale operations, the gasification pilot plant is only operated when samples are required. The large thermal mass of the gasifier and cleaning equipment make it difficult to attain truly steady state conditions in all aspects prior to sampling. Commercial operations will still suffer from inconsistencies in sampling lines, but the TWA-SPME method can extract samples directly from the process stream

eliminating this unwanted variation as well. The TWA-SPME data that indicated the dynamic nature of the system was also available within hours, compared to the 1-3 days it required for data to be returned from the conventional analysis.

## **Conclusions**

The TWA-SPME concept for analysis of syngas tar at elevated temperatures is a valuable measurement technique compared to the conventional solvent-based impinger approach. The presence of a secondary boundary layer as shown in original proof-of-concept testing was confirmed in multicomponent testing, but was found again to have minimal effect on the usefulness of the method. Validation of the concept against a conventionally accepted technique was performed using a pilot-scale gasification and gas cleaning system. Data indicated the method was capable of staying within 20% of the standard method for light tars downstream of a syngas cleaning unit. The poor performance of the conventional method and inherent difficulties of both methods were evident when obtaining raw syngas samples. The isokinetic sampling rates often deviated from their intended set points, temperature and pressure fluctuations in the pressure cooker and sample lines made steady-state sampling and gas measurements difficult, and complicated sample matrices required repeated wet chemical analyses for verification of analyte concentrations. The TWA-SPME samples also required multiple corrections for temperature, pressure, and gas-phase composition, but still provided useful data for comparison. In addition, the method was capable of showing the dynamic nature of the syngas, and was able to identify and quantify more analytes than that of the conventional solvent-based approach.

Future comparisons to other conventional approaches that do not suffer from the same difficulties as the impingers would be highly helpful useful to confirm and more accurately test this method. SPA/SPE is a potential candidate given its similar resilience to SPME, despite the

need for solvent-based lab work [7, 19, 21]. Expand the laboratory testing environment to include multiple other temperatures may yield help develop a full model for compounding effects of different temperatures, pressures, and analytes (carbon/hydrogen numbers or molecular weight correlation).

A major disadvantage of the method is the 300 °C or lower temperature limit on the SPME fibers, which currently restricts sampling to only GC-detectable tars. Currently under development is a new internally-cooled SPME device that would enable sample extraction from higher temperature environments. Future work may also consider testing the effects of thermophoresis on this device and its potential for sampling all high temperature contaminants directly from process gas streams such as pyrolysis or combustion processes. This technique would potentially avoid the time consuming and complicated conventional sampling trains.

### **Author Information**

\*Corresponding author: [koziel@iastate.edu](mailto:koziel@iastate.edu), 515-294-4206

<sup>a</sup>Iowa State University, 3122 Biorenewables Research Laboratory (BRL), Center for Sustainable Environmental Technologies (CSET), Ames, Iowa, 50011 USA

### **Acknowledgements**

The authors of this work appreciate the financial contributions of Phillips66 to fund this work. Appreciation to Dr. Derrick Rollins is also expressed for his assistance with statistical analysis.

## **CHAPTER 5. CHALLENGES AND POTENTIAL SOLUTIONS TO ANALYZING ALTERNATIVE THERMOCHEMICAL PROCESS GAS STREAMS**

The following work reflects the additional thermochemical process applications currently under investigation for the TWA-SPME analytical method. Pyrolysis vapors are of primary interest given the widespread development of fast pyrolysis based processes for replacement of petroleum-based fuels and chemicals. TWA-SPME sampling was performed at several locations along the vertical axis of a free-fall pyrolysis reactor tube, which equates to the residence time of the biomass particles in the reactor. These samples captured the time-evolution of light pyrolysis compounds such as acetic acid, styrene, and levoglucosan. The trial highlighted the challenges of sampling in environments near the limits of typical commercial-grade SPME fibers. An internally-cooled SPME fiber was constructed to address this limitation, similar to the fiber created by Pawliszyn's research group in Canada [265, 266]. Initial trials have shown the apparatus is capable of RSDs of less than 6 % when applied directly to the pyrolysis environment. Unlike previous generations of the device, the new internally-cooled fiber was also tested successfully on commercial GC-FID and GC-MS equipment, with only minor adjustments to the injection port and no special equipment required.



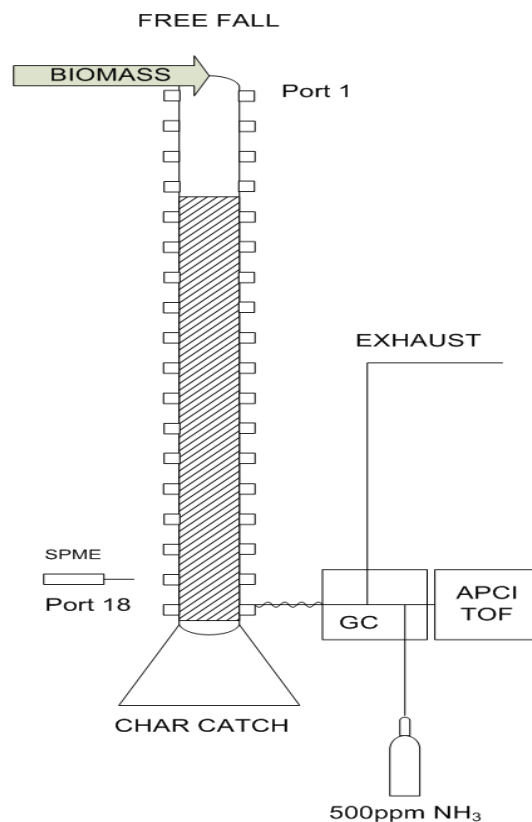


**Figure 1:** Pyrolysis Free-Fall Reactor

A free-fall reactor was constructed at Iowa State University for the purposes of testing pyrolysis kinetics [267]. This reactor system (Figure 1) was also equipped with dual sampling ports along the longitudinal axis to represent the residence time of a biomass particle within a pyrolysis environment. One of these sets of ports was dedicated to sampling with SPME.

Carboxen/polydimethylsilosane (CAR/PDMS) fibers used near the 300 °C limit showed substantially lower sample extractions than was possible in lower temperature environments, as shown in Figure 2. Thermal desorption, a key concept in chemical engineering, is one cause of this phenomenon. The molecular diffusion rates of analytes and the adsorptive/absorptive properties of SPME fibers change drastically with temperature as well, making it difficult to

extract definitive or quantitative information given the sometimes significant temperature differences between sampling ports (up to 80 °C based on heater location).

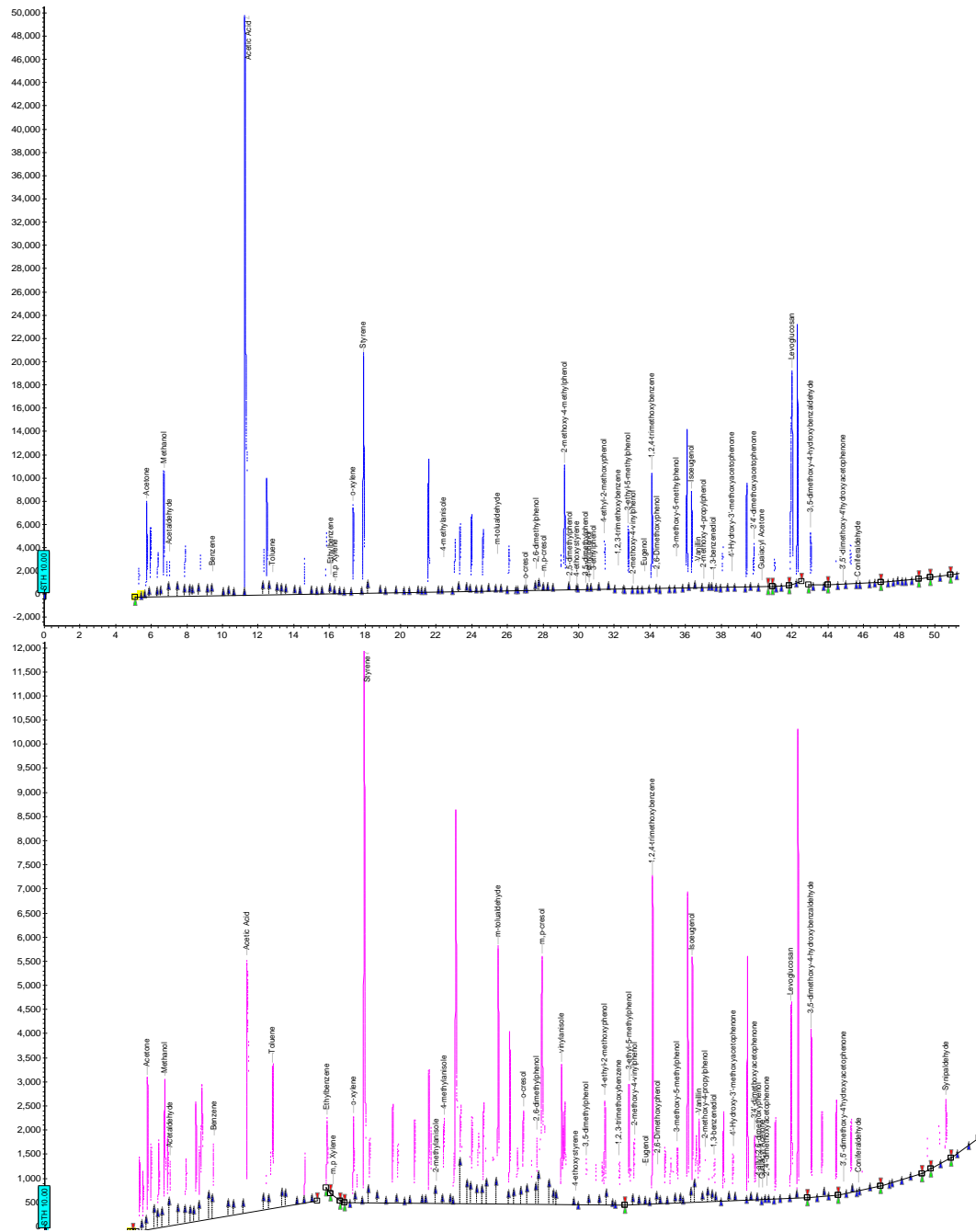


**Figure 2:** TWA-SPME chromatograms of port 14 of the free fall reactor (top) and port 18 (bottom) taken with CAR/PDMS. Environmental conditions in the ports of the reactor were approximately 0.5 psig and 200 °C for port 14 and 300 °C for port 18.

Relative differences may be discussed between chromatograms, such as the larger quantities of various light compounds in the longer residence time port (Port 18). The light ends of both chromatograms were also substantially higher than ports higher in the reactor. Secondary breakdown of heavier vapor phase molecules could be seen in the levoglucosan peak reduction as well. However, any insightful kinetic data is difficult to quantify given the many variables to consider as temperatures change so drastically. Reaching or exceeding the limitations of the fiber near 300 °C is also a concern. A highly volatile and dynamic environment such as gasification or pyrolysis will greatly benefit from a means of temperature stabilization during sampling with the TWA-SPME analytical method.

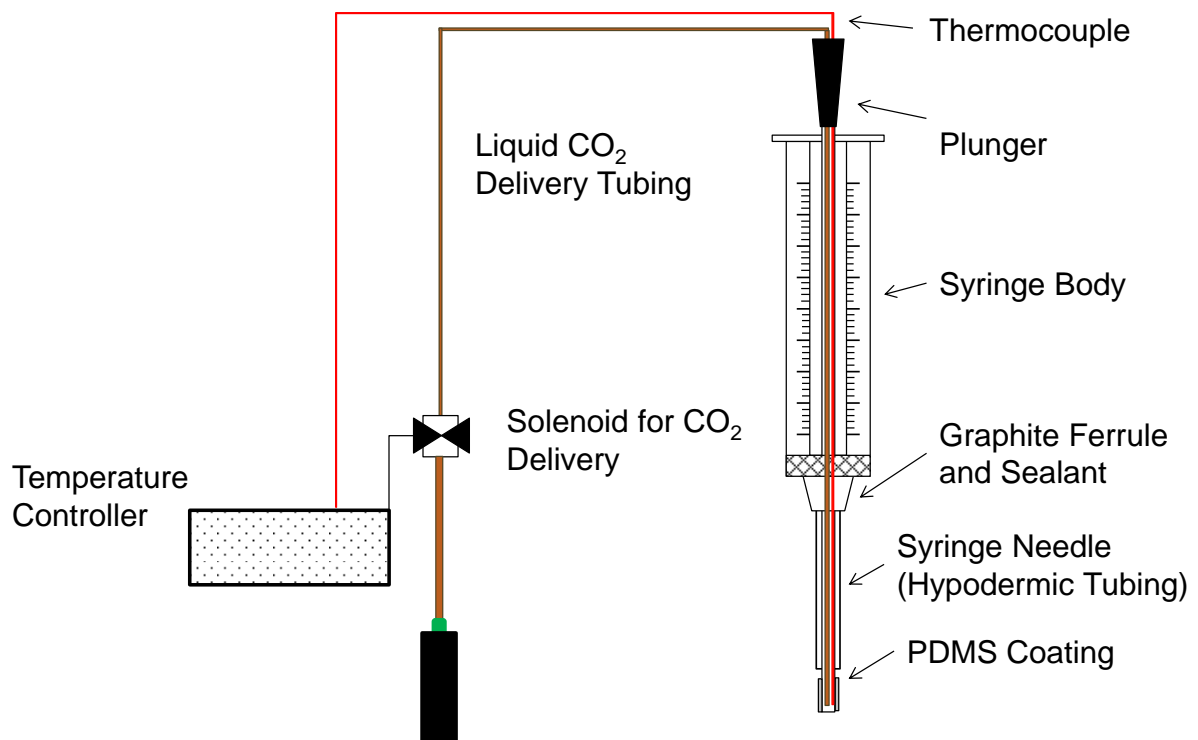


**Figure 3:** Schematic for the internally-cooled SPME device.

An internally-cooled SPME device may be a potential solution to the temperature complication in thermochemical conversion processes. Essentially a hybrid SPME fiber, it includes an internal cooling stream of liquid-CO<sub>2</sub> that vaporizes and escapes to the lab environment to cool the SPME fiber within its extraction environment.

A schematic for the internally-cooled SPME device is provided in Figure 3. A 100 uL Hamilton gastight syringe was purchased and the removable needle was replaced with the following series of tubes. The outer tube was then sealed in place using Red RTV, and the middle tube (the plunger) was sealed using a septum and GC ferrule to allow freedom of movement as needed.

The smallest hypodermic tubing available was 0.004" (0.102 mm) ID and 0.008" OD (0.203 mm) from McMaster-Carr. It was purchased at the maximum 3' to transfer liquid CO<sub>2</sub> from the solenoid valve to the tip of the syringe. A miniature 0.010" (0.254 mm) diameter mineral insulated thermocouple with potting adaptor was also purchased from TC Direct. This tubing was inserted into the second tube that was sealed on one end. This tube was purchased at the desired length for passing through the syringe housing and serving as the plunger (roughly 10" (25.4 cm)) was required for this experiment). 0.02" (0.508 mm) ID and 0.025" (0.635 mm) OD tubing was the smallest tube capable of easily sliding the Liquid-CO<sub>2</sub> transfer tube in and out of the device for transport to the analytical equipment (GC-FID). This tube would also have the PDMS coating placed on the end in future experiments. The final tube was cut to a length of approximately 3" to reach inside of the free-fall pyrolysis reactor sampling ports. This tubing served as the outer syringe housing to protect the plunger from the environment. A 0.042" (1.0668 mm) OD and 0.035" (0.889 mm) ID tube was selected for this apparatus to allow enough space for a PDMS coated tip at the end of the plunger.

The solenoid for CO<sub>2</sub> delivery is rated for cryogenic liquid up to 1000 psi, and was attached directly to the liquid CO<sub>2</sub> cylinder, without an intermediate pressure regulator. The extra thermal mass of an additional regulator made it difficult to obtain liquid CO<sub>2</sub> at the tip of the fiber. Even without the regular, approximately 1 minute of unregulated flow through the tubing was required to cool the solenoid and tubing with 1" insulation so that liquid CO<sub>2</sub> would begin flowing at the tip of the fiber. After this point, the tubing could be inserted into the syringe and testing could begin. Liquid Nitrogen was also attempted, but the pressures capable in cryogenic tanks for liquid nitrogen (~15 psig compared with ~600 psig for liquid CO<sub>2</sub>) were too low to obtain substantial flow rates. The large difference in temperatures between the liquid nitrogen and the equipment/lab resulted in gaseous liquid nitrogen emitted rather than liquid. Only the high mass flow of liquid CO<sub>2</sub> making contact with the fiber was able to cool the device within the high temperature environment.

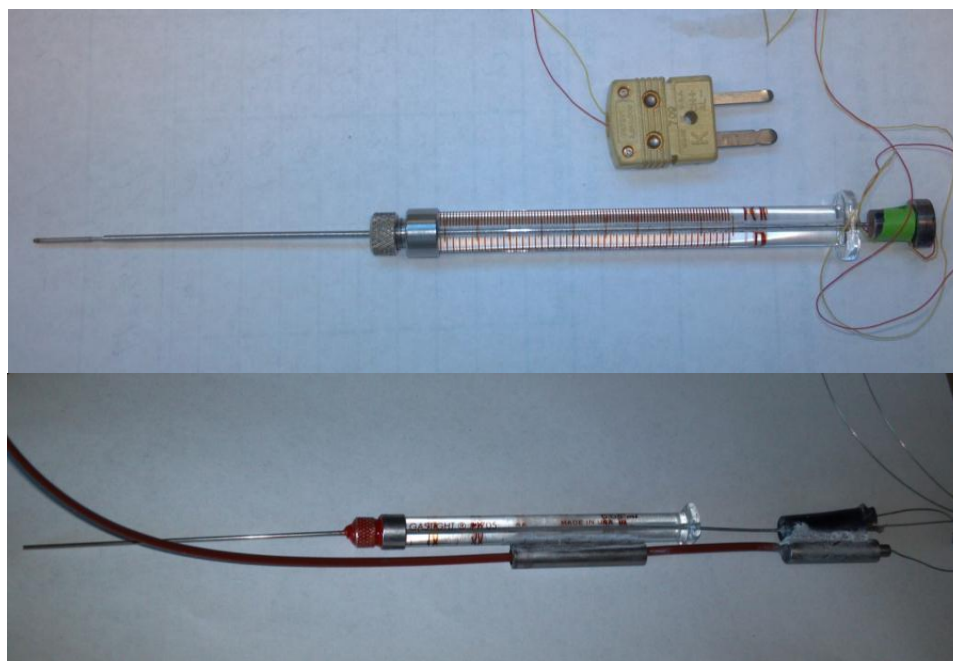


**Figure 4:** The original (top) and new (bottom) internally-cooled SPME devices

The new fiber was scaled down by nearly 25% compared to the previous internally-cooled fiber, which enabled use of regular septums in sample environments and GC-FID injection liners [265, 268]. The septums appeared to have a drastically shorter lifespan of approximately 20-30 injections, but were a substantial improvement from the expensive septumless adapter that was previously required. The only additional change that was required was to drill the injection port on the GC-FID purge port cover (Bruker part # 392597302-CAD) to a slightly larger diameter to fit the new 1.07 mm tubing.

More development of the apparatus is still required to maintain the fiber at tighter temperature tolerances. A substantial delay in the current device is often present when cycling the carbon dioxide solenoid valve. This is partially due to the solenoid spring freezing and partially due to the unregulated flow of liquid-CO<sub>2</sub> rapidly cooling the tip of the fiber, even in the high temperature pyrolysis environment. A small needle valve was attempted to regulate the flow, but it was logistically problematic to locate one of appropriate size that was rated for cryogenic liquids.

Despite these challenges, the results were very promising. RSDs obtained during red oak pyrolysis in the free-fall reactor were less than 6% for the target analyte levoglucosan. The device also operated consistently to reduce the temperature of the fiber tip from the sample environment temperature of ~360 °C to approximately 130-140 °C. The effects of this drastic temperature change are evident in Figure 5.

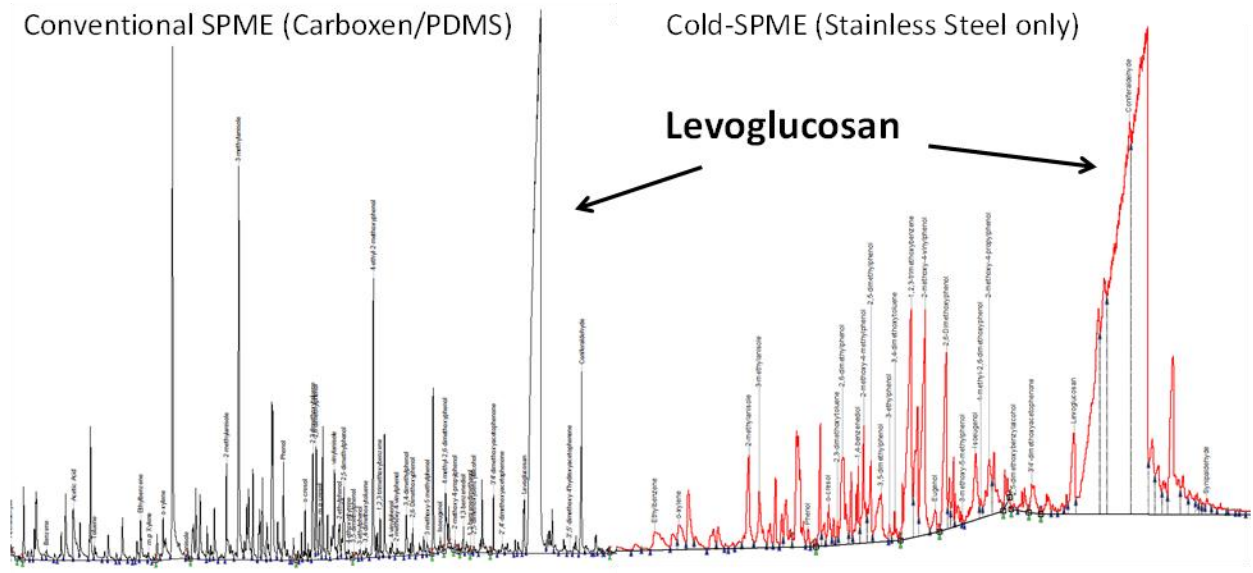


**Figure 5:** Chromatograms taken in the free-fall reactor with cellulose, showing the main peak of levoglucosan that was targeted for the extraction conditions.

Future work may also yield more valuable information on the kinetics of pyrolysis. Analyzing the samples extracted with a high-temperature GC-MS/FID may be able to identify more compounds than previously possible. Using library searches for analytes larger than 300 Da may be difficult, but desorbing the extracted analytes into a liquid medium and using HPLC can further provide information on the primary degradation products from biomass. Finally, the major benefit of the internally-cooled fiber may be the ability to flash freeze the analytes in their initial volatilized state. Conventional SPME captures the analytes and retains them in their high temperature environment until extraction is complete, and conventional liquid sampling still allows up to a few seconds before the analytes are completely cooled and restricted from further reaction. The drastic temperature reduction possible with the internally-cooled device essentially reduces the temperature of the compounds immediately upon contact, thereby capturing a more realistic picture of the compounds actually present in the first few instances following particle

devolatilization. Analyzing these compounds with a TOF-MS for up to 3000Da could be performed on the system in its current configuration, and other techniques such as SPE/SPA could be attempted to compare differences.



## CHAPTER 6. CONCLUSIONS

Thermochemical processing techniques are among the most promising means of converting waste and other forms of renewable carbon into suitable substitutes for fossil-derived fuels and chemicals. Research for improving thermochemical processing is severely hindered and commercial-scale operations are difficult to optimize without rapid and dependable analysis of process gas streams.

Substantial improvement has been made in thermochemical processing technology over the past few decades. Commercial scale facilities now exist to convert solid carbon fuels into liquid transport fuels and chemicals via gasification and downstream processing applications like catalysis and fermentation (Sasol, LanzaTech, and SunDrop Biofuels are just a few examples). New syngas cleaning technologies have also begun to address the issues inherent in conventional syngas cleanup, such as water contamination and other environmental hazards. A particular group of contaminants that have received a great deal of attention are the VOCs in syngas known as tar. These aromatic, polyaromatic, and heteroaromatic substances were typically removed in the past with water scrubbing, which created an expensive and environmentally challenging waste stream to address. New methods of tar removal via oxidation, catalysis, and oil scrubbing have drastically reduced the quantity of tar compounds found in syngas streams. However, their processes can be costly, and optimizing the cleaning process for an acceptable level of light tar contamination downstream can be economically attractive.

A substantial gap exists in the ability to measure heavy and volatile organic compounds in thermochemical processing gas streams. The analytical methods have not kept pace with the commercialization of the technology. Only recently has a standardized method been adapted in Europe and the United States to address the inconsistent reporting in research on the amount of

tar found in process gas streams from gasification. Unfortunately this procedure requires extensive use of equipment (glassware, pumps, probes, solvents, heated sampling lines), is difficult to perform with accuracy and precision, and requires large amounts of time for sampling and sample preparation/analysis. Results are typically only available after a day or more of sample analysis, and with fair reliability at best, which is unsuitable for actively monitoring commercial processes that depend on precise operation for economic success.

A novel method of measuring volatile organic compounds (VOCs) present in thermochemical process gas streams has been developed based on time-weighted average solid-phase microextraction (TWA-SPME) theory. The theory was first tested at lab scale with benzene in  $N_2$  at  $\sim 115^\circ C$  to model tar in syngas at elevated temperatures. Theoretically, the molecular diffusion coefficient ( $D_g$ ) should be unaffected with changes in sampling time and depth of fiber retraction into the SPME housing. Once determined in lab experiments or via diffusion theory, the value can be used with the appropriate sample conditions to determine concentration via Equation 2 in Chapter 3. Results showed a significant deviation from theory in this case, but despite this phenomenon there was a highly linear correlation between the depth/time ratio and the amount adsorbed on the fiber. The quantity of model compounds was increased to include all major tar constituents likely to be found downstream of major syngas cleaning processes. Similar results confirmed the presence of a secondary boundary layer developing at the tip of the fiber during TWA-SPME sample extractions. However, the highly linear nature of the response regardless of concentration also confirmed the merit of the technique for application to larger scale validation trials, as long as performed within acceptable limits on the fiber.

Substantial heat loss along the diffusion path length during sampling was also noted in the lab-scale trials, indicating that the entire sampling zone and SPME apparatus should be heated to the appropriate sampling temperature if possible. This is important for maintaining constant diffusion conditions. If not possible, using the longest retraction depth and extraction time that are still within appropriate conditions will provide the most accurate and precise response. The baseline tar compounds collected on the bare stainless steel portions of the SPME syringe housing were also found to be significant. This quantity of tar must be accounted for according to the length of time exposed to the environment. (There were no significant changes in analyte collection on the bare-fiber as a result of changes in bare-fiber retraction depths.)

The TWA-SPME method was also validated against conventional techniques used for quantifying tar compounds in a pilot-scale gasification and gas cleaning system. A recently constructed fluidized bed gasifier and gas cleanup train was used to conduct tar quantification trials using the TWA-SPME technique and the conventional impinger-based technique. Two different locations were sampled: one location downstream of a pressure cooker used to collect heavy tar compounds, and another location downstream of the tar removal process (an oil scrubber). Initial testing during the first 4 months confirmed the complicated and error-prone nature of the conventional technique. 3 successful comparisons were made at both locations between the TWA-SPME and conventional impinger approaches. Tar concentrations quantified downstream of the tar cleaning process using the TWA-SPME method were within 20% of the impinger method, and were typically within 10% or less of the impinger values.

Measuring tar concentrations downstream of the pressure cooker presented multiple challenges to obtaining valuable comparison data. Deviations from isokinetic sampling, inefficient pressure cooker heavy tar collection, and variations in sample line conditions of

pressure and temperature were likely contributors to the large discrepancies between the two methods. Engineering work performed on the tar scrubber alluded to tar aerosol formation as another potential contributor to poor pressure cooker performance. The complicated sample matrix of 2-propanol, water, and tar compounds in the impingers also created difficulty when quantifying the samples. External lab analyses were required to correct and validate the results.

Despite the challenges using TWA-SPME, the method resulted in values that were very close to those reported in literature in both sampling locations, which encourages further comparison trials to alternative methods such as SPE/SPA. The method is also appropriate as a first approximation of tar quantification in process scale gasification environments, given the many benefits of sampling directly from process piping downstream of cleaning equipment. These include elimination of sampling lines, extensive equipment, and solvents, as well as obtaining results in a matter of 1-2 h as opposed to days for the conventional technique.

Challenges in measuring higher temperature process gas streams have been identified and potential solutions have been recommended. One such solution is the further development and application of the internally-cooled SPME device. A new version of the 'cold-SPME' device has been developed that enables use of conventional analytical equipment. RSDs for the device used in a free-fall pyrolysis reactor have been less than 6 %. A major benefit of the device is its ability to essentially freeze the analyte composition onto the fiber as the temperature of the fiber may be more than 200 °C lower than the surrounding environment. More development on this device is needed to maintain a tighter tolerance on the fiber temperature for longer periods of time. This will be essential for definitive quantification using TWA-SPME measurements in higher temperature (>300 °C) environments in the future.

## APPENDIX

### GC-FID calibration issues using TWA-SPME

The following is a short communication article in preparation regarding the calibration adjustments required for solid-phase microextraction. The target journal is Journal of Chromatography A.

# Letter: Optimizing calibration for Solid-phase Microextraction using GC-FID

*Patrick J. Woolcock<sup>a</sup>, Jacek A. Koziel<sup>\*</sup>, Patrick A. Johnston<sup>a</sup>, Robert C. Brown<sup>a</sup>*

Iowa State University, 3202 NSRIC, Department of Agricultural and Biosystems  
Engineering, Ames, Iowa, 50011 USA

Keywords: solid phase microextraction, autosampler injection, calibration techniques, manual injection

**ABSTRACT.** Solid-phase microextraction (SPME) is a fairly recent, yet rapidly expanding analytical technique that is being widely adopted by many disciplines. The purpose of the technique is to combine sample extraction and preparation into a single, solvent-free step

of the analytical process, which eliminates many time-consuming processes in conventional chemical analysis. However, the process is highly susceptible to accuracy of the calibration techniques that are utilized on the analytical detection equipment. Extensive calibration work was performed using a pair of gas chromatographs coupled with flame ionization detectors (GC-FIDs) to illustrate the most accurate means of calibration for SPME experiments. Two different Varian 430-GC gas chromatographs coupled with flame ionization detectors (FIDs) were used with two different Varian CP-8400 autosamplers. Manual injections were also performed with a zero-dead-volume syringe. The calibration standards included four compounds mixed individually in acetone at 5 concentration levels each, as well as the compounds mixed together in a single acetone solution at 4 different concentrations. Results indicated a significant difference between GC-FIDs. The autosampler using individual mixtures of the compounds was the most accurate, but required a correction factor for partial volatilization of liquid in the syringe needle.

## **Introduction**

### *The Analytical Process*

A majority of the time spent during conventional chemical analysis is devoted to sampling and sample preparation. The remaining stages of analysis are relatively rapid thanks to advanced equipment such as the gas chromatograph-mass spectrometer (GC-MS) or flame ionization detector (GC-FID) which can rapidly separate and quantify components of a complex matrix. However, automating the collection and preparation of these samples for analysis by an analytical device is difficult. Conventional processes typically use an extraction medium (a sorbent for example) to obtain samples from an environment, and then apply multiple steps using organic solvents to properly prepare a sample for analysis.

*Solid-phase Microextraction (SPME)*

SPME avoids the use of these solvents by combining sampling and sample preparation into a single step, which can drastically reduce overall analysis time [36, 269]. It essentially comprises a small solid support (fused silica tubing for instance) onto which an extraction phase is placed as a coating. The entire assembly is contained within a small syringe needle (23 or 24 gauge), which can then be inserted directly into the injection port of a GC-MS or GC-FID.

The primary difference between SPME and other collection techniques (such as solid-phase extraction, or SPE) is the size of the device. Using such a small extraction phase has multiple advantages. The technique operates on an equilibrium basis, rather than exhaustive extraction. Equilibrium in this case refers to the analyte concentration in the sorbent volume (i.e. coating of extraction phase) relative to the surrounding environment. Extraction can be performed based on either the *rate* of analyte collection or *saturation* of the sorbent volume at an equal concentration to that of the surroundings. Equilibrium extraction techniques are not concerned with breakthrough, whereas exhaustive extraction techniques depend on a large sampling device to eliminate breakthrough (i.e. a situation in which more analytes are present than can be collected by the sorbent and therefore pass through the collection device, which upsets concentration measurements). The large sample volume requires extensive preparation to obtain samples of proper size for the analytical equipment, whereas a SPME fiber can be directly inserted into the analytical device. The non-exhaustive SPME technique also minimizes the likelihood that perturbations of the sample environment will occur when analytes are removed. This increases accuracy of results and enables the device to more precisely capture chemical changes occurring within the sample environment.

Accuracy and precision also depend on equipment used for sample analysis, such as GC-MS or GC-FID. Directly desorbing the SPME fiber in the injection port of the analytical equipment requires accurate calibrations for the compounds of interest. Many calibrations are performed with the same autosampling devices utilized for running samples, which eliminates any bias that evolves from the equipment. However, since the SPME fiber is used only for sample introduction to the equipment, the resulting bias from using an autosampler for calibration can substantially alter overall results.

There are multiple methods available for calibrating the analytical equipment. Autosampling devices are very common and provide superior precision and repeatability compared to classical direct injection methods. However, a disadvantage of these devices when used with SPME is the volatilization of a portion of the solution contained within the syringe. Many autosamplers utilize a syringe that retains a dead volume of solution within the syringe needle (e.g. Hamilton 10  $\mu$ L *MICROLITER* syringe). This dead volume is intended to remain in the syringe during injections and is not counted as injected volume. Unfortunately, high injection port temperatures intended to rapidly move solutions to the column will vaporize a portion of this ‘dead volume’, thereby inadvertently increasing the amount of sample that is injected.

The additional sample volume is not a concern when calibrations and samples are both run with the same autosampler because very little deviation typically exists in the amount of solution that is vaporized. However, the amount can be significant. For instance, if only a few extra tenths of a microliter are volatilized during injection of a one microliter sample (a typical maximum for direct liquid injections), the additional volume may easily exceed 25% of the intended sample amount. One potential solution to combat this issue is to manually inject the



samples using a zero dead-volume syringe. However, accuracy and precision with manual direct injections are typically poor and heavily dependent on the operator.

The objectives of this work are to evaluate the major techniques available for calibrating analytical equipment such as a GC-FID or GC-MS for SPME. An autosampler will be compared with manual injections, and two different autosamplers will be compared as well. Comparisons will also include a correction factor with the autosampler to account for the amount of dead volume that is vaporized during sample injection. Finally, calibrations using analytes mixed together and analytes injected separately will show be used to determine the most accurate calibration preparation method for the standards of interest.

### **Experimental Section**

**Chemicals.** Benzene (Sigma-Aldrich CHROMASOLV®Plus, for HPLC  $\geq 99.9\%$ ), toluene, styrene, and indene were used as model tars within an HPLC grade 2-propanol solvent. All work with chemicals was performed following lab safety protocols, using vented fume hoods and approved personal protection gear.

**Materials.** Samples were analyzed using a GC-FID (Varian GC-430), supplied with UHP hydrogen (30 mL/min), air (300 mL/min), and helium (25 mL/min). The GC injection port was held 250 °C and fitted with a regular Split/Splitless injection sleeve; 10 split was used for the manual 1 uL syringe injections of 0.5 uL, and 100 split was utilized for the 1 uL injections with the 10 uL autosampler syringe. A Phenomenex Zebron ZB-5ms column (60 m  $\times$  0.25 mm  $\times$  25  $\mu$ m) was held at a constant flow of 1.2 mL/min and used a temperature program of 50 °C for 1 min followed by heating at 10 °C/min to 150 °C. The FID was operated at 280 °C and the acquisition frequency was set at 20 Hz. A Hamilton 1 uL gastight syringe and a Hamilton 10 uL

gastight syringe were used for sample injections. The 8400 series autosampler was used for autosampler injections.

### **Results & Discussion**

**Autosampler Injection Analysis.** Discrepancy in initial  $D_g$  results from TWA-SPME testing compared to literature values prompted an investigation into the calibration curve accuracy on the GC-FID. A progression through the following experiments was performed in order to determine the most accurate and precise calibration curve for SPME testing.

1. GC-FID injections were performed using an 8400 series autosampler. Injected solutions included 5 concentration levels for all the following compounds diluted individually in 2-propanol: benzene, toluene, styrene, and indene.
2. A mixture was prepared with all 5 analytes of interest in 2-propanol, and 5 concentration levels were also analyzed using the autosampler.
3. Manual injections were performed with a zero-dead-volume (i.e. on-column) Hamilton syringe. single analytes (i.e. benzene in 2-propanol) using a 1 uL zero-dead volume (i.e. on-column) Hamilton syringe

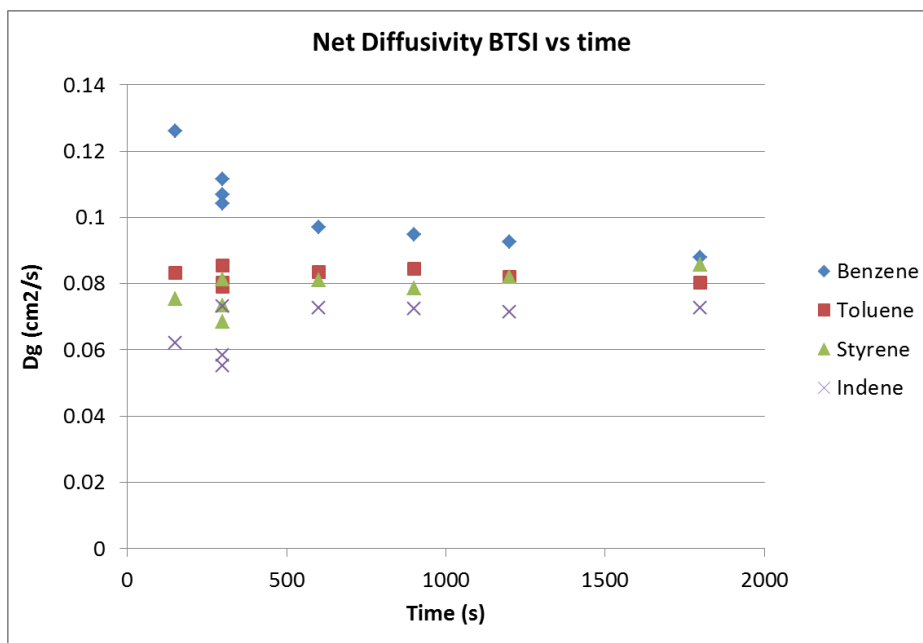


**Figure 1:**  $D_g$  values calculated with the calibration curve developed from the initial autosampler values for the BTSIN Mixture.

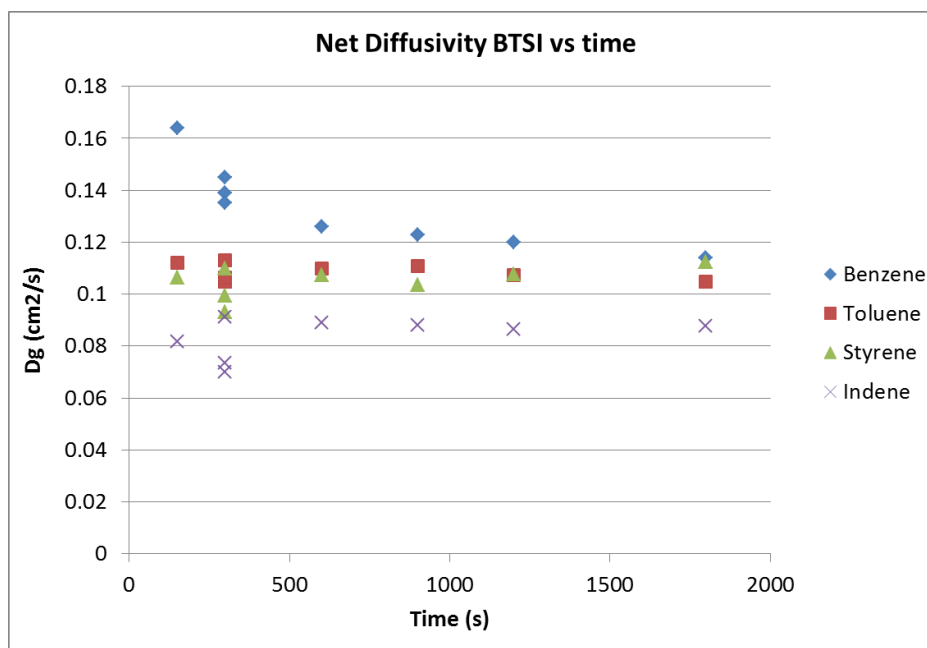


**Figure 2:**  $D_g$  values calculated with the calibration curve developed from the autosampler values for the BTSIN Mixture adjusted for the extra 20 % injection volume (0.2 uL extra).

Relative standard deviations (RSDs) for manual injections with the 1 uL syringe ranged from 10-30% depending on the analyte concentrations, with larger concentrations generally showing larger RSDs). These tests were performed using a split ratio of 10.

5 samples of each concentration (from 100 to 20,000 ppm) were performed with the autosampler, resulting in RSD values from ~1% to 5% for individual compounds in 2-propanol. RSD values for the mixtures performed on the autosampler also ranged from 2% to 5%. These were performed using a split ratio of 100.

Overall results also indicated a substantial improvement in precision using the autosamplers, but that a correction factor for the actual amount injected was required (of roughly 0.2 uL extra injected) to improve the accuracy of the autosampler. A significant difference between GC-FIDs also existed, with the second GC-FID reporting values of similar accuracy/precision, but at peak area counts of 20% lower. Differences between analyzers are generally expected however, given ages of GC-FIDs and time between thorough detector cleanings and replacement of parts etc. The autosampler using individual mixtures of the compounds was the most accurate and precise, but only once the required correction factor for partial volatilization of liquid in the syringe needle was applied.

## Supplementary material for proof-of-concept work

The supplemental material includes: (1) the progression of preliminary fiber trials on the process environment to aid in proper fiber selection, (2) a detailed discussion of the modified SPME holder for TWA sampling, (3) a description of the custom TWA SPME temperature probe and final sampling zone configuration, and (4) the completed statistical analysis for the comparison of experimental (and theoretical)  $D_g$  values.

### Experimental Section

**Fiber Selection.** Four different SPME coatings were available for testing in this experiment: PDMS, polyacrylate, PDMS/DVB (divinylbenzene), and CAR/PDMS. The different types of coatings are well known for their advantages to pre-concentrate targeted analytes in certain situations. In addition to literature detailing this information, such as from the Supelco fiber selection guide, these coatings were tested in a more realistic sample matrix to verify the most effective choice of fiber for this work. The heavy coker gas oil (HCGO) anticipated as the scrubbing liquid in the gasification pilot plant also contains many of the same light tar compounds that are expected in syngas downstream of the primary tar removal process. These include naphthalene, benzene, and other single ring aromatics.

Figure S-1 represents a comparison between the four different fibers and their performance in collecting and concentrating these target analytes. Chromatogram C, taken using PDMS/DVB clearly enhanced the quantity of analyte that could be collected compared with the choices A and B. However, chromatogram D represents the most effective fiber during these tests as the concentration of the light aromatics (shown prior to the 13 minute mark in the chromatogram) was higher in CAR/PDMS than in PDMS/DVB. This confirms CAR/PDMS as a good choice for further developing and testing this method via tar measurement in a syngas.

**Figure S-1**

**TWA Sampling Apparatus.** A manual SPME holder was modified (See Figure S-1) to enable several levels of  $\delta$  in addition to the original 3.3 mm depth (typical depth of the retracted fiber in a conventional SPME holder) [242]. The different diffusion path lengths can be used to widen the range of conditions for which TWA is applicable. For small concentrations or stagnant air, an exposed fiber may be most logical. In the case of trace tar analysis in syngas, a retracted fiber is utilized to reduce the high quantity of compounds potentially injected to the detector. Retracting the fiber within the syringe housing has an additional benefit of protecting the fiber from dust or small particles in the gas stream, thereby increasing the reliability of the technique. In this configuration, the length of the diffusion path ( $\delta$ ) is established by the depth that the fiber is retracted within the needle housing. The original fiber retraction depth (without modification) is approximately 3.3 mm, but it can vary by a few tenths of a millimeter.

**Figure S-2**

## **Results & Discussion**

**Process Gas Sampling System Characterization.** Suspected temperature variations within the sampling zone required construction of a SPME temperature probe (Figure S-3). The inner fiber portion of an SPME fiber was removed and a small thermocouple was inserted into the remaining syringe housing. This enabled measurement of temperature to be taken in the sample system at each  $\delta$ . After verifying a discrepancy in temperatures at different  $\delta$ , the entire sampling zone was heat traced including a well that was installed for the SPME fiber holder (Figure S-4). The sampling well was a ½” NPT pipe nipple placed on top of the sampling port on the glass bulb. The entire area was then recovered in insulation. The heat trace was controlled by placing a small thermocouple through a compression tee immediately downstream of the sampling zone. This thermocouple was inserted and directed upstream until the tip was only a few millimeters from the fiber sampling point. This thermocouple was then used to control the heat tracing placed around the sampling port and the sampling well.

Measuring temperatures with the probe described above (Figure S-3) in the new sampling system configuration showed a remarkable improvement in the consistency of temperature throughout the range of retraction depths. While the original orientation showed temperature losses of 30 - 40 °C, the new heat traced system with the sampling well varied less than 1 °C from 0 to 10 mm.

**Figure S-3**

**Figure S-4**

**Statistical Design of Experiments (DOE).** The full factorial design using two factors ( $\delta$  and  $t$ ) at three levels each (3.3, 5, and 10 mm; 5, 10, and 15 min) were applied in a randomized

complete block design. According to Nelson (1985), three repetitions (i.e. blocks) provide sufficient repetition to detect a difference in factor level means of two standard deviations [270]. This creates nine repetitions for each level of each factor [3 repetitions per block \* 3 blocks = 9 repetitions]. Using these calculations it is assumed that a 5% chance exists of showing a difference in factor level means when none exists and a 10% chance of failing to detect a difference when one exists (i.e.  $\alpha = 0.05$ ;  $\beta = 0.10$ ).

**DOE Experimental Results.** Figure 8 showed a significant trend in the experimental  $D_g$  values with  $\delta$  and  $t$ . These data are more easily compared to previous work using the sampling rate by Chen et al. (2003) shown in Figure S-5. The sampling rate should be a constant value as time increases to confirm the zero-sink hypothesis. Alternatively, a fiber that approaches its equilibrium value will show a steady and decline. Figure S-5 shows an initial decline before the values begin to level out to a constant sampling rate, which is even more evident with greater  $\delta$ . A possible explanation for this phenomenon is the existence of a second boundary layer, which is discussed in the main article.

### Figure S-5

**Statistical Analysis.** Providing an accurate and precise concentration value using TWA-SPME in process gas streams depends on maintaining a constant rate of diffusion through the syringe tip to the fiber. A gas stream with constant benzene concentration was tested at different conditions (3 different depths and times) to determine if any significant differences in the experimental  $D_g$  values could be detected according to Equation 3. The following model was created during the experimental design to test which parameters were statistically significant.



**Equation S-1:**  $E[X_{ijk}] = \mu_{ijk} = \mu + \alpha_i + \beta_j + \gamma_{ij} (+ \Delta_k)$  (where  $i = 1, 2, 3; j = 1, 2, 3; k = 1, 2, 3$ )

Where:

$\alpha$  = Depth

$\beta$  = Time

$\gamma_{ij}$  = The interaction effect between  $\alpha_i$  and  $\beta_j$

$\Delta$  = Experimental Blocks (and inherently the repetition)

$X_{ijk}$  = experimentally determined molecular diffusion coefficient value ( $D_g$ )

The null hypothesis states insufficient proof for any effect due to the parameter of interest, and the alternative hypothesis states that there is sufficient proof that at least one level of the parameter has a significant effect on the expected diffusivity value.

$H_{0A}: \alpha_1 = \alpha_2 = \alpha_3 = 0$

$H_{0B}: \beta_1 = \beta_2 = \beta_3 = 0$

$H_{0C}: \Delta_1 = \Delta_2 = \Delta_3 = 0$

$H_{aA}: \text{at least one } \alpha_i \neq 0$

$H_{aB}: \text{at least one } \beta_j \neq 0$

$H_{aC}: \text{at least one } \Delta_k \neq 0$

An analysis of variance (ANOVA) for the experimental data was performed using JMP statistical software. Results are shown below in Table S-1, indicating significant effects due to both fiber depth and time.

### Table S-1

Given the apparent lack of interaction effect in Table S-1 between  $t$  and  $\delta$ , an analysis of covariance (ANCOVA) was performed to test the significance of an individual factor without the

confounding effect of the other. Depth was used as a covariate to determine if the change in  $D_g$  with  $t$  was still significant. Although the F-statistic is reduced by half for  $t$ , it is still significant with a P-ratio of 0.000 as shown in Table S-2. Testing the effects of  $\delta$  using  $t$  as a covariate is unnecessary given the larger significance of  $\delta$  as stated in the F-ratio of Table 1.

### Table S-2

The significant effects of depth and time can be visually depicted using a three dimensional plot (Figures S-6 and S-7).

### Figure S-6

### Figure S-7

The nine combinations of depths and times were tested to determine which configurations were responsible for a statistical difference from the expected theoretical  $D_g$  value. Before determining a difference in means, the theoretical mean was subtracted from each of the sample and theoretical values. The difference from zero for the new mean values was then used to determine statistically significant effects from each of the depth and time parameter combinations.

**Equation S-2:** 
$$E[X_{ijk}'] = \mu_{ij}' = (\mu - \mu_{\text{theory}}) + \alpha_i + \beta_j$$

Where: 
$$X_{ijk}' = X_{ijk} - \mu_{\text{theory}}$$

$$\text{Ho: } \mu_{ij}' = 0 \quad (i = 1, 2, 3; j = 1, 2, 3)$$

$$\text{Ha: } \mu_{ij}' \neq 0 \quad (i = 1, 2, 3; j = 1, 2, 3)$$

The results from Equation S-2 are tabulated in Table 2, and indicate that sufficient proof was found to reject the null hypothesis for at least 4 combinations of  $\delta$  and  $t$ .

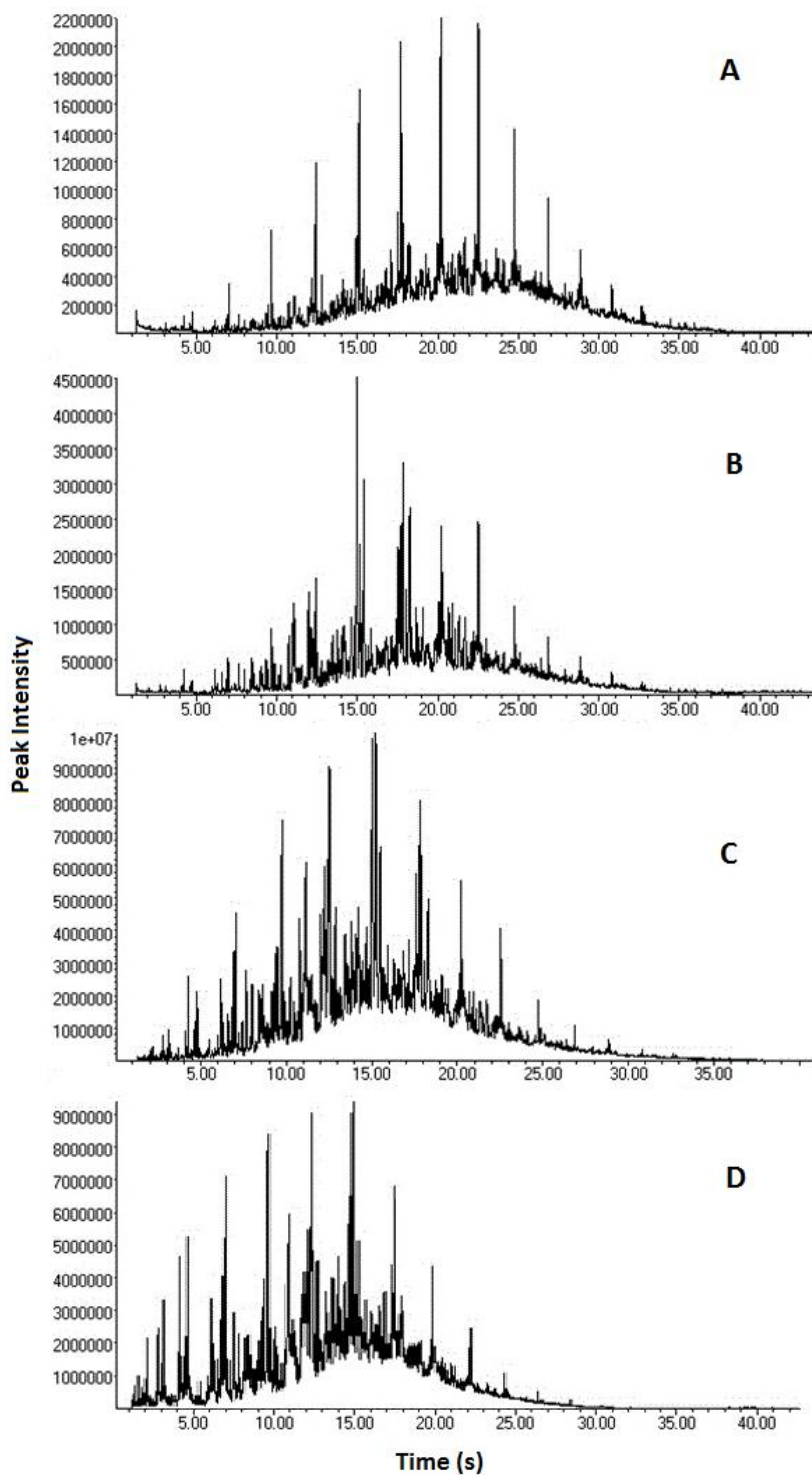
**Table S-1:** Statistical analysis of variance (ANOVA) testing the effects of  $t$  and  $\delta$  treatments.

ANOVA Effect Tests						
Source	Nparm	DF	Sum of Squares	F Ratio	Prob > F	
Experimental Block	2	2	0.0000752	1.8886	0.1835	
Fiber Depth (mm)	2	2	0.00535842	134.58	<.0001*	
Time (s)	2	2	0.00139672	35.0794	<.0001*	
Fiber Depth (mm)*Time (s)	4	4	0.00006636	0.8333	0.5236	

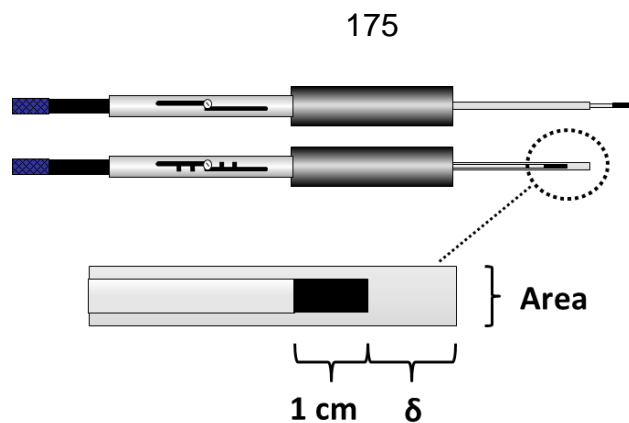
(\* indicates factors that have a significant effect on the resulting empirical  $D_g$ .)

**Table S-2:** Statistical analysis of covariance (ANCOVA). Testing the effects of time assuming depth as a covariate (i.e. confounding variable).

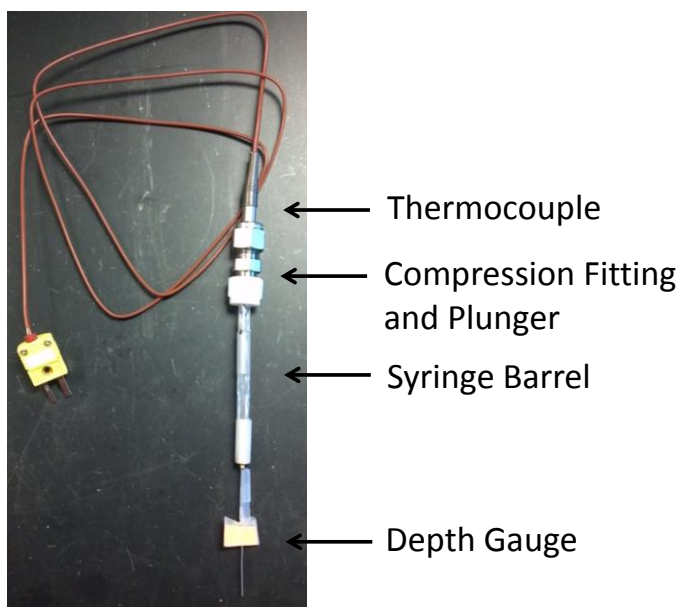
ANCOVA Effect Tests						
Source	DF	Seq SS	Adj SS	Adj MS	F	P
Depth	1	0.004971	0.00497	0.00497	134.91	0.000
Time (s)	2	0.001397	0.00140	0.00070	18.95	0.000
Error	23	0.000848	0.00085	0.00004		
Total	26	0.007215				



**Figure S-1:** Analyses of the syngas tar scrubbing oil taken at 100 °C, 1 minute exposure time, and mass spectroscopy for analyte identification. Four different fibers were analyzed, including: A) PDMS, B) polyacrylate, C) PDMS/DVB, and D) CAR/PDMS.



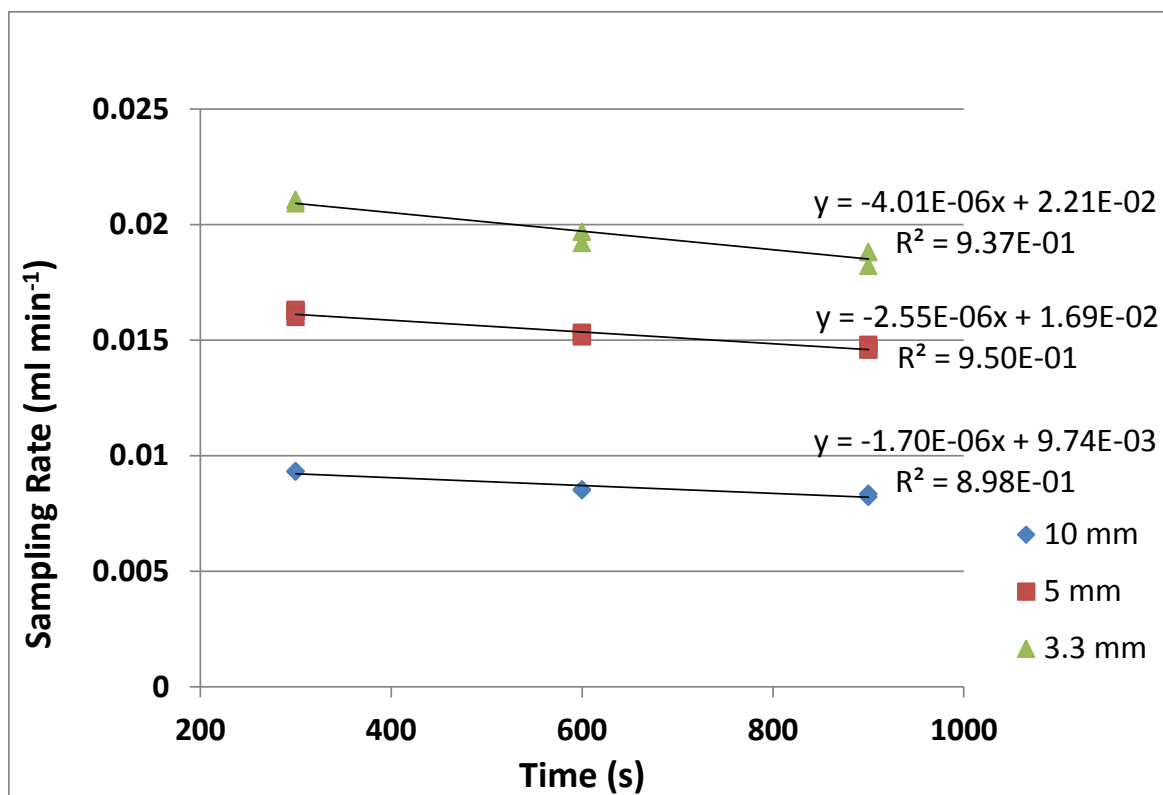
**Figure S-2:** SPME device with fiber exposed from the needle housing (top) and fiber retracted (bottom). Note the additional slots in the modified holder (bottom version) to enable retraction depths of 5, 10, 15, and 20 mm. A 24-gauge needle housing is commonly used, with a target inner diameter of 0.0140" (0.3556 mm), range 0.0135-0.0150" (0.343-0.381 mm) [242].



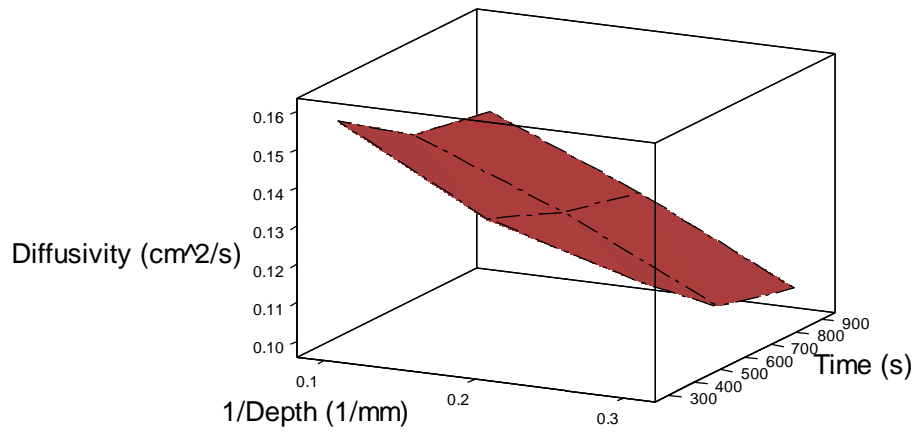
**Figure S-3:** SPME temperature probe developed to measure temperature profile along depth of retraction. Thermocouple purchased from Omega (KMTSS-010E-6)



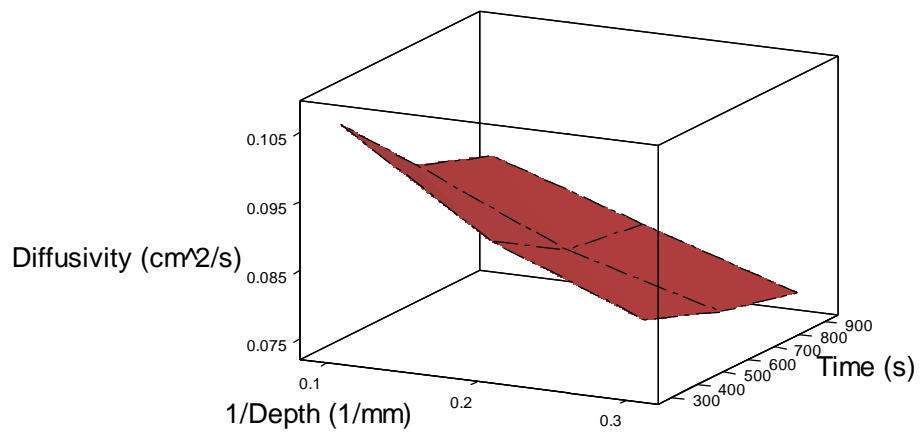
**Figure S-4:** Heated sampling apparatus for TWA passive sampling at 115°C. Note the thermocouple wire entering the exit side of the glass sampling bulb through a compression T placed in the line (right hand of picture). This thermocouple was routed through the line and placed a few mm from the sampling zone inside the glass bulb. The temperature at this location was used to control the heat tracing for the sample zones (glass bulb and sampling well).



**Figure S-5:** Sampling rates of benzene at different  $t$ . All tests performed at normal conditions of 115 °C, 0.39 g m<sup>-3</sup> (160 ppm<sub>w</sub>), 1 atm, and 5.7 SLPM N<sub>2</sub> flow rate.

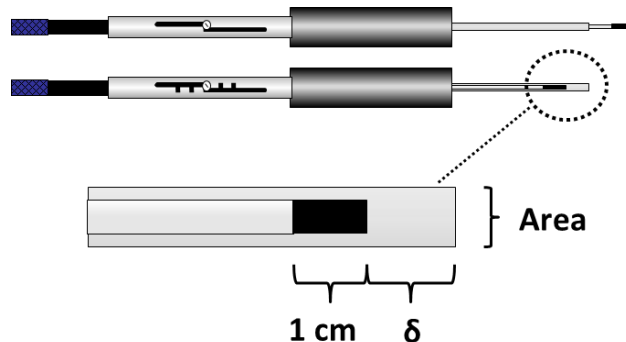


**Figure S-6:** 3-D plot of experimental  $D_g$  values at 115 °C versus time and inverse depth according to Equation 3.



**Figure S-7:** 3-D plot of experimental  $D_g$  values at 25 °C versus time and inverse depth according to Equation 3.



**Supplementary Work for TWA-SPME Pilot-Scale Validation Manuscript**

**Figure S-1:** SPME device with fiber exposed from the needle housing (top) and fiber retracted (bottom). Note that a 24-gauge needle housing is commonly used, with a target inner diameter of 0.0140" (0.3556 mm), range 0.0135" to 0.0150" (0.343 mm to 0.381 mm).[242]

The initial tests to generate standard gases using the 5 compound mixture encountered severe difficulties in maintaining a homogenous gas stream. This is likely a result of the high molecular weight of naphthalene and the physical properties surrounding the expulsion of high pressure liquid from a syringe tip. The sampling system was modified with heat tracing to provide preheated  $N_2$  at the point where the tar mixture is injected into the  $N_2$  stream to assist in maintaining gas homogeneity and volatilizing some of the analytes. This approach was unsuccessful in maintaining naphthalene at a constant concentration in the gas stream, and it was ultimately removed to maintain the other four analytes under more steady and repeatable conditions. The final analysis for  $D_g$  values was centered upon benzene, toluene, styrene and indene.

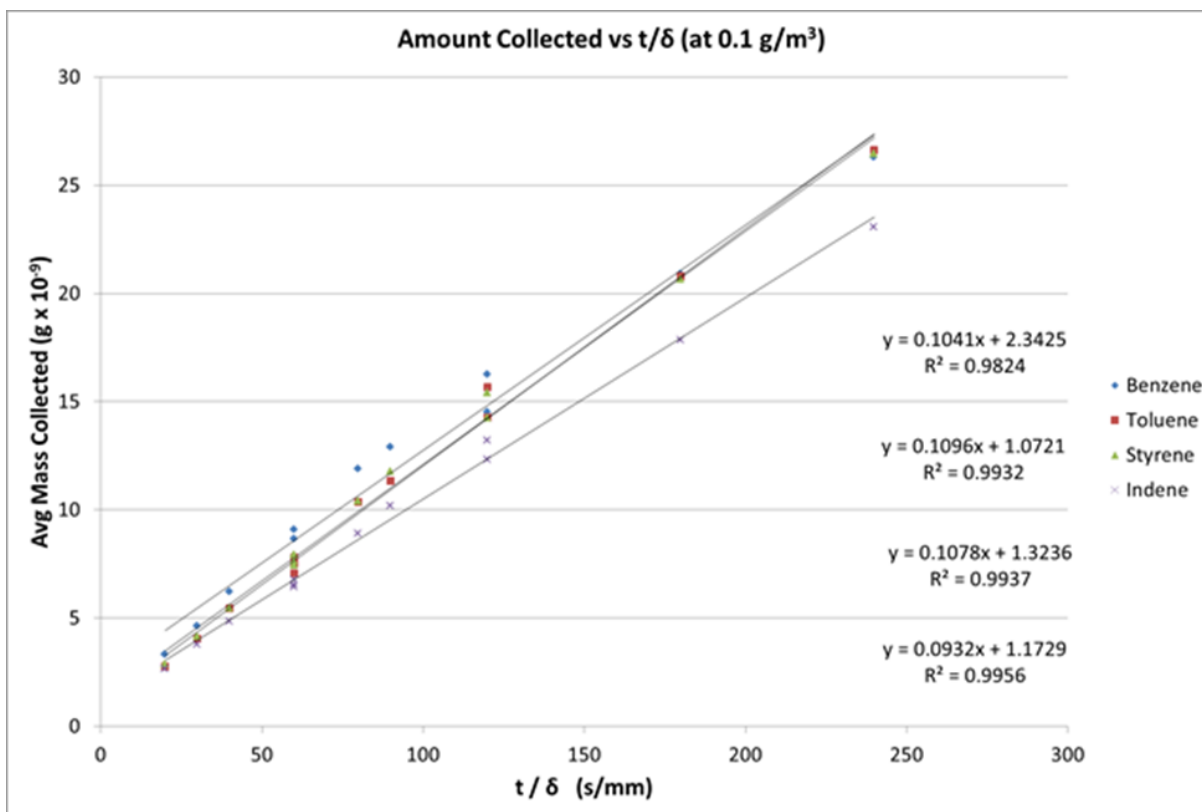


**Figure S-2:** Mass of the target analytes adsorbed on SPME fiber vs. changes in sampling time and SPME fiber retraction depth (see Figures S-3 and S-4 for benzene and toluene trends individually)

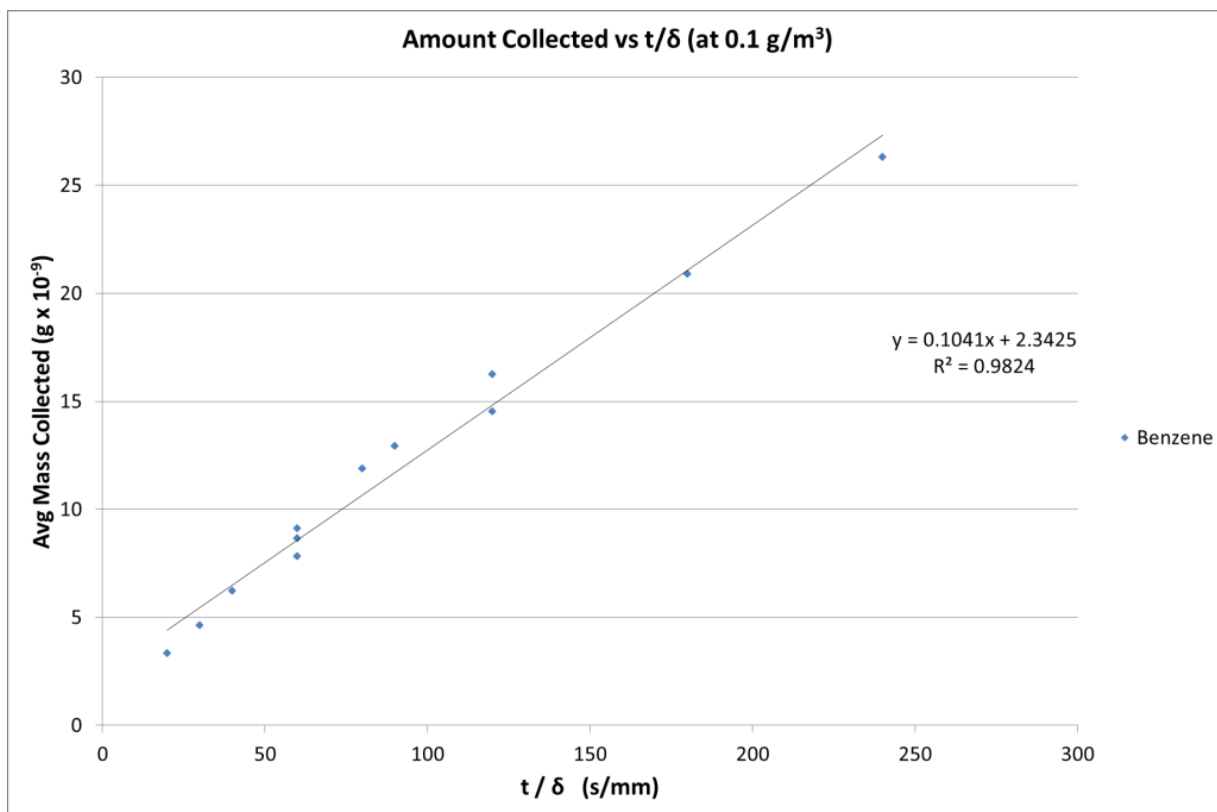


**Figure S-3:** Benzene response to changes in time and depth. Note the strong linear correlation, but also the tendency to under estimate the lowest and highest ratios of  $t/\delta$  (see plot of residuals **Figure S-5**) while overestimating the central points (suggesting a more curvilinear model due to the expected preconcentration effect at the surface of the fiber tip). The lack of fit test was performed to test this phenomenon.

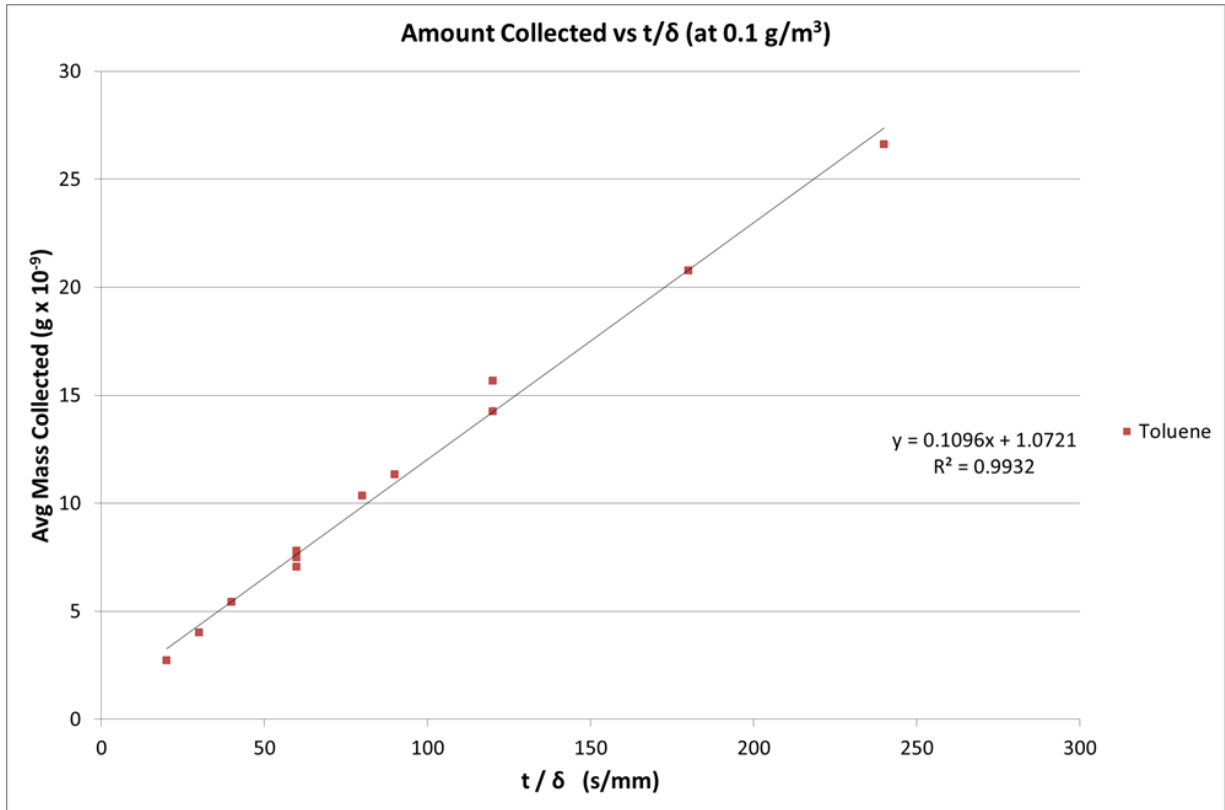


**Figure S-4:** Toluene response to changes in time and depth. Note the stronger linear correlation compared to benzene and a corresponding reduction in the over and under estimating phenomenon. The F and p values in Tables S-1 and S-2 reflect this more linear response with the heavier analytes.

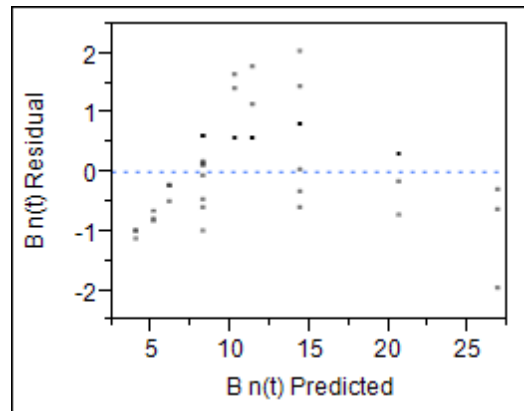


**Figure S-5:** Benzene  $n(t)$  residual by predicted plot. Note the over estimation at the extreme ends of the model calibration.

**Table S-1:** ANOVA, model parameters, and LOF results for Benzene

<b>Benzene Analysis of Variance (ANOVA)</b>					
<b>Source</b>	<b>DF</b>	<b>Sum of Squares</b>	<b>Mean Square</b>	<b>F Ratio</b>	
Model	1	1487.8526	1487.85	1692.186	
Error	34	29.8945	0.88	<b>Prob &gt; F</b>	
C. Total	35	1517.7471		<.0001*	
<b>Lack of Fit (LOF)</b>					
<b>Source</b>	<b>DF</b>	<b>Sum of Squares</b>	<b>Mean Square</b>	<b>F Ratio</b>	
Lack Of Fit	7	18.581418	2.65449	6.3353	
Pure Error	27	11.313037	0.419	<b>Prob &gt; F</b>	
Total Error	34	29.894456		0.0002*	
				<b>Max R<sup>2</sup></b>	0.9925
<b>Parameter Estimates</b>					
<b>Term</b>		<b>Estimate</b>	<b>Std Error</b>	<b>t Ratio</b>	<b>Prob&gt; t </b>
Intercept		1.9895528	0.278868	7.13	<.0001*
t/d		0.1036466	0.00252	41.14	<.0001*

**Table S-2:** ANOVA, model parameters, and LOF results for Toluene

<b>Toluene Analysis of Variance (ANOVA)</b>					
<b>Source</b>	<b>DF</b>	<b>Sum of Squares</b>	<b>Mean Square</b>	<b>F Ratio</b>	
Model	1	1637.9087	1637.91	5255.869	
Error	34	10.5956	0.31	<b>Prob &gt; F</b>	
C. Total	35	1648.5042		<.0001*	
<b>Lack Of Fit</b>					
<b>Source</b>	<b>DF</b>	<b>Sum of Squares</b>	<b>Mean Square</b>	<b>F Ratio</b>	
Lack Of Fit	7	6.299326	0.899904	5.6555	
Pure Error	27	4.296238	0.15912	<b>Prob &gt; F</b>	
Total Error	34	10.595563		0.0004*	
				<b>Max R<sup>2</sup></b>	0.9974
<b>Parameter Estimates</b>					
<b>Term</b>		<b>Estimate</b>	<b>Std Error</b>	<b>t Ratio</b>	<b>Prob&gt; t </b>
Intercept		0.5616835	0.166022	3.38	0.0018*
t/d		0.1087477	0.0015	72.5	<.0001*

Testing with the conventional method was first attempted only downstream of the tar scrubber. A long sampling line was used to route the syngas to the impingers on the ground level of the facility, which caused an inordinate amount of variability due to poor ability to heat trace. The sampling line was shortened by ~3 m and impingers were moved to the second story mezzanine to reduce this complication. Simultaneously a second sampling comparison zone was started downstream of the pressure cooker. Samples in this location could not be taken until the data collection for the joint research was completed, which typically required several hours of steady state sampling with the conventional method. Only five samples were able to be collected due to fluctuations in gasifier steady-state conditions after 2-3 h and complications with the data collection during the conventional impinger method.

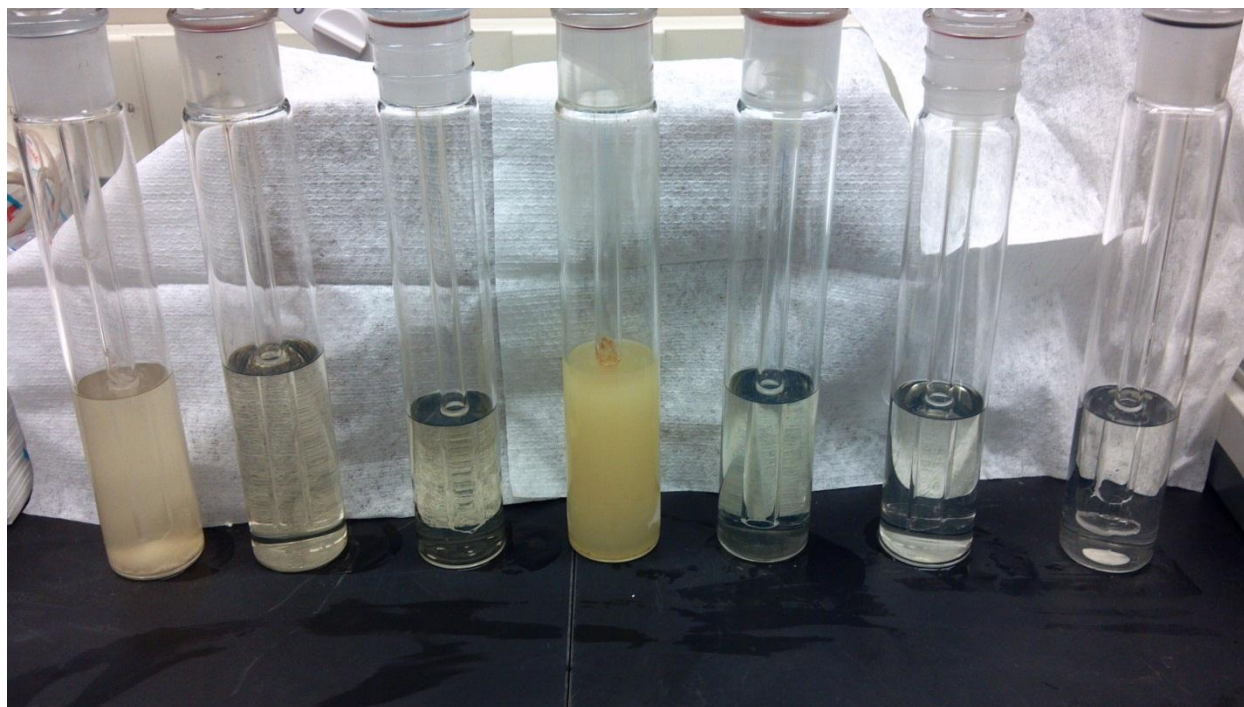


**Figure S-6:** Impingers from comparison run 3. From left, impingers 1-3 are from the impinger train at sampling location B and 4-7 are from location A. Note the high amount of contaminants reaching the impingers from sampling location A (impinger 4) compared to the samples downstream of the oil scrubber (impinger 1).

The presence of indene and naphthalene were completely void downstream of the cleaning equipment (verified by visual inspection of piping following tests, and the impingers in Figure S-6), suggesting that the cleaning equipment operated well. The direct contact cooling and spray impingement utilized in the tar removal cleaning unit was more efficient than the PC given the presence of indene and naphthalene in samples taken at location A.

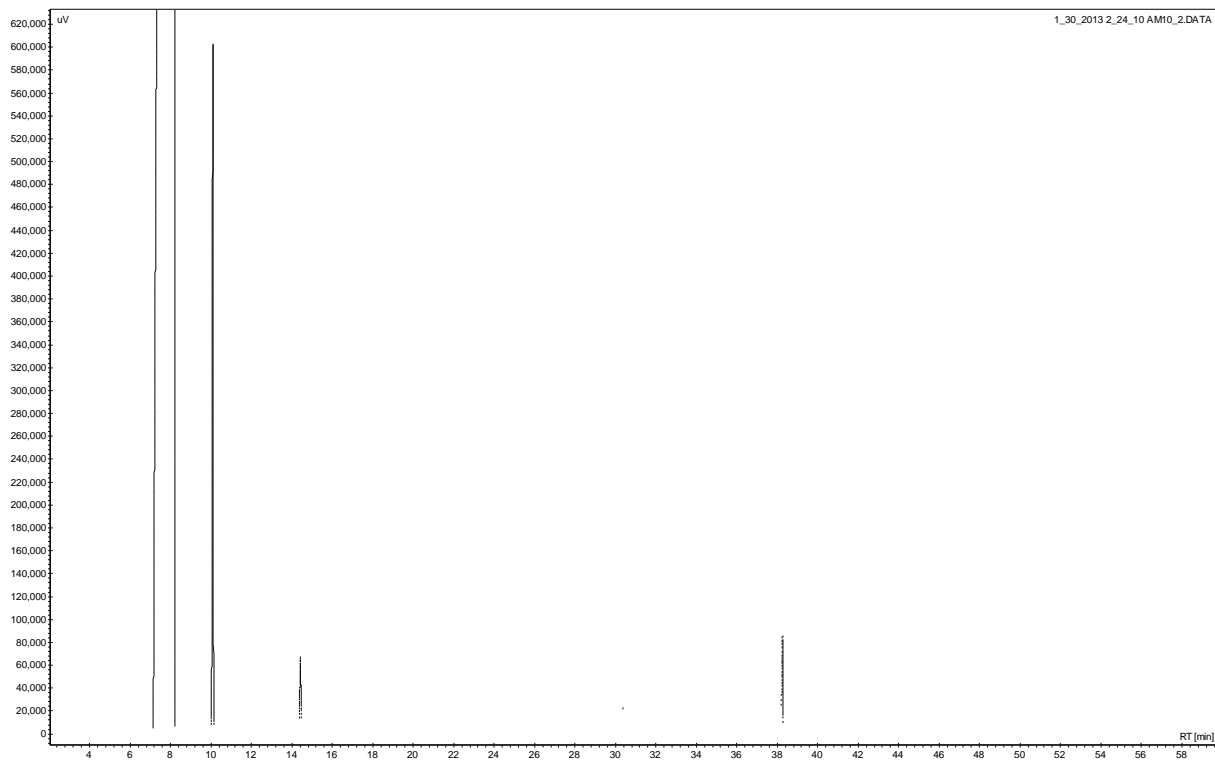


**Figure S-7:** Impinger 4 (first impinger downstream of pressure cooker) analyzed for tar compounds.



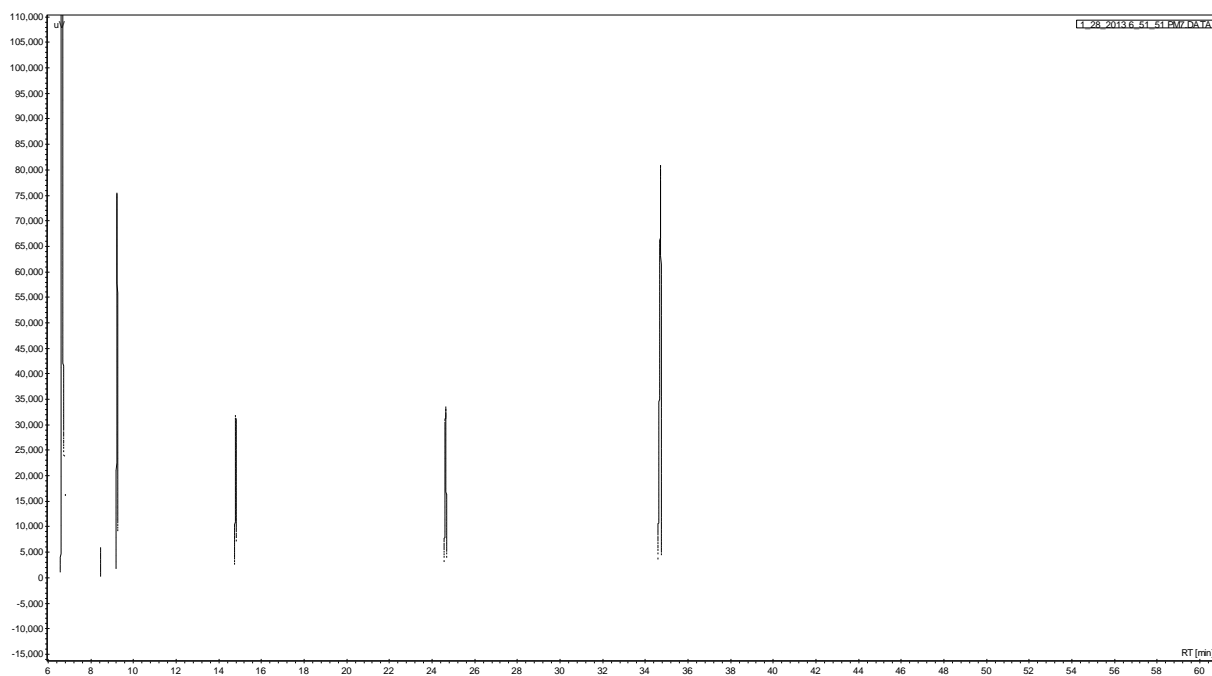


**Figure S-8:** TWA-PSME sample taken from the slipstream during the sample of Figure S-7 above. Note the higher resolution of the TWA-SPME results and the greater number of quantifiable peaks compared to the conventional impinger approach

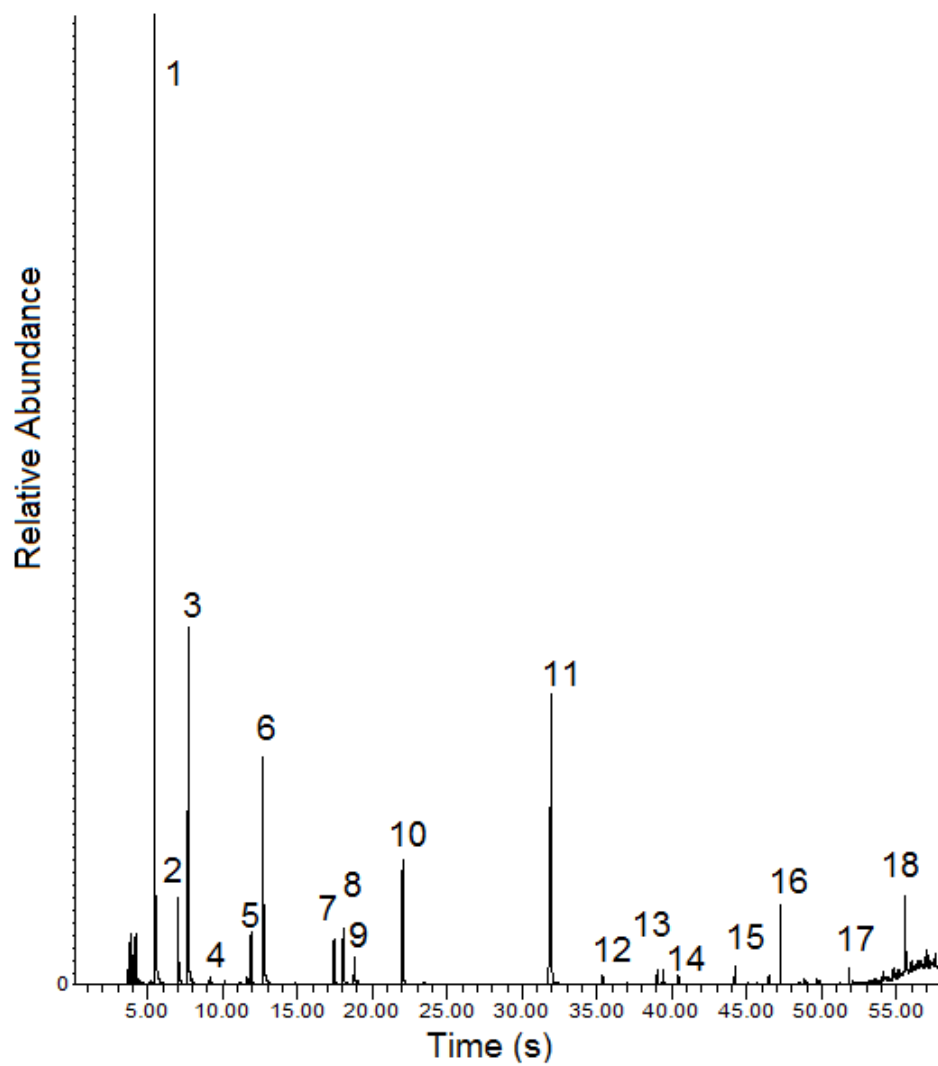


**Figure S-9:** TWA-SPME analysis of post-pressure cooker tar at 170°C for high temperature identification of tar compounds.

**Table S-3:** TWA-SPME analysis of post-pressure cooker tar at 170 °C for high temperature identification of tar compounds. The “Initial” column represents the largest tar compounds present above the baseline, which is normalized to these 18 tar compounds in the adjacent column.

Peak #	Ret Time (min)	Area %		Compound
		Initial	Normalized	
1	5.469	21.7%	28%	Benzene
2	6.987	2.06%	2.7%	Pyridine
3	7.706	8.47%	11%	Toluene
4	9.194	0.28%	0.36%	Methyl Pyridine
5	11.906	1.69%	2.2%	Ethynyl Benzene (phenylethyne)
6	12.719	8.54%	11%	Styrene
7	17.444	2.23%	2.9%	Phenol
8	18.064	2.50%	3.2%	Benzonitrile
9	18.802	1.06%	1.4%	Benzofuran
10	22.025	4.90%	6.4%	Indene
11	31.974	18.1%	24%	Naphthalene
12	35.375	0.42%	0.55%	Quinoine
13	39.028	0.61%	0.79%	Indole
14	40.424	0.36%	0.47%	Methyl Naphthalene
15	44.2	0.50%	0.65%	Biphenyl
16	47.257	2.00%	2.6%	Acenaphthylene
17	51.834	0.37%	0.48%	Fluorene
18	55.559	1.16%	1.5%	Phenanthrene
		77%	100%	

Increasing the operational temperature at which syngas exits the pressure cooker to approximately 170 °C resulted in the major tar components displayed in Table S-3. 77% of all analytes present were able to be identified as these 18 compounds. Due to the higher temperatures of the sampling line, these compounds include up to 3 ring PAHs (shown with phenanthrene) during steam/O<sub>2</sub> gasification of switchgrass in a fluidized bed gasifier.

### **Gas cleaning system design: optimizing oil scrubbing for tar removal**

The amount of tar and particulate matter (PM) present in syngas varies drastically between the types of gasifiers (updraft, downdraft, fluidized bed, oxygen-blown, etc.) [201, 226]. Syngas tars for instance can range from 1 g/m<sup>3</sup> to more than 100 g/m<sup>3</sup>, but are generally ~10-30 g/m<sup>3</sup> in syngas from fluidized bed gasifiers. Particulate matter is also perhaps up to 10% or more of the solid feed input, but is generally removed by hot cleanup devices before the gas is cooled. The process development unit (PDU) that was designed employed a series of two cyclones (designed by Karl Broer), each projected to reduce 90% of the incoming PM (resulting in a 99% overall PM removal rate). Therefore, the scrubber under consideration in this design was primarily designed to remove problematic tars, which begin to condense and foul piping/equipment when temperatures fall below 400°C.

An initial design for the oil scrubber included the following considerations: HETP and HTU calculations [271, 272], physical constrictions inside the bay, and costs of materials based on off the shelf sizes and components. A preliminary estimate of mass flow rates was developed in AspenPLUS and HYSYS to determine approximate sizing considerations for vessels and equipment (pumps, valves, heat exchangers etc.). However, after an extensive shakedown period it was determined that a redesign of the oil column was necessary.

The original design was constructed with a focus on absorption in the design calculations. The water spray that was originally intended for use directly upstream of the oil scrubber was ineffective and caused severe coking, and its use was discontinued. Without a water spray to cool the incoming gas, the syngas entered the oil scrubber at nearly 400°C compared to the original design condition of 280 to 300°C. This increased temperature required a much higher

flow rate of oil and an extensive change in column internals to provide the necessary surface area and thermal mass to cool the syngas to the desired outlet temperature. Unfortunately, tar aerosols were not effectively removed with this simplistic heat transfer design.



**Figure 1:** Pilot-scale 20 kg/h fluidized bed gasifier and gas cleaning PDU



**Figure 2:** Oil scrubber for tar removal in the PDU

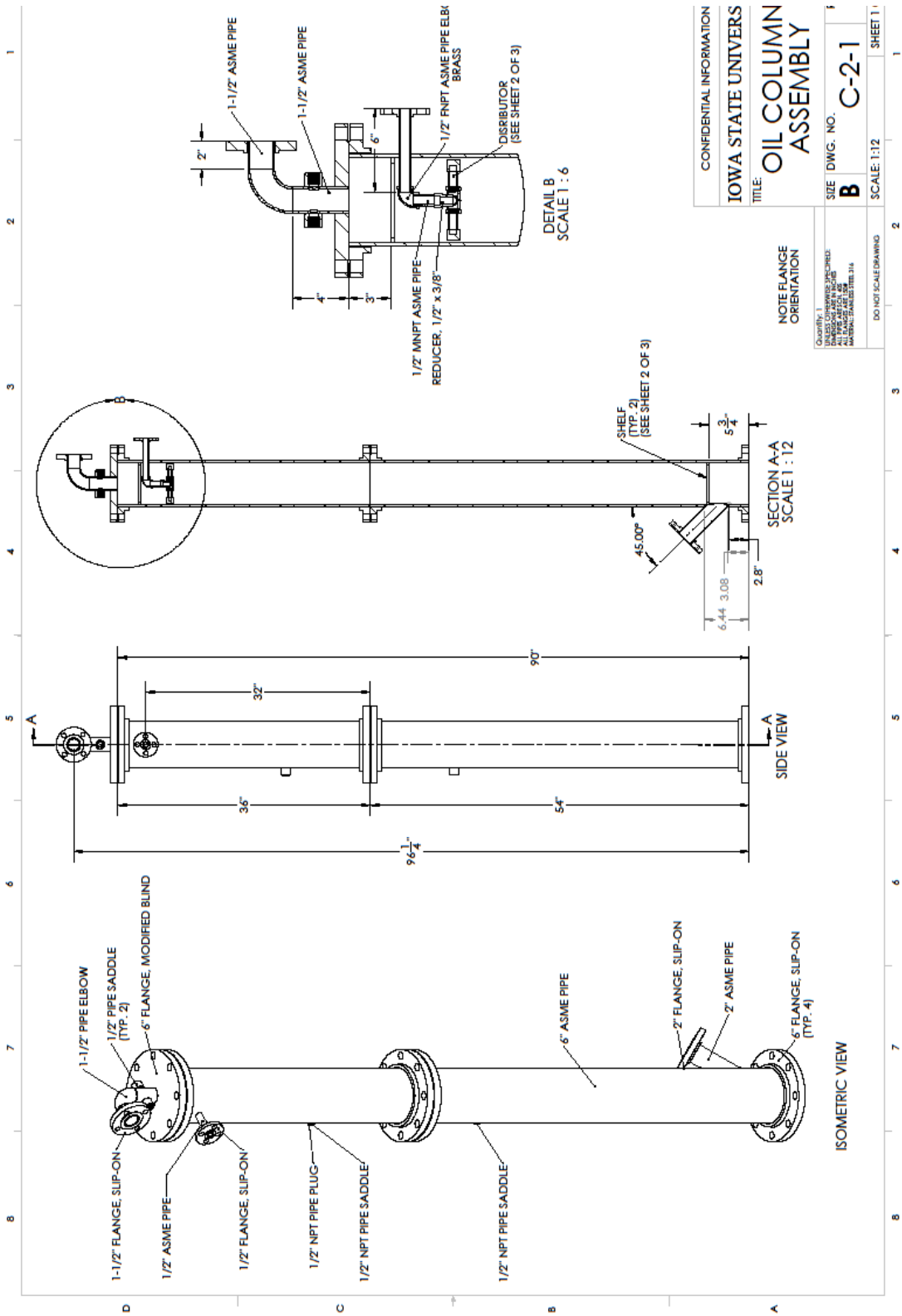


Figure 3: Oil scrubber column original design

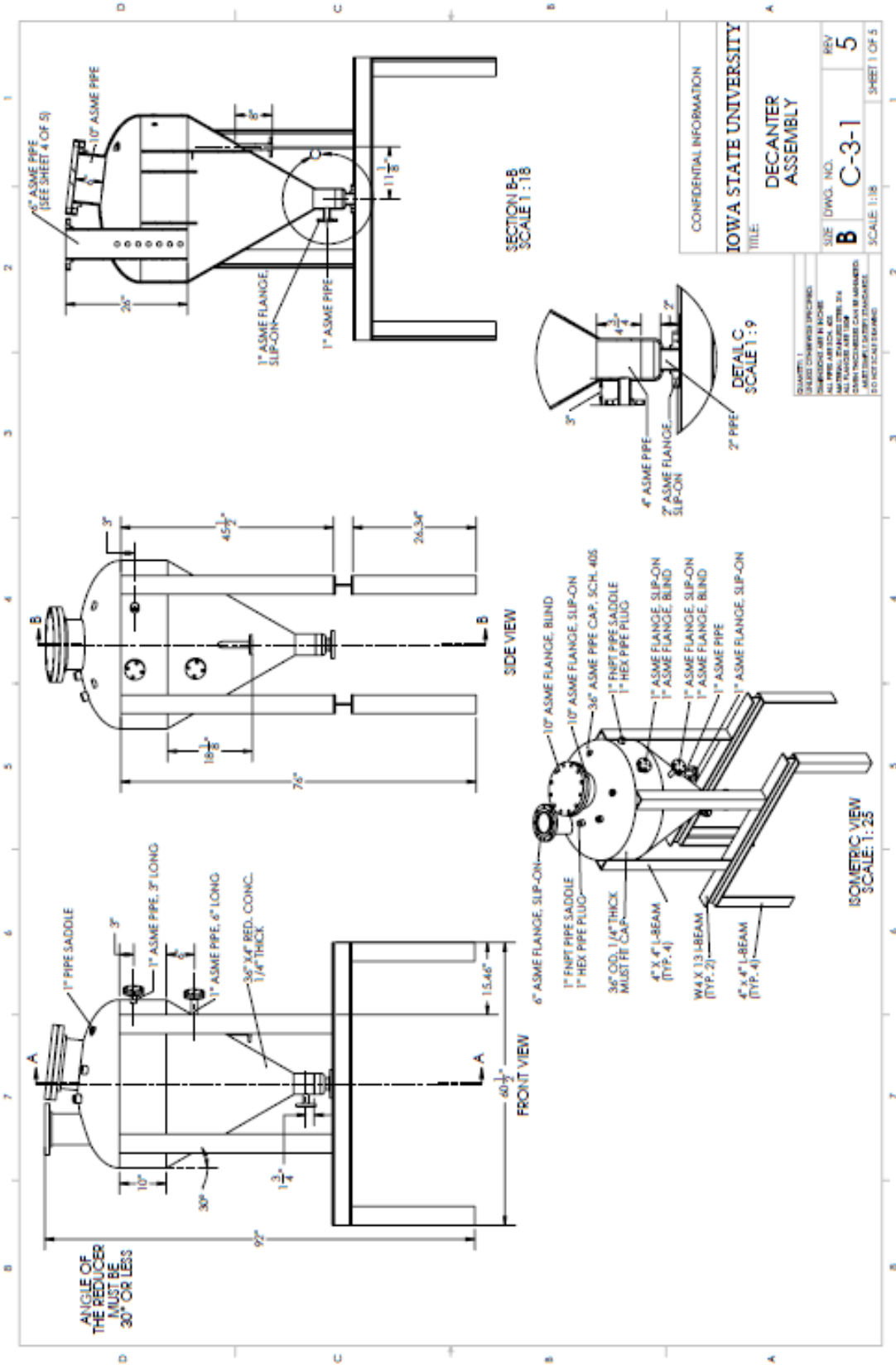


Figure 4: Oil scrubber decanter design



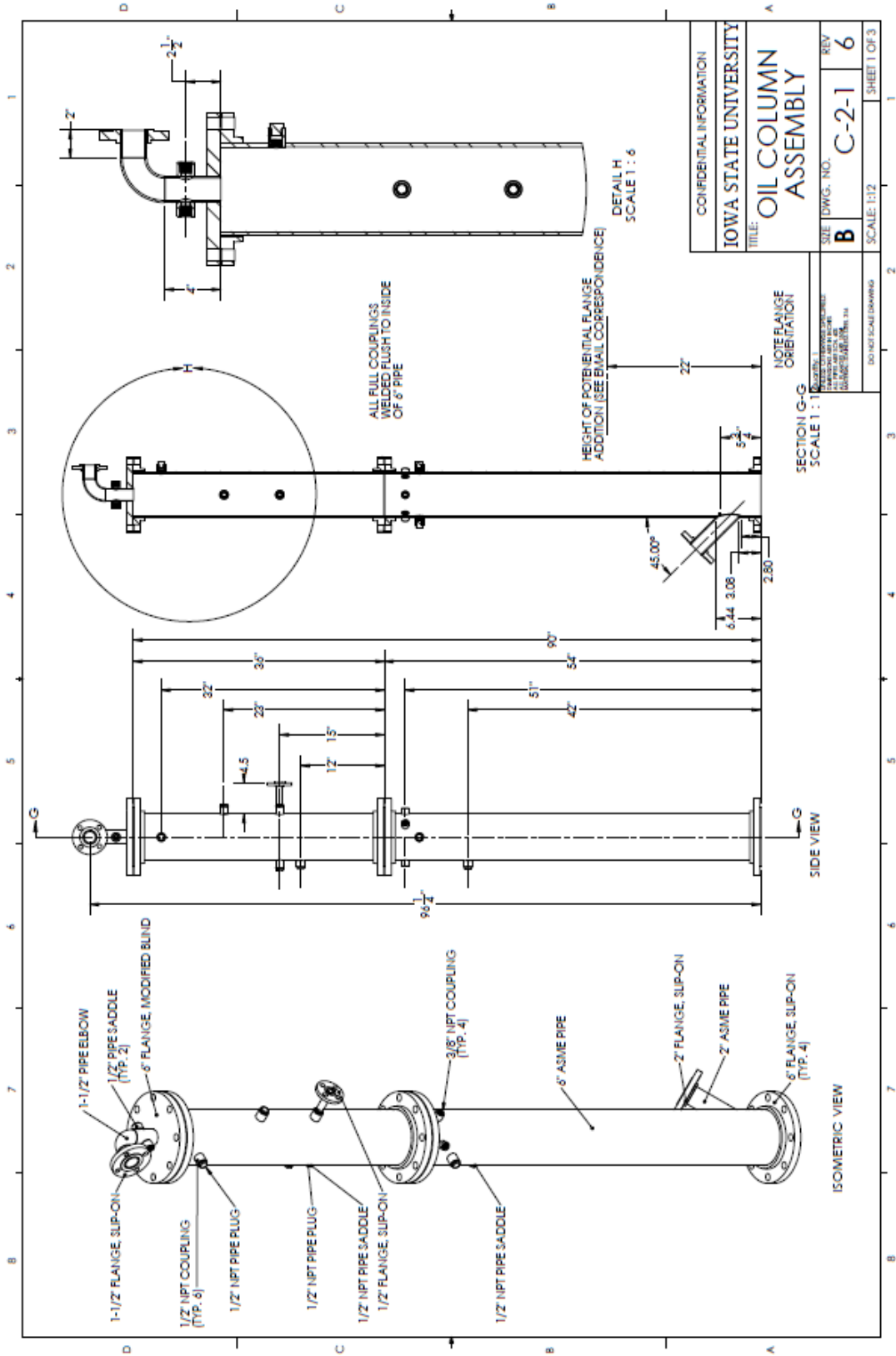


Figure 5: Oil scrubber column new design

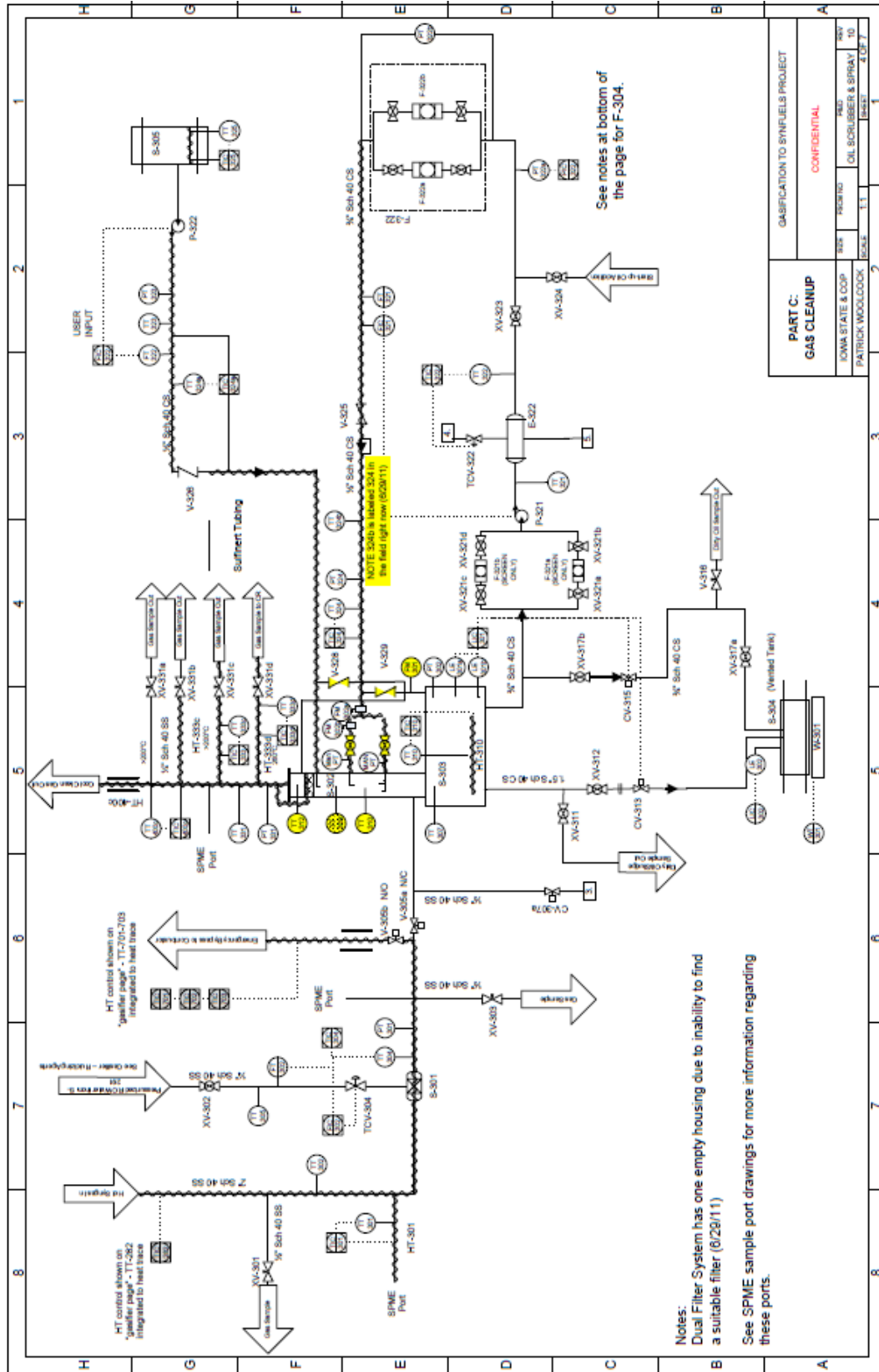


Figure 6: Oil scrubber system P&ID

An extensive redesign took place to improve the heat exchange capacity of the column while simultaneously allowing room for tar aerosol removal. The redesign was limited by the dimensions of the pilot-scale PDU that was already constructed and in operation (See Figure 1 and Figure 2). Adding a secondary column or ESP was not possible given the constrictions in space. The redesign followed a simple logic: cool the syngas down from 400 °C to ~100 °C within the first meter of column space, and use the second meter for removal of aerosols generated by the syngas cooling.

The first step was to ensure the necessary mass flow rates and heat exchange potential of for the first meter of column were possible with current hardware. Heat transfer potential of Flexipac structured packing was estimated to improve the surface area contact between the cool oil and the hot syngas. This packing had proven in previous tests to allow high volumes of used decanter oil to flow without flooding the column, which was a high priority as well in the new design. A series of oil sprays were located within the column directly above the structured packing to provide a majority of the cool oil. This oil is recycled from the large decanter vessel located beneath the column, and is used to both wet the packing and create a swirl effect in the center of the column to have good gas/liquid contact. Final, a small stream of fresh oil was sprayed down from the top of the vessel in very fine droplets. This counter-current flow of oil increased the Stokes number for collection of aerosols compared with a stationary fiber mesh. An 8" demister pad was also located at the top of the column to collect any aerosols that remained entrained in the syngas flow.

**Equation 1:** Stokes flow  $\rightarrow St = \frac{2 \cdot \rho_p \cdot R_p^2 \cdot U \cdot C_s}{9 \cdot \mu \cdot R_c}$

Where:  $\rho_p$  = density of particle being removed

$R_p$  = radius of particle

$U$  = characteristic velocity of flow

$C_s$  = Cunningham correction factor

$\mu$  = fluid viscosity (.00001755 kg/m\*s for syngas in this case)

$R_c$  = characteristic length of collector (radius of counter flowing droplet in this case)

**Table 1:** Key calculations for oil scrubber column

<u>Vapor Removal Method</u>	<u>AKSP-12</u>	<u>Inert Granules</u>	<u>Counter-flow oil</u>
Relative gas velocity	0.36 m/s	0.36 m/s	1.5 m/s
Collector $R_c$	50 $\mu$ m	2 mm	50 $\mu$ m
Stokes #	0.023	0.0013	0.10

(AKSP-12 is wire mesh demister material; counter-flow oil velocity and  $R_c$  are very conservative)

Various design issues were considered in establishing the final design shown in Figures 5, 6, and 7. Nozzle variations had to avoid clogging and maintain appropriate line pressures while maintaining proper flow characteristics (droplet radius and velocity). Overflow precautions were made in the scrubber to avoid pooling of oil in the lines and contamination of analytical and downstream process equipment. The stokes number was calculated for various configurations, of which the counter-flow oil spray was the most promising [273, 274]. Even with the considerably conservative characteristic length of the droplets (likely a fraction of that shown in Table 1), the stokes number reaches the minimum recommended level of 0.1. All other scenarios were not able to meet the minimum criteria.

The redesign successfully improved the oil scrubber performance substantially. The outlet temperature of the syngas decreased to the intended 100°C exit temperature. Visual inspection of the downstream piping verified the low tar concentrations exhibited by the tar measurements

discussed in previous chapters. Also, the time online without disruption has exceeded 6 h without signs of clogging occurring.

Final adjustments that are required include: continuous operation longer than 4-6 h to determine steady state operating parameters, identification of proper oil scrubber recycle loop protocols to determine intervals for regular filter changes, testing fresh/recycle oil ratios to maintain economic optimization for certain desired concentrations of tar in the syngas.

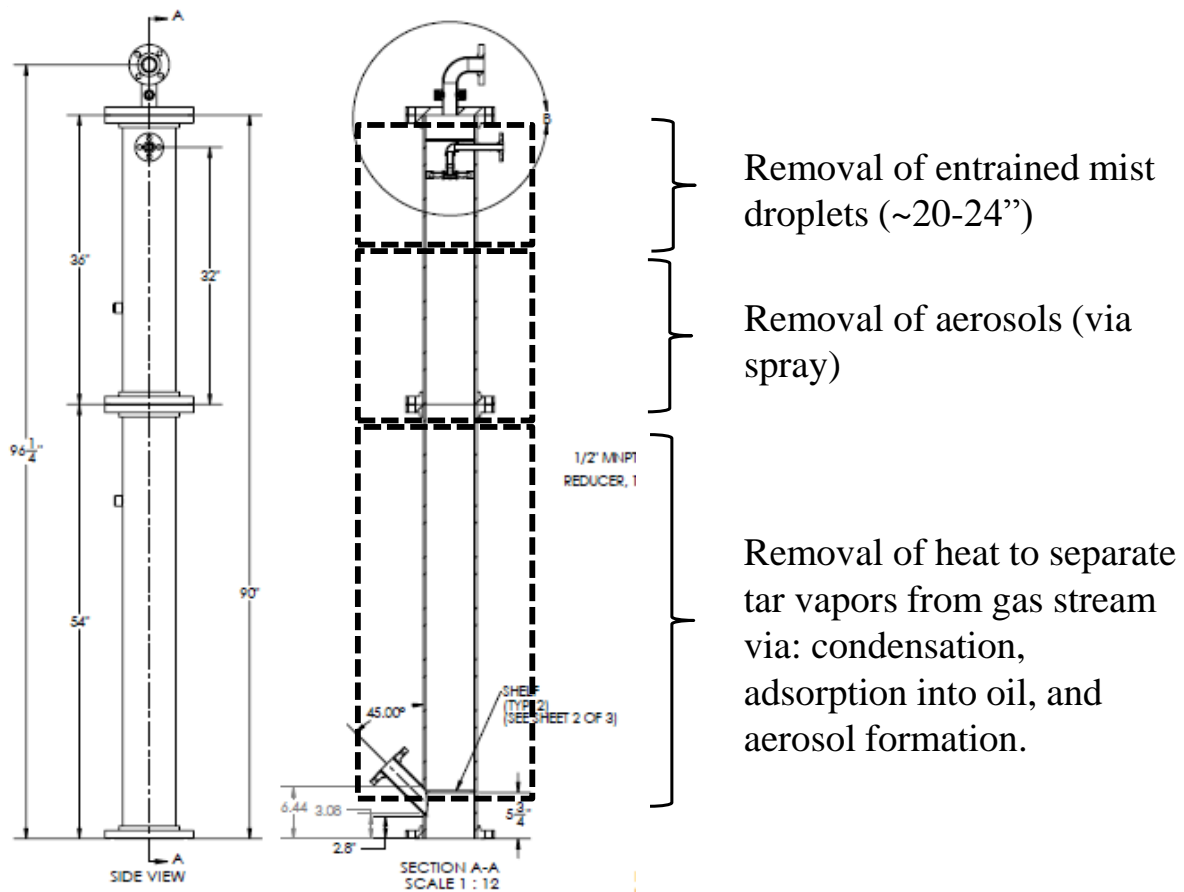


**Figure 7:** Oil scrubber column schematic and sectors for tar removal



**Figure 8:** Oil scrubber column top view

## References

1. *World Energy Outlook 2012, 2013*, International Energy Agency: Paris, France
2. *International Energy Outlook: 2010*, US Energy Information Administration: Washington DC. p. 327
3. Marker, T.L., et al., *Integrated hydrolysis and hydroconversion (IH2) for the direct production of gasoline and diesel fuels or blending components from biomass, part 1: Proof of principle testing*. Environmental Progress & Sustainable Energy, 2012. **31**(2): p. 191-199
4. Mohan, D., C.U. Pittman, and P.H. Steele, *Pyrolysis of wood/biomass for bio-oil: A critical review*. Energy & Fuels, 2006. **20**(3): p. 848-889
5. Stahlberg, P., et al., *Sampling of contaminants from product gases of biomass gasifiers*, 1998, VTT Energy: Technical research center of Finland. p. 49
6. Woolcock, P., et al., *Process Development Unit for Integrated Studies of Syngas Cleaning*, in *Annual ASABE International Meeting 2011*: Louisville, Kentucky
7. Osipovs, S., *Sampling of benzene in tar matrices from biomass gasification using two different solid-phase sorbents*. Analytical and Bioanalytical Chemistry, 2008. **391**(4): p. 1409-17
8. Pollard, A.S., M.R. Rover, and R.C. Brown, *Characterization of bio-oil recovered as stage fractions with unique chemical and physical properties*. Journal of Analytical and Applied Pyrolysis, 2012. **93**(0): p. 129-138
9. Sipilä, K., et al., *Characterization of biomass-based flash pyrolysis oils*. Biomass and Bioenergy, 1998. **14**(2): p. 103-113
10. Patwardhan, P.R., R.C. Brown, and B.H. Shanks, *Product Distribution from the Fast Pyrolysis of Hemicellulose*. ChemSusChem, 2011. **4**(5): p. 636-643
11. Kuzhiyil, N., et al., *Pyrolytic Sugars from Cellulosic Biomass*. ChemSusChem, 2012. **5**(11): p. 2228-2236
12. Spath, P.L. and D. Dayton. *Products from Syngas - Fischer-Tropsch Synthesis Products*. 2008 Nov 11 2008 [cited 2010 April 20]; Available from: <http://bioweb.sungrant.org/SGBioWeb/Templates/Technical/TechnicalPrintable.aspx?NRMODE=Published&NRORIGINALURL=/Technical/Bioproducts/Bioproducts%2Bfrom%2BSyngas/Fischer-Tropsch%2BSynthesis/Default.htm&NRNODEGUID={07DB8879-1942-4EF2-9346-1D8B19EEF966}&NRCACHEHINT=NoModifyGuest>
13. Vreugdenhil, B.J. and Z. R., *Tar formation in pyrolysis and gasification*, 2008, Energy Research Center of the Netherlands (ECN)
14. Kiel, J., et al., *Primary measures to reduce tar formation in fluidised-bed biomass gasifiers*, 2004, Energy Research Center of the Netherlands (ECN). p. 108
15. Li, C. and K. Suzuki, *Tar property, analysis, reforming mechanism and model for biomass gasification--An overview*. Renewable and Sustainable Energy Reviews, 2009. **13**(3): p. 594-604
16. Maniatis, K. and A.A.C.M. Beenackers, *Tar Protocols. IEA Bioenergy Gasification Task*. Biomass and Bioenergy, 2000. **18**(1): p. 1-4
17. Kamp, W.L.v.d., et al., *Tar measurement in biomass gasification, standardisation and supporting R&D*, in *CEN Technical Specification 2006*: Netherlands. p. 168
18. CEN, *Biomass Gasification — Tar and Particles in Product Gases — Sampling and*

- Analysis*, 2005, European Commission and the European Free Trade Association
19. Bull, D., *Performance improvements to a fast internally circulating fluidized bed (FICFB) biomass gasifier for combined heat and power plants*, in *Chemical and Process Engineering* 2008, University of Canterbury: Canterbury, New Zealand. p. 232
  20. Paasen, S.V.B.v. and J. Kiel, *Tar formation in a fluidised bed gasifier*, 2004, Energy Research Center of the Netherlands
  21. Dufour, A., et al., *Comparison of two methods of measuring wood pyrolysis tar*. *Journal of Chromatography A*, 2007. **1164**(1-2): p. 240-7
  22. Kaufman Rechulski, M.D., et al., *Liquid-Quench Sampling System for the Analysis of Gas Streams from Biomass Gasification Processes. Part 2: Sampling Condensable Compounds*. *Energy & Fuels*, 2012. **26**(10): p. 6358-6365
  23. Hernández, J.J., R. Ballesteros, and G. Aranda, *Characterisation of tars from biomass gasification: Effect of the operating conditions*. *Energy*, 2013. **50**(0): p. 333-342
  24. Wellinger, M., et al., *Sampling and Online Analysis of Alkalis in Thermal Process Gases with a Novel Surface Ionization Detector*. *Energy & Fuels*, 2011. **25**(9): p. 4163-4171
  25. Biollaz, S.M.A., et al., *PSI's Diagnostic Toolbox for On-line and Off-line Tar Analysis*, 2011, Gas Technology Institute (GTI): TCBIomass Conference 2011
  26. Xu, M., et al., *Comparison of a Solvent-Free Tar Quantification Method to the International Energy Agency's Tar Measurement Protocol*. *Energy & Fuels*, 2005. **19**(6): p. 2509-2513
  27. Aigner, I., U. Wolfesberger, and H. Hofbauer, *Tar Content and Composition in Producer Gas of Fluidized Bed Gasification and Low Temperature Pyrolysis of Straw and Wood – Influence of Temperature*, in *International Conference on Polygeneration Strategies (ICPS)2009, BIOENERGY 2020+*: Vienna
  28. Kurkela, E., P. Stahlberg, and J. Laatikainen, *Pressurised fluidised-bed gasification experiments with wood, peat and coal at VTT in 1991-1992: Part 1. Test facilities and gasification experiments with sawdust*. VTT Publications, 1993. **871**(161): p. 3-55
  29. Kurkela, E., et al., *Development of simplified IGCC-processes for biofuels - supporting gasification research at VTT*. *Bioresource Technology*, 1993. **46**(1-2): p. 37-47
  30. Kurkela, E. and P. Stahlberg, *Air gasification of peat, wood and brown coal in a pressurized fluidized-bed reactor. 1. Carbon conversion, gas yields and tar formation*. *Fuel Processing Technology*, 1992. **31**(1): p. 1-21
  31. Leppalahti, J. and E. Kurkela, *Behaviour of nitrogen compounds and tars in fluidized bed air gasification of peat*. *Fuel*, 1991. **70**(4): p. 491-497
  32. Rabou, L.P.L.M., et al., *Tar in Biomass Producer Gas, the Energy research Centre of The Netherlands (ECN) Experience: An Enduring Challenge*. *Energy & Fuels*, 2009. **23**(12): p. 6189-6198
  33. Bergman, P.C.A., Sander V.B. van Paasen, Harold Boerrigter, *The novel "OLGA" technology for complete tar removal from biomass producer gas*, in *Pyrolysis and Gasification of Biomass and Waste, Expert Meeting2002*: Strasbourg, France
  34. Zwart, R.W.R., A. Bos, and J. Kuipers, *Principle of OLGA tar removal system*, 2010, Energy research Centre of the Netherlands (ECN). p. 2
  35. Boerrigter, H. and P.C.A. Bergman, *Method and System for Gasifying Biomass*, in *United States Patent Application Publication*, U.S.P. Office, Editor 2002: Netherlands (NL)
  36. Pawliszyn, J., *Handbook of solid phase microextraction* 2009, Beijing: Chemical Industry Press. 410 p.



37. Bernardo, M.S., et al., *Determination of aromatic compounds in eluates of pyrolysis solid residues using HS-GC-MS and DLLME-GC-MS*. *Talanta*, 2009. **80**(1): p. 104-108
38. Torri, C. and D. Fabbri, *Application of off-line pyrolysis with dynamic solid-phase microextraction to the GC-MS analysis of biomass pyrolysis products*. *Microchemical Journal*, 2009. **93**(2): p. 133-139
39. Fabbri, D., et al., *Determination of Tetrachloroethylene and Other Volatile Halogenated Organic Compounds in Oil Wastes by Headspace SPME GC-MS*. *Chromatographia*, 2007. **66**(5): p. 377-382
40. Fabbri, D., A. Adamiano, and C. Torri, *GC-MS determination of polycyclic aromatic hydrocarbons evolved from pyrolysis of biomass*. *Analytical and Bioanalytical Chemistry*, 2010. **397**(1): p. 309-317
41. Brage, C., et al., *Use of amino phase adsorbent for biomass tar sampling and separation*. *Fuel*, 1997. **76**(2): p. 137-142
42. Woolcock, P.J. and R.C. Brown, *A review of cleaning technologies for biomass-derived syngas*. *Biomass and Bioenergy*, 2013. **52**: p. 54-84
43. Knoef, H., ed. *Handbook biomass gasification*. 2012, BTG Biomass Technology Group: Enschede (NL)
44. Bain, R.L. and K. Broer, *Gasification*, in *Thermochemical Processing of Biomass: Conversion into Fuels, Chemicals and Power*, C.B. Robert, Editor 2011, John Wiley & Sons: UK. p. 47-77
45. Spath, P.L. and D.C. Dayton, *Preliminary Screening -- Technical and Economic Assessment of Synthesis Gas to Fuels and Chemicals with Emphasis on the Potential for Biomass-Derived Syngas*, December 2003: Golden, CO. p. 160
46. Hirohata, O., et al., *Release Behavior of Tar and Alkali and Alkaline Earth Metals during Biomass Steam Gasification*. *Energy & Fuels*, 2008. **22**(6): p. 4235-4239
47. Korens, N., D.R. Simbeck, and D.J. Wilhelm, *Process Screening Analysis of Alternative Gas Treating and Sulfur Removal for Gasification: Revised Final Report*, 2002, Engineering consultant (SFA Pacific) Report for U.S. DOE NETL
48. Babu, S.P., *Thermal gasification of biomass technology developments: End of task report for 1992 to 1994*. *Biomass and Bioenergy*, 1995. **9**(1-5): p. 271-285
49. Good, J., et al., *Sampling and Analysis of tar and particles in biomass producer gases*, C.T. Committee, Editor 2005. p. 1-44
50. *Biomass Feedstock Composition and Property Database*, 2004, US Department of Energy
51. *Phyllis (biomass and waste composition database)*, Energy research Centre of the Netherlands (ECN)
52. Hoffmann, A.C. and L.E. Stein, *Gas cyclones and swirl tubes : principles, design, and operation*. 2nd ed 2008, Berlin ; New York: Springer. xxvi, 422 p.
53. Szemmelveisz, K., et al., *Examination of the combustion conditions of herbaceous biomass*. *Fuel Processing Technology*, 2009. **90**(6): p. 839-847
54. Gustafsson, E., M. Strand, and M. Sanati, *Physical and Chemical Characterization of Aerosol Particles Formed during the Thermochemical Conversion of Wood Pellets Using a Bubbling Fluidized Bed Gasifier*. *Energy & Fuels*, 2007. **21**(6): p. 3660-3667
55. Atimtay, A.T., *Cleaner energy production with integrated gasification combined cycle systems and use of metal oxide sorbents for H<sub>2</sub>S cleanup from coal gas*. *Clean Technologies and Environmental Policy*, 2001. **2**(4): p. 197-208

56. Newby, R.A., W.-C. Yang, and R.L. Bannister, *Fuel Gas Cleanup Parameters in Air-Blown IGCC*. Journal of Engineering for Gas Turbines and Power, 2000. **122**(2): p. 247-254
57. Stiegel, G.J. and R.C. Maxwell, *Gasification technologies: the path to clean, affordable energy in the 21st century*. Fuel Processing Technology, 2001. **71**(1-3): p. 79-97
58. Seville, J.P.K., *Gas cleaning in demanding applications*. 1st ed 1997, London ; New York: Blackie Academic & Professional. xv, 308 p.
59. *Remediation Technologies Screening Matrix and Reference Guide: Technology - Air emissions/off-gas treatment: scrubbers*. [Web Page from FRTR] 2008; Available from: <http://www.frtr.gov/matrix2/section4/4-60.html>
60. Stevens, D., *Hot Gas Conditioning: Recent Progress with Larger-Scale biomass Systems*, 2001, Pacific Northwest National Laboratory. p. 103
61. Torres, W., S.S. Pansare, and J.G. Goodwin, *Hot gas removal of tars, ammonia, and hydrogen sulfide from Biomass gasification gas*. Catalysis Reviews-Science and Engineering, 2007. **49**(4): p. 407-456
62. Devi, L., K.J. Ptasiński, and F.J.J.G. Janssen, *A review of the primary measures for tar elimination in biomass gasification processes*. Biomass & Bioenergy, 2003. **24**(2): p. 125-140
63. Bridgwater, A.V., *The Technical and Economic-Feasibility of Biomass Gasification for Power-Generation*. Fuel, 1995. **74**(5): p. 631-653
64. Ciferno, J.P. and J.J. Marano, *Benchmarking Biomass Gasification Technologies for Fuels, Chemicals and Hydrogen Production*, U.S.D.o. Energy, Editor 2002
65. Elliott, D.C., ed. *Relation of reaction time and temperature to chemical composition of pyrolysis oils*. Pyrolysis oils from Biomass, ed. E. Soltes and T. Milne. Vol. ACS Symposium Series; vol 376 1988, American Chemistry Society: Denver CO. 55-65
66. Boerrigter, H. and H. Den Uil, *Green Diesel from Biomass via Fischer-Tropsch synthesis: New Insights in Gas Cleaning and Process Design*, in *Pyrolysis and Gasification of Biomass and Waste, Expert Meeting 2002*: Strasbourg, France
67. Vreugdenhil, B.J., *Thersites: the ECN tar dew point site*, 2009, Energy Research Centre of the Netherlands (ECN)
68. Paasen, S.V.B.v., et al., *Tar dewpoint analyser; For application in biomass gasification product gases*, 2005, ECN. p. 32
69. Gupta, R.P., et al., *Desulfurization of syngas in a transport reactor*. Environmental Progress, 2001. **20**(3): p. 187-195
70. Jazbec, M., K. Sendt, and B.S. Haynes, *Kinetic and thermodynamic analysis of the fate of sulphur compounds in gasification products*. Fuel, 2004. **83**(16): p. 2133-2138
71. Leibold, H., A. Hornung, and H. Seifert, *HHP syngas cleaning concept of two stage biomass gasification for FT synthesis*. Powder Technology, 2008. **180**(1-2): p. 265-270
72. Lovell, R., S. Dylewski, and C. Peterson, *Control of Sulfur Emissions from Oil Shale Retorts*, 1981, U.S. Environmental Protection Agency: Cincinnati Ohio. p. 190
73. Dou, B.L., et al., *High-temperature removal of NH<sub>3</sub>, organic sulfur, HCl, and tar component from coal-derived gas*. Industrial & Engineering Chemistry Research, 2002. **41**(17): p. 4195-4200
74. Malhotra, S. and R. Pandey, *Desulfurization of gaseous fuels with recovery of elemental sulfur: An overview*. Critical Reviews in Environmental Science and Technology, 1999. **29**(3): p. 229-268

75. Vamvuka, D., C. Arvanitidis, and D. Zachariadis, *Flue gas desulfurization at high temperatures: A review*. Environmental Engineering Science, 2004. **21**(4): p. 525-547
76. Hansson, K.M., et al., *Formation of HNCO, HCN, and NH<sub>3</sub> from the pyrolysis of bark and nitrogen-containing model compounds*. Combustion and Flame, 2004. **137**(3): p. 265-277
77. Zhou, J., et al., *Release of Fuel-bound Nitrogen in Biomass During High Temperature Pyrolysis and Gasification*, in *32nd Intersociety Energy Conversion Engineering Conference* 1997. p. 1785-1790
78. Espinal, J.F., T.N. Truong, and F. Mondragon, *Mechanisms of NH<sub>3</sub> formation during the reaction of H-2 with nitrogen containing, carbonaceous materials*. Carbon, 2007. **45**(11): p. 2273-2279
79. Becidan, M., O. Skreiberg, and J.E. Hustad, *NO<sub>x</sub> and N<sub>2</sub>O precursors (NH<sub>3</sub> and HCN) in pyrolysis of biomass residues*. Energy & Fuels, 2007. **21**(2): p. 1173-1180
80. Glazer, M.P., et al., *Alkali Metals in Circulating Fluidized Bed Combustion of Biomass and Coal: Measurements and Chemical Equilibrium Analysis*. Energy & Fuels, 2005. **19**(5): p. 1889-1897
81. Khan, A.A., et al., *Biomass combustion in fluidized bed boilers: Potential problems and remedies*. Fuel Processing Technology, 2009. **90**(1): p. 21-50
82. Smeenk, J., R.C. Brown, and D. Eckels. *Determination of vapor phase alkali content during biomass gasification in Fourth Biomass Conference of the Americas* 1999. Oakland CA
83. Dayton, D.C., R.J. French, and T.A. Milne, *Direct Observation of Alkali Vapor Release during Biomass Combustion and Gasification. 1. Application of Molecular Beam/Mass Spectrometry to Switchgrass Combustion*. Energy & Fuels, 1995. **9**(5): p. 855-865
84. Turn, S.Q., et al., *The fate of inorganic constituents of biomass in fluidized bed gasification*. Fuel, 1998. **77**(3): p. 135-146
85. Smeenk, J. and R.C. Brown. *Evaluation of an Integrated Gasification/Fuel Cell Power Plant*. in *Third Biomass Conference of the Americas*. 1997. Montreal, Canada
86. Trembly, J.P., R.S. Gemmen, and D.J. Bayless, *The effect of IGFC warm gas cleanup system conditions on the gas-solid partitioning and form of trace species in coal syngas and their interactions with SOFC anodes*. Journal of Power Sources, 2007. **163**(2): p. 986-996
87. Valmari, T., et al., *Field Study on Ash Behavior during Circulating Fluidized-Bed Combustion of Biomass. 2. Ash Deposition and Alkali Vapor Condensation*. Energy & Fuels, 1998. **13**(2): p. 390-395
88. Kling, Å., et al., *Alkali deactivation of high-dust SCR catalysts used for NO<sub>x</sub> reduction exposed to flue gas from 100 MW-scale biofuel and peat fired boilers: Influence of flue gas composition*. Applied Catalysis B: Environmental, 2007. **69**(3-4): p. 240-251
89. Dou, B.L., et al., *Single and combined removal of HCl and alkali metal vapor from high-temperature gas by solid sorbents*. Energy & Fuels, 2007. **21**(2): p. 1019-1023
90. Turn, S.Q., *Chemical Equilibrium Prediction of Potassium, Sodium, and Chlorine Concentrations in the Product Gas from Biomass Gasification*. Industrial & Engineering Chemistry Research, 2007. **46**(26): p. 8928-8937
91. Higman, C. and M.v.d. Burgt, *Gasification*. 2nd ed 2008, Amsterdam ; Boston: Gulf Professional Pub./Elsevier Science. xvi, 435 p.

92. Trembly, J.P., R.S. Gemmen, and D.J. Bayless, *The effect of coal syngas containing HCl on the performance of solid oxide fuel cells: Investigations into the effect of operational temperature and HCl concentration*. Journal of Power Sources, 2007. **169**(2): p. 347-354
93. Lyczkowski, R.W. and J.X. Bouillard, *State-of-the-art review of erosion modeling in fluid/solids systems*. Progress in Energy and Combustion Science, 2002. **28**(6): p. 543-602
94. Cummer, K.R. and R.C. Brown, *Ancillary equipment for biomass gasification*. Biomass & Bioenergy, 2002. **23**(2): p. 113-128
95. Stairmand, C.J., *Design and Performance of Cyclone Separators*. Transactions of the Institution of Chemical Engineers, 1951. **29**: p. 356-383
96. Koch, W. and W. Licht, *New Design Approach Boosts Cyclone Efficiency*. Chemical Engineering, 1977. **84**(24): p. 80-88
97. Rosin, P., E. Rammler, and W. Intelmann, *Bases and boundaries of cyclone dust removal*. ZEITSCHRIFT DES VEREINES DEUTSCHER INGENIEURE, 1932. **76**: p. 433-477
98. Salcedo, R.L. and M.J. Pinho, *Pilot- and Industrial-Scale Experimental Investigation of Numerically Optimized Cyclones*. Industrial & Engineering Chemistry Research, 2002. **42**(1): p. 145-154
99. Lee, K. and B. Liu, *Theoretical study of aerosol filtration by fibrous filters*. Aerosol Science and Technology, 1982. **1**(2): p. 147-161
100. Peukert, W., *High temperature filtration in the process industry*. Filtration & Separation, 1998. **35**(5): p. 461-464
101. Sharma, S.D., et al., *A critical review of syngas cleaning technologies - fundamental limitations and practical problems*. Powder Technology, 2008. **180**(1-2): p. 115-121
102. Sharma, S.D., et al., *Recent developments in dry hot syngas cleaning processes*. Fuel, 2009. **In Press, Corrected Proof**
103. Desu, S. and C.-H. Peng, *Coating Porous Materials with Metal oxides and other ceramics by Metal Organic Chemical Vapor Deposition (MOCVD)*, USPTO, Editor 1993, Center for Innovative Technology: United States of America
104. Schildermans, I. and J. Baeyens. *Reviewing the growing potential of porous sintered metal filters*. 2006. Prague, Czech republic: Czech Society of Chemical Engineering
105. Gardner, B., et al. *Hot gas filtration meeting turbine requirements for particulate matter*. 2005. Reno-Tahoe, NV, United states: American Society of Mechanical Engineers
106. Stanghelle, D., T. Slungaard, and O.K. Sønju, *Granular bed filtration of high temperature biomass gasification gas*. Journal of Hazardous Materials, 2007. **144**(3): p. 668-672
107. Macías-Machín, A., et al., *New granular material for hot gas filtration: Use of the "Lapilli"*. Chemical Engineering and Processing, 2006. **45**(9): p. 719-727
108. Ritzert, J.A., R.C. Brown, and J. Smeenk. *Filtration Efficiency of a Moving Bed Granular Filter*. in *Science in Thermal and Chemical Biomass Conversion*. 2004. Victoria, B.C., Canada
109. Brown, R.C., J. Smeenk, and C. Wistrom. *Design of a moving bed granular filter for biomass gasification*. in *Progress in Thermochemical Biomass Conversion*. 2000. Tyrol, Austria
110. Brown, R., et al., *Similitude study of a moving bed granular filter*. Powder Technology, 2003. **138**(2-3): p. 201-210

111. Smid, J., et al., *Moving bed filters for hot gas cleanup*. Filtration & Separation. **42**(6): p. 34-37
112. Smid, J., et al., *Hot gas cleanup: new designs for moving bed filters*. Filtration & Separation, 2005. **42**(10): p. 36-39
113. El-Hedok, I.A., L. Whitmer, and R.C. Brown, *The influence of granular flow rate on the performance of a moving bed granular filter*. Powder Technology, 2011. **214**(1): p. 69-76
114. Ma, L. and G.V. Baron, *Mixed zirconia-alumina supports for Ni/MgO based catalytic filters for biomass fuel gas cleaning*. Powder Technology, 2008. **180**(1-2): p. 21-29
115. Rapagna, S., et al., *In Situ Catalytic Ceramic Candle Filtration for Tar Reforming and Particulate Abatement in a Fluidized-Bed Biomass Gasifier*. Energy & Fuels, 2009. **23**(7): p. 3804-3809
116. Lloyd, D.A., *Electrostatic precipitator handbook* 1988, Bristol [England] ; Philadelphia: A. Hilger. xiv, 239 p.
117. McDonald, J.R. and A.H. Dean, *Electrostatic precipitator manual*. Pollution technology review, 1982, Park Ridge, N.J.: Noyes Data Corp. xi, 484 p.
118. Probststein, R.F. and R.E. Hicks, *Synthetic fuels* 2006, Mineola, N.Y.: Dover Publications. xiv, 490 p.
119. McKenna, J.D., J.H. Turner, and J.P. McKenna, *Electrostatic Precipitators*, in *Fine Particle (2.5 Microns) Emissions* 2008. p. 135-174
120. Theodore, L., *Electrostatic Precipitators*, in *Air Pollution Control Equipment Calculations* 2008, John Wiley & Sons, Inc. p. 399-450
121. !!! INVALID CITATION !!!
122. Han, J. and H. Kim, *The reduction and control technology of tar during biomass gasification/pyrolysis: An overview*. Renewable & Sustainable Energy Reviews, 2008. **12**(2): p. 397-416
123. Nair, S.A., et al., *Streamer corona plasma for fuel gas cleaning: comparison of energization techniques*. Journal of Electrostatics, 2005. **63**(12): p. 1105-1114
124. Kwan, W., et al., *Removal of suspended fine particles from gases by turbulent deposition*. ASHRAE Transactions, 1997. **103**: p. 213-222
125. Dullien, F., *Theory and practice of a new class of equipment for separation of particulates from gases: the turbulent flow precipitator*. Revue de l'Institut français du pétrole, 1999. **54**(5): p. 565-575
126. Ahrenfeldt, J., et al., *Validation of a continuous combined heat and power (CHP) operation of a two-stage biomass gasifier*. Energy & Fuels, 2006. **20**(6): p. 2672-2680
127. Brandt, P., E. Larsen, and U. Henriksen, *High Tar Reduction in a Two-Stage Gasifier*. Energy & Fuels, 2000. **14**(4): p. 816-819
128. Steynberg, A. and M. Dry, *Fischer-Tropsch technology*. Studies in surface science and catalysis, 2004, Amsterdam ; Boston: Elsevier. xxi, 700 p.
129. Visconti, C.G., et al., *Fischer-Tropsch synthesis on a Co/Al<sub>2</sub>O<sub>3</sub> catalyst with CO<sub>2</sub> containing syngas*. Applied Catalysis A: General, 2009. **355**(1-2): p. 61-68
130. Riedel, T., et al., *Comparative study of Fischer-Tropsch synthesis with H<sub>2</sub>/CO and H<sub>2</sub>/CO<sub>2</sub> syngas using Fe- and Co-based catalysts*. Applied Catalysis A: General, 1999. **186**(1-2): p. 201-213
131. Tregrossi, A., A. Ciajolo, and R. Barbella, *The combustion of benzene in rich premixed flames at atmospheric pressure*. Combustion and Flame, 1999. **117**(3): p. 553-561

132. Fjellerup, J., et al., *Formation, Decomposition, and Cracking of Biomass Tars in Gasification*, 2005, Technical University of Denmark. p. 60
133. Houben, M.P., H.C. de Lange, and A.A. van Steenhoven, *Tar reduction through partial combustion of fuel gas*. *Fuel*, 2005. **84**(7-8): p. 817-824
134. Brandt, P. and U. Henriksen, *Decomposition of tar in gas from updraft gasifier by thermal cracking*, in *1st World Conference on Biomass for Energy and Industry* 2001, James & James (Science Publishers) Ltd.: Sevilla, Spain. p. 1756-1758
135. Dayton, D., *Review of the literature on Catalytic Biomass Tar Destruction*, 2002: Golden, CO. p. 33
136. Dutta, A., R.L. Bain, and M.J. Bidy, *Techno-economics of the production of mixed alcohols from lignocellulosic biomass via high-temperature gasification*. *Environmental Progress & Sustainable Energy*, 2010. **29**(2): p. 163-174
137. Phillips, S., et al., *Thermochemical Ethanol via Indirect Gasification and Mixed Alcohol Synthesis of Lignocellulosic Biomass*, 2007, NREL. p. 132
138. Dutta, A. and S.D. Phillips, *Thermochemical Ethanol via Direct Gasification and Mixed Alcohol Synthesis of Lignocellulosic Biomass*, 2009: Golden, CO. p. 144
139. Sutton, D., B. Kelleher, and J.R.H. Ross, *Catalytic conditioning of organic volatile products produced by peat pyrolysis*. *Biomass and Bioenergy*, 2002. **23**(3): p. 209-216
140. Houben, M.P., et al. *An analysis and experimental investigation of the cracking and polymerisation of tar*. in *12th European conference on biomass for energy, industry and climate protection*. 2002. Netherlands, Amsterdam
141. Boudart, M. and G. Djéga-Mariadassou, *Kinetics of heterogeneous catalytic reactions*. *Physical chemistry* 1984, Princeton, NJ: Princeton University Press. xviii, 222
142. Satterfield, C.N., *Heterogeneous catalysis in industrial practice*. 2nd ed 1996, Malabar, Fla.: Krieger Pub. xvi, 554 p.
143. Mastellone, M.L. and U. Arena, *Olivine as a tar removal catalyst during fluidized bed gasification of plastic waste*. *AIChE Journal*, 2008. **54**(6): p. 1656-1667
144. Dou, B., et al., *Catalytic cracking of tar component from high-temperature fuel gas*. *Applied Thermal Engineering*, 2003. **23**(17): p. 2229-2239
145. Sutton, D., B. Kelleher, and J.R.H. Ross, *Review of literature on catalysts for biomass gasification*. *Fuel Processing Technology*, 2001. **73**(3): p. 155-173
146. Yung, M.M., W.S. Jablonski, and K.A. Magrini-Bair, *Review of Catalytic Conditioning of Biomass-Derived Syngas*. *Energy & Fuels*, 2009. **23**(4): p. 1874-1887
147. Xu, C., et al., *Recent advances in catalysts for hot-gas removal of tar and NH<sub>3</sub> from biomass gasification*. *Fuel*, 2010. **89**(8): p. 1784-1795
148. Abu El-Rub, Z., E.A. Bramer, and G. Brem, *Review of catalysts for tar elimination in biomass gasification processes*. *Industrial & Engineering Chemistry Research*, 2004. **43**(22): p. 6911-6919
149. Simell, P.A., et al., *Steam Reforming of Gasification Gas Tar over Dolomite with Benzene as a Model Compound*. *Industrial & Engineering Chemistry Research*, 1999. **38**(4): p. 1250-1257
150. Simell, P.A. and J.B.s. Bredenberg, *Catalytic purification of tarry fuel gas*. *Fuel*, 1990. **69**(10): p. 1219-1225
151. Tamhankar, S., K. Tsuchiya, and J. Riggs, *Catalytic cracking of benzene on iron silica - catalyst activity and reaction mechanism*. *Applied catalysis. A, General*, 1985. **16**(1): p. 103-121

152. El-Rub, Z.A., E.A. Bramer, and G. Brem, *Experimental comparison of biomass chars with other catalysts for tar reduction*. Fuel, 2008. **87**(10-11): p. 2243-2252
153. Simell, P., et al., *Catalytic hot gas cleaning of gasification gas*. Catalysis Today, 1996. **27**(1-2): p. 55-62
154. Miyazawa, T., et al., *Catalytic properties of Rh/CeO<sub>2</sub>/SiO<sub>2</sub> for synthesis gas production from biomass by catalytic partial oxidation of tar*. Science and Technology of Advanced Materials, 2005. **6**(6): p. 604-614
155. Pansare, S.S., J.G. Goodwin, and S. Gangwal, *Simultaneous Ammonia and Toluene Decomposition on Tungsten-Based Catalysts for Hot Gas Cleanup*. Industrial & Engineering Chemistry Research, 2008. **47**(22): p. 8602-8611
156. Luengnaruemitchai, A. and A. Kaengsilalai, *Activity of different zeolite-supported Ni catalysts for methane reforming with carbon dioxide*. Chemical Engineering Journal, 2008. **144**(1): p. 96-102
157. Buchireddy, P.R., et al., *Biomass Gasification: Catalytic Removal of Tars over Zeolites and Nickel Supported Zeolites*. Energy & Fuels. **24**(4): p. 2707-2715
158. Brown, R.A., et al., *Production and characterization of synthetic wood chars for use as surrogates for natural sorbents*. Organic Geochemistry, 2006. **37**(3): p. 321-333
159. Zhang, T., et al., *Preparation of activated carbon from forest and agricultural residues through CO<sub>2</sub> activation*. Chemical Engineering Journal, 2004. **105**(1-2): p. 53-59
160. Chembukulam, S.K., et al., *Smokeless Fuel from Carbonized Sawdust*. Industrial & Engineering Chemistry Product Research and Development, 1981. **20**(4): p. 714-719
161. Zanzi, R., K. Sjostrom, and E. Bjornbom, *Rapid high-temperature pyrolysis of biomass in a free-fall reactor*. Fuel, 1996. **75**(5): p. 545-550
162. Rodríguez-Reinoso, F., M. Molina-Sabio, and M.T. González, *The use of steam and CO<sub>2</sub> as activating agents in the preparation of activated carbons*. Carbon, 1995. **33**(1): p. 15-23
163. Linares-Solano, A., et al., *Activated carbons from bituminous coal: effect of mineral matter content*. Fuel, 2000. **79**(6): p. 635-643
164. Hosokai, S., et al., *Mechanism of decomposition of aromatics over charcoal and necessary condition for maintaining its activity*. Fuel, 2008. **87**(13-14): p. 2914-2922
165. Yu, J., et al., *Char-supported nano iron catalyst for water-gas-shift reaction - Hydrogen production from coal/biomass gasification*. Process Safety and Environmental Protection, 2006. **84**(B2): p. 125-130
166. Hauserman, W.B., *High-yield hydrogen-production by catalytic gasification of coal or biomass*. International Journal of Hydrogen Energy, 1994. **19**(5): p. 413-419
167. Raveendran, K., A. Ganesh, and K.C. Khilar, *Influence of mineral matter on biomass pyrolysis characteristics*. Fuel, 1995. **74**(12): p. 1812-1822
168. Fahmi, R., et al., *The effect of alkali metals on combustion and pyrolysis of Lolium and Festuca grasses, switchgrass and willow*. Fuel. **86**(10-11): p. 1560-1569
169. Brown, R.C., Q. Liu, and G. Norton, *Catalytic effects observed during the co-gasification of coal and switchgrass*. Biomass & Bioenergy, 2000. **18**(6): p. 499-506
170. Pemen, A.J.M., et al., *Pulsed corona discharges for tar removal from biomass derived fuel gas*. Plasmas and Polymers, 2003. **8**(3): p. 209-224
171. Nair, S.A., et al., *Tar removal from biomass-derived fuel gas by pulsed corona discharges*. Fuel Processing Technology, 2003. **84**(1-3): p. 161-173

172. Neeft, J.P.A., H.A.M. Knoef, and P. Onaji, *Behaviour of Tar in Biomass Gasification Systems: Tar Related Problems and their Solutions*, 1999, ECN Netherlands Energy Research Foundation, BTG Biomass Technology Group: Petten
173. Ober, J.A., *Sulfur. In: Mineral Commodity Summaries.*, 2009, USGS (United States Geological Survey) Minerals
174. Westmoreland, P.R. and D.P. Harrison, *Evaluation of candidate solids for high-temperature desulfurization of low-Btu gases*. Environmental Science & Technology, 1976. **10**(7): p. 659-661
175. Tamhankar, S.S., et al., *Mixed-Oxide Sorbents for High-Temperature Removal of Hydrogen-Sulfide*. Industrial & Engineering Chemistry Process Design and Development, 1986. **25**(2): p. 429-437
176. Gangwal, S.K., R. Gupta, and W.J. McMichael, *Hot-gas cleanup--sulfur recovery technical, environmental, and economic issues*. Heat Recovery Systems and CHP, 1995. **15**(2): p. 205-214
177. Ohtsuka, Y., et al., *Recent progress in Japan on hot gas cleanup of hydrogen chloride, hydrogen sulfide and ammonia in coal-derived fuel gas*. Powder Technology, 2009. **190**(3): p. 340-347
178. Sud-Chemie, *General Catalogue*, Sud-Chemie, Editor 2010
179. Sanchez-Hervas, J.M., J. Otero, and E. Ruiz, *A study on sulphidation and regeneration of Z-Sorb III sorbent for H<sub>2</sub>S removal from simulated ELCOGAS IGCC syngas*. Chemical Engineering Science, 2005. **60**(11): p. 2977-2989
180. Sanchez, J.M., E. Ruiz, and J. Otero, *Selective removal of hydrogen sulfide from gaseous streams using a zinc-based sorbent*. Industrial & Engineering Chemistry Research, 2005. **44**(2): p. 241-249
181. Gupta, R.P. and W.S. O'Brien, *Desulfurization of Hot Syngas Containing Hydrogen Chloride Vapors Using Zinc Titanate Sorbents*. Industrial & Engineering Chemistry Research, 2000. **39**(3): p. 610-619
182. Jun, H.K., et al., *Decomposition of NH<sub>3</sub> over Zn-Ti-based desulfurization sorbent promoted with cobalt and nickel*. Catalysis Today, 2003. **87**(1-4): p. 3-10
183. Busca, G. and C. Pistarino, *Abatement of ammonia and amines from waste gases: a summary*. Journal of Loss Prevention in the Process Industries, 2003. **16**(2): p. 157-163
184. Mojtahedi, W., et al., *Catalytic Decomposition of Ammonia in Fuel Gas Produced in Pilot-Scale Pressurized Fluidized-Bed Gasifier*. Fuel Processing Technology, 1995. **45**(3): p. 221-236
185. Mojtahedi, W. and J. Abbasian, *Catalytic Decomposition of Ammonia in a Fuel Gas at High-Temperature and Pressure*. Fuel, 1995. **74**(11): p. 1698-1703
186. Punjak, W.A., Uberoi, M., Shadman, F., *Control of Ash Deposition Through the High Temperature Adsorption of Alkali Vapors on Solid Sorbents*, in *Symposium on Ash Deposition, 197th Annual Meeting of the American Chemical Society*: Dallas, TX
187. Mulik, P.R., M.A. Alvin, and D.M. Bachovchin, *Simultaneous high-temperature removal of alkali and particulates in a pressurized gasification system. Final technical progress report, April 1981-July 1983*, 1983. p. Medium: X; Size: Pages: 337
188. Punjak, W.A., M. Uberoi, and F. Shadman, *High-temperature adsorption of alkali vapors on solid sorbents*. AIChE Journal, 1989. **35**(7): p. 1186-1194
189. Dou, B.L., et al., *Adsorption of alkali metal vapor from high-temperature coal-derived gas by solid sorbents*. Fuel Processing Technology, 2003. **82**(1): p. 51-60



190. Dou, B., et al., *HCl Removal and Chlorine Distribution in the Mass Transfer Zone of a Fixed-Bed Reactor at High Temperature*. Energy & Fuels, 2006. **20**(3): p. 959-963
191. Dou, B.-l., J.-s. Gao, and X.-z. Sha, *A study on the reaction kinetics of HCl removal from high-temperature coal gas*. Fuel Processing Technology, 2001. **72**(1): p. 23-33
192. Weinell, C.E., et al., *Hydrogen chloride reaction with lime and limestone: kinetics and sorption capacity*. Industrial & Engineering Chemistry Research, 1992. **31**(1): p. 164-171
193. Dou, B., et al., *High-Temperature HCl Removal with Sorbents in a Fixed-Bed Reactor*. Energy & Fuels, 2003. **17**(4): p. 874-878
194. Timmer, K., *Carbon conversion during bubbling fluidized bed gasification of biomass*, in *Mechanical Engineering* 2008, Iowa State University: Ames. p. 171
195. Dou, B., et al., *Reaction of Solid Sorbents with Hydrogen Chloride Gas at High Temperature in a Fixed-Bed Reactor*. Energy & Fuels, 2005. **19**(6): p. 2229-2234
196. Shemwell, B., Y.A. Leventis, and G.A. Simons, *Laboratory study on the high-temperature capture of HCl gas by dry-injection of calcium-based sorbents*. Chemosphere, 2001. **42**(5-7): p. 785-796
197. Schifftner, K.C. and H.E. Hesketh, *Wet scrubbers*. 2nd ed 1996, Lancaster, Pa: Technomic. xv, 206
198. *Industrial Filtration and Product Recovery Systems*, 2003, MikroPul Filtration Solutions, Beacon Industrial Group
199. Bologna, A., et al., *Novel wet electrostatic precipitator for collection of fine aerosol*. Journal of Electrostatics, 2009. **67**(2-3): p. 150-153
200. Balsam T. Mohammad, M.C.V., Christian Kennes., *Mesophilic and thermophilic biotreatment of BTEX-polluted air in reactors*. Biotechnology and Bioengineering, 2007. **97**(6): p. 1423-1438
201. Brown, R.C., *Thermochemical Processing of Biomass - Conversion into Fuels, Chemicals and Power* 2011: Wiley & Sons
202. Kohl, A.L. and R. Nielsen, *Gas purification*. 5th ed 1997, Houston, TX: Gulf Publishing. viii, 1395
203. Larson, E.D., H. Jin, and F.E. Celik, *Large-scale gasification-based coproduction of fuels and electricity from switchgrass*. Biofuels, Bioproducts and Biorefining, 2009. **3**(2): p. 174-194
204. Nagl, G.J., *Update your sulfur management program; Flexibility of liquid redox processing can optimize refinery sulfur handling*. Hydrocarbon Processing, 2005. **84**(11): p. 43-50
205. Watson, J., K.D. Jones, and T. Barnette, *Remove hydrogen sulfide from syngas*. Hydrocarbon Processing, 2008. **87**(1): p. 81-84
206. Plummer, M., *Sulfur and hydrogen from H<sub>2</sub>S*. Hydrocarbon Processing, 1987. **66**(4): p. 38-40
207. Jensen, A.B. and C. Webb, *Treatment of H<sub>2</sub>S-containing gases: A review of microbiological alternatives*. Enzyme and Microbial Technology, 1995. **17**(1): p. 2-10
208. Fortuny, M., et al., *Biological sweetening of energy gases mimics in biotrickling filters*. Chemosphere, 2008. **71**(1): p. 10-17
209. Satoh, H., *Bacteria help desulfurize gas*. Hydrocarbon Processing, 1988. **67**(5): p. 76
210. Proll, T., et al., *Removal of NH<sub>3</sub> from biomass gasification producer gas by water condensing in an organic solvent scrubber*. Industrial & Engineering Chemistry Research, 2005. **44**(5): p. 1576-1584

211. Pinto, F., *Effect of experimental conditions on gas quality and solids produced by sewage sludge cogasification. 1. Sewage sludge mixed with coal*. Energy & Fuels, 2007. **21**(5): p. 2737
212. Koveal, R. and D. Alexion, *Gas Conversion with Rejuvenation Ammonia Removal*, U.S.P. Office, Editor 1999: USA
213. Bai, H. and A.C. Yeh, *Removal of CO<sub>2</sub> Greenhouse Gas by Ammonia Scrubbing*. Industrial & Engineering Chemistry Research, 1997. **36**(6): p. 2490-2493
214. Fortier, H., et al., *Ammonia, cyclohexane, nitrogen and water adsorption capacities of an activated carbon impregnated with increasing amounts of ZnCl<sub>2</sub>, and designed to chemisorb gaseous NH<sub>3</sub> from an air stream*. Journal of Colloid and Interface Science, 2008. **320**(2): p. 423-435
215. Baxter, L.L., et al., *The behavior of inorganic material in biomass-fired power boilers: field and laboratory experiences*. Fuel Processing Technology, 1998. **54**(1-3): p. 47-78
216. Turn, S.Q., C.M. Kinoshita, and D.M. Ishimura, *Removal of inorganic constituents of biomass feedstocks by mechanical dewatering and leaching*. Biomass and Bioenergy, 1997. **12**(4): p. 241-252
217. Davidsson, K.O., et al., *The effects of fuel washing techniques on alkali release from biomass*. Fuel, 2002. **81**(2): p. 137-142
218. Zwart, R.W.R., et al., *Oil-based gas washing - Flexible tar removal for high-efficient production of clean heat and power as well as sustainable fuels and chemicals*. Environmental Progress & Sustainable Energy, 2009. **28**(3): p. 324-335
219. Spooren, T., et al., *Semiwet scrubbing: Design and operational experience of a state-of-the-art unit*. Environmental Progress, 2006. **25**(3): p. 201-207
220. Kameda, T., et al., *Removal of hydrogen chloride from gaseous streams using magnesium-aluminum oxide*. Chemosphere, 2008. **73**(5): p. 844-847
221. Diaz-Somoano, M., M.A. Lopez-Anton, and M.R. Martinez-Tarazona. *Solid sorbents for trace element removal at high temperatures in coal gasification*. in *9th International Conference on Environmental Science and Technology*. 2005. Rhodes Isl, Greece: Univ Aegean
222. Alptekin, G., *Novel Sorbent-Based Process for High Temperature Trace Metal Removal*, May 2009, TDA Research, Inc.: Wheat Ridge CO. p. 99
223. Woolcock, P.J., et al., *Analysis of trace contaminants in hot gas streams using time-weighted average solid-phase microextraction: Proof of concept*. Journal of Chromatography A, 2013. **1281**: p. 1-8
224. Woolcock, P. and R. Brown, *A review of syngas cleaning technologies (submitted & accepted)*. Biomass & Bioenergy, 2013
225. Bahng, M.-K., et al., *Current technologies for analysis of biomass thermochemical processing: A review*. Analytica Chimica Acta, 2009. **651**(2): p. 117-138
226. Brown, R.C., *Biorenewable resources: engineering new products from agriculture*. 1st ed2003, Ames, Iowa: Iowa State Press. xii, 286 p.
227. Wang, J., et al., *Sampling atmospheric pesticides with SPME: laboratory developments and field study*. Environmental pollution, 2008. **157**(2): p. 365-370
228. Ouyang, G. and J. Pawliszyn, *Recent developments in SPME for on-site analysis and monitoring*. TrAC. Trends in analytical chemistry, 2006. **25**(7): p. 692-703

229. Carasek, E. and J. Pawliszyn, *Screening of tropical fruit volatile compounds using solid-phase microextraction (SPME) fibers and internally cooled SPME fiber*. Journal of agricultural and food chemistry, 2006. **54**(23): p. 8688-96
230. Vas, G. and K. Vékey, *Solid-phase microextraction: a powerful sample preparation tool prior to mass spectrometric analysis*. Journal of Mass Spectrometry, 2004. **39**(3): p. 233-254
231. Ouyang, G. and J. Pawliszyn, *A critical review in calibration methods for solid-phase microextraction*. Analytica Chimica Acta, 2008. **627**(2): p. 184-197
232. Cai, L., J.A. Koziel, and M.E. O'Neal, *Determination of characteristic odorants from Harmonia axyridis beetles using in vivo solid-phase microextraction and multidimensional gas chromatography–mass spectrometry–olfactometry*. Journal of Chromatography A, 2007. **1147**(1): p. 66-78
233. Koziel, J., M. Jia, and J. Pawliszyn, *Air Sampling with Porous Solid-Phase Microextraction Fibers*. Analytical Chemistry, 2000. **72**(21): p. 5178-5186
234. Ouyang, G., et al., *Time-weighted average water sampling with a diffusion-based solid-phase microextraction device*. Journal of Chromatography A, 2007. **1138**(1–2): p. 42-46
235. Wang, J., et al., *Flexibility of solid-phase microextraction for passive sampling of atmospheric pesticides*. Journal of Chromatography A, 2009. **1216**(15): p. 3031-3037
236. Hlina, M., et al. *Tar measurement in synthetic gas produced by plasma gasification by solid phase microextraction (SPME)*. in *ISPC Conference*.
237. Chen, Y., J. Koziel, and J. Pawliszyn, *Calibration for on-site analysis of hydrocarbons in aqueous and gaseous samples using solid-phase microextraction*. Analytical Chemistry, 2003. **75**(23): p. 6485-93
238. Isetun, S., et al., *Air sampling of organophosphate triesters using SPME under non-equilibrium conditions*. Analytical and Bioanalytical Chemistry, 2004. **378**(7): p. 1847-53
239. Koziel, J.A., J. Noah, and J. Pawliszyn, *Field sampling and determination of formaldehyde in indoor air with solid-phase microextraction and on-fiber derivatization*. Environmental Science & Technology, 2001. **35**(7): p. 1481-6
240. Ceballos, D., et al., *Characterization of solid-phase microextraction and gas chromatography for the analysis of gasoline tracers in different microenvironments*. Journal of the Air & Waste Management Association, 2007. **57**(3): p. 355-65
241. Chen, Y. and J. Pawliszyn, *Time-weighted average passive sampling with a solid-phase microextraction device*. Analytical Chemistry, 2003. **75**(9): p. 2004-2010
242. *Personal Communication – Supelco representative*, 2010: Bellefonte PA
243. Koziel, J., et al., *Field air analysis with SPME device*. Analytica Chimica Acta, 1999. **400**(1-3): p. 153-162
244. Koziel, J.A. and J. Pawliszyn, *Air sampling and analysis of volatile organic compounds with solid phase microextraction*. Journal of the Air & Waste Management Association, 2001. **51**(2): p. 173-184
245. Lyman, W.J., D.H. Rosenblatt, and W.J. Reehl, *Diffusion Coefficients in Air and Water*, in *Handbook of Chemical Property Estimation* 1982, American Chemical Society: Washington, D.C.
246. Karaiskakis, G. and D. Gavril, *Determination of diffusion coefficients by gas chromatography*. Journal of Chromatography A, 2004. **1037**(1-2): p. 147-189
247. Reid, R.C., J.M. Prausnitz, and B.E. Poling, *The properties of gases and liquids* 1977

248. Bird, R.B., W.E. Stewart, and E.N. Lightfoot, *Transport Phenomena*. 2 ed 2002, New York: J. Wiley
249. Martos, P.A. and J. Pawliszyn, *Time-weighted average sampling with solid-phase microextraction device: implications for enhanced personal exposure monitoring to airborne pollutants*. *Analytical Chemistry*, 1999. **71**(8): p. 1513-1520
250. Koziel, J., P. Martos, and J. Pawliszyn, *System for the generation of standard gas mixtures of volatile and semi-volatile organic compounds for calibrations of solid-phase microextraction and other sampling devices*. *Journal of Chromatography A*, 2004. **1025**(1): p. 3-9
251. Thomsen, V., D. Schatzlein, and D. Mercurio, *Limits of Detection in Spectroscopy*, in *Forensic Bioinformatics 6th Annual Conference 2007*: Dayton, Ohio
252. Semenov, S.N., J.A. Koziel, and J. Pawliszyn, *Kinetics of solid-phase extraction and solid-phase microextraction in thin adsorbent layer with saturation sorption isotherm*. *Journal of Chromatography A*, 2000. **873**(1): p. 39-51
253. Milne, T.A., R.J. Evans, and N. Abatzoglou, *Biomass Gasifier "Tars": Their Nature Formation and Conversion*, 1998, National Renewable Energy Laboratory: Golden, CO
254. Neeft, J.P.A., et al., *Behaviour of Tar in Biomass Gasification Systems: Tar Related Problems and Their Solutions* 1999: Novem
255. Bridgwater, A.V., *Progress in thermochemical biomass conversion* 2001: Oxford: Blackwell Science
256. Stahl, K., M. Neergaard, and J. Nieminen, *Varnamo Demonstration Programme - Final Report*, in *1st World Conference on biomass for Energy and Industry* 2000, James & James (Science Publishers) Ltd: Sevilla, Spain. p. 730-736
257. *Gasification and Syngas Cleaning Process Development Unit*. 2013 2011 [cited 2013 April 16 ]; Available from: <http://www.biocenturyresearchfarm.iastate.edu/capabilities/thermochemical/gasification.html>
258. Lyman, W.J., W.F. Reehl, and D.H. Rosenblatt, *Handbook of chemical property estimation methods: environmental behavior of organic compounds* 1990, Washington, D.C.: American Chemical Society
259. Leahy-Dios, A. and A. Firoozabadi, *Unified model for nonideal multicomponent molecular diffusion coefficients*. *AIChE Journal*, 2007. **53**(11): p. 2932-2939
260. Larroque, V., V. Desauziers, and P. Mocho, *Comparison of two solid-phase microextraction methods for the quantitative analysis of VOCs in indoor air*. *Analytical and Bioanalytical Chemistry*, 2006. **386**(5): p. 1457-64
261. Larroque, V., V. Desauziers, and P. Mocho, *Development of a solid phase microextraction (SPME) method for the sampling of VOC traces in indoor air*. *Journal of environmental monitoring*, 2006. **8**(1): p. 106-11
262. Chen, C.-Y., C. Hsieh, and J.-M. Lin, *Diffusive sampling of methylene chloride with solid phase microextraction*. *Journal of Chromatography A*, 2006. **1137**(2): p. 138-144
263. Tsai, S.-W. and K.-K. Wu, *Determination of ethylene oxide by solid-phase microextraction device with on-fiber derivatization*. *Journal of chromatography. A*, 2003. **991**(1): p. 1-11
264. Chen, Y., *New calibration methods for solid phase microextraction for on-site analysis*, in *Chemistry* 2004, University of Waterloo: Ontario, Canada

265. Chen, Y. and J. Pawliszyn, *Miniaturization and automation of an internally cooled coated fiber device*. Analytical Chemistry, 2006. **78**(14): p. 5222-6
266. Woolcock, P., J. Koziel, and R. Brown, *Characterization of pyrolysis kinetics using internally-cooled solid-phase microextraction* [In Preparation] 2013
267. Ellens, C.J. and R.C. Brown, *Optimization of a free-fall reactor for the production of fast pyrolysis bio-oil*. Bioresource Technology, 2012. **103**(1): p. 374-380
268. Ghiasvand, A.R., S. Hosseinzadeh, and J. Pawliszyn, *New cold-fiber headspace solid-phase microextraction device for quantitative extraction of polycyclic aromatic hydrocarbons in sediment*. Journal of Chromatography A, 2006. **1124**(1-2): p. 35-42
269. Kataoka, H., et al., *Developments and applications of capillary microextraction techniques: A review*. Analytica Chimica Acta, 2009. **655**(1-2): p. 8-29
270. Nelson, W., *Weibull Analysis of Reliability Data with Few or No Failures*. Journal of Quality Technology, 1985. **17**(3): p. 168-169
271. Peters, M., *Plant design and economics for chemical engineers / Max S. Peters, Klaus D. Timmerhaus*
272. Sinnott, R.K., *Coulson & Richardson's Chemical Engineering*. 2nd ed. Vol. 6. 1996: Butterworth-Heinemann. 966
273. Friedlander, S.K., *Smoke, Dust, and Haze: Fundamentals of Aerosol Dynamics; Second Edition* 2000, New York: Oxford University Press. 407
274. Tien, C., *Granular filtration of aerosols and hydrosols* 1989: Butterworth Publishers. 365